PATRICK LEAHY
Lake Champlain
Basin Program

TECHNICAL REPORT NO. 120

Development of a Comprehensive Binational Phosphorus Mass Balance Analysis Toolkit for the Missisquoi Bay Watershed

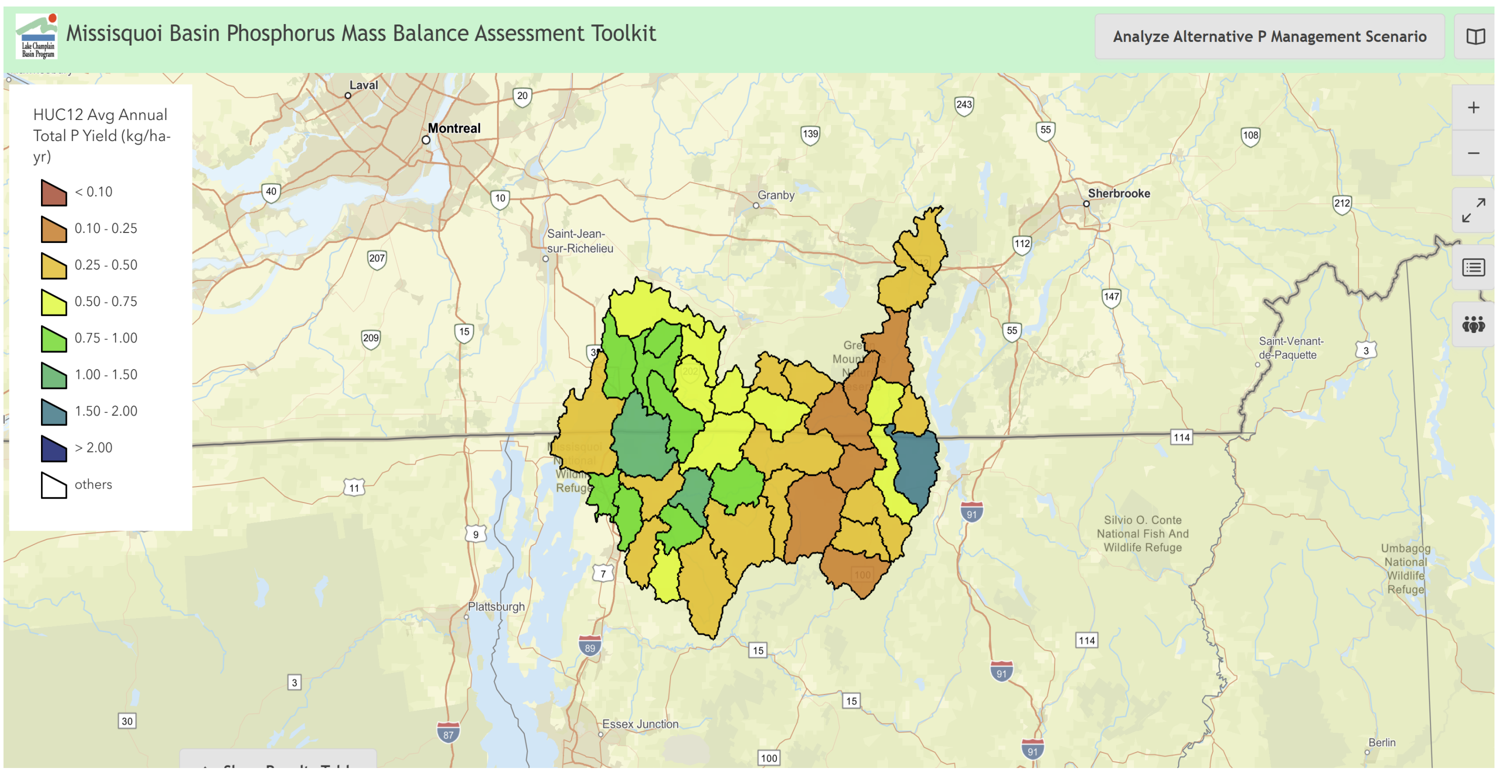

July 2026

Prepared by: Michael Winchell, M.S., Stone Environmental, Inc.; Aubert Michaud, Ph.D., OBVBM; Andrew Schroth, Ph.D., University of Vermont; Eric Roy, Ph.D., University of Vermont; Joshua Faulkner, Ph.D., University of Vermont Patrick Clemins, Ph.D., University of Vermont

For:
The Lake Champlain Basin Program and NEIWPCC

This report was funded and prepared under the authority of the Lake Champlain Special Designation Act of 1990, P.L. 101-596 and subsequent reauthorization in 2002 as the Daniel Patrick Moynihan Lake Champlain Basin Program Act, H. R. 1070, through the US EPA. Publication of this report does not signify that the contents necessarily reflect the views of the states of New York and Vermont, the Lake Champlain Basin Program, the US EPA or the Great Lakes Fishery Commission.

The Lake Champlain Basin Program has funded more than 100 technical reports and research studies since 1991. For complete list of LCBP Reports please visit:
https://www.lcbp.org/news-and-media/publications/technical-reports/

NEIWPCC Job Code: 0357-002-001
Project Code: L-2022-010

FINAL REPORT

NEIWPCC Job Code:	0357-002-001
Project Code:	L-2022-010
Contractor:	Stone Environmental, University of Vermont, OBVBM
Prepared By:	Michael Winchell, M.S., Stone Environmental, Inc. Aubert Michaud, Ph.D., OBVBM Andrew Schroth, Ph.D., University of Vermont Eric Roy, Ph.D., University of Vermont Joshua Faulkner, Ph.D., University of Vermont Patrick Clemins, Ph.D., University of Vermont
Project Period:	February 10, 2022 to September 30, 2025
Date Submitted:	May 21, 2025
Date Revision Submitted:	September 15, 2025
Date Approved:	September 15, 2025

DEVELOPMENT OF A COMPREHENSIVE BINATIONAL PHOSPHORUS MASS BALANCE ANALYSIS TOOLKIT FOR THE MISSISQUOI BAY WATERSHED

CONTACT INFORMATION

Stone Environmental, Inc.
535 Stone Cutters Way
Montpelier, VT 05602
mwinchell@stone-env.com

This is a United States Environmental Protection Agency funded project.

This project was funded by an agreement awarded by United States Environmental Protection Agency to NEIWPCC in partnership with the Lake Champlain Basin Program

PROJECT SUMMARY

This project has merged existing basin-wide data and scientific expertise from Quebec and Vermont to quantify the inventory of different P stocks within the Missisquoi Basin's terrestrial and aquatic compartments, applied physically based and empirical models and data to quantify the fate and transport of P across the basin, and produced a Missisquoi Bay Watershed P Mass Balance Assessment Toolkit for analysis of the P mass balance over the next 30 years under various alternative management scenarios.

Key outputs of this project include:

1. Creation of a binational P inventory providing a formal assessment of the current inventory and distribution of P within all terrestrial and aquatic compartments of the Missisquoi Basin;
2. A modeling approach for evaluating the water quality response of Missisquoi Bay to long-term changes in P loadings. The approach is based on a spatially-explicit binational terrestrial P export metamodel for evaluating the terrestrial landscape storage and export of P for unique combinations of land use/cropping system, soil characteristics, and climate, both under current and future alternative management practices;
3. The P Mass Balance Assessment Toolkit that allows stakeholders to explore the future long-term Missisquoi watershed P mass balance under a range of alternative assumptions. Such assumptions include adopting agricultural and non-agricultural best management and conservation practices at various scales and adoption rates throughout the U.S. and Canadian portions of the Missisquoi watershed. The Toolkit can be accessed at: https://www.stone-env.net/mass_balance/.

Key outcomes of this project include:

1. A thorough understanding of the variability in terrestrial landscape contributions to the P mass loads into Missisquoi Bay, and how this variability is contributing to the current P mass imbalance in the Bay;
2. Insights into how a broad range of alternative management practices, implemented following different adoption strategies, lead to reductions in Bay P loadings and how the Bay's water quality metrics respond to these loading reductions;
3. Consistent binational dataset and analysis methodology, packaged into a user-friendly Toolkit. The Toolkit enables customized evaluation of management strategies for maximizing beneficial reductions in P loading to Missisquoi Bay within the bounds of practical and economic constraints.

Six categories of alternative P management practices were investigated, including nutrient management (BMP-1), erosion control (BMP-2), riparian zone management (BMP-3), land use conversion (BMP-4), decentralized wastewater system upgrades (BMP-5), and centralized wastewater treatment plant improvements (BMP-6). Multiple implementation strategies for these practices were considered, including random and targeted areas at 20%, 50%, and 100% adoption rates, which showed clear benefits to targeting implementation to the critical source areas within the watershed. A summary of the P loading abatement rates from implementing the four agricultural BMP groups and different adoption strategies is provided in Figure ES1 below. Projected results on BMP effects demonstrate the substantial benefit of adopting a targeting

strategy when it comes to P non-point sources control. For example, a 7.4% P abatement rate is projected at the watershed scale for a random implementation of composite scenario BMPs 1+2+3 (nutrient, crop system, and riparian management) over 20% of the cropland. A targeted implementation over the same total surface area (20% of the cropland) would generate more than a three-fold increase in P loading abatement rate (23%). A similar pattern is projected with a rate of 50% BMP implementation over cropland. Although the random implementation is projecting a 15.6% reduction of watershed P loading, the abatement rate nearly doubles (26.8%) when considering a targeting strategy.

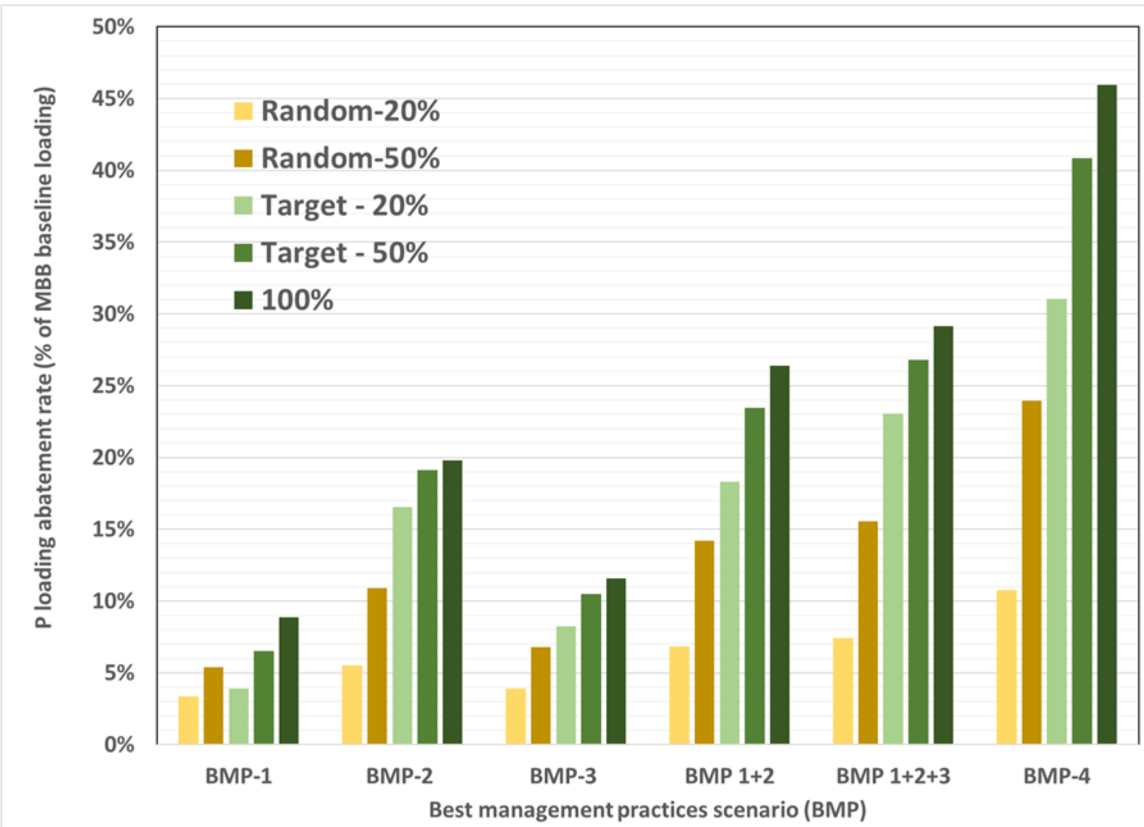

Figure ES1. Projected phosphorus loading abatement rates with respect to Missisquoi Bay watershed baseline loading from random, targeted, and global implementation of best management practices (BMP) scenarios on cropped land (including a 34% abatement rate systematically applied to residential and urban point sources).

The land conversion scenario (BMP-4) has the most effective abatement rate of P loading compared to the other agricultural BMPs. When applied to the most vulnerable farmland (target Critical Source Areas (CSAs)), the projected reduction in P loading is thus highly significant. Figure ES2 illustrates the effect of including land conversion scenarios to a targeting strategy (50% of cropped land) for the agricultural BMPs. Without land conversion, the watershed scale P loading abatement rate resulting from BMPs 1+2+3 is projected at 26.8%. A 5% area substitution of the most critical cropped land source areas to permanent forage cover leads to a projected abatement rate of 32.2%. The same logic applies to 10% and 20% substitution of composite BMPs (BMP 1+2+3) by land conversion, for resulting P abatement rates of 34.4% and 37.3% at the watershed scale. The marginal effect of land conversion diminishes with the importance of targeted area. Considering the important spatial discrimination in baseline P loadings, the 5% land conversion scenario has a significantly higher efficiency in reducing P loadings than the 10% or 20% scenarios which are converting gradually less vulnerable land. Considering that land conversion scenarios would presumably involve the largest cost-share costs, as compared to other agricultural BMPs, a practical implication of these projections would be to restrain land conversion scenarios to the most critical CSAs.

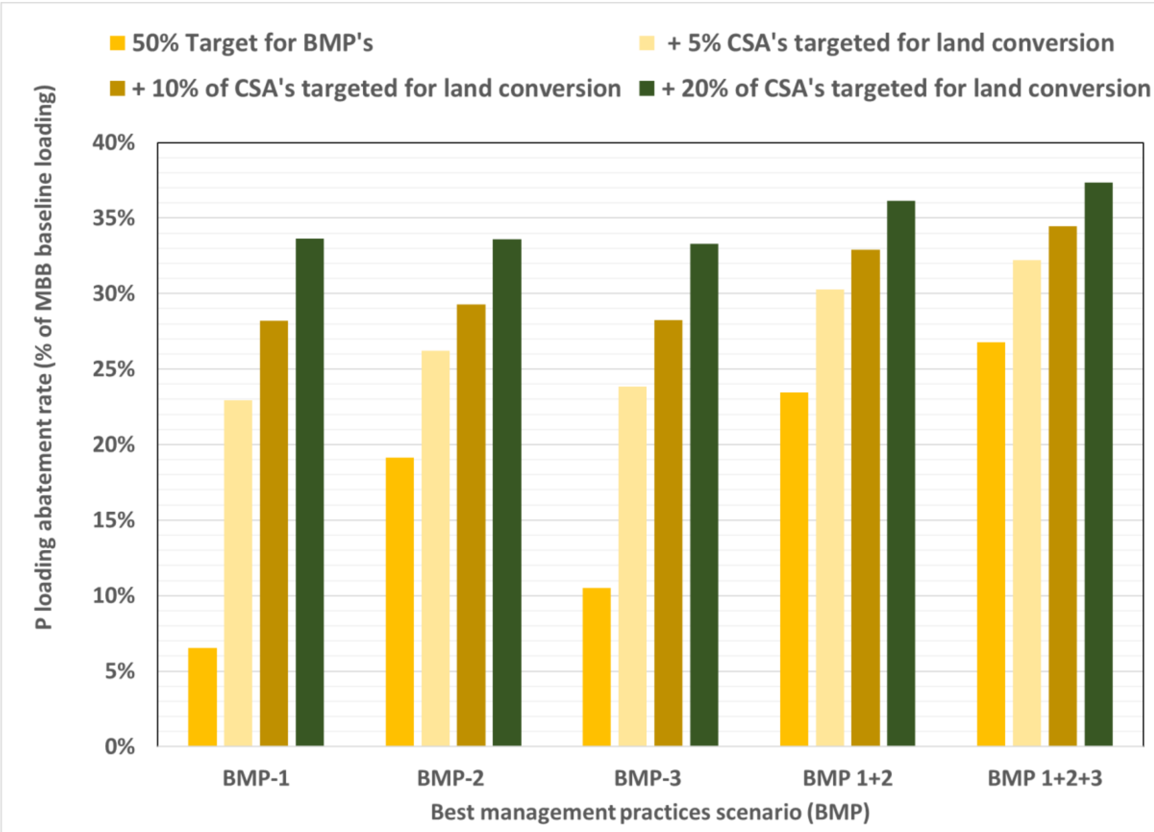

Figure ES2. Projected phosphorus loading abatement rates with respect to Missisquoi Bay watershed baseline loading from a targeted (50% of CSA area) adoption of BMP scenarios, together with an increasing level of land conversion scenarios (0, 5%, 10%, 20%). A 34% abatement rate was systematically applied to residential and urban point sources.

The simulations of the P dynamics in Missisquoi Bay resulting from baseline landscape P loadings and the alterative management scenario loadings simulations demonstrate a substantial P imbalance in the bay with more P coming into the bay from its tributaries relative to what the bay exports (positive P imbalance) at an annual scale (see Figure ES3). As landscape P reduction scenarios are implemented, the magnitude of P imbalance decreases. Dryer years with less riverine loading approach equilibrium under maximum P reduction (P imbalance near zero and inputs similar to outputs). However, higher external loading years with extreme high flow events, even under maximum P reduction, remain well above P balance with substantial accumulation of P in the bay's sediment. In those years, external loads are extremely high and notably high P imbalance persists irrespective of P load reduction simulations. This result highlights the relative importance of large events in impacting the overall system's P budget, as has been demonstrated elsewhere (Vidon et al, 2018), which has substantial relevance to climate change impacts on P imbalance.

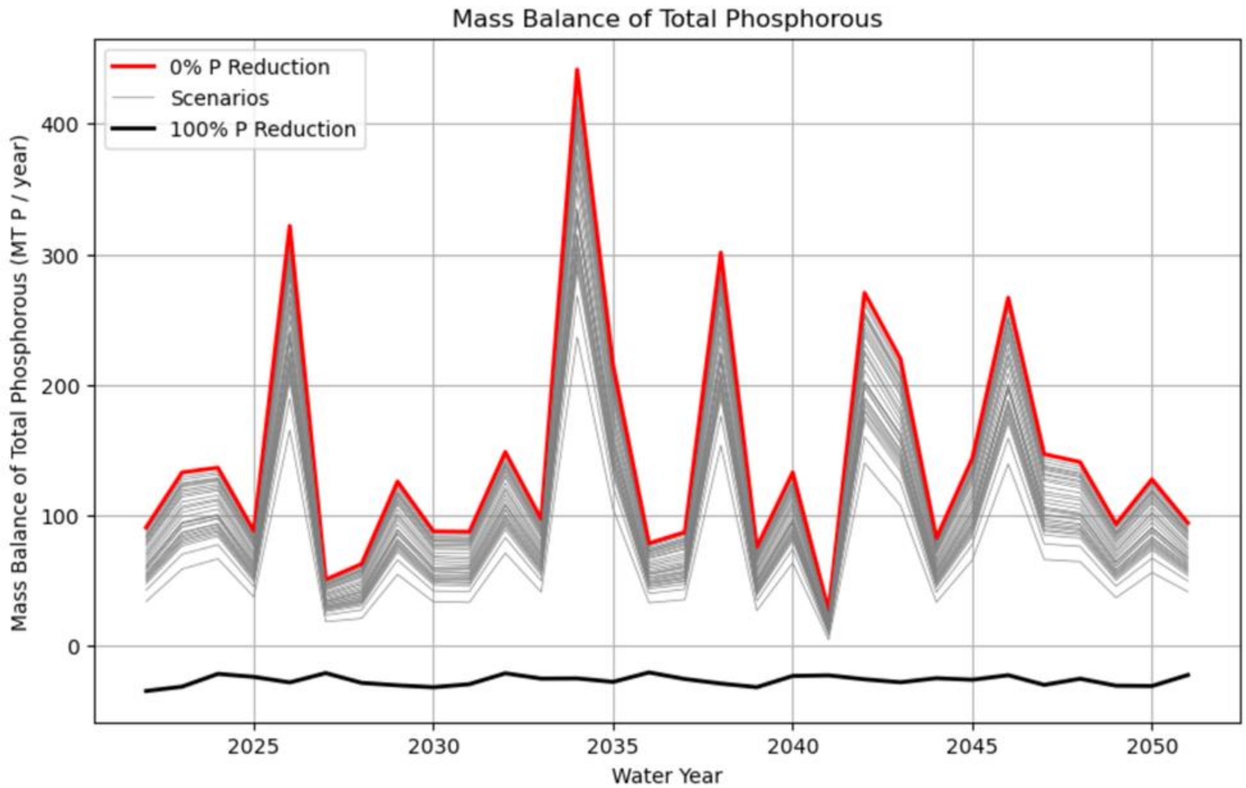

Figure ES3: Bay-wide P mass balance for simulation years (inputs from tributaries-output from the causeway) in metric tons (MT). Positive values indicate that P is accumulating in the bay, whereas negative values indicate scenarios where the bay is becoming depleted in P and zero would be P equilibrium where P inventories would theoretically remain constant. The red line is the baseline scenario. The grey lines are the range of watershed P reduction scenarios implemented. The black line shows results when tributary loading of P is zero and represents annual export of legacy P from the bay's sediment.

Unfortunately, all P reduction scenarios had minimal impact on the number of days that the bay is simulated to have cyanobacteria bloom conditions at a threshold of 20 μg/L or higher bay wide average chlorophyll-a concentrations. Predicted summer chlorophyll-a concentrations under baseline, maximum simulated tributary P loading reduction, and 100% tributary P loading reduction scenarios are shown in Figure ES4 below. Under the largest P reduction scenario, the cyanobacteria bloom duration decreased by only a few days in the summer or up to a week when considering the entire year. This result is due to the persistence of large stores of legacy phosphorus in the bay's sediment that provide P to cyanobacteria under conditions where they naturally thrive (hot and dry portions of the summer). Once initiated, those blooms are often resilient and can persist well into fall. Conversely, watershed tributary P input reductions impact water column P inventories in Missisquoi Bay most during shoulder seasons when conditions are often unfavorable for cyanobacteria dominance (turbid, cool water).

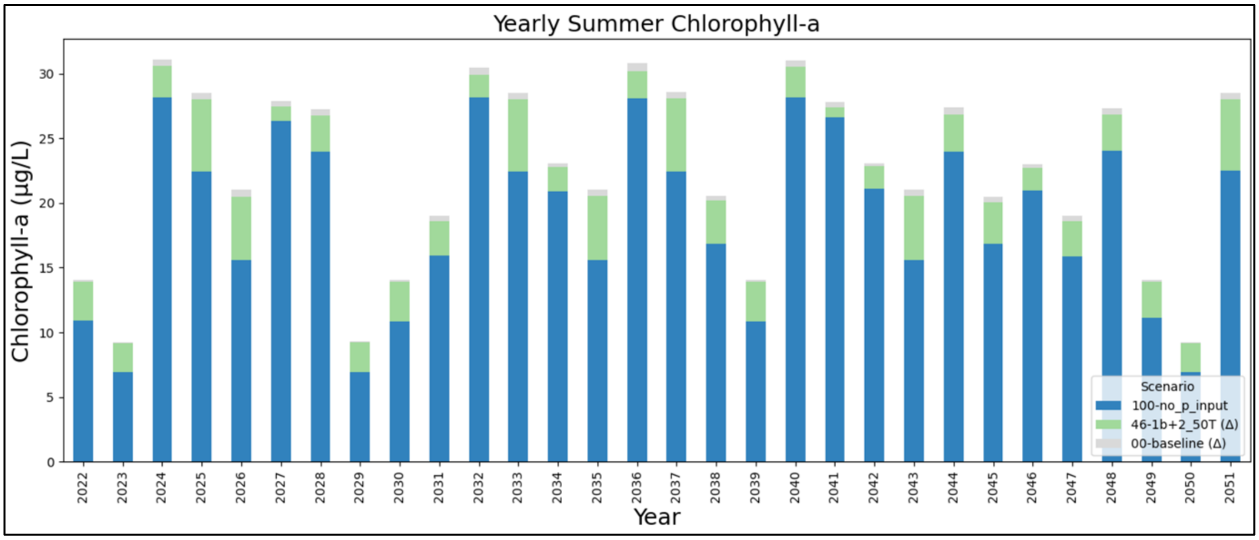

Figure 31: Average annual summer (June through September) chlorophyll-a concentrations in Missisquoi Bay in response to baseline (0% reduction) in gray, maximum achieved reduction in metamodel simulations in green, and no tributary P input in blue.

Given the most optimistic estimates of terrestrial P loading reductions under the alternative management scenarios assessed (average annual P load reduction of 45%), the modeling conducted in this study suggests that summer period P concentrations would average near 36 µg/L (a 29% reduction in concentration from current conditions), resulting in only small reductions in the frequency of cyanobacteria blooms. The modeling predictions of both terrestrial P loads to the Bay under alternative management scenarios and the Missisquoi Bay's response to those load reductions made several conservative assumptions, including constant P inputs and terrestrial P saturation levels in soils over time and constant benthic P concentrations within the Bay's sediment over time. This conservatism suggests that over the next 30 years, both terrestrial P loads and the Bay's P imbalance could be reduced beyond that presented in this report. Nevertheless, it is clear from this project's assessment that the current P imbalance is significant, and that more aggressive and strategic adoption of improved management practices will be necessary to meaningfully close the P mass imbalance gap in Missisquoi Bay. The P Mass Balance Toolkit should serve as a valuable guide in developing and evaluating these strategies.

CONTENTS

Project Summary 3
1. Project Introduction 12
2. Tasks Completed 13
Task 1: Develop a QAPP 13
Task 2: Identify PAC and Conduct Project Startup Meeting 13
Task 3: Quantify Terrestrial P Inventories Throughout the Missisquoi Basin 14
Task 4: Quantify Inventories of P in Missisquoi Bay 15
Task 5: Develop SWAT-Based Terrestrial P-Export Metamodel 15
Task 6: Apply Metamodel to Simulate Bay Mass Balance Input Changes Under Alternative Conditions 16
Task 7: Simulate and Quantify P Fate and Transport Within and From Missisquoi Bay 17
Task 8: Develop the Missisquoi Basin P Mass Balance Assessment Toolkit 17
Task 9: Project Reporting 18
3. Methodology 18
Task 3: Quantify Terrestrial P Inventories Throughout the Missisquoi Basin 18
Task 3a: Quantify Terrestrial P Inventories Throughout the Missisquoi Basin, Quebec 18
Task 3b: Quantify Terrestrial P Inventories Throughout the Missisquoi Basin, Vermont 23
Task 4: Quantify Inventories of P in Missisquoi Bay 32
Sediment Inventories 32
Water Column Inventories 33
Task 5: SWAT-Based Metamodel Development 33
Concepts and Rationale 33
Spatial Structure and Development of MM 43
Rationale 44
Framework 44
Alternate Management Scenarios for Agricultural Land Uses 45
Alternate Management Scenarios for the Point Sources of Urban and Residential Developed Land Uses 46
Composite Scenarios (Multiple BMP Groups Combined) 46
Task 7: Simulate and Quantify P Fate and Transport Within and From Missisquoi Bay 46
Task 8: Develop the Missisquoi Basin P Mass Balance Assessment Toolkit 48
Mass Balance Toolkit Data Sources and Compilation 48
Mass Balance Toolkit Functionality and Development Process 49

Mass Balance Toolkit Technological Infrastructure 49
4. Quality Assurance Tasks Completed 50
Task 3: Quantify Terrestrial P Inventories Throughout the Missisquoi Basin 50
Task 4: Quantify Inventories of P in Missisquoi Bay 50
Task 5: SWAT Metamodel Development 50
Task 6: Simulate Mass Balance Input Changes Under Alternative Conditions 51
Task 7: Simulate and Quantify P Fate and Transport Within and From Missisquoi Bay 52
Task 8: Develop the Missisquoi Basin P Mass Balance Assessment Toolkit 52
5. Deliverables Completed 53
Task 3: Quantify Terrestrial P Inventories Throughout the Missisquoi Basin 53
Task 3a: Quantify Terrestrial P Inventories Throughout the Missisquoi Basin, Quebec 53
Task 3b: Quantify Terrestrial P Inventories Throughout the Missisquoi Basin, Vermont 63
Task 4: Quantify Inventories of P in Missisquoi Bay 69
Redox Sensitive Sediment P Inventory 69
Total Sediment P Inventory 69
Water Column Sediment P Inventory 69
Task 5: SWAT Metamodel Development 70
Model parametrization 70
Geophysical properties 70
Soil and Crop Management 73
P inputs 74
Metamodel Calibration and Validation 77
Spatial Heterogeneity of Metamodel Projections 80
TASK 6: SIMULATE BAY MASS BALANCE INPUT CHANGES UNDER ALTERNATIVE CONDITIONS 84
Agricultural BMPs Simple and Multi-Group Effects 85
Nutrient Management Group Effects (BMP-1) 87
Cropping System Group Effects (BMP-2) 88
Riparian Zone Management (Buffers and Sedimentation Structures, BMP-3) 90
Multi-Group Agricultural BMPs Effects 91
Land Conversion (BMP-4) 92
Residential and Urban Land Uses Point Sources (BMP-5 and BMP-6) 93
Composite Scenarios (Multiple Groups Combined) 94
Task 7: Simulate and Quantify P Fate and Transport within and from Missisquoi Bay 98
Bay-Wide P Mass Balance 98
Seasonal P Imbalance and the Relative Roles of Internal and External Loading 103

Impacts of P Reductions on Cyanobacteria Blooms and Achieving the TMDL Target Concentration 105

Task 8: Develop the Missisquoi Basin P Mass Balance Assessment Toolkit 111

Linear Regression Models for Bay P Mass Balance from Watershed Load Reductions ... 111

Web-Based Toolkit 113

6. Conclusions 123

7. References 125

8. Appendices 134

Appendix 1: Results tables of Terrestrial P Inventories Throughout the Missisquoi Basin, Quebec. 134

Table A1-1: Land Use Distribution within Individual Subwatersheds of Missisquoi bay Basin. 134

Table A1-2: Distribution of Phosphorus Inputs, Crop Uptakes and Balances per Land Use Classes for Individual Subwatersheds (HUC12) of Missisquoi Bay Basin 134

Table A1-3: Area Weighted Mehlich-3 Soil Test Phosphorus, Aluminium and P Saturation per Land Use Classes for Individual Subwatersheds (HUC12) of Missisquoi Bay Basin .. 134

Table A1-4: Soil Phosphorus Saturation Distribution 134

Table A1-5: Wastewater Treatment Plant Characteristics 134

Table A1-6: Population and Estimated Loadings from Septic Systems for Missisquoi Bay Watershed 134

Appendix 2: Results tables of Terrestrial P Inventories Throughout the Missisquoi Basin, Vermont 135

Table A2-1: Agricultural P Inputs by HUC12 and Land Use 135

Table A2-2: Agricultural P Inputs Variability by HUC12 and Land Use 135

Table A2-3: Soil Characteristics by HUC12 and Land Use 135

Table A2-4: Soil Characteristics Variability by HUC12 and Land Use 135

Table A2-5: Wastewater P Effluent Concentrations 135

Table A2-6: Wastewater P Solids 135

Table A2-7: Septic System P Load Estimations 135

Appendix 3: Results tables of Missisquoi Bay P Inventories 135

Table A3-1: Sediment Samples, Ascorbate Extraction 135

Table A3-2: Sediment Samples, Total Digestion 135

Table A3-3: Water Samples, DEC 135

Table A3-4: Water Samples, UVM Platform 135

Table A3-5: Water Samples, UVM Spatial 135

Appendix 4: Metadata of Key Inputs to the Terrestrial Metamodel 135

Appendix 5: Quality Assurance Project Plan..135

1. Project Introduction

This project was a binational collaborative effort between Stone Environmental, Inc. (Stone), the University of Vermont (UVM), Research and Development Institute for the Agri-Environment (IRDA), and Organisme de Bassin Versant de la Baie Missisquoi (OBVBM) to develop a comprehensive, binational phosphorus (P) mass balance model for the Missisquoi Bay watershed. The analysis of this model's results are publicly accessible through a web-based P Mass Balance Assessment Toolkit. The primary goals of the project directly align with recommendations of the International Joint Commission (IJC, 2020) to:

- Compile available data to quantify the distribution of P across the different compartments of the basin-wide system, including imports and exports of P to and from the Canadian and U.S portions of the basin
- Link existing watershed and lake models to quantify the fate and transport of P across the terrestrial and aquatic components of the basin
- Develop a Toolkit for evaluating the impacts of alternative management/conservation practices on the basin-wide P balance and P flux out of Missisquoi Bay

The analysis approach described in this project's approved Workplan and QAPP specified the use of a SWAT-based terrestrial metamodel linked to the AEM3D lake model to quantify the response of the Missisquoi Bay to changes in watershed P loadings. Given the significance of these models in this project's approach to understanding the Missisquoi Bay and watershed P mass balance, the approach followed for the P inventory efforts ensured that the necessary P inputs and storages required by these two models were explicitly compiled at each model's required scales. For terrestrial modeling, this ultimately led to Hydrologic Response Unit (HRU) scale inputs, where HRUs represent unique combinations of land cover/crop, soil characteristics, topographic characteristics, climate inputs, and management practices. Across Vermont and Quebec, approximately 175,000 HRUs were defined, representing a very highly resolved spatial modeling foundation for this assessment.

The project team members had well defined roles and responsibilities throughout the duration of the project from startup in early summer of 2022 through project completion in the summer of 2025. Stone served the project manager role, leading coordination across team members, Lake Champlain Basin Program (LCBP), and the Project Advisory Committee (PAC), contributing to the technical approaches of each task, and providing oversight and review of all project deliverables. Data compilation necessary to conduct the quantitative terrestrial P balance inventory was co-led by UVM and OBVBM/IRDA, with each organization contributing the local knowledge and expertise to understand the available data sources and their limitations necessary to complete this task. UVM also led the compilation of the Bay P inventory, which was required to parameterize the AEM3D model of Missisquoi Bay. The development of the SWAT-based metamodel to cover the entirety of the binational Missisquoi watershed, followed by generating and interpreting metamodel simulations under both current (baseline) and alternative management scenario, was led by OBVBM/IRDA. This significant effort produced some of the most important outputs from this project, which were terrestrial P loading reduction scenarios used as input to the AEM3D model of the Bay. The approach for defining and parameterizing the alternative management scenarios run through the metamodel was a collaborative effort between OBVBM/IRDA and Stone. Quantification of the Bay's response to long-term reductions in P tributary loadings was based on UVM's AEM3D model simulations and results analysis. The terrestrial metamodel inputs and results, linked with the Bay P dynamics model outputs, generated the data necessary to develop the P Mass Balance Assessment Toolkit. Stone led the design and technical development of the Toolkit.

This "Development of a Comprehensive Binational Phosphorus Mass Balance Analysis Toolkit for the Missisquoi Bay Watershed" project contributes to multiple goals, objectives, and strategies outlined in the LCBP's 2022 Opportunities for Action. These goals most directly include:

- Goal 1: Clean Water
    - Objective 1.A: Improve understanding of water quality conditions and trends; determine the effectiveness of past management and inform future management decisions
        - Strategy: I.A.2 – Fund and interpret research on management decisions and best management practices (BMPs)
        - Strategy I.A.3 – Fund and interpret research to better understand nutrient dynamics and limit their impact
- Goal 4: Informed and Involved Public
    - Objective: IV.A – Enhance formal learning at all educational levels
    - Strategy: IV.A.2 – Maintain and expand digital/online tools and resources

This project's outputs include the most comprehensive analysis to date of terrestrial P inputs and storages across both sides of the Missisquoi watershed's international boundary. The calibrated and validated modeling approaches implemented in the project estimate how those P inputs and storages translate to tributary P loading to the Bay and how the Bay's P mass balance is projected to respond to these long-term changes in P loadings. Details of the project tasks, methodology, quality assurance performed, and results and deliverables are provided in the sections that follow.

2. Tasks Completed

Task 1: Develop a QAPP

A secondary data and modeling Quality Assurance Project Plan (QAPP) was developed to guide this project. Key components to the QAPP included identification of data sources, intended uses of these existing data, limitations of existing data, the development of the SWAT-based metamodel, integration with the AEM3D Missisquoi Bay model, and development of the P Mass Balance Toolkit. In addition, this project relied upon previously initiated work conducted for the LCBP, which had its own associated QAPP, namely for the project entitled "Evaluating Alternatives to Control Internal Phosphorus Loading in Missisquoi Bay Using a 3-Dimensional Coupled Hydrodynamic-Aquatic Ecosystem Model". The final QAPP was approved and signed on 7/12/2022.

Task 2: Identify PAC and Conduct Project Startup Meeting

A project advisory committee (PAC) was formed and consisted of US and Quebec scientists and stakeholders. The PAC included the following members:

- Quebec-based
  - Pierre Leduc, President, OBVBM
  - Urbain Swennen, Agricultural Producer, UPA Local Delegate and OBVBM Administrator
  - Daniel Tremblay, Env. Dept (MELCC, Qc)
  - Carl Bélec, Science and Technology Branch, Agriculture and Agri-Food Canada
- US-based
  - Marli Rupe, Agricultural Water Quality Section Chief, VT DEC
  - Karen Bates, Tactical Basin Planner
  - Kent Henderson, DVM, Friends of Northern Lake Champlain
  - Judson Peck, Water Quality Program Coordinator, VAAFM
  - Matthew Vaughan, Ph.D., Project Officer, LCBP

The first PAC meeting was held on 5/20/2022. The meeting focused on review of the approved workplan and discussion on data to be collected throughout Task 3 (Quantify Terrestrial P Inventories Throughout the Missisquoi Basin). Feedback from the PAC during this meeting helped guide the compilation and analysis methods for P inventory data.

The second PAC meeting was held on 11/29/23, when the results of Task 3 (Quantify Terrestrial P Inventories Throughout the Missisquoi Basin), Task 4 (Quantify Inventories of P in Missisquoi Bay), and Task 5 (Develop SWAT-Based Terrestrial P-Export Metamodel) were presented and discussed. In addition, the committee discussed potential strategies for developing alternative scenarios to be considered in Task 6 (Apply Metamodel to Simulate Bay Mass Balance Input Changes Under Alternative Conditions). The discussion provided guidance for the approach used to construct alternative scenarios for simulation with the metamodel.

The third and final PAC meeting was held on 2/25/25. Topics included presentation and discussion of the results of Task 6 (Apply Metamodel to Simulate Bay Mass Balance Input Changes Under Alternative Conditions), discussion of preliminary results from Task 7 (Simulate and Quantify P Fate and Transport Within and From Missisquoi Bay), and a live demonstration of a Beta version of Task 8 (P Mass Balance Assessment Toolkit web application). Feedback provided technical insights concerning the results obtained from the metamodel alternative scenario analysis and helped in guiding further development of the Toolkit.

Task 3: Quantify Terrestrial P Inventories Throughout the Missisquoi Basin

The goal of this task was to develop a compartmentalized P inventory for the entire basin that supported Objective 1 of this project: Compile Available Data to Quantify the Distribution of P Across the Different Compartments of the Basin-Wide System.

A key outcome from Task 3 included the foundational data that would be used as inputs to the SWAT-based metamodel used to quantify terrestrial P loadings to the Bay. While the differences in data availability and data sources between Quebec and Vermont necessitated this task be completed for each respective county independently, the end results were consistent in terms of the quantified data elements. These elements included:

- Land cover layer for the Missisquoi Basin
- Agricultural land typology needed for the spatial estimation of P flows and soil metrics
- Manure application characteristics

- Estimated P flows (manure, fertilizer, crop harvest)
- Partial P mass balance for agricultural land
- Predicted soil metrics by HUC12 and agricultural land use
- Estimated P loads from wastewater systems
- Estimated P loading assumptions for non-agricultural land use

The deliverables from Task 3 included the detailed data compilation and analysis methodology as presented in Section 3 (Methodology) and the results and deliverables presented in Section 5 (Deliverables Completed). In addition, detailed tables in Excel format were compiled as primary deliverables describing land use distribution, agricultural P inputs, soil P concentrations and P saturation levels, municipal wastewater flows and concentrations, and decentralized (septic system) P loads at the HUC12 sub-watershed scale for the Vermont and Quebec portions of the basin.

TASK 4: QUANTIFY INVENTORIES OF P IN MISSISQUOI BAY

The goal of this task was to compile many years of water column monitoring data from an assortment of studies to provide the best estimate of the current inventory of P in Missisquoi Bay and its sediment, resulting in the comprehensive and up-to-date integrated dataset of bay-wide phosphorus inventories. This task also supported Objective 1 of this project: Compile Available Data to Quantify the Distribution of P Across the Different Compartments of the Basin-Wide System.

The resulting datasets compiled in Task 4 were used as the basis to calibrate and validate the AEM3D model. Quantities compiled for the Bay P inventory included:

- Redox sensitive sediment P mass at the top 1 cm and top 10 cm
- Total sediment P mass at the top 1 cm and top 10 cm
- Water column P mass as soluble reactive O, dissolved P, and total P

Deliverables from Task 4 included the detailed data compilation and analysis methodology as presented in Section 3 (Methodology) and the results and deliverables presented in Section 5 (Deliverables Completed). In addition, detailed tables in Excel format were compiled as primary deliverables that included detailed sample-level data for sediment and water column P values used to characterize the Bay-wide P inventory and derive inputs to the AEM3D model.

TASK 5: DEVELOP SWAT-BASED TERRESTRIAL P-EXPORT METAMODEL

The goal of this task was to develop a metamodel, derived from the physically-based SWAT model simulations, to allow simplified simulations of the impacts of a broad range of alternative land management/conservation practice assumptions on the terrestrial P balance and exports to the Bay. This task also supported Objective 2 of this project: Apply Watershed and Lake Models to Quantify the Fate and Transport of P Across the Terrestrial and Aquatic Components of the Basin and Bay.

The metamodel was expanded from the P-EDIT modeling approach developed by IRDA (Michaud et al., 2008, 2018; Drouin et al., 2014) to enable simulation of the entire Vermont and Quebec portions of the Missisquoi Bay watershed. This required analysis of the terrestrial P inventory data compiled in Task 3 to generate Hydrologic Response Unit (HRU) level metamodel inputs. The key outcomes from the metamodel task completion included:

- A geodatabase composed of data layers containing P inputs, P stores, soil properties, topographic parameters, and agronomic management information for 99,673 HRUs in Quebec and 77,205 HRUs in Vermont
- An ArcGIS-based Python script that automates running the metamodel for Quebec and Vermont based on the HRU-level inputs compiled for current (baseline) conditions within the watershed
- HRU-level metamodel outputs based upon the baseline conditions
- Validation of the modeling approach based on available tributary monitoring data

Deliverables from Task 5 included the detailed data compilation and analysis methodology as presented in Section 3 (Methodology) and the results and deliverables presented in Section 5 (Deliverables Completed). In addition, a geodatabase was provided that contained the spatial HRU delineations and all input parameters required to run metamodel simulations and the metamodel Python code itself.

Task 6: Apply Metamodel to Simulate Bay Mass Balance Input Changes Under Alternative Conditions

The goal of this task was to generate alternative tributary P loading scenarios by modifying the input assumptions of the baseline scenario to reflect a range of potential P management behavior modifications throughout the watershed. This task also supported Objective 2 of this project: Apply Watershed and Lake Models to Quantify the Fate and Transport of P Across the Terrestrial and Aquatic Components of the Basin and Bay.

The key outcome from this task was an ensemble of Bay input P load changes from baseline, allowing the quantification of a probability distribution of baseline Bay input percent changes used to adjust the observed P loads from the Missisquoi, Pike, and Rock rivers. In total, 90 alternative P management scenarios and subsequent metamodel simulations were generated for the entire Missisquoi Bay watershed, which included modification to the following:

- Agricultural Land Use BMPs:
  - Nutrient Management (modification of manure application method and timing)
  - Cropping System Erosion Management (cover crops and modification to no till/conservation tillage)
  - Riparian Zone Management (buffers and sediment basins)
  - Land Conversion (conversion of most cultivated land to permanent grass meadow)
- Agricultural Land Use Implementation/Adoption Strategies
  - 20% Random, 20% Targeted
  - 50% Random, 50% Targeted
  - 100%
- Developed Land Uses
  - Residential Decentralized Wastewater P Reduction
  - Urban Centralized Wastewater Effluent P Reduction

The deliverables from Task 6 included the detailed data compilation and analysis methodology as presented in Section 3 (Methodology) and the results and deliverables presented in Section 5 (Deliverables Completed). In addition, tables of HUC12-level metamodel results from each of the 90 alternative scenarios quantifying the P load reductions from baseline conditions were compiled, ultimately providing the necessary tributary P load inputs for Task 7.

Task 7: Simulate and Quantify P Fate and Transport Within and From Missisquoi Bay

The goal of this task was to generate long-term (30-year) simulations of the Bay P mass balance under baseline conditions as well as under a range of alternative tributary P loading scenarios defined from the metamodel simulations. This task also supported Objective 2 of this project: Apply Watershed and Lake Models to Quantify the Fate and Transport of P Across the Terrestrial and Aquatic Components of the Basin and Bay.

The key outcomes from this task were the results from the 31 AEM3D model simulations (baseline and a sub-sample of 30 alternative scenarios) which allowed for quantification of:

- Relative contribution of watershed vs. lake sediment sources to the Bays' overall water column inventory of P
- An assessment of the flux of P from the bay through the Rte. 78 causeway
- Analysis of how P fluxes are partitioned seasonally and inter-annual variability
- Quantification of major P mass balance elements for integration in the Toolkit, including:
    - Long-term (30-year) P mass balance
    - Water column P concentrations
    - Estimated cyanobacteria bloom days

The deliverables from Task 7 included the detailed data compilation and analysis methodology as presented in Section 3 (Methodology) and the results and deliverables presented in Section 5 (Deliverables Completed). In addition, AEM3D model outputs for the baseline and 30 alternative scenarios were compiled in tables and used as inputs to the P Mass Balance Assessment Toolkit.

Task 8: Develop the Missisquoi Basin P Mass Balance Assessment Toolkit

The goal of this task was to develop a web-based stakeholder accessible application where core conclusions around the state of the basin's P mass balance/imbalance can be understood, and the relative impacts of different P management options can be assessed. The resulting Toolkit enables stakeholders to quantitatively assess the long-term P-balance throughout the Missisquoi watershed and Bay based on baseline conditions in comparison to alternative future scenarios for the watershed. This task also supported Objective 3 of this project: Develop a Toolset for Stakeholders to Evaluate Impacts of Adopting Alternative Management/Conservation Practices on the Binational P Balance.

The key outcome from this task was the publicly accessible P Mass Balance Assessment Toolkit that allows stakeholders to:

- Evaluate the impacts of P management alternatives at the HUC12 and full watershed scale, considering:
    - Total P load (mass/time)
    - Total P yield (mass/area-time)
    - Change in P load/yield from baseline
- Construct their own alternative P management scenario, for the entire watershed by individual HUC12, based on:
    - Residential wastewater improvement
    - BMP implementation strategy
    - Agricultural BMPs implemented

  - Land conversion rate
- Evaluate the impacts of reductions in watershed P loadings on the P mass balance, P concentrations, and days of cyanobacteria blooms in Missisquoi Bay

Deliverables from Task 7 included the detailed data compilation and analysis methodology as presented in Section 3 (Methodology) and the results and deliverables presented in Section 5 (Deliverables Completed). The P Mass Balance Assessment Toolkit is available at: https://www.stone-env.net/mass_balance/.

TASK 9: PROJECT REPORTING

The project reporting task has included quarterly annual progress reports over the project's duration, as well as this Final Report.

3. METHODOLOGY

TASK 3: QUANTIFY TERRESTRIAL P INVENTORIES THROUGHOUT THE MISSISQUOI BASIN

Task 3a: Quantify Terrestrial P Inventories Throughout the Missisquoi Basin, Quebec

This section presents the compartmentalized P inventory for the Quebec portion of the Missisquoi Bay (MB) basin, as specified under Task 3a of the project work plan. This inventory is a determinant input to parameterization of the Terrestrial P-Export metamodel (MM), a principal deliverable of the project. To predict P export to surface waters and P storage within the basin landscape, the MM requires a detailed spatial portrait of the physical characteristics of the basin, together with its land use and management. Critical components of the P mass balance requiring quantification for MM simulations include the timing and amount of P applied as manure or other organic inputs, as well as mineral fertilizer.

Data for the non-agricultural inputs have been collected for the Quebec portion of the Missisquoi Basin by OBVBM. Conceptually, the urban land use polygons of the project geographic information system (GIS) have been delineated according to the presence of centralized water treatment systems. Data collected for individual treatment units include information on types of water treatment, retention time, population, daily flow conception criteria, P concentrations, and loadings of emissions. The stormwater overflows have also been described in terms of number of structures, annual discharges, P concentration, and annual P loadings of stormwater. Developed/residential land use has been delineated into high density and low density residential areas based on population census. Data have also been collected on the number of decentralized (septic) systems and P loadings have been estimated from the population census and loadings.

The inventory of P sources from the agricultural, residential, and urban sectors in Quebec meets the needs for the comprehensive modeling of terrestrial phosphorus emissions to surface waters of the Missisquoi Bay basin (MBB).

Land Use Layer

The final Vermont/Quebec land use classification consists of 15 different land use classes, including three developed classes and seven agricultural classes. Land use typology for the agricultural sector in Quebec was developed from the *Banque de données des cultures assurées (BDPPAD)* from the crop insurance board *La Financière agricole du Québec* (FAQ) for the reference year 2021. The BDPPAD polygons cover most of the cropped area of the Quebec sector of MBB. The land use classification for the area not covered by the BDPPAD (uninsured cropped area) has been supported by the map units of the *Carte écoforestière* from the *Ministère de l'Énergie et des ressources naturelles* (MERN, 2021b), which includes a generic agricultural land layer. The final classification of agricultural seven land use classes for the 9176 management units of MBB were aggregated as follows.

- Grain corn (corn stalks non harvested)
- Silage corn (corn stalks harvested)
- Soybean
- Small grain (generic), including all straw cereals, together with canola and leguminous annuals
- Hay (generic), including variable compositions of perennial legumes and grasses
- Pasture and Meadows, refer to generic agricultural land from Carte Écoforestière, which is not included within BDPPAD polygons. For Quebec, where pastures are not abundant, this land use class mostly includes grass dominant natural prairies and were not attributed organic or mineral fertilization
- Other agricultural (generic), which includes fruit and vegetable production, or crop production that is not insurable

The developed land use classes were defined and mapped as follows:

- The urban land use class includes all developed areas served by centralized sanitary systems (OBVBM, 2021)
- Developed, residential high density includes urban cores which are not connected to centralized sanitary systems and present relatively high population density
- Developed, residential low density includes residential areas with a relatively low population density
- Paved roads have been edited as polygons from the linear road vectors of the *Base de données topographiques du Québec* (MERN, 2021b)
- Unpaved roads polygons followed the same procedure

The undeveloped land use typology was defined as follows:

- Forest land use class (generic) that includes all deciduous and coniferous trees map units described within the *Carte écoforestière* (MERN, 2021)
- Brush, unmanaged agricultural land use that includes an extensive selection of land use mapped by MERN (2021) that have been disturbed by human activity, including hydro lines, fallows, or gravel pits
- Wetland land use derived from MERN (2021) that includes various types of wetlands, flooded sites and unregenerated exogenous sites
- Water land use class polygons obtained from MERN (2021)

Because different sources of land use polygons were merged for the overall classification of MBB area, topologic problems must be addressed. Orphan polygons, typically “spaghetti” shaped, resulted principally from the merging of BDPPAD and *Carte Écoforestière.* This issue was related to different polygon geometries and was rectified by smoothing polygon boundaries, merging orphan and spaghetti polygons into larger adjacent polygons, and establishing a minimum polygon area of 2 ha for the agricultural management units. The final land use layer includes 99,671 polygons for the MBB in Quebec. We have described map units and land use statistics within section 5.0.

Phosphorus Inputs to Cropland and Mass Balance

The principal source of phosphorus inputs data for the agricultural land use in Quebec was the phosphorus reports census, which is updated yearly by the *Ministère de l'Environnement, Lutte contre les changements climatiques, Faune et Parcs* (MELCCFP), for 2021. The information contained in the Phosphorus Report is used in applying environmental cross-compliance as a measure of eligibility for certain programs by the Financière agricole du Québec (FAQ) and the *Ministère de l'Agriculture, des Pêcheries et de l'Alimentation* (MAPAQ). Phosphorus reports estimating organic and mineral phosphorus production, imports and exports are mandatory in Quebec for every farm with animal production under liquid manure management or that generates over 1,600 kg P_2O_5 annually. The mandatory census also applies to farms cropping over 15 ha of annual cash crops, or over 5 ha of horticultural and fruit crops. The information is compiled by certified agronomists, while issuing the agri-environmental nutrient management of individual farms.

A total of 313 phosphorus reports (MELCCFP, 2021a) from agricultural production sites are documented for the crop year 2021 for the MBB. The data, geopositioned to the individual production units, include the following yearly information for the individual agricultural production sites:

- Manure P production (kg P_2O_5)
- Imported manure P (kg P_2O_5)
- Exported manure P (kg P_2O_5)
- Manure P applied (kg P_2O_5)
- Residual matter P applied (kg P_2O_5)
- Mineral P applied (kg P_2O_5)
- Annual crop area (ha)
- Hay and pasture area (ha)
- Fruits and horticulture area (ha)
- Crop area below 7.6% P saturation (ha)
- Crop area 7.6-13.1% P saturation (ha)
- Crop area 13.1-20% P saturation (ha)
- Crop area over 20% P saturation (ha)

To project P emissions to surface waters and P storage within the basin landscape, the mass balance metamodel developed for the study area requires a detailed spatial portrait of the P inputs and soil P status, expressed at field scale. The P budget data (n=313) from phosphorus reports for individual farm centroids thus must be projected at field scale to individual, fertilized field unit polygons (n=9,100). Organic and mineral P inputs were not attributed to the pasture/meadow land use units. The method of distributing P inputs from farm unit centroids to agricultural field polygons followed a three-step approach:

First, global P mass balance and soil P saturation distribution were generated for each municipality (n=18) from the MBB based on the extraction of centroid data from individual animal and crop production units and land use statistics.

As a second step, mineral and organic mass inputs were distributed to individual crop classes (grain corn, silage corn, small grains, soy, hay) within each municipality and further distributed into distinct periods of manuring (spring, summer, and early and late fall), reflecting local nutrient management plans. Seasonal organic P inputs to individual crop classes were allocated assuming 45%, 25%, 20%, and 10%, respectively, of global manure P inputs are applied during spring (corn, small grains), summer (hay and small grains), early fall (soybean) and late fall (grain corn).

As a third step, P input rates and periods, as well as soil P saturation levels were allocated to individual field management units (MGU polygons). This allocation procedure, from farm centroids to field polygons, relied on the robust assumptions that fields with relatively higher P levels are associated with historically higher P inputs, and that P-rich fields tend to be closer to animal production sites. Following a spatial request procedure, individual field polygons (MGU units) were ranked (decreasing order) against the manure P input of their nearest farm centroid. The distribution of soil P saturation estimated for the overall municipality was subsequently attributed to individual field polygons, based on the proximity of farm with elevated inputs of manure P. In short, acreages with elevated soil P saturation were primarily attributed to field polygons close to farm centroids showing highest P mass inputs. Manure P inputs distribution to individual field polygons followed the same order of attribution as for the P saturation level, based on farm centroid locations and respective P mass balance. P input specific rates were limited to 85 kg P_2O_5/ha, considering typical N:P ratios of manure production (dominantly liquid) and target N levels for crops.

The global mineral P inputs estimated for individual municipalities were distributed to field polygons which were not attributed manure P inputs. Constant specific rates of mineral P input were attributed to individual municipalities' cropland, given by the ratio of total mineral P input to the municipality from MELCCFP census to the crop acreages without manure.

Phosphorus mass balances for individual cropland polygons were derived from the difference between estimated total P mass inputs (organic and mineral) and estimated crop P uptakes. Phosphorus uptakes were estimated using 10-year crop yield averages from local municipalities of MBB (FAQ, 2021) and generic crop P uptake rates from fertilizer management guide edited by CRAAQ (2010).

Table 1 presents the reference data used to document P uptakes for individual classes of agricultural land use. Small grain and other agricultural production classes were attributed generic uptake values, estimated from mean P uptakes data for barley and wheat categories.

Table 1. Crop yields and specific P uptake (harvested) per crop type.

	Harvested Crop Yield, T/ha Dry Weight Basis [1]									
Municipality	**Silage Corn**	**Grain Corn**	**Soybean**	**Hay [3]**	**Barley**	**Oats**	**Wheat**	**Rye**	**Canola**	**Small Grain (generic) [4]**
Farnham	18.20	8.70	2.90	7.00	2.7	2.10	2.70	2.60	1.60	
Sainte-Sabine	18.20	8.70	2.90	7.00	2.7	2.10	2.70	2.60	1.60	
Saint-Alexandre	17.60	10.10	3.20	7.60	3.3	1.50	3.40	2.60	1.60	

	Harvested Crop Yield, T/ha Dry Weight Basis [1]									
Municipality	**Silage Corn**	**Grain Corn**	**Soybean**	**Hay [3]**	**Barley**	**Oats**	**Wheat**	**Rye**	**Canola**	**Small Grain (generic) [4]**
Pike River	17.30	10.10	3.30	7.30	2.9	2.20	3.40	2.60	1.60	
Bedford	15.60	8.70	2.90	7.10	1.2	1.80	2.50	2.60	1.60	
Frelighsburg	15.60	8.70	2.90	6.70	1.2	1.80	2.50	2.60	1.60	
Saint-Armand	17.30	8.70	2.90	7.30	2.9	2.20	3.40	2.60	1.60	
MBB Average crop yield (harvested) T/ha	17.11	9.10	3.00	7.14	2.41	1.96	2.94	2.60	1.60	
Specific P uptake (harvest) kg P_2O_5/T (Dry weight) [2]	5.00	7.30	14.90	7.25	7.25	10.80	10.20	8.50	19.00	8.73
Total P uptake (harvest) kg P_2O_5/ha (Dry weight)	85.57	66.43	44.70	51.79	17.50	21.14	30.02	22.10	30.40	23.76

[1] La Financière Agricole du Québec (2021), Average crop yields 2012-2020; straws left on field

[2] CRAAQ, 2010. Guide de référence en fertilisation, 2e édition.

[3] Average for 2nd cut, 40% leguminous (50%) and grasses (50%)

[4] Mean of barley and wheat category data. Uptake rate also applied to "Other agricultural" land use class.

Projections of organic inputs and mineral inputs, together with crop uptakes and P mass balance were finally cumulated at MGU scale to give a detailed portrait of P input and soil stock across the MBB, which reflect contrasting local gradients in animal density and manure imports, legacy soil P, and cropping systems. Field-scale P stock and inputs data were further aggregated at subwatershed (HUC12) scale to present a hydrologically coherent perspective of agricultural P mass inventory for the MBB.

Soil P and Physical Properties Metrics

The soil P levels of MBB cropped land were derived from the farm phosphorus reports from MELCCFP (2021a), where soil P status of cropland acreages are documented according to their soil P saturation. The latter expressed the ratio between extractable P to Al through the Mehlich-III soil test and is used as the agri-environmental indicator in Quebec in compliance with regulations for agricultural operations (REA; MELCCFP, 2020). Soil P saturation within farm phosphorus reports is expressed in four categories: below 7.6%, from 7.6 to 13.1%, from 13.1 to 20%, and over 20% P saturation. The saturation levels of 7.6% P/Al and 13.1% P/Al represent respectively the agri-environmental thresholds for clayey and sandy soils within Quebec's regulations. The median values of soil P saturation classes have been selected to document the individual P status of cropland polygons. A 22.75% soil P saturation level was arbitrarily attributed to cropland with a P/Al saturation class over 20%.

The spatial allocation of soil P saturation levels to individual cropland polygons of MBB followed the procedure expressed earlier for the P inputs distribution. Following a ranking procedure, cropland polygons near farm units (centroids) with the highest documented P loadings were attributed to the highest soil P saturation levels. For each individual municipality, the attribution of soil saturation classes to cropland polygons matched the surface area distribution of soil P saturation classes. Median soil P saturation levels for cropland polygons were further expressed in Mehlich-III extractable units (mg/kg), where:

*Mehlich-III P (ug/kg) = Mehlich-III Al (ug/kg) * P saturation ratio (%)*

Extractible soil Al levels for individual cropland polygons were obtained from the hydro-pedological data bank from IRDA (2017), which document Al levels for individual sol map units of the MBB. For municipalities within the MBB where soil P saturation data from farm phosphorus reports were not available, generic soil P saturation and Mehlich-III soil P levels were obtained from municipal averages of soil text values documented by Beaudet et al. (2009).

The natural inherent total P content of individual soil map units of MBB were also documented from IRDA (2017) hydro-pedological database. The database documents total native P in dominant soil series for the MBB watershed, determined through total-P extraction procedure from subsoil (B horizon) samples. Soil series that did not have analytical results had their native soil P levels attributed using mean values of total natural P by texture classification, as compiled from the analysis of soils B horizons from 158 soil series in Quebec (Michaud et al., 2008).

Complementary soil physical properties of soil map units of the MBB were also documented from the IRDA (2017) hydro-pedological database. Hydrologic soil group, surface soil texture (clay, silt, sand %) and soil erodibility factors were included as attributes to the soil map unit polygons of MBB, as they are determinant inputs to the metamodel algorithms for runoff and erosion rates projections. Slope gradients and lengths of individual field polygons, estimated through the metamodel spatial algorithms, complete the soil physico-chemical properties inventory used as inputs to runoff, sediment, and P emissions estimates by the metamodel.

Residential and Urban Human P Sources

Phosphorus inventory data from residential and urban land use within the Quebec part of MBB include P loadings related to wastewater treatment plants, sewage overflows, and autonomous septic systems. Most of these data have been compiled by OBVBM (2015, 2017, 2021), through their update of MBB Master Water Plan (*Plan directeur de l'eau*). A detailed description of these P fluxes within MBB is presented in section 5.0.

Task 3b: Quantify Terrestrial P Inventories Throughout the Missisquoi Basin, Vermont

For Task 3b, we constructed an inventory of data to estimate agricultural land partial P mass balance, soil P metrics, P loading rates for non-agricultural land uses, and additional terrestrial P sources (e.g., wastewater) for the Vermont portion of the Missisquoi Bay Basin (MBB-VT) in northwestern Vermont, USA. This work has been published in Bondeson et al. (2024).

Given the importance of agricultural land use for P dynamics in the MBB-VT, we invested substantial effort in determining and executing an optimized method to estimate P mass balance components for agricultural lands given the data available. See Figure 1 below for the final method used. We first created a spatial layer of land cover within the MBB-VT and then leveraged field-level data from publicly available nutrient management plans (NMP) for ten dairy farms operating within the MBB-VT, including 1422 fields that collectively accounted for ~21% of the agricultural land area in the MBB-VT. Next, we identified parameters available for the entire watershed (e.g., field slope, soil clay percentage) to characterize all field polygons. We tested the use of pairs of these parameters in k-means clustering to establish a typology for agricultural land (including hay and corn) in the watershed, and selected a final typology based on which parameter pair resulted in clusters of fields having meaningful differences for key P parameters (modified Morgan P, modified Morgan Al, and P saturation ratio). Finally, we extrapolated known nutrient management and soil test data to hay and corn fields across the entire watershed based on the agricultural land typology, used available soil test data to fill gaps for soybeans, “other agriculture”, and pasture, and completed inventories of partial P mass balance and soil P metrics for the MBB-VT by HUC12 watershed and land use.

We provide more details on our methodology and results for agricultural land, as well as other terrestrial P sources, in the sections below.

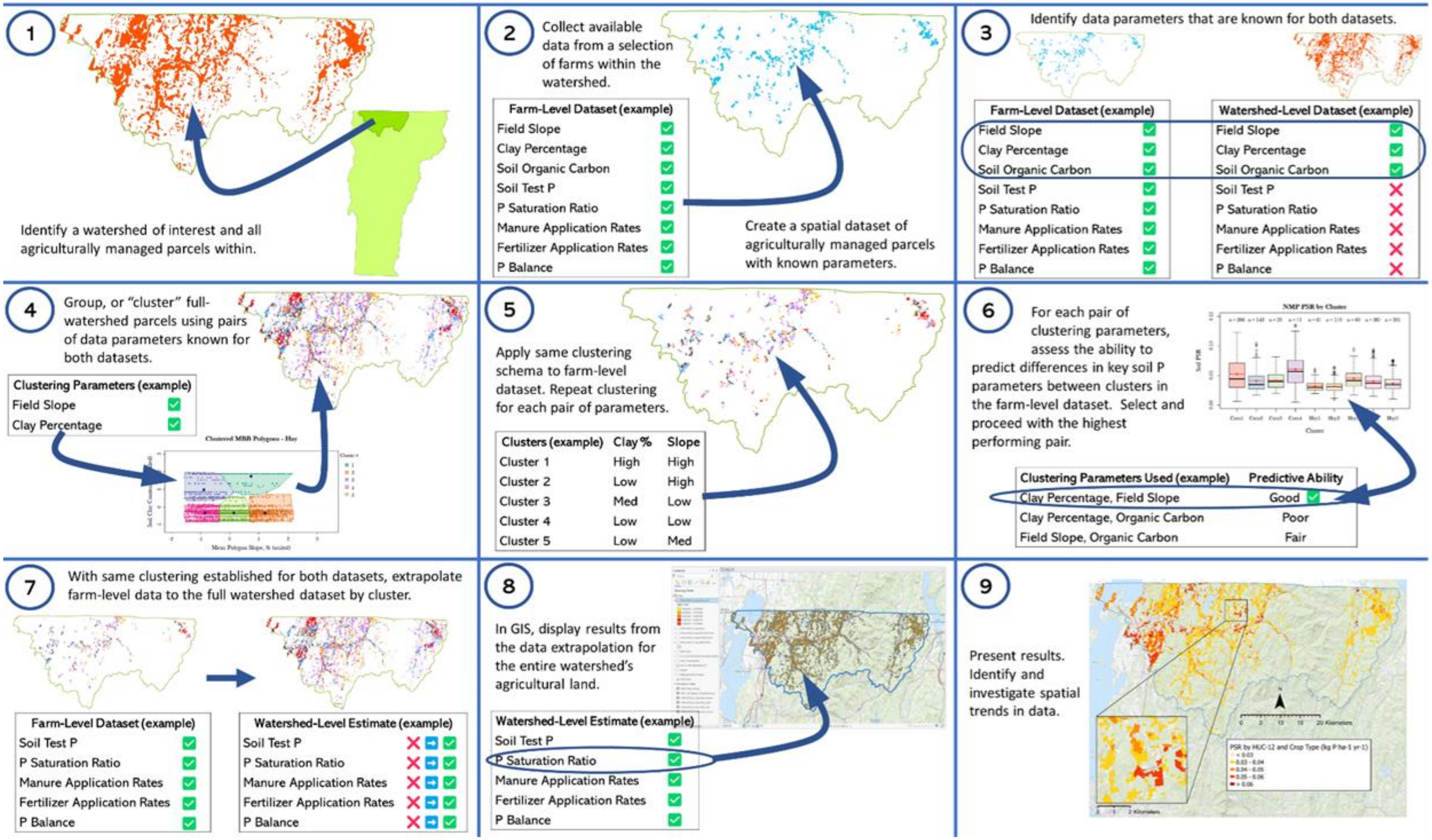

Figure 1. Methodology to extrapolate farm-level nutrient management and soil test data to cropland at the watershed scale for the Vermont portion of the MBB-VT (Bondeson et al., 2024).

Land Use Layer

We created a vector layer for the MBB-VT representing the distribution of land cover types. The base dataset for our land cover layer was a 0.5 m resolution raster sourced from the VCGI's Open Geodata Portal (VCGI, 2016). This high-resolution land cover dataset portrayed cover classification based on 2016 imagery, and included some, but not all, of the land classifications necessary for our output layer. The 2016 land cover layer contained a supplemental vector dataset for agricultural land, characterized by three land use types: pasture, hay, and crops. Due to the dominance of silage corn in our watershed (USDA NASS, 2017), and the lack of available data to distinguish silage from grain corn in the MBB-VT, we first assumed all land categorized as "crops" by the VCGI to be silage corn. Next, to identify areas of agricultural land as "soybean" or "other ag", we sourced 2016 raster data at a 30 m resolution from the USDA Cropland Data Layer (CDL) (USDA NASS, 2016). We compared the CDL with the VCGI supplemental agricultural land layer across the watershed and incorporated any areas classified as "soybean" or "other ag" in the CDL that were greater than one contiguous acre and within the extent of the 2016 VCGI supplemental agricultural land use layer. We then used a vector dataset of common land units, or CLUs (Winchell et al., 2011), to segment the 2016 VCGI supplemental agricultural land cover layer into fields.

For wetland land cover, we used the supplemental vector layer of wetlands available from the VCGI containing classifications for emergent, scrub-shrub, and forested wetlands. If an area classified as a forested wetland in the supplemental layer overlapped with the forest land cover type in the base raster, we assigned it the "forest" land cover type in the output layer. We re-classified emergent and scrub-scrub wetlands as "wetland" in the output layer.

To identify urban areas, we first sourced vector data from the VCGI of all areas within the MBB served by centralized wastewater treatment facilities (WWTPs). All areas within the WWTP polygons which had been classified as "buildings, "other paved surfaces", or "bare earth" were given the "urban" classification for our final layer.

To identify developed/residential areas, we created 100-meter buffers around all areas classified as "buildings" in the original VCGI base land use layer. We assigned all areas within the 100 m buffer which had been classified as "buildings, "other paved surfaces", or "bare earth" in the VCGI base layer to the "developed/residential, low density" classification for our final layer. Additionally, we obtained a vector dataset of farmsteads, or areas identified as central agricultural production areas, in the 2011 CSA analysis (Winchell et al., 2011). We designated farmsteads as either medium ("developed/residential, high density" classification) or small ("developed/residential, low density" classification).

We crosschecked the land cover types herein described (agricultural land, urban, and developed/residential) to ensure that there were no overlaps. In cases of overlap, agricultural land took precedence, and we trimmed the other layer to the agricultural land boundary. All gaps were filled in with the brush/unmanaged classification. Because the VCGI base layer did not differentiate between paved and dirt roads, we used the vector dataset of classified roads used in the 2011 CSA analysis (Winchell et al., 2011). We "burned" these into our land use layer, taking precedence over all other layers. We reclassified very little agricultural area in this process.

Due to the mixed format of the data sources and conversion to and from raster format, the land use layer, although in vector format, initially appeared pixelated at close range. Numerous orphan and spaghetti polygons existed that would have increased the complexity and unwieldiness of the vector layer in subsequent hydrologic modeling. Spaghetti polygons were a byproduct of using the CLUs to segment fields in the VCGI supplemental layer, due to these layers having slight differences in polygon geometry. Thus, spaghetti polygons had the same crop type as the larger adjacent agricultural land polygon. Spatial analyst Mohamed Niang at the IRDA rectified these issues by smoothing polygon boundaries, merging orphan and spaghetti polygons into larger adjacent polygons, and establishing a minimum polygon area of 2 ha, while retaining the characteristics of the CLU field segmentation and maintaining total agricultural land area and typology ratios. Before post-processing by the IRDA, there were 15,180 field polygons included in the MBB-VT agricultural land dataset. After post-processing, the total number of field polygons decreased to 5,557, but the important characteristics of the data were preserved.

Agricultural Land Typology

As a first step in developing our agricultural land typology for the MBB-VT, we gathered information on soil properties and field slope. We compiled data from the Soil Survey Geographic (SSURGO) database (NRCS, 2022) for the MBB-VT watershed, including:

- MUKEY (map unit ID)
- the name of the dominant soil component within the MUKEY
- the unique component ID of the of the dominant soil component
- the soil's hydrologic group
- the unique ID specifying the surface soil layer
- the top of the surface soil layer depth (cm)
- the bottom of the surface soil layer depth (cm)
- clay content (%)
- sand content (%)
- organic carbon content (%)
- pH
- k-Factor, a measurement of soil texture developed by Williams (1995)
- Soil texture

We generated a 10-m resolution soils raster for the MBB-VT characterized by MUKEY. We then used Zonal Statistics in ArcGIS to determine the dominant MUKEY within each agricultural land field polygon. Next, we used Spatial Analyst tools in ArcGIS to derive a 10-m raster of slope for the entire MBB watershed. The data source for slope calculations was the 10-m resolution digital elevation model (DEM) included as part of the NHDPlus HR. Using Zonal Statistics, we calculated the mean value of the slope raster contained within each agricultural land field polygon.

We identified four key parameters (mean slope, soil clay percentage, soil organic carbon percentage, and soil pH) as potential predictors of key P properties in the NMP dataset for the MMB-VT. We tested six distinct pairings of these parameters for k-means clustering (Hartigan and Wong, 1979) of field polygons within each crop type (corn and hay) using the "kmeans" function in base R (R Core Team, 2022). We used the R function "fviz_nbclust" from the `factoextra` package to run three common diagnostics (the elbow method, the average silhouette method, and the gap statistic) to determine the number of clusters to specify in k-means clustering for each crop type (Kodinariya and Makwana, 2013), with greatest weight given to the elbow method results. Next, we determined the number of statistically significant differences between the distributions of modified Morgan P, modified Morgan Al, and P saturation ratio for observations sorted into each cluster (Kruskal-Wallis non-parametric test with multiple post-hoc Dunn-Bonferroni pairwise comparisons) (Table 2). The combination of mean slope ('slope') and soil clay percentage ('clay') was the best-performing pairing, and we therefore chose these two parameters for the final redistribution of NMP dataset characteristics to MBB-VT agricultural land. An added advantage of using slope and clay is that these parameters are unlikely to be affected by agricultural land management, while soil organic carbon and pH can change due to practices such as tillage, manure input, and liming (Albrecht et al., 2005; Fenton et al., 2008).

Table 2. Results from statistical analyses to determine optimal clustering parameters for MBB-VT agricultural land.

Corn						
Predictors Used	**Number of Clusters**	**Number of Pairwise Comparisons**	**Number of Statistically Significant Comparisons**			**% Significant**
			MMP	**MMAL**	**PSR**	
Slope and Clay	4	6	4	4	3	61%
Slope and OC	4	6	1	2	2	28%
OC and Clay	5	10	3	4	3	33%
pH and Clay	5	10	2	3	1	20%
Slope and pH	5	10	1	3	1	17%
OC and pH	4	6	0	1	0	6%
Hay						
Predictors Used	**Number of Clusters**	**Number of Pairwise Comparisons**	**Number of Statistically Significant Comparisons**			**% Significant**
			MMP	**MMAL**	**PSR**	
Slope and Clay	5	10	5	6	6	57%
Slope and OC	4	6	4	4	4	67%
OC and Clay	5	10	3	5	4	40%
pH and Clay	4	6	0	4	0	22%
Slope and pH	5	10	1	3	1	17%
OC and pH	3	3	0	2	0	22%

In the sections that follow, we describe in more detail how certain P flows (e.g., manure P input, fertilizer P input, crop P harvest) and soil P characteristics were estimated for all agricultural land polygons in the MBB-VT watershed.

Manure P Inputs to Agricultural Land

We obtained field-level manure application data from nutrient management plans (NMP) provided by the Vermont Agency of Agriculture, Food and Markets (VAAFM) for ten dairy farms operating within the MBB-VT. This dataset included 1422 fields (0.08 to 49.9 ha each) that collectively accounted for ~21% of the agricultural land area in the MBB-VT (incl. 16% of the area in hay and 38% of the area in corn).

The relationships between manure application timing and crop type are important to P mass balance watershed-wide, and we aimed to preserve the proportions of manure applied by season when extrapolating agricultural land data from the NMPs out to the entire watershed. To do this, we:

- Determined the proportion of fields in the NMPs receiving manure for each individual combination of crop type, cluster designation, and application period
- Calculated the mean value of the nonzero application rates (in kg P/ha-yr) for each of these combinations
- Applied this mean to the same proportion of the matching cluster in the MBB-VT dataset (for example, if 5 out of the 10 fields in NMP Corn Cluster 3 received manure in May-September, and the average of those 5 values was 50 kg P/ha-yr, we assigned 20 out of the 40 fields in Corn Cluster 3 a manure application rate of 50 kg P/ha-yr for May-September)

We ran a spatial redistribution model 10,000 times to account for the effects of uncertainty in spatial assignments of manure inputs within each agricultural land typology cluster. We based our final estimates for manure P input by HUC12 and land use on an iteration of the spatial distribution model that was within 10% of standard deviations of the central values for mean watershed P balance and mean P saturation for all crops over 10,000 runs, and within 25% of the standard deviations of mean corn land and hay land P balance and mean P saturation over 10,000 runs.

Fertilizer P Inputs to Agricultural Land

We obtained field-level fertilizer application data from NMPs provided by VAAFM for ten dairy farms operating within the MBB-VT. This was the same dataset used for manure. We used the same method of extrapolating from NMP data to the entire watershed for fertilizer that we described above for manure, although there was no temporal component for fertilizer P input.

Crop P Uptake

We obtained field-level crop yield and P uptake per mass of harvested crop data from NMPs provided by VAAFM for ten dairy farms operating within the MBB-VT. This was the same dataset used for manure and fertilizer. We used the same method of extrapolating from NMP data to the entire watershed for crop uptake that we described above for manure, although there was no temporal component for crop P uptake.

Agricultural P Balance

We calculated a partial P mass balance for agricultural land (units = kg P/ha-yr) as:

P balance = P applied via manure + P applied via fertilizer – Crop P uptake

We did not account for atmospheric deposition into nor leaching/export out of the system boundary for this calculation in Task 3b (hence, the “partial” mass balance).

To estimate a partial P mass balance for the agricultural land of the MBB-VT, we multiplied the result of each per-field P mass balance rate by the area of that field to produce a net P excess or deficit in terms of mass for each field. We then summed these P masses to determine the net mass balance for individual agricultural land clusters and different spatial units. When assigning a proportion of MBB-VT fields in each agricultural land cluster with manure or fertilizer application values, we randomly chose those fields. Thus, each iteration of the spatial distribution is only one of numerous possible solutions. Consider, for example, that by random chance, we assigned all the manure applications to the largest fields. This would result in a more positive agricultural land P balance for the watershed than if we had assigned manure applications to the smallest fields. To counteract the possibility that random chance would give us a result that was far away from the theoretical "mean" situation, we ran the NMP to MBB-VT spatial distribution 10,000 times, determining mean partial P balance by agricultural land cluster and for all agricultural land.

Soil P Metrics

We collected agricultural soil P information from two sources: (1) the same database of NMPs mentioned above for manure, fertilizer, and crop P uptake, and (2) the UVM Agricultural and Environmental Testing Lab (AETL). In both datasets, soil test P and Al results are based on Modified Morgan extraction. To provide soil P information in an identical format as the Quebec team (Mehlich-3 extraction) and determine the P saturation ratio, we used several conversions based on past studies.

To convert from Modified Morgan P (MMP) to Mehlich-3 P (M3P), we used the equation developed by Winchell et al. (2011):

$$M3P = (6.718 * MMP) - (11.83 * pH) - (32.757 * (MMP/MMAl) + 90.73$$

Where:

MMA = Modified Morgan Al and units for M3P, MMP, and MMAl are mg/kg.

We calculated Mehlich-3 Al (M3Al) using an equation developed by Magdoff et al. (1999) (units = mg/kg):

$$M3Al = 534.68 + (10.47 * MMAl) - (0.028 * MMAl^2)$$

P saturation was estimated as M3P divided by M3Al (mass basis) for input into the metamodel. We also estimated Mehlich-3 P saturation ratio using P divided by (Al + Fe) (on a molar basis) by following a conversion for Quebec soils having similar characteristics to the MBB-VT developed by Khiari et al. (2000). We used the latter version to inform the spatial distribution model.

For corn and hay, we used similar methods to estimate soil P metrics for agricultural land polygons as we did for P flows and P balance. The NMP dataset, augmented using the conversions described above, contained values of MMP, MMAl, M3P, M3Al, and P saturation for all field polygons included in the NMP dataset. After we determined agricultural land clusters for the NMP dataset (as described above), each cluster had a unique distribution of values for these soil metrics. We then assigned the same distribution of P saturation ratio values (molar ratio based on P, Al, and Fe) from each cluster in the NMP dataset to its corresponding cluster in the MBB-VT dataset. To illustrate, consider that NMP Hay Cluster 5 has 100 P saturation ratio observations, while MBB-VT Hay Cluster 5 has 400 observations. We randomly selected 400 P saturation observations from NMP Hay Cluster 5 to populate MBB-VT Hay Cluster 5, with the stipulation that some observations must be taken multiple times to fully populate the MBB-VT cluster. For each P saturation ratio observation used, we also assigned the associated

MMP, MMAl, M3P, and M3Al that went into calculating it. In this way, we preserved the variability of the original values in the NMP dataset when extrapolating to the MBB-VT agricultural land. Finally, we estimated soil metrics by HUC12 and crop type, based on an iteration of the spatial distribution model that was within 10% of standard deviations of the central values for mean watershed P balance and mean P saturation for all crops over 10,000 runs, and within 25% of the standard deviations of mean corn land and hay land P balance and mean P saturation over 10,000 runs.

For the “other agriculture”, pasture, and soybean crop types, the AETL database was our only data source, so we used it to extrapolate soil test data, by municipality, basin-wide. We organized results from the AETL database by town. To attribute soil test data to any towns that did not have data, we identified all towns sharing a boundary with it, identified the mean of the soil test values in that town, and used the mean of the surrounding towns’ values. The AETL soil test values for “other agriculture”, pasture, and soybean were in the same range as the NMP soil test values for corn and hay. Considering this, and the fact that corn and hay account for >97% of the agricultural land in the MBB-VT, we do not consider the AETL data to be highly influential in the final analyses.

We estimated native soil P in the MBB-VT using mean values of total natural P by texture classification, as compiled from an analysis of soils from 158 soil series in Quebec (Michaud et al., 2022). Texture classifications for MBB-VT soils were derived from SSURGO and were sub-classified to match the three texture classifications in the Michaud et al. (2009c) analysis: clayey, loamy, and sandy.

Human P Sources

We estimated P inputs from human waste using a combination of wastewater treatment plant (WWTP) discharge data and estimated loadings from septic systems. Average measured discharge and average effluent P concentration at WWTPs located within the MBB-VT were sourced from NPDES permits for six municipal facilities and one paper mill (VTANR, 2023). Average measured discharge and average effluent P concentration were multiplied to calculate annual P discharge. The annual P discharge for each facility was then multiplied by the area of urban polygons associated with each facility, previously identified in the land use layer using VCGI data, to determine P discharge rate for urban polygons (kg P/ha-yr).

We estimated septic P loading rates using population data at the town level (US Census Bureau, 2020). For towns that lie entirely inside the MBB-VT watershed and are not served by a WWTP, all residents were assumed to be served by septic. For towns partially inside the MBB-VT watershed, the population served by septic was estimated proportionate to the percent of land area of each town within the watershed. For towns that are partially served by WWTPs, the population served by septic was estimated as the total population minus the estimated population served by WWTPs. Estimated septic P load was calculated as population served by septic multiplied by the estimated loading rate of 1.6 g P/person-day (US EPA, 2002) as a high estimate. The high estimate assumes the entire septic P load eventually reaches surface waters. A low estimate was also calculated, based on the findings of Oldfield et al. (2020) indicating that 34% of total septic P load reaches surface waters. The low estimate for septic P load to surface waters is likely more realistic.

P Loading for Non-Agricultural Land Uses

We sourced P loading rates for remaining land use types from Winchell et al. (2011).

Task 4: Quantify Inventories of P in Missisquoi Bay

Sediment Inventories

Sediments were collected by gravity core at predetermined grid locations. The sediment chemistry data that were used for sediment P inventories are described in detail in the QAPP and collected under previous Lake Champlain Basin Program and NSF EPSCoR sampling programs in 2020 and 2021. Redox sensitive P concentrations are derived from ascorbate extractions as referenced in the QAPP and are operational definitions of sediment P pools most likely to contribute to internal loading of phosphorus. Total phosphorus concentrations were obtained by Aqua Regia digestion and include both labile and recalcitrant forms of P. Sediment inventories were partitioned by the most reactive depth interval (0-1 cm) and the 0-10 cm interval. These data were then interpolated following the below method to determine P mass ranges in the different sediment intervals for the entire bay. The interpolation scheme described below was for the minimum and maximum P values for each bin within the bay to produce the range of possible P inventories in the bay's sediments.

The mapping software ArcGIS Pro was used to interpolate the sediment bulk density and the concentration of P in Missisquoi Bay in between sampling sites. Spatially autocorrelated data can be modeled with a semivariogram which plots average dissimilarity of paired points against separation distance between those points. The semivariogram was then used as the underlying model to create a prediction surface (kriging) by taking a weighted average of known points (Isaaks and Srivastava, 1989; Olea, 2006).

Kriging methods have been used in previous studies to estimate sediment phosphorus concentrations (Puttonen et al., 2014; John et al., 2021). Empirical Bayesian Kriging (EBK) was chosen as the interpolation method for this study because parameters are assigned through a process of multiple simulations on data subsets to minimize error. New values are estimated successively at each input location and a new semivariogram is estimated from each set of simulated data. This process is repeated to obtain an average semivariogram from multiple results. EBK has been shown to model complex environmental datasets better than other kriging methods because it includes the uncertainty of the underlying semivariogram and can account for moderately nonstationary data (Samsonova et al., 2017; Krivoruchko and Gribov, 2019).

Measured point values were mapped in ArcGIS Pro, and EBK analysis was run in the geostatistical analysis package for each sediment depth fraction. Prediction surface results were cross validated by successively excluding experimental points and comparing the known value with the interpolated value at that location. Results were generalized by calculating the root mean square error (RMSE) of interpolation:

$$\sqrt{\frac{\sum_{i=1}^{n}\left(\hat{z}(s_i) - z(s_i)\right)^2}{n}}$$

Where:

$\hat{z}(s_i)$ is the interpolated value
$z(s_i)$ is the is the measured value at point s_i

The resulting estimation raster was clipped by the Missisquoi Bay border shapefile and binned to estimate the total area for each range of values. Sediment bulk density and P mass were also interpolated in this way.

Water Column Inventories

As described in the QAPP, we compiled data from the EPSCoR BREE program, the Lake Champlain Long-Term Monitoring Program and UVM's data from the LCBP funded project to assess options to suppress internal loading in Missisquoi Bay going back to 2017 when the BREE project began. We identified the minimum and maximum concentration values for the different measured P parameters, and then calculated a mass based on an estimated volume of 2.12*10^11 L of bay water at each minimum and maximum P fraction (TDP, TP, SRP) concentration value. We provide estimates from each dataset separately, as they each have different strengths and biases, which provides additional insight. The UVM BREE P data is the highest frequency, captures internal and external loading events most thoroughly, and includes 3 phosphorus operational forms (SRP, TDP, and TP) at one location. The UVM-Stone dataset is the most spatially expansive but also focused on summer conditions and biases towards internal loading events given the goals of that study (bottom water was sampled and the study was focused on describing internal loading). The composite long-term monitoring data is least biased to bottom water concentrations and captures a range of seasonal conditions at two locations. Given that all these samples were collected by boat, there is also some bias towards collection during weather conditions where boating is feasible (e.g., samples were not collected during big storms). Although these data do not include winter field campaigns, the only published winter P concentrations for Missisquoi Bay fall within the ranges captured by the other datasets (e.g., Schroth et al. 2015, Joung et al. 2017).

TASK 5: SWAT-BASED METAMODEL DEVELOPMENT

The approach to develop the metamodel was built upon the P-EDIT modeling approach developed by IRDA (Michaud et al. 2009c, 2018; Drouin et al., 2014). The metamodel (an empirical model derived from the physically based SWAT model simulations) has been developed to enable simplified simulations of the impacts of a broad range of alternative land management/conservation practice assumptions on the terrestrial P balance and exports to the bay, in order to satisfy the requirement of the MBB P-Balance Toolkit.

Concepts and Rationale

The empirical metamodel predicts P storage and export based upon the physical characteristics of a landscape unit (e.g., land cover, soil properties and slope), the climate characteristics of MBB agriclimatic sub-region (precipitation and temperature), and the management of that landscape unit, either agricultural (crop rotation, fertilizer inputs, tillage practices, drainage), residential, urban or forested.

The geophysical parametrization of the metamodel derived through GIS analysis remains static for all simulations of the model. The land use and land management inputs, and potentially climate inputs, vary based on user specifications and temporal horizon. **Error! Reference source not found.** illustrates the conceptual diagram of spatial data treatment, including:

- Agricultural P inputs (manure and mineral) and soil P level/saturation, which are distributed (spatially) to agricultural land use/management units (MUs) based on agronomic census data

- Urban, forest, roads, residential and natural P non-point sources are projected through export coefficient obtained from anterior modeling studies (Deslandes et al., 2006; Michaud et al., 2007; Winchell et al., 2011)
- Cropping systems characteristics for agricultural land use/management units (MU)
- Soil and landscape properties defined respectively at the soil map unit and micro-catchment scales
- The P emissions module, estimating runoff, sediment and P yields based on all input parameters
- All baseline dynamic parameters custom modified to generate alternate scenarios

The soil P stock is updated when considering different projections in time, based on cumulative manure and mineral P inputs.

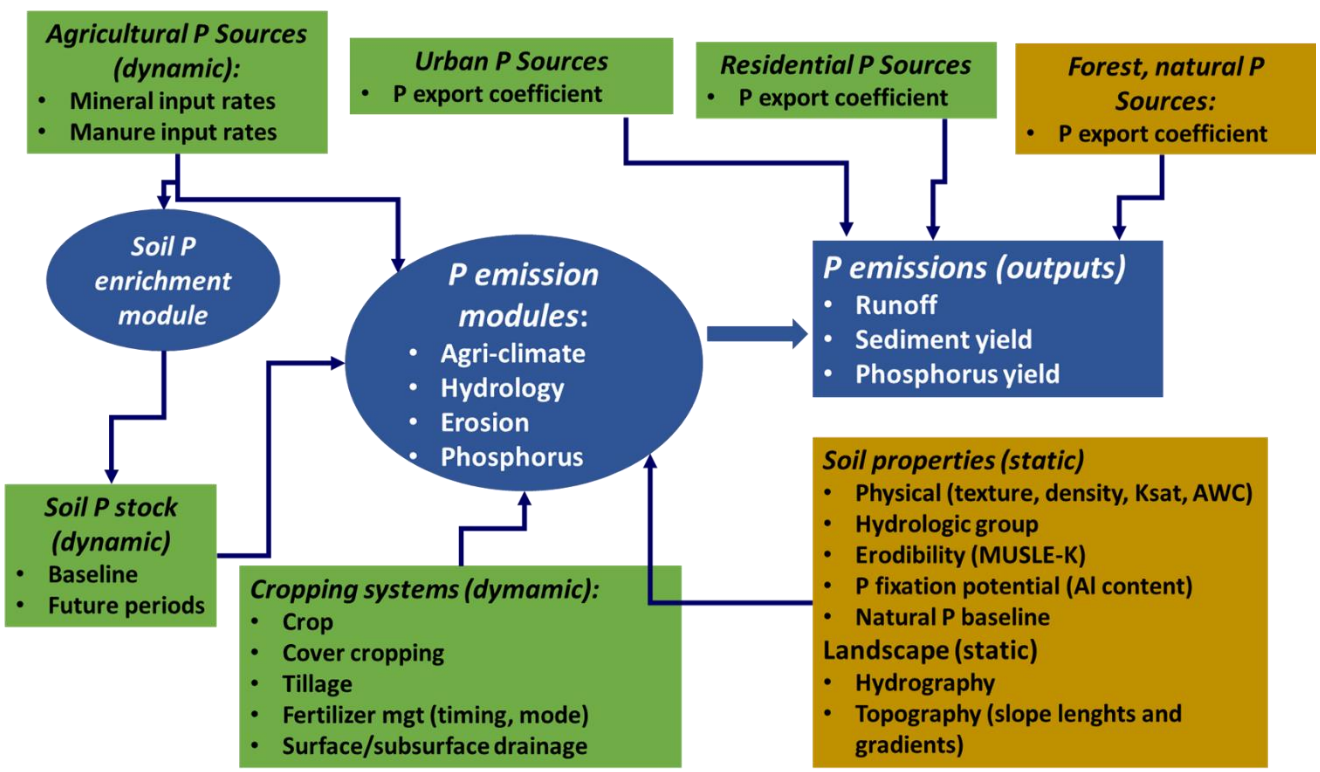

Figure 2. Conceptual diagram of spatial data treatment.

The P emission modules of the MM feed each other, including Climate, Hydrology, Erosion, and Phosphorus.

Climate Module

The agriclimate module represents the regional variability in precipitation and temperature gradients across the MBB watershed, from the mountainous areas to the lake shores. The MM outputs the relative effect of the subregional climate in inducing surface runoff and total water yield across the watershed, and potentially, future climate effects.

Agriclimatic parameters have been developed from precipitation, evapotranspiration, and snowmelt data from the SWAT modeling conducted as part of the Missisquoi basin critical source area project (Winchell et al., 2011) for the years from 1996 – 2009. In addition, rainfall intensity data (2-year recurrence interval annual maximum 6 hour rainfall) was derived at the SWAT subbasin level from NOAA Atlas 14 precipitation frequency data (Perica et al., 2019). The agriclimatic parameters were classified into four zones and spatially distributed based on subbasin-level elevation (Table 3).

Table 3. Agriclimate factors estimated for the MBB subregions based on elevation range.

MBB Agri-Climate Group	Elevation Range (m)	Annual Runoff Weight Factor (Cs(i))	Water Export Weight Factor (CT(i))
1 (Reference Region)	<= 125	1.00	1.00
2	125 - 250	1.05	1.23
3	250 - 425	1.34	1.50
4	> 425	1.89	2.02

To infer the relationships developed in the lowest elevation “reference” region to the other agriclimatic regions of the watershed, two climatic weighting factors were used.

Water Export Weighting Factor: This factor expresses the difference in the total exported water (surface and subsurface) between MBB upstream region of interest and the “reference” region. This gradient is derived from the difference between the two regions’ respective precipitation and evapotranspiration. The export factor is thus calculated based on the average long-term precipitation and evapotranspiration rate (derived from Winchell et al., 2011) associated with the region of interest (*i*) and the “reference” region (*r*):

$$CT(i) = \frac{QT(i)}{QT(r)}$$

Where:

CT(*i*) = annual water export weighting for region “i”
QT(*i*) = annual water export index for region “i”
QT(*r*) = annual water export index for reference region “r”

$$CT(i) = \frac{PPT(i) - Etr(i)}{PPT(r) - Etr(r)}$$

Where:

PPT(*i*), PPT(*r*) = average annual total precipitation for regions “i” and “r”
Etr(*i*), Etr(*r*) = average annual evapotranspiration for region “i” and “r”

Annual Runoff Weighting Factor: This factor accounts for the influence of snow melt and the frequency of intense rain events as these affect the distribution, surface or subsurface, of total water exported from the land unit. The effect of snowmelt is captured by a snowmelt factor which is based on the ratios of annual snowmelt in the “reference” region (r) and the target region (i) (Winchell et al., 2011). The effect of the frequency and intensity of rain events was calculated based on long-term average of days receiving more than 25 mm of rain and the 6-hour duration 2-year recurrence interval rainfall event. Since snow melt is a major contributor to annual runoff, a weighting factor of 1.5 was assigned to this portion of the calculation. Therefore, the annual runoff weighting for the target region (i) as a function of the reference region (r) is:

$$Cs(i) = \frac{(Csh(i) * 1.5 + Csp(i))}{2.5}$$

Where:

Cs(i) = annual runoff weighting factor for region “i”
Csh(i) = snowmelt runoff factor for region “i”
Csp(i) = rain event runoff factor for region “i”

And,

$$Csh(i) = \frac{Fp(i)}{Fp(r)}$$

$$Csp(i) = \frac{P\max(i) * Jr(i)}{P\max(r) * Jr25(r)}$$

Where:

Fp(i), Fp(r) = Annual snowmelt (mm) for target region “i” and reference region “r”
Pmax(i), Pmax(r) = maximum probable rain lasting 6 hours with a recurrence interval of 2 years for target region “i” and reference region “r”
Jr25(i), Jr25(r) = number of days with daily precipitation exceeding 25 mm for target region “i” and reference region “r”

Hydrology Module

The hydrology module predicts surface water runoff and tile drain flow. The annual water yields are based on SWAT simulation outputs, calibrated, and validated against hydrometric historic data from MBB stations (Deslandes et al., 2006; Michaud et al., 2007). SWAT model outputs were reduced to distribution curves for the average annual surface runoff and subsurface flow for different combinations of crops and HRUs modeled in the P-EDiT metamodel (Michaud et al., 2009c). For fields that are not tile drained, the metamodel assumes a subsurface drainage yield through deep ditches, which are typically spaced at 100 m, while typical tile spacing is in the order of 12 to 15 m for drained fields. Subsurface drainage amount is based on its relationship to surface runoff, as predicted by SWAT algorithms for individual crop classes.

Surface drainage class refers to historic land improvement, where a good condition implies the implementation of (laser) precision land leveling, average condition implies drainage improvement to limit surface ponding, while deficient class implies the presence of narrow beds or no leveling of natural surface drainage with presence of surface ponding.

Conceptually, the amount of surface runoff and drain flow exported from a field (or parcel) is based on the following factors:

- hydrologic soil group (HSG)
- subsurface drainage class (systematic, partial, none)
- surface drainage class (good, average/default, deficient)
- condition of the cultivated soil profile (good, presence of compacted zones, dominance of compacted zones)

Mathematically, the combination of these 4 factors allows the metamodel to assign a global *hydro-pedological class* to the field or parcel. The classes range from 1 to 9, with 1 being the least vulnerable to runoff and 9 being the most vulnerable. For a selected crop, the MM determines the amount of runoff based on the HSG of the soil (undrained HRU), and assigns a value to the class as follows:

- HRU A = 3
- HRU B = 5
- HRU C = 7
- HRU D = 9

The value assigned based on the HSG can be modified based on data entered for the three other factors. This step can result in an improvement or in further degradation of the risk value. The global *hydro-pedological class* for the parcel, as determined by the four factors, is then used as an input to estimate the average annual surface runoff for the parcel under the specified crop. In turn, the runoff estimate is used as input to determine subsurface drainage yield, following distribution functions developed from SWAT modeling outputs. Distribution curves for surface runoff and drainage yields for various combinations of crop and soil HSG can be found in Michaud et al. (2009c). The four factors used to adjust the final hydro-pedological class for a given HRU are described below:

1) Hydrological Soil Group

The USDA-NRCS hydrologic soil group (HSG) classification criteria for Quebec soils were selected from Gagné et al. (2013), and HRU HSG classification for Vermont soils were selected from the Soil Survey Geographic (SSURGO) Database (NRCS, 2022).

2) Subsurface Drainage Class Adjustment

The field subsurface drainage adjustment was classified into three categories:

- Absent: no change
- Partial: minus 1 pt
- Systematic: minus 2 pts

3) Surface Drainage Class

The field surface drainage adjustment was classified into the following categories:

- Deficient (presence of depressions): plus 1 pt
- Average (default): no change
- Good (precision levelling): minus 1 pt

4) Condition of Cultivated Soil Profile

The condition of the cultivated soil profile adjustment was classified into the following categories:

- Good (default): no change
- Presence of zones at risk: plus 1 pt
- Dominance of zones at risk: plus 2 pts

Considering the extent of the area under study, average surface drainage class and good condition of soil profiles have been retained as default values within the initial metamodel parameterization.

Erosion Module

The erosion module predicts net sediment loads following a similar approach to that for water yields. Daily SWAT model runs, calibrated against MBB rivers monitoring data, enabled a net annual sediment export to be associated with variable combinations of crops and soil types at the HRU scale. The metamodel model estimates the sediment yield similarly to SWAT following the MUSLE equation (Williams 1995), using the surface runoff estimate from the Hydrology module. The following equation, used in the metamodel, relates predicted net erosion to predicted runoff generated in the Hydrology module:

$$Sed = (a * Qs - b) * C * k * LS$$

Where:

Sed = annual net export of sediment (t/ha)
Qs = annual runoff (mm/ha)
k = erodibility factor of soil (MJ mm/ha h)
C = crop factor
L = slope length factor
S = slope factor
a and b = model calibration parameters

K for Quebec soils is selected from the hydro-pedological database (IRDA, 2017) and K for Vermont soils is determined from SSURGO database (NCRS, 2022).

L and S factors represent the influence of the length of the slope and its steepness on erosion rate and were derived from the NHDPlus-HR DEM (USGS, 2021) available for both Quebec and Vermont sides of MBB. Longest flow paths from individual Flow Path Units (FPU) and their slope gradient were estimated using ARCHYDRO tool kit (ESRI, 2011). When a null slope gradient was determined due to a convex profile, the average slope of the FPU's pixels was determined using the nearest neighbour estimates.

The crop factor (C) considers the vegetative cover (leaves, branches that intercept rain drops), soil surface cover (crop residues, live vegetation) and soil management practices (type, timing and frequency of working the soil). C values were determined based on calibrated SWAT modeling (Deslandes et al., 2006; Michaud et al., 2007) and from reference values (Wall et al. 2002). To account for the effect of preceding crop, C factor values were multiplied by 0.5 following hay crop, while soybean, corn and vegetable crops increase the C factor by a factor of 1.2.

Table 4 presents the C factors used for the MBB metamodel.

Table 4. Crop factors (C) used in ODEP in the prediction of net sediment exports (adapted from Michaud et al. 2007, and Wall et al. 2002).

Crop and Management Combination	C Value
Corn, fall moldboard plowing	0.45
Corn, fall surface tillage	0.30
Corn, spring surface tillage	0.20
Corn, no till	0.15
Cereals, fall moldboard plowing	0.30
Cereals, fall surface tillage	0.20
Cereals, spring surface tillage	0.15
Cereals, no till	0.10
Soybean, fall moldboard plowing	0.55
Soybean, fall surface tillage	0.50
Soybean, spring surface tillage	0.30
Soybean, no till	0.25
Cover crop	0.15
Hay	0.03

Calibration parameters “a” (slope) and “b” (intercept) for individual crop X tillage class combinations were estimated following a linear regression procedure relating SWAT-predicted annual surface runoff of individual HRU’s (independent “X” variable) to their respective sediment yield ratios (dependent variable “Y”) expressed as the ratio of the HRU’s specific sediment yield to the product of K, LS, and C parameters. Distribution curves and equations for sediment yield ratios (specific sediment yield/KLSCP) for various combinations of crop and tillage management scenarios can be found in Michaud et al. (2009c).

Phosphorus Module

The phosphorus module calculates the annual average P export and separately calculates surface runoff and subsurface P losses, as well as soluble and particulate P forms. Predictions are based on a mixed approach, relying on SWAT/metamodel outputs for runoff and sediment yield, and on empirical relationships developed in field experiments. Although Hydrology and Erosion modules of the metamodel provide water volumes and sediment exports, the P module determines P concentration and P speciation. Experimental results used to develop the P module were selected from studies in Québec completed in the last 25 years, either in plot studies under natural precipitation or under simulated precipitation, and in field studies. All analytical determinations of P fractions were completed at IRDA’s the agri-environmental laboratory (IRDA, 2022) following identical protocols. Four P fractions are considered in the metamodel:

- total P (TP)
- particulate P (PP)
- total dissolved P (TDP)
- dissolved reactive P (DRP)

Soluble P Loss in Surface Runoff

P loading in surface runoff is estimated from predicted surface runoff and sediment yield, and concentrations of phosphorus in the soil. In Québec, Giroux et al. (2008) showed that Mehlich-3 P (M3-P) and the P saturation index (M3-P/M3-Al) are correlated with TDP in runoff:

$$DP = 17{,}1\ (PSR) + 40$$

Where:

DP is the dissolved P concentration in surface runoff (ug/L)
PSR is the phosphorus saturation ratio (%)

And the annual total dissolved P loading is expressed as:

$$TDP(kg/ha) = runoff(L/ha) * [DP](g/L) \quad \text{([ ] = concentration)}$$

Particulate P Export in Surface Runoff

Particulate phosphorus (PP) export in surface runoff is calculated based on sediment loads from the Erosion Module, to which a P concentration is applied:

$$PP(g/ha)=sediment(t/ha)*[PP](g/t)$$

And,

$$PP(mg/kg)=Total\_soil\_P(mg/kg)*E$$

The concentration of PP in the sediments is modeled based on soil total P and a runoff enrichment factor “E” to account for the sediments enrichment in P during the erosion process. The method is driven by research from Iowa (NRCS-IOWA, 2004; Mallarino et al., 2005). Soil total P is not a common analysis. Within the metamodel, soil total P is estimated based on soil P content of the soil in its natural state, here forth referred to as “total natural P”, and anthropogenic enrichment.

Total natural P of dominant soil series of MBB in Quebec were determined from total P extraction of “B horizons” of soil samples. Average values were further classified by textural groupings and used to fill data for soil series that were not analyzed in Quebec and for Vermont soils (Table 5).

Table 5. Mean total natural P and Mehlich-3 P by textural groupings for 158 soil series in Quebec.

Textural Groupings	P Total		P_{M-3}	
	Mean	SE	Mean	SE
	(mg/kg)			
Clayey soils	713	255	16.8	14.9
Loamy soils (including sandy loams)	634	232	19.4	16.7
Sandy soils	537	299	27.0	18.2
Mean of all soils	662	295	20.0	16.6

Enrichment of total P by anthropogenic sources was determined based on available P (M3-P), considering the proportionality factor (k1) that relates total P increases to increases in available P. The k1 factor was estimated to be 2.3 based on the relationship between total P and M3-P of 158 selected soil series in Québec (Michaud et al., 2009c). The metamodel soil's total soil P is thus estimated by:

$$Total\ Soil\ P = Total\ natural\ P + 2.3*(M3\text{-}P\text{-}20)$$

The enrichment factor (E) represents the ratio between the concentration of PP (mg/kg) of the sediments and the total P of the soil (mg/kg). Studies have shown that E decreases exponentially with an increase in sediment load. Giroux et al. (2008) highlighted this relationship using data from numerous natural and simulated rainfall experiments. For the current metamodel, the E factor was optimised based on the hydrologic modeling in the MBB to ensure coherence between surface runoff volumes, sediment loads, and P loads predicted by the metamodel.

Therefore:

$$E = 7.25 * Sed^{-0.25}$$

Where:

Sed = Sediment concentration in surface runoff (mg/L)

Surface Runoff P Enrichment from Non-Incorporated Manure or other Organic Amendment

The MM estimates the enrichment of surface runoff resulting the spreading of unincorporated organic amendments. No surface runoff enrichment is associated to manure incorporated into the soil, following the literature's general assumption that soil tillage generally cancels the effect of manure left on soil surface. Within the MM, dissolved P concentration of surface runoff following the spreading of manure or other organic amendment is estimated from a two-step approach. First, the concentration of dissolved P in surface runoff is estimated from soils' P saturation level, as presented previously, without considering the effect of the amendment. As a second step, the surface runoff DRP concentration resulting from the effect of non-incorporated amendment is based on the P application rate:

$$DRP_{amend} = (1.55\ (DRP_{SOiL})\ +182)*\ Rate\_Manure * 0.4364/59)*F_{Période}$$

Where:

DRP_{SOiL} (ug/l), is the concentration of dissolved reactive P as estimated by P-EdiT algorithm without considering the effect of the amendment
Rate_Manure is the amendment P input rate (kg P_2O_5/ha) (0.4364 is the conversion factor from P_2O_5 to P units; 59 is the experimental reference input rate)
$F_{Période}$ is the seasonal factor (spring and fall: 1.0; summer: 0.5)

This empirical relationship relating P organic amendment input rate and soil P saturation to enrichment of surface runoff in DRP (Michaud et al., 2021) has been derived from the results of an experiment performed under rainfall simulation on 36 field plots from the lower Pike River watershed, within MBB (Michaud and Laverdière, 2004). The experimental set-up, comparing side-to-side hay and bare soil, with or without liquid manure, yielded significant relationships expressing the enrichment of surface runoff in DRP in response to unincorporated manure. Although the soil P saturation of the soil and P manure input were shown to have a determinant effect on surface DRP enrichment of surface runoff, soil cover (bare soil vs hay) did not. Details of the experimental set-up and results can be found in Michaud and Laverdière (2004).

The seasonal factor, empirical in nature, reflects the influence of biological activity on the mobility of phosphorus documented in various early runoff plot experiment and field trials in Quebec (Côté et al., 1999) and more recent studies. From a five-year runoff plot monitoring experiment, Gangbazo et al. (1996) documented a more than two-fold greater reactive soluble P loading from fall liquid manure application on hay as compared to a side-dress application in the Estrie region (Quebec). Bernard and Côté (1997) documented a 150% increase in P losses from a fall application of pig manure as compared to spring application from a runoff plot experiment in Quebec. Landry (2006) described the dynamics of soluble P fluxes on long-term experimental plots fertilized with liquid manure, where side-dressed manure P exerted a 35-40 fold increase in P on ion exchange membranes (IEM). IEM-P levels were shown to return rapidly to equilibrium (14 days) following the summer side-dress application.

P Loss in Subsurface Drainage

The estimate of P loss in subsurface pathways is based on the drain water yield estimated within the Hydrology Module and published PP and TDP concentrations reference values. The P concentration values (either PP or TDP) in response to soil texture and crop type effects (

Table 6) were adapted from drain water yield and quality monitoring on field scale and experimental plot runoff studies in Quebec (Giroux and Royer, 2006a,b; Enright and Madramootoo,(2004; Gollamudi et al., 2007).

*TDP (g/ha) = volume of drain water (L/ha) * [TDP in drain water] (g/L)*

*TPP (g/ha) = volume of drain water (L/ha) * [PP] (g/L)*

Table 6. Average reference concentrations used in metamodel for different fractions of P in drain water based on soil texture and crop type.

Annual Crops			
Texture	**Particulate P**	**Total Dissolved P**	**Dissolved Reactive P**
	ug/L		
>30% clay	262	44	30
>20% clay <70% sand	150	51	42
< 20% clay <70% sand	38	57	54
>70% sand	10	6	4
Perennial Crops			
Texture	**Particulate P**	**Total Dissolved P**	**Dissolved Reactive P**
	ug/L		
>30% clay	156	38	25
>20% clay <70% sand	97	50	40

< 20% clay <70% sand	38	62	54
>70% sand	10	6	4

Spatial Structure and Development of MM

The projection of P emissions in space and time requires the integration of different input parameters that are documented at distinct scales. Hydrological parameters are generated at subwatershed or micro-catchment scale (SUB). Attributes of land use and management units (MU) polygons include all the information related to cropping systems of agricultural MUs, and non-point P export coefficients from urban, residential, forest and other natural land occupations. The spatial structure of the data (polygons) is developed as follows:

Subwatersheds/Catchments Delineation (SUB):

- SUBs are derived from flow path analysis of the DEM using a Python script. The minimum size of subwatersheds/catchments has been optimized, considering the 10 m spatial resolution of the GIS data layers.
- Defined SUBs include subwatersheds associated to the 11 water quality monitoring stations. MM aggregated P emissions projections for these subwatersheds support the validation and calibration of the MM.
- The HUC-12 subwatersheds are the scale at which the metamodel results are presented within the final tool kit.

Land Use/Management Units (MU):

- MUs are classified into 14 hybrid land use classes, uniform for QC and VT sectors of MBB.
- Attributes of the MUs document several key parameters of the MM, including soil P and P inputs, crop management, and land development for agricultural Mus.

Flow Path Units (FPU):

- FPU polygons are the spatial entities at which the topographic factors are estimated (LS-MUSLE, Modified Universal Soil Loss Equation).
- FPU layout is derived from the spatial intersection of subwatersheds, land use (MU), hydrographic network, and roads polygons.
- Systematic buffers were generated within FPUs to avoid artifacts when estimating flow path statistics (longest length and slope gradient). These artifacts are related to spatial shifts between the boundaries of fields (land use polygons) and the locations of farm ditches revealed by the DEM. The identification and treatment of water pathways at the FPU level is supported in the MM by a custom script developed in Python language to enable bypassing the instability problems of the ARCHYDRO module. DEM analysis is first supported by converting FPU's to matrix mode, followed by determination of flow-accumulation directions and concentrations. The analysis of flow paths then supports the identification of the longest route, converted subsequently in vector mode to determine its properties (L-length and S-slope gradient). The assessment is based on the longest flow path of the FPU polygon, for its portion included between and 10-85% of its route toward the FPU outlet, ditch, or stream. The calculation of parameters L and S are then applied to the section according to the methodology proposed by Wall et al. (2002).

Hydrologic response units (HRU):

- HRUs are derived from the spatial intersection of FPU (already integrating SUB and MU delineation) and soil map units.
- Final emissions outputs (surface runoff, sediment yield and total P yield) are projected at this scale.
- The management attributes of the MUs and LS factors from the FPUs are merged within HRUs following a joint spatial procedure.

A summary of the data elements required for the metamodel are provided in Appendix 4.

Task 6. Simulate Bay Mass Balance Input Changes Under Alternative Conditions

In accordance with the project objective 3, the metamodel has been designed to assess the impacts of various management options (e.g., changing farm practices, watershed loading reductions) on the P balance in the terrestrial and aquatic components of the system.

In practice, the metamodel compares the long-term P-balance throughout the MBB based on "baseline" conditions to alternative future scenarios for agricultural and developed land. The project advisory committee (PAC) has been solicited to comment on the approach and to validate a set of alternate scenarios to be routed through the MM. A subset of these scenarios has in turn served as inputs to AEM3D Missisquoi Bay model, as described in the Workplan.

Rationale

The following rationale guided the development of alternate management scenarios:

- Selected alternative best management practices (BMPs) are considered effective to reduce P emissions into surface water and are promoted practices in both Quebec and Vermont, and should be prioritized according to their expected cost-efficiency ratio (cost ($)/kg P abated; Michaud et al., 2019a).
- Efficiency in reducing P loading is optimal when both BMPs targeted on P sources (input management) and transport (runoff and erosion control) are introduced together, promoting synergistic effects.
- Targeting the BMPs according to most critical P source areas is desirable to promote the overall efficiency of P reduction strategies within the MBB.

Framework

The BMPs used to build the alternative scenarios have been organized into three agricultural best management practices (BMP) groups and two developed land BMP groups. The groups are designed to capture categories of alternative management strategies, including nutrient management, erosion control, landscape/structural controls, and point sources from developed land uses.

In practice, the approach involved the modification of the management input parameters of individual hydrological response units (HRUs) within the metamodel attributes table. The resulting change in P loadings (%) is expressed relative to the baseline P loading estimates of individual HRUs.

Alternate Management Scenarios for Agricultural Land Uses

Agricultural BMPs have been designed according to four groups, namely P fertilizer management (Group no. 1), Cropping system management (Group no. 2), Riparian zone management (Group no. 3) and Land conversion (Group no. 4).

P Sources Management Scenario (Nutrient Management, BMPs Group 1)

These scenarios consist of the incorporation of organic fertilizers, where originally surface applied within the baseline scenario, and displacement of manure inputs from late fall period to summer period. In practice, the scenario's effects on the P loading are solely applied to HRUs from the baseline scenario where manure is not incorporated. The projected reduction in soluble P loading (exclusively) is modeled through the change of the Manure application mode class parameter from Surface applied (Class 4) to Early Incorporation (Class 1), while the Manure period class parameter is fixed to summer period (Class 2). The relative effect on individual HRU P loadings depends on the initial soil P richness and P input rate, as described in the methodology section (Task 5, MM development). No surface runoff enrichment is projected by the metamodel when manure is incorporated (Manure incorporation classes 1 to 3).

Cropping System (Soils and Crop Management, BMPs Group 2)

These scenarios include the introduction of cover crops into corn silage and soybean stubbles (Cover crop class parameter no. 1), together with no-tillage for grain corn and small grains (Soil tillage parameter class 4). Through the MM algorithms, the reductions in sediment P loadings are proportional to the change in the Crop cover "C" factor from the erosion predictive equation MUSLE. In turn, the new sediment loading rate determines the P enrichment factor of the sediment. A practical implication of this relationship is that a reduction in erosion rate, through crop residues or cover crop, implies an increase in P level of sediments. As presented in the methodology section, the baseline P status of the individual HRUs, including natural P level and enrichment (Mehlich-II P level and P saturation) are also determinants of the total P loading rate resulting from the implementation of BMPs.

Riparian Zone Management (Buffers and Sedimentation Structures, BMPs Group 3)

An empirical abatement factor of 18.7% of the sediment loading in surface runoff resulted from this scenario, where extended riparian strips are considered (Buffer class 4; over 3 m width), together with the implementation of catch basins. This abatement rate reflects the water quality response to this type of land development assessed in the catchment study *Ruisseau Au Castor* (Michaud et al., 2005), a tributary of downstream Pike River. Because the abatement is solely applied to the particulate P fraction of surface runoff, the effect on total P loading depends on the relative fractions (soluble vs particulate) of P initially projected for a given HRU, within the baseline scenario. A practical implication of this method is that the percent reduction in total P loading resulting from buffers and catch basins is proportional to the initial sediment and particulate P of a given HRU. For example, the Riparian zone scenario will be more effective in reducing the elevated total P loading from silage corn on hilly ground, than from a no-till grain corn or hay, with relatively low baseline sediment yields.

Land Conversion Scenarios (BMPs Group 4)

The land conversion scenarios have also been projected for the most severe critical source areas (CSAs) of P emissions. In practice, the scenario implies the change from the baseline land use class to permanent grass meadows (Land use class "Pasture"), without P fertilizer input.

Agricultural BMPs Allocation/Implementation Methods

The BMP implementation methods include both targeted and random implementation of selected BMPs. Three levels of implementation have been selected for the Vermont and Quebec territories including 100%, 50% and 20% of cropped land surface area of each individual state/province. The target allocation followed a ranking approach based on specific P loadings (kg P/ha) of individual HRUs. Additional target rates of 5 and 10% of state/province cropped land have also been projected for the land conversion of the highest baseline P loading CSAs.

Alternate Management Scenarios for the Point Sources of Urban and Residential Developed Land Uses

Alternate management scenarios for developed residential (BMPs group 5) and urban land use (BMPs group 6) are projecting the improvement of the efficiencies of centralized wastewater treatment systems urban zones and the decentralized (septic) wastewater treatment systems within the low and high density residential areas. A generic abatement rate of 34% of the baseline P loadings estimated within the P Inventory project has been selected for both urban and residential land use point sources alternative management scenarios.

Composite Scenarios (Multiple BMP Groups Combined)

Additional alternative scenarios have been designed based on combining multiple BMP groups and targeting strategies. The rationale behind the projection of composite scenarios is to optimize the reduction in P loadings through the cumulative effects of BMPs, while targeted implementations favor their cost-efficiency.

The overall set of alternate management scenarios was designed as follows:

- A gradual implementation rate on crop land, comparing 100%, 20% random, 20% target, 50% random, and 50% target rates for the agricultural BMPs groups, including:
    - Simple effects of BMP-1, BMP-2, BMP-3, and BMP-4 (20 scenarios)
    - Composite effect of BMP-1 + BMP-2 (5 scenarios)
    - Composite effect of BMP-1 + BMP-2 + BMP-3; (5 scenarios)
- A targeted simple and composite agricultural BMPs scenarios implementation on 50% of cropped land, complemented by land conversion scenarios of 5, 10 and 20% of cropped land area (15 scenarios).
- Alternate management scenarios for developed residential (BMPs group 5) and urban land use (BMPs group 6) effects on P loadings were added to the agricultural BMPs effects

There are 45 alternative scenarios that included only agricultural BMPs and 45 alternative scenarios that included both agricultural and urban/residential BMPs together.

TASK 7: SIMULATE AND QUANTIFY P FATE AND TRANSPORT WITHIN AND FROM MISSISQUOI BAY

To simulate phosphorus (P) mass balance in Missisquoi Bay in response to a range of P reduction scenarios outlined in previous chapters of this report, we implemented the same model developed previously for the Lake Champlain Basin that is outlined in Braun et al. (2024), AEM3D. Important processes that impact P balance represented in the model include phosphorus inputs from all tributaries, phosphorus uptake by cyanobacteria, scavenging by suspended particles, deposition and resuspension of particulate P, release of dissolved P from sediments (internal loading), and phosphorus transport out of Missisquoi Bay into the Inland Sea. In this portion of the project, our core objectives were to 1) quantify P mass balance for the entire bay across a range of scenarios informed by the research team's metamodel of the watershed to quantify how different reduction scenarios impacted P mass balance, 2) examine the seasonality of phosphorus mass balance and the relative importance of sources (lake sediment vs tributary), 3) examine how reduction scenarios impact summer cyanobacteria blooms and bay-wide P concentrations relative to the TMDL target concentration.

AEM3D model capabilities, development, and calibration and validation performance statistics for the model used here are described in extensive detail in Chapter 4 (sections 4.1-4.3) of Braun et al. (2024). We used this published model of the bay to assess various components of P balance within the lake, as well as P-reduction impacts on cyanobacteria blooms. To implement the model, tributary inputs of water were sequenced from the same sequence of calendar years (2010; 2012-2022) as in Braun et al. (2024) with the same timing and magnitude. Baseline P fluxes implemented were also identical and derived from WRTDS-K output for the same years (Zhang and Hirsh, 2019). To examine the impact of the different reduction scenarios, P reductions were implemented instantaneously (at the beginning of model year 1) and then uniformly on daily WRTDS loading projections throughout the remainder of the time series. In general, reduction scenarios ranged from a minimum of 2% reduction to a maximum of 46% reduction. The specific subset of scenarios implemented from the larger body of metamodel runs to feed lake model simulations were selected through a prescribed process. Briefly, the 90 alternative P management scenarios simulated with the metamodel were ranked according to the average annual reduction in total P load to Missisquoi Bay. Based on that ranking, within each 1/30th of the distribution of scenarios, the single scenario with the highest amount of P reduction relative to baseline conditions was chosen as a scenario to represent the P load inputs to the AEM3D model. For these 30 selected alternative scenarios, the reductions in P load for each of the three Bay tributaries (Missisquoi River, Pike River, and Rock River) were calculated independently and used to adjust the baseline condition daily time series of P load inputs to the Bay AEM3D model.

To calculate the phosphorus flux leaving Missisquoi Bay, an AEM3D "curtain" from which to extract model output was created across the relatively narrow connection between the Missisquoi Bay and the Northeast Arm. In the AEM3D model implemented for this project, this curtain is 2 surface grid cells (500 m) long. The daily mean of the direction of the flow across the 2 cells that make up the curtain was used to determine whether water is flowing into or out of the Bay each day. The daily mean of the concentration of the phosphorus components are then assigned a positive value if the flow for the cell is out of the lake and a negative value if the flow is into the lake. Next, these daily mean concentrations are multiplied by the average depth at the curtain (4.84 m) and the length of the curtain (500 m) to calculate the amount in metric tons (MT) of phosphorus component moving in or out of the Bay each day. Finally, these quantities are summed over the year to calculate the yearly net export from the Bay for each phosphorus component.

For quantifying impacts on cyanobacteria and impacts relative to TMDL targets, we extracted chlorophyll and total phosphorus concentrations from each model simulation. The bay was considered to be blooming if bay wide average chlorophyll concentrations were 20 μg/L or greater to be consistent with Braun et al. (2024). Bay wide phosphorus component (TP, PO_4, etc.) and chlorophyl concentrations were extracted from AEM3D's integrated time series (ITS) output. These ITS files provide bay-wide mass balance and concentration values at a specified time step during the simulation. The daily average of these values was then calculated and these daily averages used to calculate the mass balance parameters provided.

AEM3D does have a limitation for this application in that it does not capture the impact of changing P fluxes on the pool of phosphorus in the sediment that can contribute to internal loading (described in detail in Braun et al., 2024). Thus, if large watershed reductions in P were decreasing sediment P stores in the bay to the extent that P release from sediment would decrease, the model as configured would not capture that process. The model also does not capture diagenetic processes including burial and phase transformations that further could impact the pool of P and its behavior in the sediment. Although these limitations are important to acknowledge, they are also unlikely to substantially impact results at the timescales and watershed reduction scenarios modeled here given the high mass of legacy P present in the bay's sediment (Braun et al., 2024; Giles et al., 2016).

Task 8: Develop the Missisquoi Basin P Mass Balance Assessment Toolkit

The Missisquoi Bay metamodel, compiled from a suite of land-use/policy/agricultural practice scenarios and developed in consultation with the Project PAC, was integrated to develop a tool for understanding the P mass balance in the basin. The Missisquoi Basin Phosphorus Balance Assessment Toolkit has been designed for analysis of the current P imbalance in the system, drivers of this imbalance, and impacts of various management options (e.g., changing farm practices, wastewater improvements) on the P balance in the terrestrial and aquatic components of the system. The Toolkit synthesizes insights derived from output of the complex terrestrial and aquatic models through a web-based application where core conclusions around the state of the basin's P balance can be understood. The key aspects of the Toolkit development process are provided in the sections that follow.

Mass Balance Toolkit Data Sources and Compilation

The data sources used to develop the Toolkit included the following:

- Average annual total P loads (mass/time), yields (mass/area-time), and loading reductions (percent change) from baseline conditions for the baseline and each of the 30 alternative scenarios selected to represent the range (high to low) of P mass reduction potential used as inputs to the AEM3D lake model defined at the HUC12 watershed scale
- Missisquoi Bay 30-year average total P load reduction (mass/time), Bay mass balance (mass), Bay total P concentration (mass/volume), and days of cyanobacteria blooms (blooms/time) associated with the baseline conditions simulation and the 30 representative alternative scenarios
- HUC12 watershed boundaries obtained from the US Geological Survey (USGS) Watershed Boundaries Database (WBD) for mapping purposes (USGS, 2021)

Further analysis of the data inputs was required to enable user projections of Bay mass balance outputs from watershed P loading predictions from the 90 alternative management scenarios simulated with the metamodel. Having generated Bay model simulations based on "worst case" (baseline) conditions and "best case" conditions (most impactful alternative management scenario), we developed an interpolation approach to predict Bay P mass balance responses to a continuous range of watershed P load reduction scenarios. This approach was accomplished through linear regression models that estimated Bay P quantities (P mass balance, P aquatic concentration, and cyanobacteria bloom days) from watershed total P load reductions under the alternative P management scenarios. The results of these linear regression models will be discussed in Section 5.

Mass Balance Toolkit Functionality and Development Process

The mass balance Toolkit is based on HUC12-scale P load outputs from the metamodel and linkages to resulting P mass balance outcomes from the AEM3D Bay model. The primary functionality requirements that were designed into the development of the toolkit were as follows:

- The Toolkit users must be able to evaluate watershed and Bay P mass balance outcomes from the 90 alternative P management watershed loading scenarios simulated.
- The Toolkit users must have the option of evaluating different alternative scenarios within different geographic regions within the watershed. For example, an evaluation of land conversion from crops to meadow could be considered in targeted HUC12 sub-watersheds, with erosion control practices implemented in the remaining HUC12 sub-watersheds.
- The Toolkit should provide visual and tabular P mass watershed loading results at the HUC12 and full watershed scales, in addition to the Bay P mass balance response results.

The design of the Toolkit focused on simplicity and clarity such that users are able to quickly determine the steps necessary to generate maps and tables of P mass balance quantities associated their own interactive selection alternative management scenarios. The user feedback cycle followed through the development of the Toolkit was as follows:

- An initial version Toolkit version provided to LCBP Project Officer for review.
- The Beta version of the Toolkit was presented to the Project PAC, with feedback gathered to inform updates and improvements.
- Further testing and feedback from LCBP Project Officer resulted in additional modifications and improvements implemented to final Beta version.
- Final testing and evaluation of the Toolkit by the Project PAC, Project Office, and interested TAC members resulted in the final Toolkit updates.

Mass Balance Toolkit Technological Infrastructure

The P Mass Balance Toolkit uses a JavaScript build tool called Vite configured for React with TypeScript. It uses a user interface component library called Daisy UI with styling provided by the Tailwind Cascading Style Sheets framework. The map is built with ArcGIS software development kit for JavaScript and renders a feature layer from ArcGIS Online but the symbology is rendered based on calculations made within the Toolkit application. There is no database associated with the Toolkit, but it does use Jotai state management and is hosted on a Windows Server on Stone Environmental’ s virtual server network.

4. Quality Assurance Tasks Completed

The following represents a summary of the quality assurance tasks completed during this study.

Task 3: Quantify Terrestrial P Inventories Throughout the Missisquoi Basin

The realization of the terrestrial P inventories for Quebec and Vermont met the data-quality objectives to collect, analyze, display, and document valid locational data. These data were used to accurately estimate and relate terrestrial phosphorus inputs within the MBB (transboundary) watershed, as well as P stocks within agricultural soils of the MBB. Recent geophysical and land use locational data targeted for the project provided complete coverage of Vermont and Quebec, with similar scales and data attributes.

Distinct methodologies were followed for the inventories of P inputs and soil P status in Quebec and Vermont, due to different data sources. In Quebec, P inputs and soil P levels were supported by geolocalized data sets (MELCCFP, 2021a) documented for all individual production units of MBB. Because similar extended data sets were not available for Vermont, UVM's team project members invested substantial effort to estimate P mass balance components for agricultural lands given the data available. The methodology was peer-reviewed through a scientific publication (Bondeson et al., 2024), as was part of a thesis conducted at UVM (Bondeson, 2023).

Task 4: Quantify Inventories of P in Missisquoi Bay

We relied on published and previously screened data from the long-term monitoring program and Braun et al. (2024) to make bay-wide P inventory estimates to ensure data quality control. The assumptions and limitations of these datasets and our calculations are discussed in detail in the project QAPP (Appendix 5).

Task 5: SWAT Metamodel Development

The metamodel development benefited from expertise and an array of scientific inputs which make the Missisquoi Bay watershed region important in the scientific understanding of nonpoint sources of surface water contamination, especially phosphorus. Numerous hydrometric monitoring data sets, experimental plot-level studies, field and micro-watershed experiments, as well as several deterministic hydrological modeling exercises conducted on both sides of the border supported the completion of this study. These assets, together with the current project methodology developments made it possible to meet the three main insurance quality issues related to the MM development, namely:

- The model parameterization: Are the geophysical environment, land use and management adequately represented?
- The model algorithms: Are the equations used within the MM adequately representative of the processes specific to the study area?
- The validation of the model: Are the projected results from the MM adequately supported by observations from the area of study?

Model parameterization: The configuration of the model geophysical parameters benefited from detailed and similar hydro-pedological data sources documented at the soil map unit scale in Quebec (IRDA) and Vermont (SSURGO). The land occupation parameters also relied on recent, spatially-explicit land use maps for Quebec (La Financière and Natural Resources Dept) and Vermont (UVM Spatial Analysis Laboratory). The parametrization of P inputs and soil P status were supported by the P inventories carried out with task 3.

Model algorithms: This MM development task relied on metamodel (Michaud et al., 2009c, 2018; Drouin et al., 2014) and deterministic (SWAT) modeling development in the study region in Quebec (Deslandes et al., 2006; Michaud et al., 2007) and Vermont (Winchell et al., 2011). These results were published in peer-reviewed scientific journals (Deslandes et al., 2006; Michaud et al., 2007) or reviewed by LCBP (Winchell et al., 2011). The algorithms used in projecting concentrations and flows of P are empirical and were from observations collected in Quebec, with a large portion coming from the MM study region. Sources of observations and algorithms are described in the methodology section of the report.

Validation of metamodel projections: The hydrometric monitoring of P flux in eleven stations within the study area were used to calibrate and evaluate metamodel performance. The linear regression of modeled and observed data (R^2=0.94) indicated satisfactory quality assurance of the projected P loadings of the baseline scenario.

Task 6: Simulate Mass Balance Input Changes Under Alternative Conditions

This task involved testing of the metamodel through simulations of alternate land use and management scenarios. The first quality insurance issue concerned the selection of alternate best management practices (BMPs) to reduce P emissions into surface water and are promoted practices in both Quebec and Vermont. Following an initial proposal of alternate scenarios for P loadings simulation, the PAC reviewed the proposed approach and proposed set of alternate scenarios to be routed through the MM. The recommendations of the PAC were considered in the final selection of alternate management scenarios, which in turn served as inputs to the AEM3D Missisquoi Bay model.

A second quality assurance challenge related to the modeling of alternate management scenarios is the validation of projected abatements in P loadings. Although the P loadings from the baseline scenario can be validated via comparison with historic hydrometric monitoring data, this is not the case for alternate management scenarios. Because the alternate scenarios are computed within the MM through changes in management parameters, a general assumption is that the validated results from the baseline scenario serve as a rationale for the validity of alternative scenario projections. Same algorithms, with new management parameters, will generate realistic projected loadings following a similar methodology. The empirical nature of the MM algorithms projecting the soluble and particulate P concentrations from contrasting soil P level or loading rates of unincorporated manure, support this assumption.

Regarding the cropping system BMPs (residue and cover cropping), the projection of sediment loading is from SWAT/MM algorithms, which is essentially driven by the MUSLE equation crop cover factor (factor C). Considering the abundant literature on C factor documentation, the MM projections for sediment loadings following no till or cover cropping are considered robust. However, the effect of these soil conservation practices on P loading is less documented. The general state of knowledge indicates a reduction in particulate P loading rate following residue or cover cropping introduction but also report an increase in soluble P export depending on soil P level. According to the meta-analysis of Daryanto et al. (2017), for example, direct seeding in grain corn and soybean reduces the losses of particulate P of 55% on average compared to conventional tillage (ploughing) or chisel. Conversely, the P in soluble reactive form tends to increase. The current MM algorithms ensure a sound representation of contrasting abatement rates in sediment vs P loads by modeling the concentrations in soluble and particulate P separately and considering P enrichment ratios (E) for particulate P projections. The E factor in the MM model reflects the finer grain size, and respectively higher reactive P level of exported sediments following erosion control. In the present study, the erosive protection scenario (BMP 2) is associated with an area-weighted 46-47% reduction in sediment loads and respective 26-28% in P loads, which is representative of the Daryanto et al. (2017) meta-analysis.

Finally, the projections of riparian zone management scenario (BMP-3) is also empirical in nature and is based on sediment and P loadings abatement monitored locally. Conceptually, the MM empirical abatement rate involves projecting the effect of extended riparian strips and in-ditch catch basins on water quality, as documented at the catchment scale for a tributary of downstream Pike River (Michaud et al., 2005). Although the BMP-3 projection is considered robust on a short-time scale, the projection is questionable on a longer-time scale (30 or more years). A review of long-term monitored effects of erosion control on P loads in North America (Dodd and Sharpley, 2016) showed that particulate P trapping sites become long-term sources of soluble phosphorus emissions. The MM algorithms partially accounts for this phenomenon, by applying a fixed P abatement rate to “incoming” particulate P loading rate. A reduction in particulate P loading projected for residue or cover cropping (BMP-2) thus implies a reduced effect of the riparian BMP-3 on final total P loading.

Task 7: Simulate and Quantify P Fate and Transport Within and From Missisquoi Bay

To ensure quality control on model runs, we used the same forcing data as Braun et al. (2024) that was previously vetted with the same AEM3D code. We confirmed that baseline simulation data were consistent with the Braun et al. (2024) TP model output for a similar time series as discussed in detail in the project QAPP (Appendix 5). Where possible, we also compared our output to the P balance simulations of Limnotech (2012) to confirm that our values for the various P fluxes (tributaries to lake, deposition from water column to sediment, outflow from model domain to the rest of the lake, release from sediment to water column, etc.) are in a similar range as discussed in the report (or note where and why there is deviation). In addition, where applicable, we also ran our updated Python analysis code on the Limnotech (2012) output files to verify the code returned the same analysis values as the original Limnotech (2012) Matlab analysis code.

Task 8: Develop the Missisquoi Basin P Mass Balance Assessment Toolkit

The P Mass Balance Toolkit was based upon data generated in Tasks 6 and 7. The data from Task 6 used by the Toolkit includes the HUC12-scale P load, yield, and change from baseline condition values. These data are displayed on the Toolkit map and summarized in Toolkit results tables. Both map-level data and summarized tabular data were checked independently against the raw data provided from the Task summary spreadsheets to confirm accuracy. The data from Task 7 used by the Toolkit consisted of the linear regression models used to calculate Bay P mass balance quantities as a function of the reduction in watershed P loadings derived by the user-defined alternative scenario. The results from these regression equations displayed in the Toolkit tabular output summary were checked independently against the linear regression equations and AEM3D model output results to confirm accuracy and agreement.

The functional behavior of the Toolkit was quality controlled through multiple interactions of testing and feedback between the application development team and both internal project team members and external project stakeholders. These quality control and revision steps were conducted to ensure error-free Toolkit functionality and allow for clear and intuitive workflow.

5. Deliverables Completed

Task 3: Quantify Terrestrial P Inventories Throughout the Missisquoi Basin

Task 3a: Quantify Terrestrial P Inventories Throughout the Missisquoi Basin, Quebec

Deliverables completed for Task 3a include:

- A land use layer for the Missisquoi Bay Basin, Quebec (MBB-QC)
- Physiographic layers and attributes for MBB-QC, including topography, pedology, and hydrology
- An agricultural P input layer at field scale (management units–MGU polygons) describing rate and timing of organic (manure and residual materials) and mineral fertilizer inputs to MBB-QC cropland, together with P crop uptake and P balance
- A soil P layer describing phosphorus levels (total and available), and saturation of MBB-QC cropland at field-scale estimations of phosphorus loadings emitted from individual wastewater treatment plants and storm overflows structures in MBB-QC
- Estimated phosphorus loadings emitted from septic systems in MBB-QC

Land Use

The final land use classification for the Quebec portion of MBB is illustrated in Figure 3. Overall, the forest, agricultural land, and developed land area occupies 57%, 29% and 2% of MBB, respectively (135,978 ha). Table 7 presents the global land use class distributions for the Missisquoi Bay basin in Quebec. The distribution of land use classes surface areas for individual subwatersheds of MBB is presented in Appendix 1, Table A1-1.

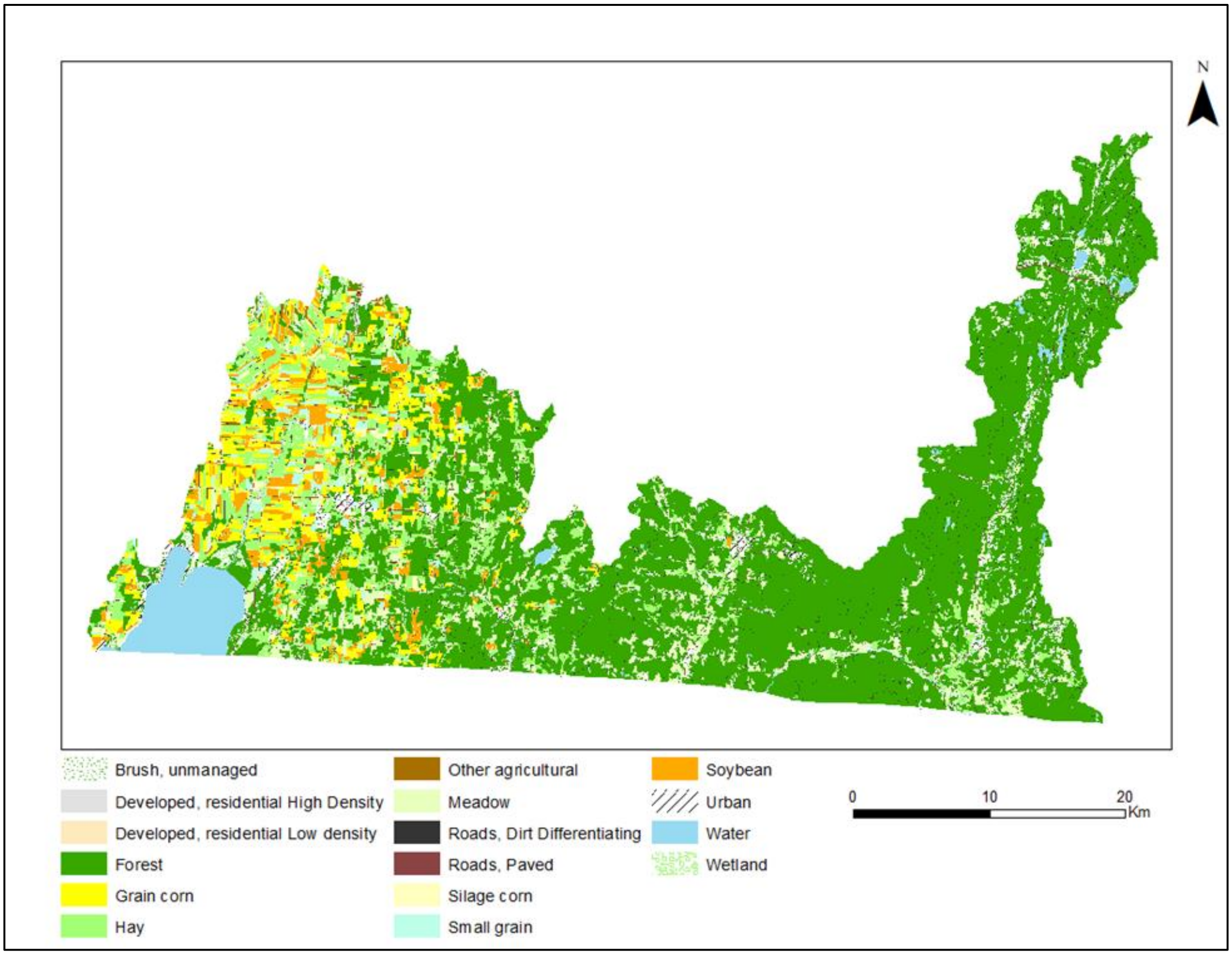

Figure 3. Land cover / land use map of Missisquoi Bay Basin for the Quebec territory.

Phosphorus Inputs to Cropland

Table 8 reports the totals of phosphorus inputs to the overall Missisquoi Bay watershed from the farming sector based on production site locations (MELCCFP, farm census, 2021a). Manure P inputs to the MBB watershed are estimated by summing on-farm (centroids located within the watershed boundaries) production and imports of manure P from which manure P exports are subtracted. Based on this method, estimated manure inputs within MBB are 1,087 T P_2O_5 per year which accounts for two thirds (66%) of phosphorus inputs. These manure P inputs include on-farm production (1,181 T P_2O_5/yr) and imported manure P from distinct production sites (627 T P_2O_5/yr), from which the manure P exported from the same group of production units (722 T P_2O_5/yr) are subtracted. Reflecting the specialization of the agricultural sector in the MBB, most manure P applied on farmland (58%) is moved from one farm operation to another. Uncertainty is associated with these estimates because the relative portions of P imports and exports that come from the basin are unknown.

Table 7. Land use class distributions for the Missisquoi Bay Basin in Quebec.

Land Use Class	Area (ha)	Area (%)
Grain corn	8,869	6.5%
Silage corn	957	0.7%
Soybean	5,640	4.1%
Small grain	1,578	1.2%
Other agricultural	396	0.3%
Hay	10,960	8.1%
Pasture	11,194	8.2%
Brush, unmanaged	4,733	3.5%
Developed, residential low density	429	0.3%
Developed, residential high density	398	0.3%
Forest	79,793	58.7%
Roads, Dirt	1,797	1.3%
Roads, Paved	872	0.6%
Urban	1,187	0.9%
Water	5,876	4.3%
Wetland	1,300	1.0%
Total	**135,978**	**100.0%**

Table 8. Distribution of phosphorus input sources to Missisquoi Bay watershed from phosphorus reports of farming operations (MELCCFP, 2021a).

Source	Mass (T P_2O_5)
Manure P production	1,182
Imported manure P	627
Exported manure P	722
Manure P applied	1,087
Residual matter P applied (RMP)	81
Mineral P applied	475
Total organic P applied	1,168
Total P applied	1,643

Table 9 presents the distribution of organic and mineral P inputs to MBB at the watershed scale (Pike, Rock, Missisquoi and MBB), together with crop type classification. This distribution results from the projection of phosphorus reports for individual production site centroids (n=313) to individual fertilized field unit polygons (n=9,100) as described in section 3a. This estimate (1,231 T P_2O_5 per year) is a more reliable estimate of organic P applied within the MBB farmland compared to the figure cited in Table 8 as it considers production unit centroids on the close outskirts of MBB boundaries. In Quebec, 1,231 T of organic fertilizer (P_2O_5 units) were attributed to 41% of MBB cropped area (18,037 ha). The area-weighted loading rate for organic inputs is

68.2 kg P_2O_5/ha, with the highest input for grain corn fields averaging 75.0 kg P_2O_5/ha. A total of 460 T of P mineral inputs (P_2O_5 units) were attributed to 12,450 ha of cropland, for an average loading rate of 37,0 kg P_2O_5/ha. Overall, the Pike River watershed fertilized cropland area (23,689 ha) comprises 83% of P inputs to MBB. Direct tributary subwatersheds, Rock River, and Missisquoi River, received 6.2%, 6.7%, and 3.9%, respectively, of annual farm P inputs. A detailed description of organic and mineral P inputs for individual MBB subwatershed (HUC12) and crop classes can be found in Appendix 1, Table A1-2.

Table 9. Distribution of mass and specific phosphorus inputs per land use class and individual watershed of Missisquoi Bay Basin soil P and physical properties metrics.

			Organic P Input					Mineral P Input					Total P Input	
Watershed		**Total Area (ha)**	**Area (ha)**	**% Total Area**	**Mass (kg P_2O_5/yr)**	**Rate (kg P_2O_5/yr)**		**Area (ha)**	**% Total Area**	**Mass (kg P_2O_5/yr)**	**Rate (kg P_2O_5/yr)**		**Mass input (kg P2O5/yr)**	**Specific P Input (kg P_2O_5/ha-yr)**
Total Bay direct discharge		2,565	1,400	0.55	71,848	51.3		1,071	0.42	32,443	30.3		104,291	40.7
Total Missisquoi River		1,628	760	0.47	60,893	80.1		229	0.14	5,055	22.1		66,029	40.6
Total Pike River		23,689	14,107	0.60	1,022,244	72.5		10,215	0.43	385,884	37.8		1,408,128	59.4
Total Rock		1,839	1,770	0.96	75,582	42.7		936	0.51	37,155	39.7		112,737	61.3
MBB-QC		**29,720**	**18,037**	**0.61**	**1,230,568**	**68.2**		**12,450**	**0.42**	**460,536**	**37.0**		**1.691,185**	**56.9**
	Land use													
Total MBB-QC	Grain corn	9,229	7,187	0.78	538,675	75.0		2,417	0.26	77,633	32.1		616,308	66.8
Total MBB-QC	Hay	11,516	4,634	0.40	304,498	65.7		6,195	0.54	241,334	39.0		545,832	47.4
Total MBB-QC	Other agricultural	415	294	0.71	824	2.8		377	0.91	15,423	40.9		16,248	39.1
Total MBB-QC	Silage corn	987	780	0.79	48,949	62.7		491	0.50	15,622	31.8		64,571	65.4
Total MBB-QC	Small grain	1,622	1,441	0.89	104,179	72.3		280	0.17	11,418	40.7		115,596	71.3
Total MBB-QC	Soybean	5,950	3,701	0.62	233,442	63.1		2,690	0.45	99,106	36.8		332,549	55.9

Figures 4 5, illustrate the pedological and topographic gradient within MBB, respectively, where dominant clayey material from the Saint-Lawrence marine plain to the west contrast with low and high Appalachian tills of coarser textures at highest elevations.

Area-weighted averages of soil P, Al, and saturation levels for individual cropland classes of MBB are presented in Table 10. Detailed P status results for individual subwatersheds and cropland-class combinations of MBB are presented in Appendix 1, Tables A1-3 and A1-4.

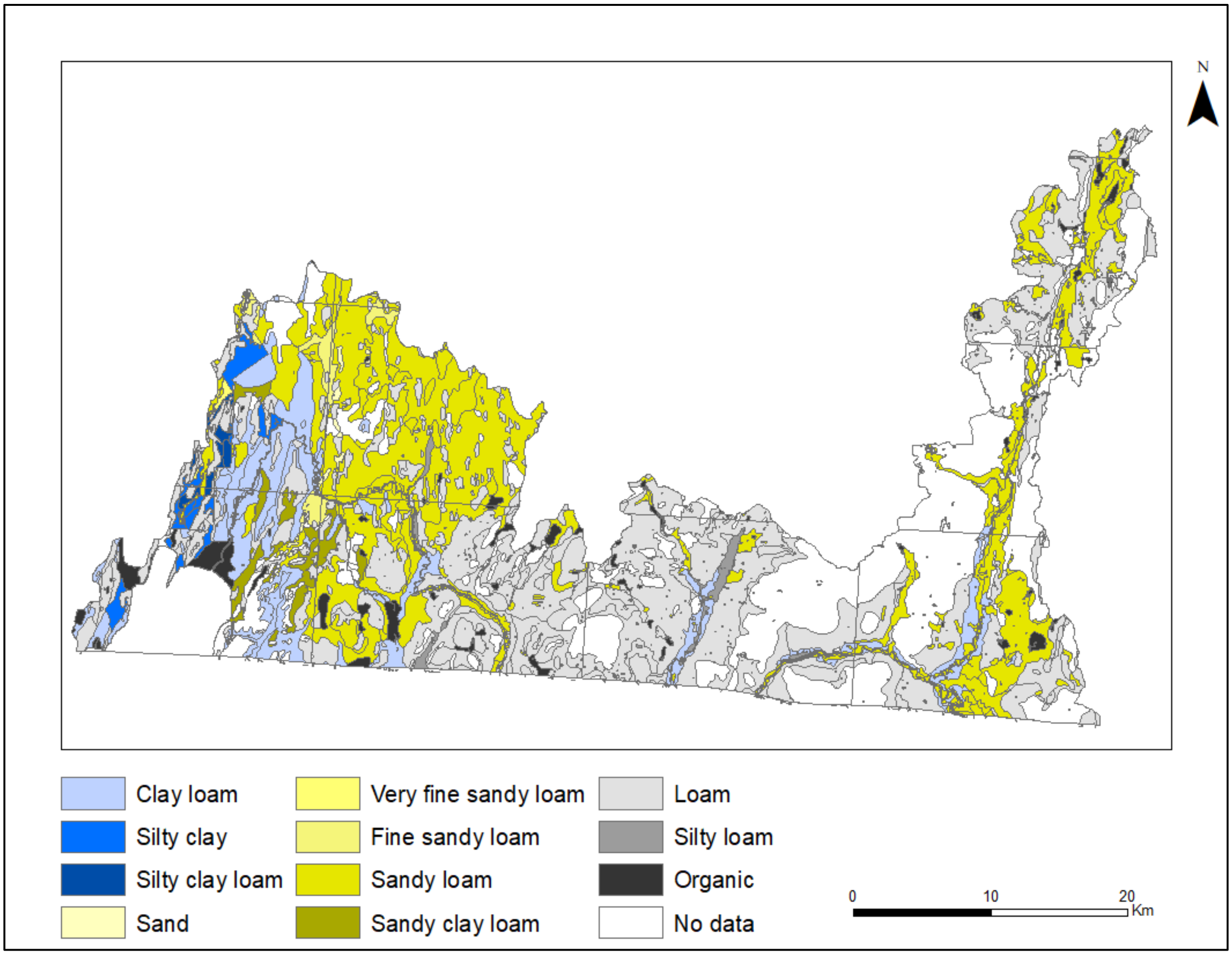

Figure 4. Surface texture classes of soil map units from Missisquoi Bay Basin in Quebec.

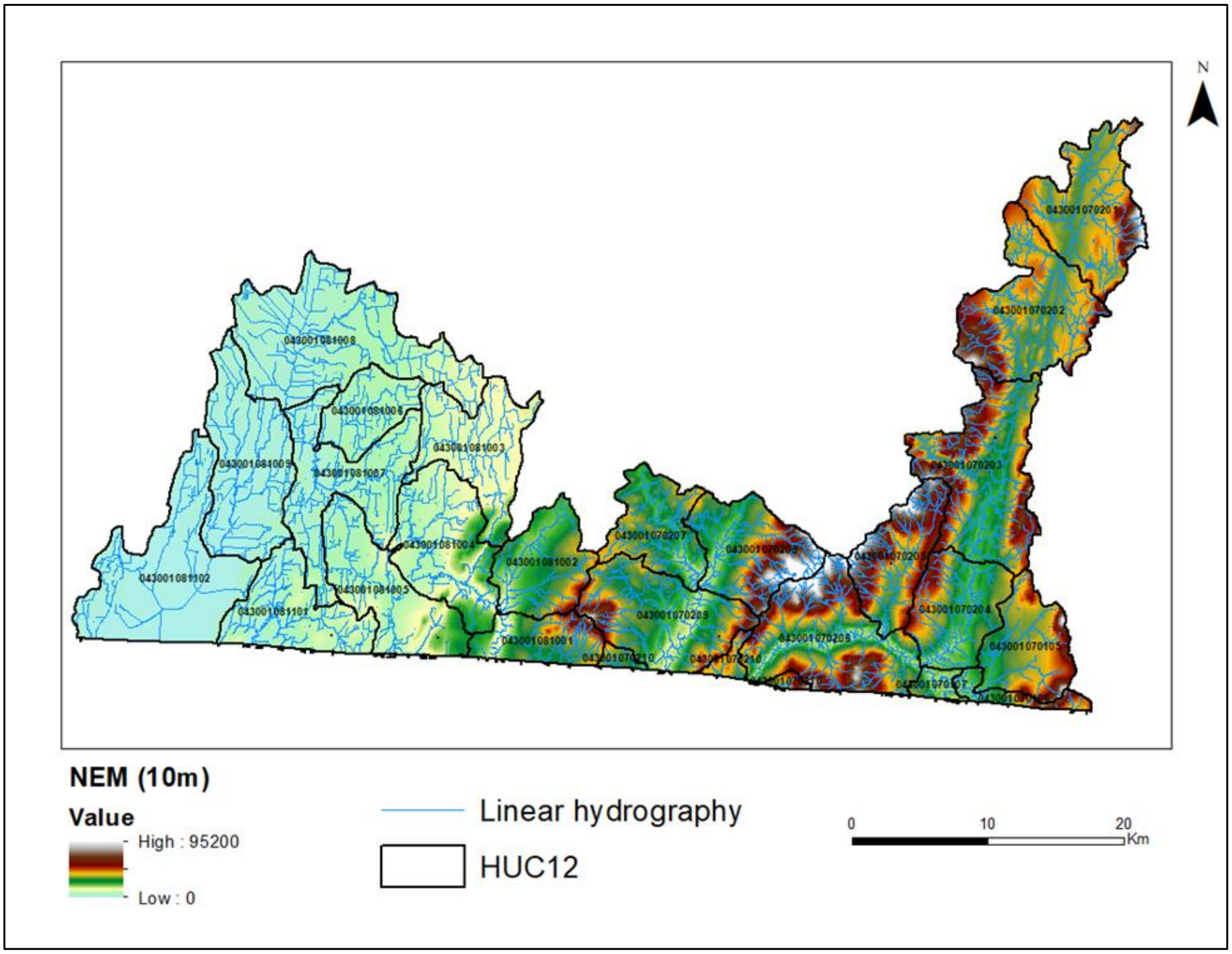

Figure 5. Numerical elevation model, linear hydrography and subwatersheds (HUC12) of Missisquoi Bay Basin in Quebec.

Table 10. Area-weighted Mehlich-3 soil test phosphorus, aluminum, and P saturation for land use classes of Missisquoi Bay Basin.

Land Use	Area (ha)	Mehlich-3 P		
		P (mg/kg)	Al (mg/kg)	P Saturation
Grain corn	1,076,301	116.6	1,064	11.00
Hay	590,336	51.3	1,108	4.55
Other agr.	23,389	56.3	1,086	5.28
Silage corn	43,314	43.9	1,086	4.06
Small grain	74,707	46.1	1,060	4.36
Soybean	593,140	99.7	1,078	9.39

Urban and Residential Human P Sources

Wastewater treatment plants. The performance characteristics of the eleven wastewater treatment plants in MBB in Quebec are presented in Appendix 1 (Table A1-5). Their locations are illustrated in Figure 6. Phosphorus annual loadings from the MBB treatment plants assessed by MELCCFP (2021b) are presented in Table 11. In 2017-2019, average annual P loadings for the ten plants with discharges in MBB were 0.97 metric tons of phosphorus per year, which slightly exceeds the total of wastewater allocation for the MBB (0.85 T P/year). The Bedford plant contributes 55% of the annual P loading from the wastewater treatment plants, due to its relatively large population (2,961 inhabitants, 8% of MBB watershed; ISQ, 2017). The municipalities of Frelighsburg and Notre-Dame-de-Stanbridge need to improve their sanitation performance at their treatment plant, as their artificial marsh treatment technology did not yield the expected returns.

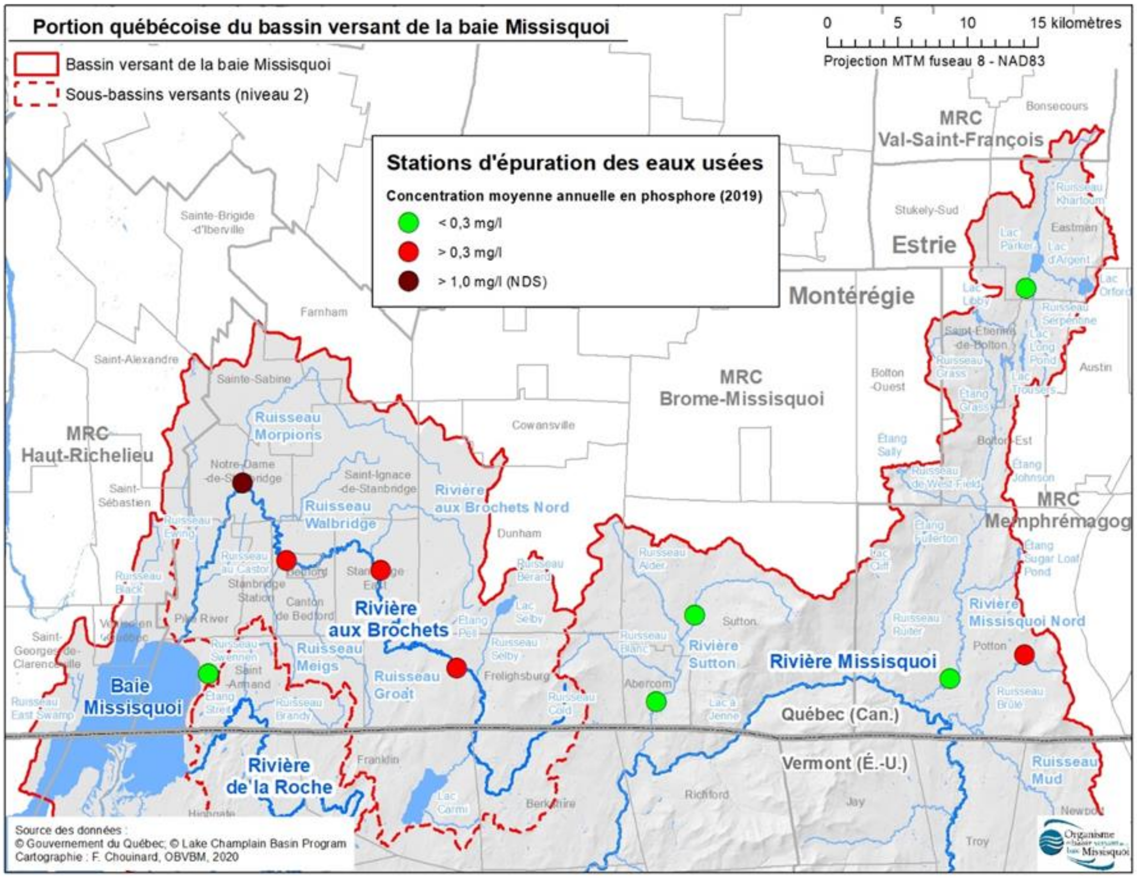

Figure 6. Location of wastewater treatment plants in MBB in Quebec (OBVBM, 2015).

Table 11. Phosphorus concentrations and loadings from wastewater treatment plants in Quebec.

Wastewater Treatment Plant ID	P Conc. 2017 (mg P/l)	P Conc. 2018 (mg P/l)	P Conc. 2019 (mg P/l)	P Loading 2017 (T P/year)	P Loading 2018 (T P/year)	P Loading 2019 (T P/year)	Wasteload Allocation (T P/year)
Abercorn	0.40	0.40	0.20	0.00	0.00	0.00	0.02
Bedford	0.40	0.40	0.50	0.51	0.55	0.58	0.47
Eastman	0.30	0.40	0.20	0.00	0.04	0.00	0.03
Frelighsburg	2.60	2.70	2.80	0.07	0.15	0.11	0.02
Notre-Dame-de-Stanbridge	3.30	3.00	3.30	0.11	0.11	0.07	0.08
Potton	0.30	0.30	0.20	0.04	0.04	0.04	N/A
Potton (Owl's Head)	0.20	0.50	0.40	0.00	0.00	0.00	0.04
Saint-Armand	0.20	0.20	0.20	0.00	0.00	0.00	0.01
Stanbridge East	1.50	1.30	1.10	0.04	0.04	0.04	N/A
Sutton	0.20	0.30	0.30	0.11	0.11	0.15	0.16
Venise-en-Québec (Discharge outside MBB)	N/A	N/A	N/A	N/A	N/A	N/A	N/A
Eastman - Camping Normand	N/A	N/A	N/A	N/A	N/A	N/A	0.02
St-Armand - Usine de filtration de Bedford	N/A	N/A	N/A	N/A	N/A	N/A	Nd
Québec (Total MBB)				**0.88**	**1.04**	**0.99**	**0.85**

Sewage overflows. The 24 stormwater overflow structures in the MBB (Figure 7) had their overflows characterized for the 2017-2019 period. The total number of overflow events (all infrastructures combined, at least 12-minute durations) varied from 301 to 355 events annually (MELCCFP, 2021b). Cumulative P loadings estimated for the stormwater structures of MBB varied annually from 91 to 104 kg P/year, as reported in Table 12. From theoretical estimation overflow volume, three municipalities from the MBB - Bedford, Sutton, and Venise-en-Québec - need sanitary network improvements. Most overflows occurred in the town of Bedford, with annual overflow volume estimations of 41,000 to 53,000 m^3 in 2017-2019 (Cliche et al., 2020).

Table 12. Estimated P loadings from stormwater overflow structures.

Municipality	2017 (kg)	2018 (kg)	2019 (kg)
Abercorn	N/A	0.08	N/A
Bedford	84.78	126.86	95.43
Eastman	N/A	N/A	N/A
Frelighsburg	N/A	N/A	N/A
Notre-Dame-de-Stanbridge	N/A	N/A	0.04
Potton	N/A	N/A	N/A
Saint-Armand	N/A	N/A	N/A
Stanbridge East	N/A	N/A	N/A
Sutton	3.53	0.16	5.76
Venise-en-Québec	0.79	N/A	0.73
Total (kg/P)	**91.12**	**129.12**	**103.98**

Source: MELCCFP, 2021b.

Note: "N/A" indicates no monitoring for years indicated

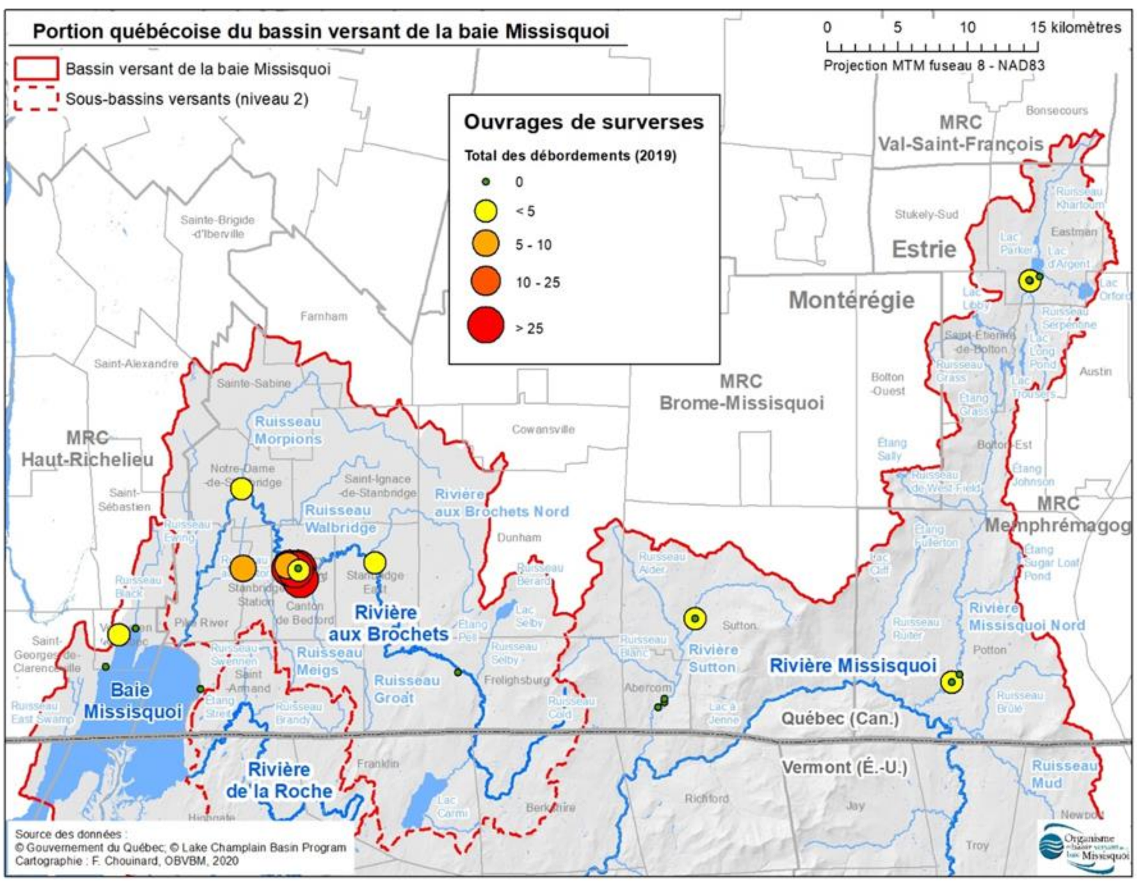

Figure 7. Location of storm overflow structures in MBB in Quebec (OBVBM, 2015).

Septic systems. From a survey of MBB municipalities (OBVBM, 2015), there are 9,245 residential and 235 commercial septic systems in MBB (prorated for surface area within the basin). Phosphorus loadings from these autonomous septic systems for the MBB were estimated based on population served, an estimated loading rate of 1.6 g P/person-day (US EPA, 2002) and an average removal efficiency of 66%, based on the findings of Oldfield et al. (2020) for tributaries of the Canadian portion of the Lake Erie Basin.

Population per municipality was prorated based on the proportion of municipal land included in the watershed (Appendix 1, Table A1-6). The permanent population of the Quebec portion of the Missisquoi Bay watershed was estimated at approximately 23,634 in 2017 (ISQ, 2017). The seasonal population, which includes occupants of second homes and cottages primarily concentrated in Sutton, Venise-en-Québec, Potton, and Eastman, is estimated to be about 15,325 (MRCBM, 2016; MRC de Memphrémagog, 2009). The total population of the Quebec portion of the watershed is estimated at approximately 38,960 people for the reference year 2017. The permanent population of the BVBM Québec portion increased by about 17% between 1996 and 2017 (ISQ, 2017).

Assuming six months residence time to the seasonal population within MBB and the aforementioned loading rate and removal efficiency, estimated P loadings from septic systems into MBB are 4.65 T P/year (Appendix 1, Table A1-6). This estimate is general in nature and does not consider the disparity in compliance or vulnerability of septic systems. Many septic systems are installed near the basin's rivers and lakes, or even directly in the littoral and flood zones. According to the available data, there are more than 400 buildings including campsites in high current flood zones (0-20 years), flood risk zones, and river corridors (generally 0-2 years) in the MBB which cannot be connected to the municipal sewer systems (MELCCFP, 2022; MRCBM, 2016; MRC de Memphrémagog, 2009; Biron et al., 2013).

Point sources of P to MBB rivers from the residential and urban sectors of the basin are estimated to be 5.73 T P annually, including loadings from wastewater treatment plants, sewage overflows, and septic systems. These loadings do not include non-point source phosphorus emissions from the residential and urban sectors of MBB, which will be addressed through P specific export coefficient (kg P/year) in the metamodel development procedure.

Task 3b: Quantify Terrestrial P Inventories Throughout the Missisquoi Basin, Vermont

Deliverables completed for Task 3b, also documented in Bondeson et al. (2024), included:

- A land cover layer for the Missisquoi Basin, Vermont (MBB-VT)
- An agricultural land typology needed for the spatial estimation of P flows and soil metrics
- Manure application characteristics
- Estimated P flows (manure, fertilizer, crop harvest) and partial mass balance by HUC12 and agricultural land use
- Partial P mass balance for agricultural land in the entire MBB-VT
- Predicted soil metrics by HUC12 and agricultural land use
- P flows from wastewater systems
- P loading assumptions for non-agricultural land use

Land Use

The final land cover layer for the MBB-VT is shown in Figure 8 and summarized in Table 13 below.

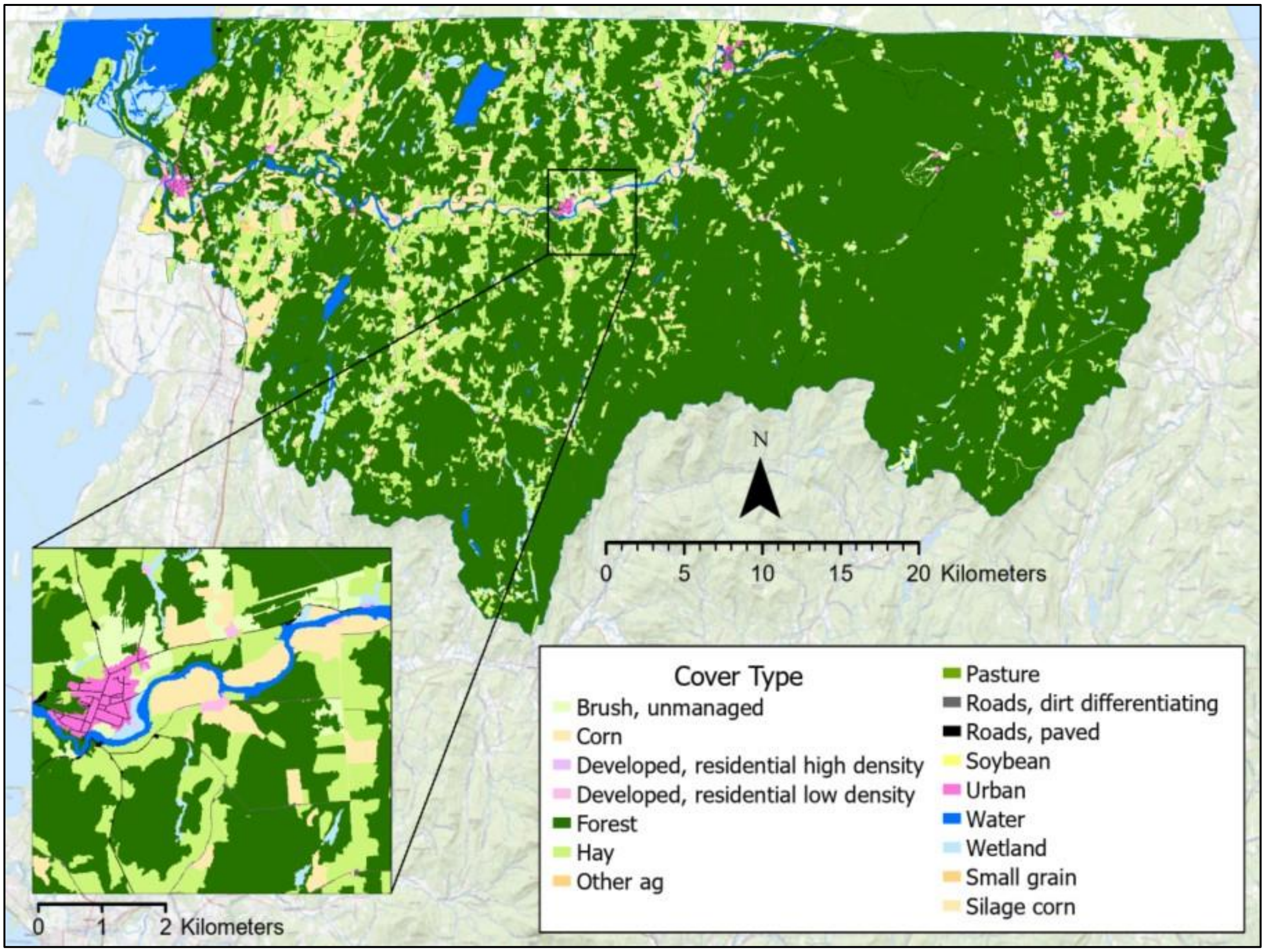

Figure 8. Land cover layer for the MBB-VT.

Table 13. Distribution of land cover within the MBB-VT.

Cover Type	Area (ha)	% of MBB-VT by area
Forest	131,277	65%
Hay	26,772	15%
Corn	8,258	6%
Water	5,847	4%
Wetland	4,557	3%
Brush, unmanaged	3,704	3%
Roads, dirt	1,114	1%
Developed, residential low density	870	1%
Roads, paved	781	0.4%
Urban	423	0.3%
Pasture	417	0.2%
Other ag	153	0.1%
Soybean	86	0.0%
Developed, residential high density	39	0.0%
Total	**184,297**	

Agricultural P Sources

Clusters of agricultural land field polygons for hay and corn for the MBB-VT watershed and the subset of fields having NMP data are shown in Figure 9. We used these clusters to distribute NMP data (from ~21% of agricultural land) to all corn and hay polygons in the MBB-VT.

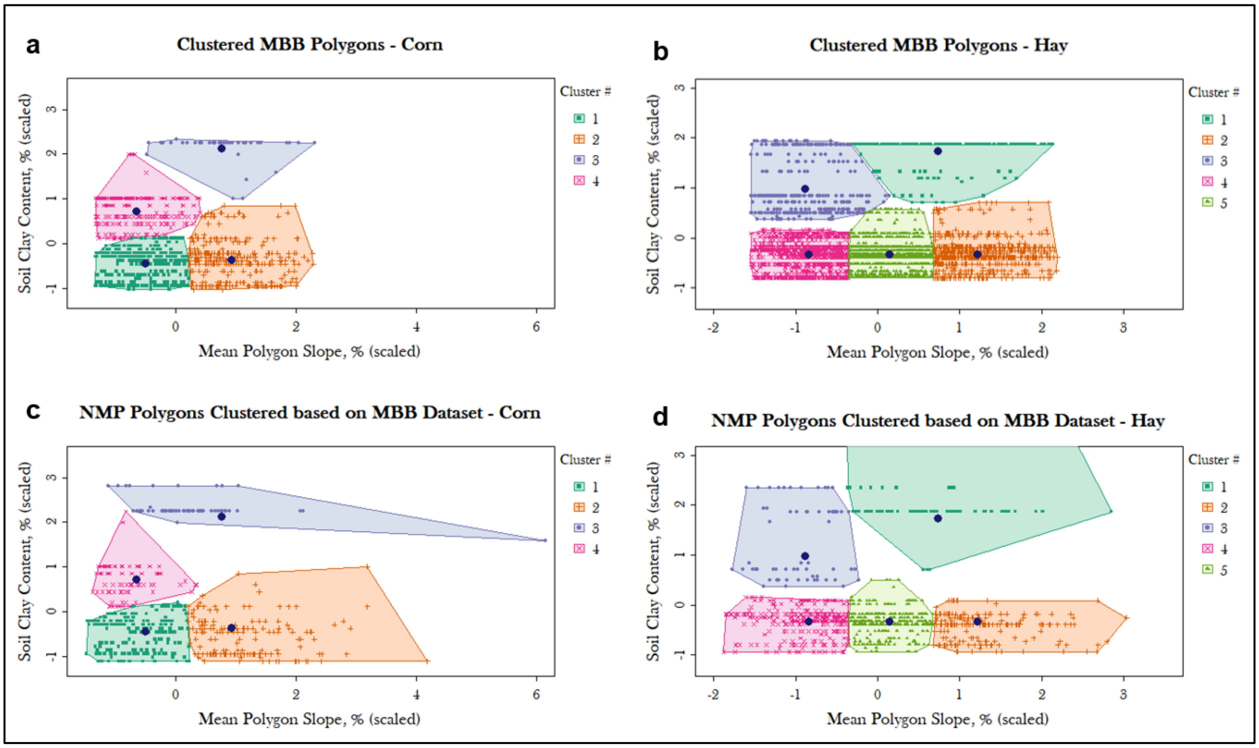

Figure 9. Clustered agricultural land polygons for the entire MBB-VT watershed (a, b) and the subset of fields having Nutrient Management Plan (NMP) data (c, d) (Bondeson et al., 2024).

Table 14 shows manure application characteristics of the NMPs used here.

Table 14. Temporal manure application characteristics in the NMPs (% of Total P applied).

Manure Application Period	Corn	Hay	All NMPs
April	4%	<1%	4%
May - September	14%	32%	46%
October - December 15	32%	18%	50%
Total	50%	50%	100%
Dominant incorporation method	Spade or injection	None	

A small amount of manure was applied in April, with May-September manure disproportionately applied to hay, and late fall manure disproportionately applied to corn. Across the NMPs, manure applied to corn cropland was almost entirely incorporated into the soil, while almost no manure applied to hay was incorporated. These trends are likely due to a variety of factors, including field access restrictions during wet times, ease of incorporating manure when a field is under tillage (i.e., corn), and planting and harvest timing. The VAAFM enforces a winter manure spreading ban, and thus no manure was spread in the MBB-VT between December 15 and April 1, when risk for P loss through overland transport is highest due to frozen soils inhibiting infiltration (Liu et al., 2018).

Our final estimates for manure P input, fertilizer P input, and crop P uptake by HUC12 and land use are included in Appendix 2. These estimates do not account for any inputs to or outputs from soybean fields (0.2% of watershed area), "other agriculture" (0.4% of watershed area), or pasture (1.2% of watershed area). Means reported here are spatially weighted. Mean manure P input for HUC12 watersheds ranged from 80 to 115 kg P_2O_5/ha-yr (35 to 50 kg P/ha-yr). For the entire MBB-VT, mean manure P inputs to corn and hay were 120 and 82 kg P_2O_5/ha-yr, respectively (52 and 36 kg P/ha-yr, respectively). The overall mean manure P input to agricultural land in the MBB-VT was 89 kg P_2O_5/ha-yr (39 kg P/ha-yr). Average fertilizer P inputs for HUC12 watersheds ranged from 0.2 to 4.1 kg P_2O_5/ha-yr (0.1 to 1.8 kg P/ha-yr). For the entire MBB-VT, mean fertilizer P inputs to corn and hay were 6.2 and 0.5 kg P_2O_5/ha-yr, respectively (2.7 and 0.2 kg P/ha-yr, respectively). The overall average fertilizer P input to agricultural land in the MBB-VT was 1.8 kg P_2O_5/ha-yr (0.8 kg P/ha-yr). Mean crop P uptakes for HUC12 watersheds ranged from 70 to 86 kg P_2O_5/ha-yr (31 to 38 kg P/ha-yr). For the entire MBB-VT, average crop P uptakes for corn and hay were 95 and 75 kg P_2O_5/ha-yr, respectively (41 and 33 kg P/ha-yr, respectively). The overall mean crop P uptake from agricultural land in the MBB-VT was 79 kg P_2O_5/ha-yr (34 kg P/ha-yr).

Partial P balance results by agricultural land cluster, accounting for manure inputs, fertilizer inputs, and crop harvest, are shown below for the NMP dataset (Figure 10) and for the entire MBB-VT (means of 10,000 iterations) (Figure 11).

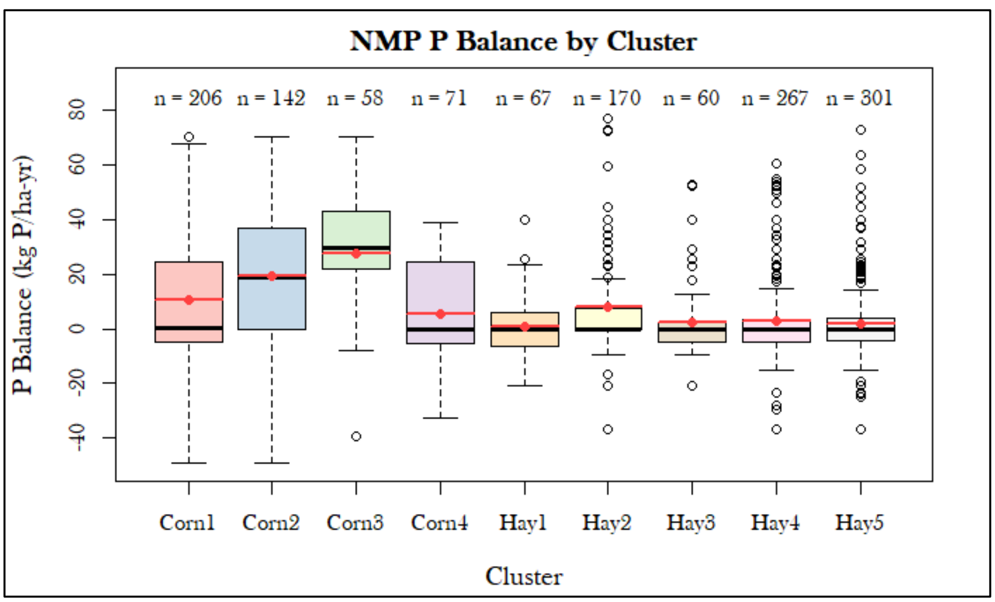

Figure 10. P balance for agricultural land clusters using the Nutrient Management Plan (NMP) dataset accounting for manure, fertilizer, and crop P uptake (Bondeson et al., 2024).

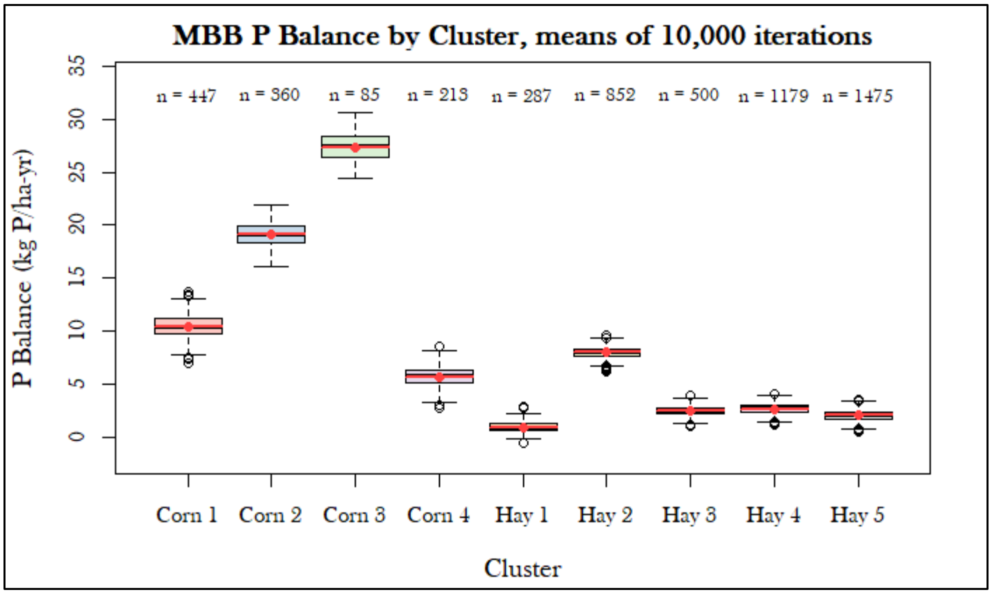

Figure 11. P balance for agricultural land clusters for the entire MBB-VT (mean values from 10,000 Iterations) accounting for manure, fertilizer, and crop P uptake (Bondeson et al., 2024).

Figure 12 depicts the results for 10,000 iterations of redistributing NMP information to the MBB-VT and calculating agricultural land partial P balance for the whole watershed. This distribution is normal, indicating consistent performance of the model. The estimated mean agricultural land partial P balance (± 1 standard deviation) for the MBB-VT watershed was 449,411 ± 18,001 kg P_2O_5/yr (196,249 ± 7,861 kg P/yr).

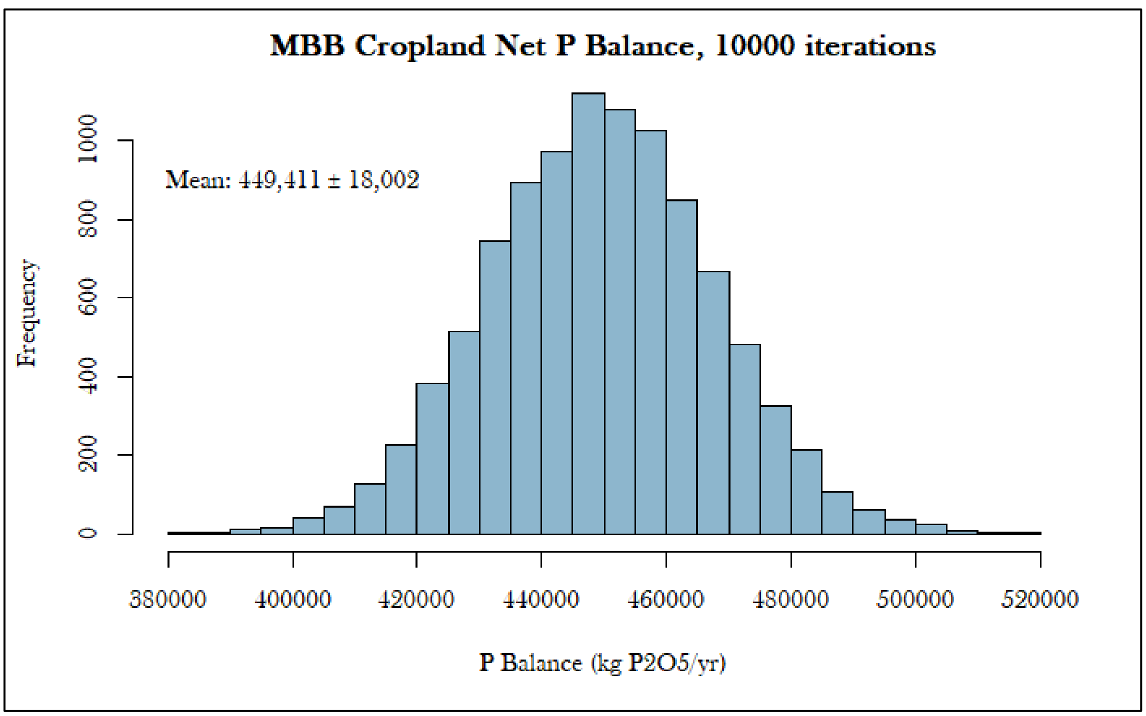

Figure 12. Overall estimated P balance for the agricultural portion of the MBB-VT accounting for manure, fertilizer, and crop P uptake (Bondeson et al., 2024).

The MBB-VT was characterized by an estimated average P balance (± 1 standard deviation) of 13 ± 0.5 kg P_2O_5/ha-yr (5.5 ± 0.2 kg P/ha-yr) for agricultural land overall, 31 ± 2 kg P_2O_5/ha-yr (13 ± 1 kg P/ha-yr) for corn cropland, and 7 ± 0.4 kg P_2O_5/ha-yr (3.23 ± 0.16 kg P/ha-yr) for hay cropland. Appendix 2, Tables A2-1 and A2-2 include results by HUC12 and agricultural land use. We also visualized these results spatially in Figure 13, which shows mean P balance for field polygons at the HUC12 level accounting for different agricultural land uses.

Predicted soil characteristics needed for the metamodel (M3P, M3Al, and M3P/M3Al on a mass basis) by HUC12 and agricultural land use are shown in Appendix 2, Tables A2-3, and A2-4. Spatially-weighted estimated mean M3P, M3Al, and M3P/M3Al at the HUC12 levels ranged from 44 to 61 mg P/kg, 898 to 1056 mg Al/kg, and 0.046 to 0.066, respectively. For the entire MBB-VT, using spatial weighting, mean estimated M3P was greatest for corn (58 mg P/kg) compared to hay (49 mg P/kg), soybean (30 mg P/kg), other agriculture (51 mg P/kg), and pasture (44 mg P/kg). Similarly, watershed-scale spatially-weighted mean P saturation (M3P/M3Al) was also greatest for corn (0.066) compared to the other land uses (0.036-0.051).

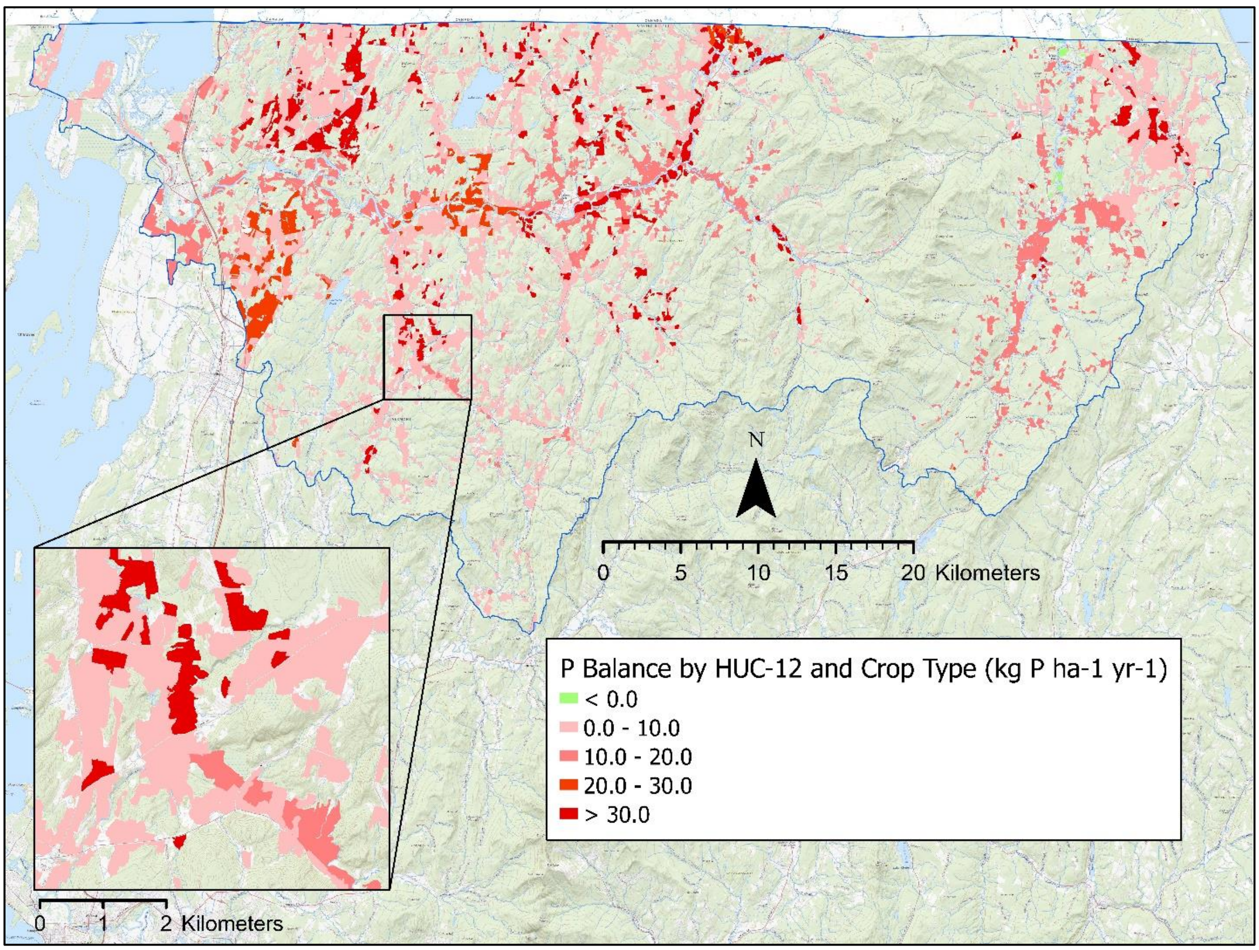

Figure 13. P Balance model predictions for MBB-VT agricultural land, using mean values for each unique HUC12 and crop type combination (Bondeson et al., 2024).

Human Waste

We estimated that annual effluent P load from WWTPs is 951 kg P/yr. Our estimate for the P load from septic systems ranges from a low estimate of 4,113 kg P/yr to a high estimate of

12,096 kg P/yr. We consider the lower estimate more realistic given that it is very unlikely all P input to septic systems is lost to surface waters. Therefore, we estimate that total loading from human waste in the MBB-VT is approximately 5,064 kg P/yr, accounting for both WWTPs and septic systems. Only one of the WWTPs land applies biosolids in the watershed. Two send sludge waste to WWTPs outside of the MBB, two to landfill solid waste, and the destination of solid waste from the remaining two is unknown. See Appendix 2, Tables A2-6, and A2-7 for more details.

Task 4: Quantify Inventories of P in Missisquoi Bay

Redox Sensitive Sediment P Inventory

The Missisquoi Bay redox sensitive phosphorus mass in the uppermost centimeter and the top 10 cm of sediment are provided in Table 15. Values of P mass for the entire bay and within the 2 m, 3 m, and 4 m depth contour are included.

Table 15. Redox sensitive sediment phosphorus mass for Missisquoi Bay.

Redox Sensitive Phosphorus Mass (x1,000 kg)					
Sediment Depth	**Whole Bay (77.5 km²)**	**> 2 m Water Depth (58.6 km²)**	**> 3 m Water Depth (39.7 km²)**	**> 4 m Water Depth (15.9 km²)**
0-1 cm	76 - 84	56 - 62	37 - 41	14-15
0-10 cm	1,157 - 1,398	869 - 1,045	601 - 720	237 - 285

Total Sediment P Inventory

The Missisquoi Bay total phosphorus mass in the uppermost centimeter and the top 10 cm of sediment are provided in Table 16. The values of P mass for the entire bay and within the 2m, 3m, and 4m depth contour are included.

Table 16. Total phosphorus sediment mass inventory for Missisquoi Bay.

Total Phosphorus Mass (x1,000 kg)				
Sediment Depth	**Whole Bay (77.5 km²)**	**> 2 m Water Depth (58.6 km²)**	**> 3 m Water Depth (39.7 km²)**	**> 4 m Water Depth (15.9 km²)**
0-1 cm	168 - 192	120 - 138	79 - 91	28 - 33
0-10 cm	3,390 - 3,791	2,410 - 2,704	1,561 - 1,760	561 - 640

Water Column Sediment P Inventory

The Missisquoi Bay water column phosphorus mass ranges derived from three different datasets are provided in Table 17. The UVM platform data were collected weekly from May through October 2017 to 2019 and include data collected at 0.5 meters below the surface and ~2-3 cm off the bottom. Thus, the data capture the widest range of concentrations, albeit at one site. The DEC data from 2017-2021 are composite water column samples and were collected biweekly across a similar seasonal period (Spring-Fall). The integrated sample thus spans a lower range of samples but may be more representative of average concentrations for the bay. The UVM spatial dataset only includes samples collected from 2-3 cm off the bottom during summer months when internal loading is more prevalent, thus it better captures a range of concentrations when the sediment may be a dominant source of P.

Table 17. Water column phosphorus mass inventory for Missisquoi Bay.

Water Column Phosphorus Mass (x1,000 kg)			
Dataset	**Soluble Reactive P**	**Dissolved P**	**Total P**
UVM Platform	3.0-196.2	3.4-224.6	44.5-320.0
UVM Spatial	NA	64.6-375.8	NA
VT DEC	NA	18.6-100	42.1-200.3

TASK 5: SWAT METAMODEL DEVELOPMENT

Model parametrization

P inventory data, land use, and geophysical attributes of MBB landscapes were spatially integrated for Vermont and Quebec in the ArcGIS geographic information system with a 10 m spatial resolution. Following the spatial structure previously described within the methodology sections, subwatershed units (SUB), land management units (MU), flow path units (FPU) and soil map polygons were intersected to generate the hydrological response units (HRU), which are the basic units of metamodel computation. Totals of 62,479 and 80,883 HRUs (0.01 ha minimum surface area), respectively, comprise the Vermont and Quebec sections of MBB metamodel, resulting in 143,362 HRUs across the bi-national watershed.

Geophysical properties

Vermont and Quebec have contrasting soil, and landscape properties. Table 18 compares the distribution of selected soil and landscape properties at the HRU scale for the agricultural land in Vermont and Quebec sections of the MBB, which exert a strong influence on runoff, sediment, and phosphorus yields estimates by the metamodel algorithms. The following gradients in soil and landscape properties are particularly important in explaining the hydrological responses across the entire MBB:

Soil P

Estimates of natural soil and soil test P estimated for Vermont tend to be lower than in Quebec. Since natural P estimates in Vermont were derived from the soil texture classes, the lower natural P levels for Vermont (-59%) reflect the coarser texture of its soils. Relatively higher soil test P in Quebec (+21%) and also relatively stronger P fixation potential (+10% in Al level) result in a difference of 9% in area-weighted P saturation ratios between Vermont (5.39) and Quebec (5.91).

Soil erodibility (K factor)

Agricultural soils of Vermont are more erodible than Quebec soils, as suggested by its higher (+21%) area-weighted erodibility factor. The important contrast in silt content of VT and QC soils (+28% in VT) explain this spatial gradient. Relatively more abundant clay soils occur in Quebec, with a 47% higher averaged clay content than Vermont soils devoted to agriculture. This gradient reflects the extent of the Saint-Lawrence plain geomorphic region occupying the north-western portion of the MBB.

Topography and land development

The agricultural landscapes differ in Vermont and Quebec due to both topography and land development patterns. The area-weighted slope average of cultivated fields is 6.16% in Vermont, which is 3.1-fold steeper than the Quebec average (1.99%). The dominance of Appalachian terrain within the cultivated sectors of the MBB in Vermont explains this topographic gradient. In Quebec, agricultural land use is concentrated in the western region, where terrain is flat to gently rolling, inherited from marine and alluvial deposits.

Although slopes are steeper in Vermont, Quebec cultivated fields generally have longer surface flow patterns. Flow path analysis of individual cultivated fields of VT and QC indicates that the average (area-weighted) flow length of Quebec fields (261.7 m) is 5.6-fold longer than Vermont fields (46.9 m). Longer slopes in QC are inherited from the historic land registry under the French regime, which imposed a division of long and narrow parcels typically along the slope gradient towards streams. Further levelling of the fields, following the subsurface drainage on the farmland, together with ditch filling, also promoted longer flow paths.

In the end, steeper field slopes in Vermont are a major contributor to the vulnerability to erosion of its agricultural soils. The average flow-length factor (USLE-LS) of the universal soil loss equation in Vermont (2.14) is 2.7-fold the Quebec average (0.79).

Another important contrast in land development of Vermont and Quebec is the predominant subsurface drainage of QC farmland, while subsurface drainage remains limited and primarily of irregular structure in Vermont. The metamodel parameterization for Quebec assigned systematic subsurface drainage to 53% of cropped land, predominantly within the flatter, easternmost section of MBB under grain corn production. Due to its limited extent, no subsurface drainage has been assigned to cropped acreages in Vermont.

Table 18. Selected distributions of geophysical characteristics of hydrological response units (HRU) for agricultural land use in Vermont (a) and Quebec (b) in MBB.

(a)

Vermont HRU parameter	Mean	Standard Deviation	Median	Max	Min	Area-Weighted Mean
Surface area (ha)	1.34	1.18	0.75	29.01	0.02	3.72
Mehlich-3 P (mg/kg)	50.5	13.8	48.2	144.0	4.0	50.8
Mehlich-3 Al (mg/kg)	1000	196	965	1513	576	993
P Saturation (M3P/M3Al)	5.31	1.75	4.73	18.22	0.68	5.39
Natural-P (mg/kg)	639.2	25.8	634.0	713.0	537.0	640.0
Hydrologic soil group [1]	7.10	1.12	7.00	9.00	3.00	7.02
Soil erodibility (K)	0.0322	0.0074	0.0342	0.0448	0.0029	0.0324
Sand (%)	49.5	18.8	47.0	97.9	0.0	47.7
Silt (%)	41.2	16.1	41.6	72.7	0.0	42.9
Clay (%)	9.4	5.2	7.0	100.0	0.5	9.2
Slope length (m)	37.9	35.4	15.0	714.0	2.0	46.9
Slope (%)	6.96	3.28	6.25	60.00	0.01	6.16
Slope-length MUSLE (LS)	2.02	1.52	1.26	19.68	0.03	2.14

[1] HSG: A=3; B=5; C=7; D=9

(b)

Quebec HRU parameter	Mean	Standard Deviation	Median	Max	Min	Area-Weighted Mean
Surface area (ha)	1.79	1.84	0.69	58.46	0.01	7.02
Mehlich-3 P (mg/kg)	50.1	32.9	38.0	348.5	18.0	64.1
Mehlich-3 Al (mg/kg)	1129	90	1110	1532	945	1108
P Saturation (M3P/M3Al)	4.54	3.083	3.800	22.75	1.90	5.91
Natural-P (mg/kg)	1014.8	311.0	868.0	1885.0	0.0	1017.2
Hydrologic soil group [1]	7.67	0.97	7.00	9.00	3.00	7.64
Soil erodibility (K)	0.0255	0.0061	0.0256	0.0562	0.0029	0.0256
Sand (%)	45.7	14.1	51.0	87.0	0.0	44.9
Silt (%)	30.5	8.9	35.0	52.3	0.0	30.9
Clay (%)	15.4	7.3	12.0	52.5	0.0	16.7
Slope length (m)	177.5	97.6	190.9	300.0	2.0	261.7
Slope (%)	2.59	2.60	1.02	60.00	0.00	1.99
Slope-length MUSLE (LS)	0.85	0.97	0.30	25.02	0.03	0.79

[1] HSG: A=3; B=5; C=7; D=9

Soil and Crop Management

Cropping systems, land drainage and phosphorus sources also differ significantly in Vermont and Quebec. Table 19 presents the crop acreages of both regions, together with their tillage systems distribution, as assigned to the initial metamodel parameterization (baseline scenario). Globally, hay is the dominant crop on predominantly dairy Vermont farmland (75%), in rotation with silage corn (23%). Most of silage corn acreages (57%) have been assigned to reduced tillage system in fall period, while 20% and 18%, respectively are considered under reduced spring tillage or no-till. Only 5% of corn acreages are thus assigned to moldboard ploughing.

Quebec cropped acreages are hay (39%), grain corn (31%), soybean (20%), and small grain (6%). Silage corn production is limited to 3% of crop acreages. Regarding tillage systems, 61%, 20%, and 18% of annual crops (corn, soybean, small grains) in the Quebec section of MBB have been assigned to fall reduced tillage, no-till and fall plowed, respectively.

Over 11,000 ha of land in the Quebec section of the MBB have been attributed to meadows. These areas correspond to agricultural land use, from SIEF (MERN, 2021b) land inventory, without appearing on crop insurance board maps (La Financière, 2021). An extensive, natural prairie land use has been attributed to these surface areas. A significant part of this unclassified agricultural land area incudes annual crops acreages, where owners do not insure their production.

Table 19. Crops and related tillage system in Vermont (a) and Quebec (b) farmland within the baseline scenario of metamodel parameterization.

(a)

Vermont	Fall Tillage		Reduced Fall Tillage		Reduced Spring Tillage		No Tillage		Total Area
	(ha)	(%)	(ha)	(%)	(ha)	(%)	(ha)	(%)	(ha)
Silage Corn	389	5%	4,685	57%	1,680	20%	1,500	18%	8,255
Hay	0	0%	0	0%	0	0%	26,759	100%	26,759
Other Agr.	0	0%	0	0%	0	0%	153	100%	153
Pasture	0	0%	0	0%	0	0%	416	100%	416
Soybean	0	0%	0	0%	0	0%	86	100%	86
Total	**389**	**1%**	**4,685**	**13%**	**1,680**	**5%**	**28,914**	**81%**	**35,669**

(b)

Quebec	Fall Tillage		Reduced Fall Tillage		Reduced Spring Tillage		No Tillage		Total Area
	(ha)	(%)	(ha)	(%)	(ha)	(%)	(ha)	(%)	(ha)
Grain corn	2,114	24%	4,596	52%	0	0%	2,159	24%	8,869
Hay	546	5%	2	0%	0	0%	10,420	95%	10,969
Other agricultural	54	14%	37	9%	2	0%	304	77%	396
Meadows	0	0%		0%	0	0%	11,196	100%	11,196
Silage corn	198	21%	523	55%	21	2%	215	22%	957
Small grain	204	13%	786	50%	27	2%	562	36%	1,578
Soybean	619	11%	4,414	78%	54	1%	552	10%	5,640
Total	**3,736**	**9%**	**10,359**	**26%**	**104**	**0%**	**25,408**	**64%**	**39,606**

P inputs

The allocation of phosphorus inputs to Quebec and Vermont farmland within the metamodel parameterization procedure highlight distinct P management practices amongst the regions. The area-weighted rates of P applied to farmland in Vermont and Quebec are estimated to be 82 and 58 kg P_2O_5/ha, respectively (Table 20.) While 98% of P applied on Vermont farmland is from organic sources, essentially manure, Quebec has a substantial mineral P input (27% of total P). Corn and hay acreages received most of phosphorus applied to crop land in both regions, in proportions of 98% (VT) and 69% (QC) of total P applied. Manure spreading in early fall following soybean harvest in Quebec accounts for 19% of total P applied.

Table 20. Mineral and organic mass and specific P inputs to Vermont (a) and Quebec (b) farmland in the baseline scenario of metamodel parameterization.

(a)

Vermont	Mineral P Input (kg P_2O_5)	Organic P Input (kg P_2O_5)	Total P Input (kg P_2O_5)	Total Area (ha)	Total Specific P Input (kg P_2O_5/ha)
Corn	50,959	986,176	1,037,134	8,255	126
Hay	13,105	2,199,956	2,213,062	26,759	83
Other Ag	0	0	0	153	0
Pasture	0	0	0	416	0
Soybean	0	0	0	86	0
Total	64,064	3,186,132	3,250,196	39,606	82

(b)

Quebec	Mineral P Input (kg P_2O_5)	Organic P Input (kg P_2O_5)	Total P Input (kg P_2O_5)	Total Area (ha)	Total Specific P Input (kg P_2O_5/ha)
Grain corn	74,123	518,366	592,489	8,869	67
Hay	232,561	317,416	549,977	10,969	50
Other agricultural	14,627	824	15,452	396	39
Meadows	10,620	0	10,620	11,196	0
Silage corn	15,274	47,272	62,546	957	65
Small grain	11,369	100,860	112,229	1,578	71
Soybean	93,205	224,693	317,898	5,640	56
Total	**451,779**	**1,209,433**	**1,661,211**	**39,606**	**42**

Regarding periods and incorporation mode, all hay and corn lands in Vermont were allocated manure inputs in the model parameterization procedure, predominantly during summer and late fall periods (Table 21a). Given that manure was considered surface applied on hay fields, and systematically incorporated on corn fields, unincorporated manure mode was assigned to 80% of manured acreages in Vermont.

In Québec, manure inputs were attributed to 52% of cropped land. Given that manure inputs were predominantly associated with annual crops, manure incorporation was assigned to 83% of manured acreages. Following the distinct management scenarios of individual crops, the proportions of manured acreages in spring, summer, early fall and late fall are, 46%, 26%, 19% and 9%, respectfully (Table 21b).

Table 21. Period and incorporation rate of manure per crop class assigned to Vermont (a) and Quebec (b) farmland within the baseline scenario of metamodel parameterization.

(a)

Vermont	Spring Pre-Seeding (ha)	Summer (ha)	Early Fall (ha)	Late Fall (ha)	Total Manured Area (ha)	Total Agric. Area (ha)	Percent Manured (%)	Percent Incor-porated (%)
Corn	992	3,205	0	5,063	9,260	8,255	100%	100%
Hay	132	21,680	0	15,248	37,060	26,759	100%	0%
Other Ag	0	0	0	0	0	153	0%	
Pasture	0	0	0	0	0	416	0%	
Soybean	0	0	0	0	0	86	0%	
Total	**1,124**	**24,884**	**0**	**20,311**	**46,320**	**35,669**	**98%**	**20%**

(b)

Quebec	Spring Pre-Seeding (ha)	Summer (ha)	Early Fall (ha)	Late Fall (ha)	Total Manured Area (ha)	Total Agric. Area (ha)	Percent Manured (%)	Percent Incor-porated (%)
Grain corn	5,065	201	3	1,284	6,553	8,869	74%	98%
Hay	462	3,084	44	0	3,590	10,969	33%	32%
Other agricultural	0	10	0	0	10	396	2%	0%
Meadows	0	0	0	0	0	11,196	0%	
Silage corn	547	45	0	0	592	957	62%	99%
Small grain	707	593	0	0	1,300	1,578	82%	100%
Soybean	0	0	2 814	0	2,816	5,640	50%	100%
Total	**6,781**	**3,934**	**2,861**	**1,284**	**1, 860**	**39,606**	**38%**	**83%**

Metamodel Calibration and Validation

Because the metamodel development was derived from deterministic (SWAT) modeling calibrated outputs and observations from the MBB region (Deslandes et al., 2006; Michaud et al., 2007), the calibration process relied essentially on the modulation of the agroclimatic factors of the MM. As presented in the methodology section, initial agroclimatic parameters values were derived from precipitation zones based on elevation. The parameters were further globally adjusted such that phosphorus yields projected by the metamodel: 1) compare optimally to the variability in average P yields estimated for the eleven MBB water quality monitoring stations operated by MELCCFP (Simoneau, 2019), and 2) reflect the basin-wide loading estimates referenced within the total maximum daily load procedure for Missisquoi Bay (TMDL-EPA) for the reference period 2002-2010 (US EPA, 2016). Because the annual P flux estimated for Quebec by US EPA (2016) and Simoneau (2019) for the common 2001-2010 period were 52 and 72.4 tons of total P, respectively, loading estimates derived from MELCCFP stations data were normalized using a 1.39 ratio (i.e., 72.4 / 52). The normalization of Simoneau (2019) P loadings estimates was supported by the comparison with independent P fluxes estimates from IRDA, VDEC, and USGS (Table 22), which are generally higher than Simoneau's (2019) for the respective periods. Differences in sampling protocols, namely the targeting of peak flow events by IRDA, USGS, or VDEC, presumably explain relatively higher P loadings than Simoneau (2019).

Table 22. Annual specific total P loadings from monitored Pike River subwatersheds (kg P/ha).

Subwatershed	MELCCFP [1]	MELCCFP Normalized for TMDL [2]	IRDA [3,4,5]	VDEC, MELCCFP [6]	USGS [7]
Ruisseau Au Castor	1.13	1.60	1.77 [3]	1.57	
Ewing	1.00	1.42	1.74 [4]	1.20	
Walbridge	0.54	0.77	0.80 [5]		
Pike downstream	0.56	0.80		0.62	0.78

[1] MELCCFP, Quebec, 1999-2017 period (Simoneau, 2019).
[2] MELCCFP, Quebec, 1999-2017 period (Simoneau, 2019), normalized for TMDL-EPA MBB reference loading 2001-2010 (US EPA, 2016).
[3] IRDA, Micro-watershed 2001-2011 period (Madramootoo et al., 2012; Michaud et al., 2002, 2004).
[4] IRDA, Micro-watershed 2007-2011 period (Madramootoo et al., 2012; Michaud et al., 2009a).
[5] IRDA, Micro-watershed 2001-2006 period (Michaud et al., 2009b)
[6] VDEC, MELCCFP. 2008. 2002-2005 period (Smeltzer and Simoneau, 2008).
[7] USGS. 2013. 1990-2011 period (Medalie, 2013).

Table 23 presents the metamodel projections of annual total phosphorus yields and average annual total P yields adapted from the eleven MELCCFP subwatershed monitoring data sets and TMDL basin wide reference loadings. Metamodel projections of basin-scale P annual loadings from Vermont and Quebec reached 105 and 71 Tons Total P, respectfully. These loading estimates represent a -23% (VT) and -2% (QC) difference compared to the 2016 TMDL's reference loadings. Metamodel loading estimates at the subwatershed scale are generally within 20% of the reference loadings from the monitoring stations, except for the Pike upstream, Morpions, and Ewing monitoring locations (Table 23). The significantly higher MM loading estimates for the Pike River upstream subwatershed in Vermont (0.73 kg P/ha), with respect to the monitoring station close to Quebec/Vermont border (0.39 kg P/ha) presumably reflects the effect of the Lake Carmi. Considering the morphology of the subwatershed, the difference in projected emissions and subwatershed outlet load more likely reflect the phenomenon that Lake Carmi acts as a catch basin for the dominantly sediment-bound phosphorus emitted from the surrounding farmland. Recurrent and severe algal blooms observed in the lake support this hypothesis.

For Ruisseau Aux Morpions and Ewing River subwatersheds, located within the intensive agricultural production zone in the downstream portion of Pike River, two factors are considered to contribute to the underestimation of the metamodel projections of P loadings. First, the underestimated annual crops acreage, considered by default as perennial forage by the metamodel, likely contributes to the lower subwatershed loadings. Also, organic soils under annual crop production comprise a significant part of these neighbouring subwatersheds. Monitoring of micro-watersheds from Morpions (Ricard et al., 2022) and from another black soils dominated subwatershed from the Monteregie region in Quebec (Michaud et al., 2012) stressed the vulnerability of organic soils in emitting elevated sediment and P loadings. Considering that the metamodel algorithms were developed and validated solely on mineral soils, its ability to predict organic soils' hydrology and P mobility are less comprehensively validated, and more likely underpredicted P fluxes.

Considering the eleven subwatersheds reference loadings and TMDL basin wide projection, the metamodel projections explain 94% of the overall variability in annual specific total phosphorus loading across the Missisquoi Bay basin (Figure 14). The slope regression coefficient (0.87) suggests that projected P loadings, globally, remain 13% below reference loadings. Conceptually, a lower metamodel projected P loading, with respect to reference P loading, is expected for two reasons. First, point source P loadings are not accounted for within the MM estimates. Referring to EPA-TDML (US EPA, 2016) and Quebec-MELCCFP (2021b), wastewater annual P loads to MBB reach approximately to 2.5 tons of phosphorus per year, which represents 1.2% of yearly total P load to the bay. Secondly, in-stream P sources from downstream sections of MBB tributaries may also be partly unaccounted for by the MM, whose algorithms have been validated at micro-watershed scale (10-30 km^2). The phosphorus TMDL (US EPA, 2016) for the Missisquoi Bay allocate 29.5% of total P loading to in-stream sources in Vermont. In Quebec, streambank erosion and resuspended sediments contribution to total P load were estimated to be 21% of the TP (Michaud et al., 2019b).

Table 23. Specific total annual phosphorus loadings projected by the metamodel and reference loadings derived from the MELCCFP monitoring datasets for eleven water quality monitoring stations used for the MM calibration procedure.

Subwatershed	Area (ha)	Specific Loading (kg P/ha)		
		Reference	Projected	Dev.
Missisquoi Upstream (VT)	36,010	0.28	0.30	7%
Missisquoi Downstream (VT, QC)	94,000	0.34	0.36	6%
Sutton (QC)	14,900	0.34	0.36	6%
Pike Upstream (VT)	9,600	0.39	0.73	89%
Walbridge (QC)	2,790	0.77	0.85	10%
Morpions (QC)	11,230	1.48	0.93	-37%
Pike Downstream (VT, QC)	58,770	0.81	0.72	-11%
Ewing (QC)	2,950	1.42	0.91	-36%
Castor (QC)	1,420	1.57	1.39	-12%
Rock Upstream (VT)	7,130	1.19	1.22	3%
Rock Downstream (VT, QC)	12,510	1.02	1.25	22%
MBB (QC)	135,990	0.53	0.52	-2%
MBB (VT)	184,152	0.74	0.57	-23%

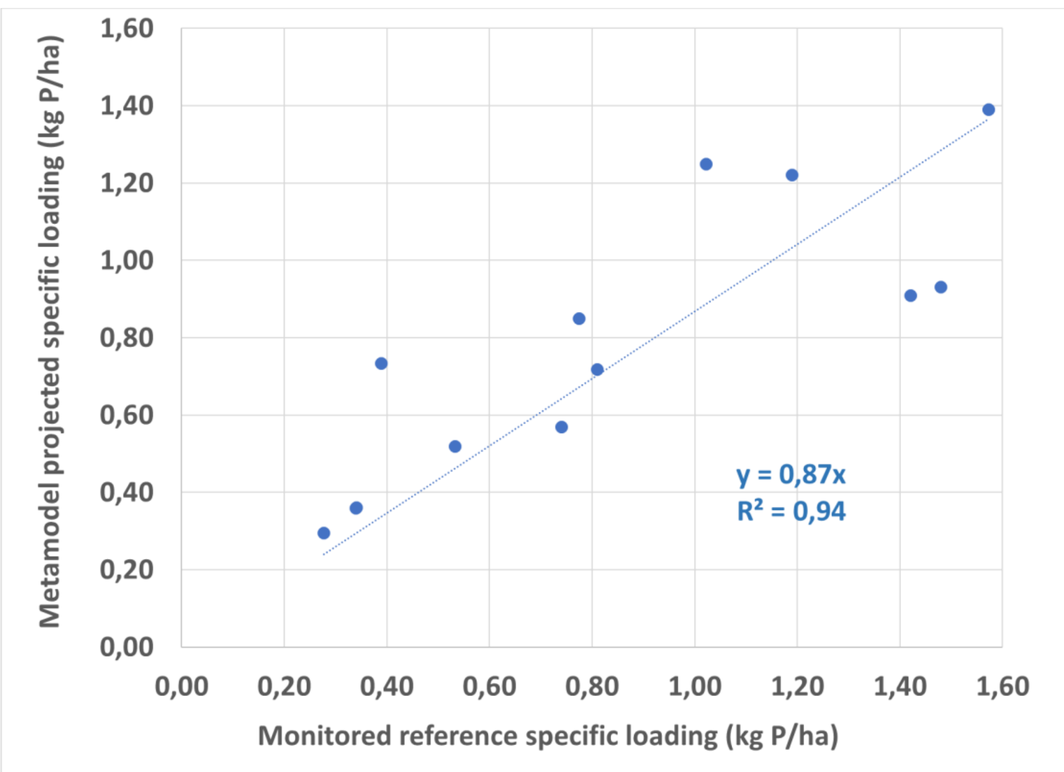

Figure 14. Specific total annual phosphorus loadings projected by the metamodel reference loadings derived from the MELCCFP monitoring datasets for eleven water quality monitoring stations used for the MM calibration procedure.

Spatial Heterogeneity of Metamodel Projections

Considering the diversity of landscapes and crop management systems across the MBB, the metamodel projections of total P loadings across the study area are highly variable. Figure 15 illustrates the variability of projected sediment and phosphorus specific yields at hydrologic response unit scale (HRU) per crop class across the Missisquoi Bay basin. Although a general gradient in projected specific sediment and P loads between crop classes, from hay to annual crops, is suggested by the illustration, significant variability per crop class is also observed. This variability reflects the effects of both geophysical and management-related factors on projected P loadings. The resulting spatial heterogeneity in sediment and P loadings projected by the MM is illustrated in Figure 16 for the Rock River subwatershed.

Amongst geophysical drivers of sediment and P projected emissions, slope gradient, hydrologic soil grouping, and soil erodibility are the most important. Regarding crop and soil management, the erosion protection given by the hay cover translates into relatively lower sediment and P emissions. However, soil P level together with manure management (rate, timing, and incorporation mode) contribute to the variability in specific P yields at the HRU scale on hay fields. For annual crops, sediment-bound P is largely driven by the crop cover, where silage corn and soybean fields are the most vulnerable. For grain corn and small grains, the tillage system (from fall plowing to no-till) significantly influence the sediment load, thus the total P projected emission.

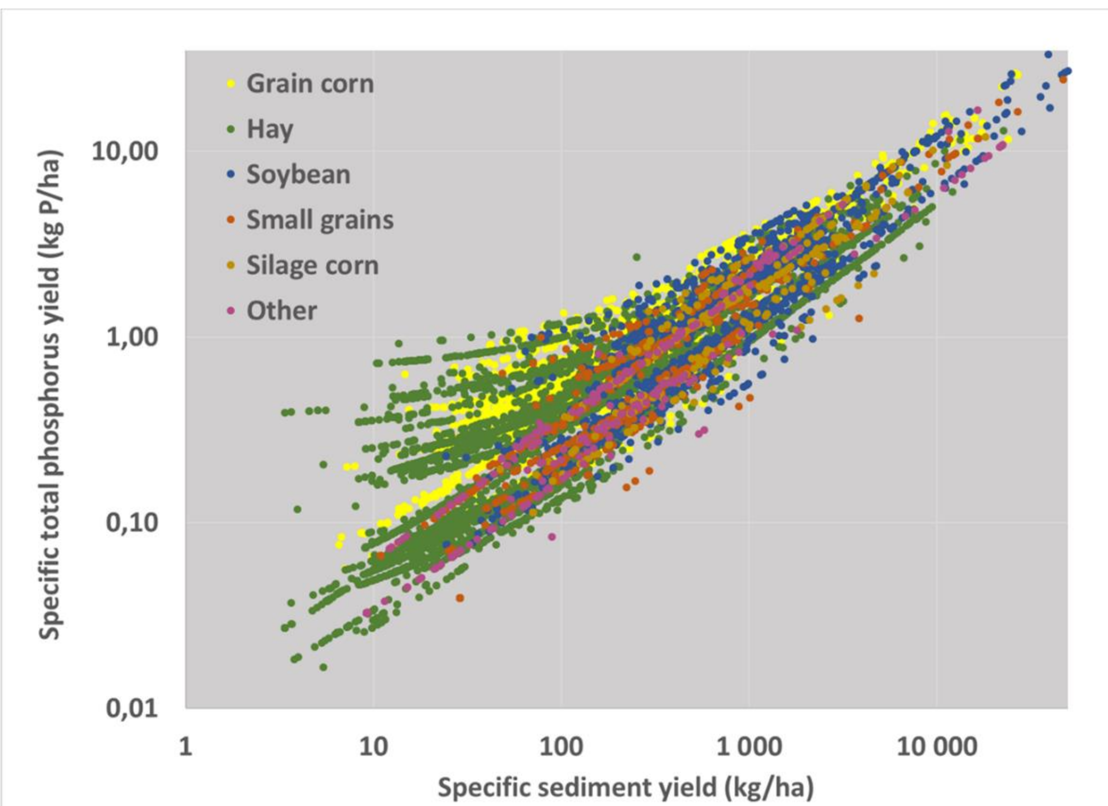

Figure 15. Variability of sediment and phosphorus specific yields at hydrologic response unit scale (HRU) per crop class across the Missisquoi Bay basin.

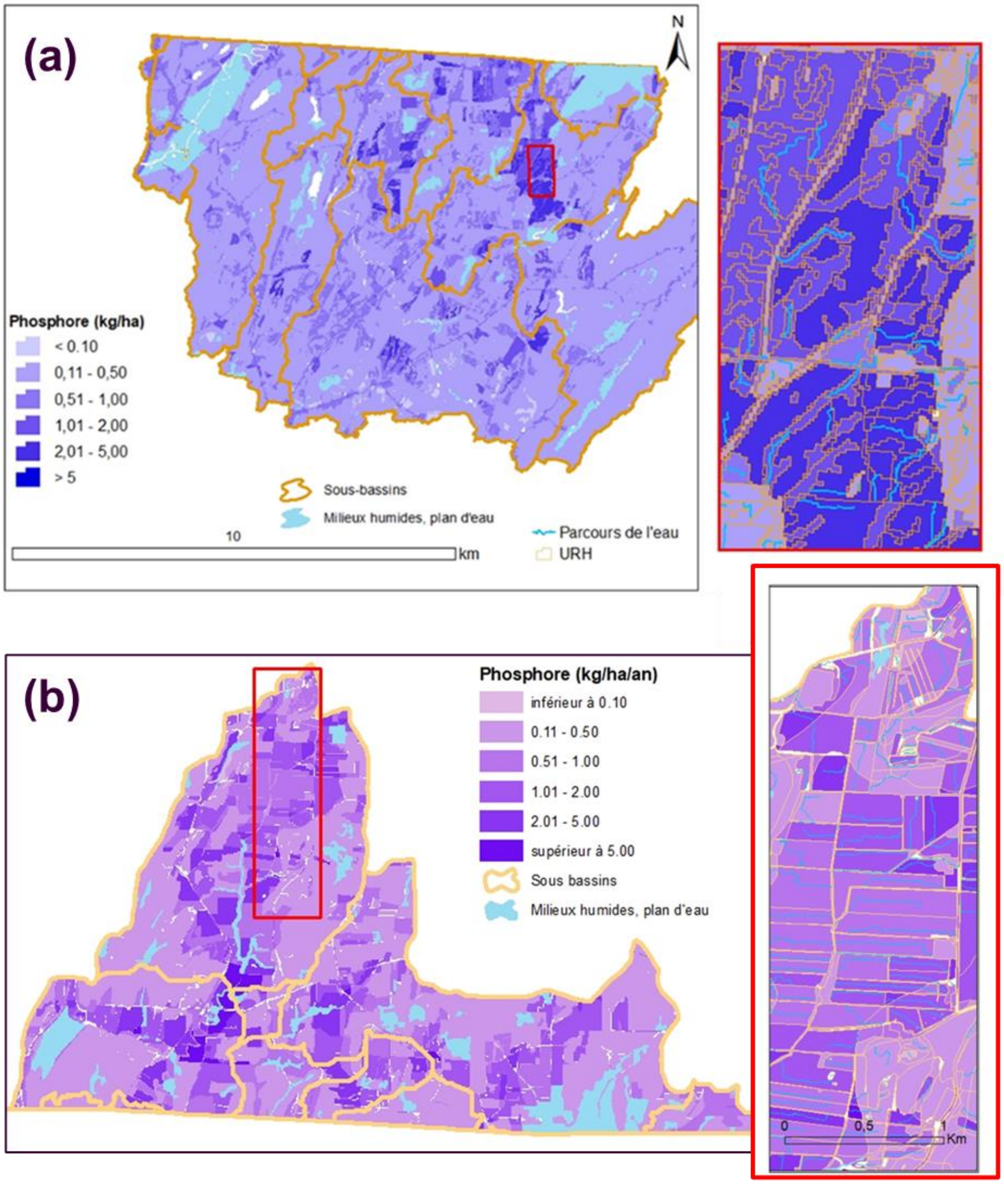

Figure 16. Metamodel spatial projections of total phosphorus loadings for Vermont (a) and Quebec (b) portions of Rock River watershed.

Tables 24 and 25 present the projected sediment and total phosphorus loadings per land use class within the Missisquoi Bay basin in Vermont and Quebec, respectively. As presented previously in the methodology section, P loadings for non-agricultural land use are estimated though P export coefficients calibrated through previous deterministic modeling studies. The same specific P export coefficients have been applied throughout the basin, for both VT and QC portions of the basin. Conversely, phosphorus loadings for agricultural land use, on average, show significant variability per crop class, in the Vermont and Quebec regions. Typically, silage corn and soybean acreages have the highest P loadings, in relation to their relatively scarce crop residue protection and related vulnerability to erosive processes. The "other crop" class also shows relatively elevated sediment and P loadings, as horticultural cropping factors have been considered within the MM parameterization. Grain corn and small grain classes, primarily in Quebec, have relatively lower specific sediment and P loadings, reflecting the adoption of conservation tillage systems and their efficient erosion protection.

Comparison of specific sediment and phosphorus loadings across crop classes and regions indicate a strong gradient between Vermont and Quebec metamodel estimates. The contrast is particularly significant for the corn and hay classes, both abundantly represented in VT and QC This projected discrimination in P specific loadings illustrates the MM cumulative sensitivity to both geophysical and management factors. An important factor explaining differences in sediment and P loadings is the omni-presence of subsurface drainage systems in Quebec, which translate to significantly lower surface runoff rates. For example, the average annual surface runoffs for grain corn and hay projected for Quebec are 91 and 112 mm, respectively. For silage corn and hay in Vermont, surface runoff averages are 142 and 154 mm/year, respectively, which represent 56 and 37% higher runoff rates, in part due to the higher precipitation and snowmelt annual rates in the hillier terrain of Vermont.

The different terrains in Vermont in Quebec also influence sediment and P yields. As previously described in the model parameterization section, the area-weighted slope average of cultivated fields is 6.16% in Vermont, which is 3.1-fold steeper than the Quebec average (1.99%). Considering the MUSLE algorithm used by the MM for sediment yield projection, the difference in slope and flow-length factor (USLE-LS) implies that sediment loadings in Vermont are 2.7-fold higher than in Quebec, all other factors of crop management and soil properties being equal. Higher soil erodibility previously reported for Vermont soils (21% on average) also contributes to elevated sediment yields. Finally, the dominance of conservation tillage over grain corn stubble in Quebec offers a relatively stronger attenuation of erosive process relative to low residue silage corn in Vermont. The interaction of subsurface drainage, terrain slopes, soil erodibility, and crop residue cover have a multiplicative effect within the metamodel algorithms, which finally express a strong spatial differentiation in sediment and related P loadings estimates across the Missisquoi Bay watershed from Quebec to Vermont.

Table 24. Projected total and specific sediment and phosphorus loadings per land use class in Missisquoi Bay basin in Vermont.

Land use	Area (ha)	Annual Sediment Loading (T TSS)	Annual Total P Loading (kg P)	Annual Specific Sediment Loading (T TSS/ha)	Annual Specific Total P Loading (kg P/ha)
Corn	8,240	84,326	38,579	10.23	4.68
Hay	26,696	42,768	44,020	1.60	1.65
Other Ag	153	665	1,293	4.36	8.48
Soybean	86	218	149	2.53	1.73
Pasture	416	966	701	2.32	1.68
Total - Agricultural	**35,592**	**128,944**	**84,743**	**3.62**	**2.38**
Brush, unmanaged	3,631		254		0.07
Developed, High Density	39		381		9.80
Developed, Low density	868		4,364		5.03
Forest	131,239		6,562		0.05
Roads, Dirt	1,109		5,402		4.87
Roads, Paved	778		1,602		2.06
Urban	423		681		1.61
Water	5,840		0		0.00
Wetland	4,555		5,010		1.10
Total - Non-Agricultural	**148,480**		**24,257**		**0.16**
Wastewater Treatment Plants			951		
Total Basin	**184,072**		**109,951**		**0.60**

Table 25. Projected total and specific sediment and phosphorus loadings per land use class in Missisquoi Bay basin in Quebec.

Land use	Area (ha)	Annual Sediment Loading (T TSS)	Annual Total P Loading (kg P)	Annual Specific Sediment Loading T TSS/ha)	Annual Specific Total P Loading (kg P/ha)
Grain corn	8,869	4,984	13,594	0.56	2.73
Silage corn	957	1,321	2,210	1.38	1.67
Small grain	1,578	857	1,888	0.54	2.20
Soybean	5,640	7,793	12,434	1.38	1.60
Hay	10,960	3,894	8,394	0.36	2.16
Other agricultural	396	312	426	0.79	1.37
Pasture	11,194	6,614	8,791	0.59	1.33
Total - Agricultural	**39,595**	**25,775**	**47,736**	**0.65**	**1.85**
Brush, unmanaged	4,733		331		0.07
Developed, Low density	429		1,678		3.91
Developed, High Density	398		3,012		7.57
Forest	79,793		7,979		0.10
Roads, Dirt	1,797		8,749		4.87
Roads, Paved	872		1,796		2.06
Urban	1,187		1,714		1.44
Water	5,876		0		0.00
Wetland	1,300		1,430		1.10
Total - Non-Agricultural	**96,384**		**26,689**		**0.28**
Wastewater Treatment Plants			1,070		
Total Basin	**135,978**		**75,495**		**0.56**

TASK 6: SIMULATE BAY MASS BALANCE INPUT CHANGES UNDER ALTERNATIVE CONDITIONS

This section presents the results of metamodel simulations of sediment and P loadings from alternate management scenarios. A total of 90 alternate management scenarios have been generated for the MBB. The scenarios captured the simple and interactive effects of the four groups of agricultural best management practices (BMPs) applied to Vermont and Quebec rural landscapes, assuming different adoption rates (20, 50 and 100% of cropped land), and under a random or targeted implementation on most critical P sources areas (CSAs). Land conversion scenarios of most vulnerable CSAs have also been considered to complement the agricultural BMPs. Finally, abatement of P loadings from developed land uses are cumulated, to generate a complete portrait of potential reductions in phosphorus emissions to surface waters of Missisquoi Bay watershed. To support the coupling of the terrestrial P emission model to the Missisquoi Bay model, P loadings from alternate management scenarios have been aggregated to tributary scale, namely Missisquoi, Pike and Rock rivers.

Agricultural BMPs Simple and Multi-Group Effects

The three groups of agricultural BMPs had distinct effects on sediment and total P projected emissions. Nutrient management group BMPs (BMP-1) solely affect soluble P emissions, and its effects depend on soil P level, as well as P input rate and mode (incorporation of nutrient or not). Cropping system BMPs (BMP-2) have important effects on erosion processes and sediment yield. Projected sediment yields translate into particulate P loadings, typically the most important component of total P in the Missisquoi Bay watershed. Finally, the riparian zone BMP group (BMP-3) solely affects particulate P emissions, though empirical abatement ratios documented in the Missisquoi Bay basin.

Tables 26 and 27 present the simple and multiple group average effects of the agricultural BMPs on sediment and P emissions per class of cropped land. The efficiencies of BMP combinations are expressed by the percentage of abatement of the sediment or P emissions for a given crop class and a given BMP scenario, with respect to the baseline simulation. On average, cropping system BMPs have the largest potential influence on P emissions. However, their effects on P emissions are highly variable, depending on the original baseline emissions, which are largely driven by the inherent properties of the soil (P level, erodibility, drainage class) and the landscape (slope gradient and length). Nutrient management effects (BMP-2), where applicable, are less variable and respond to soil P richness and rate of inputs. Finally, the riparian zone management effect is proportional to the baseline particulate P loading, to which a constant abatement rate is applied.

Table 26. Projected average sediment and P loadings for baseline and alternate agricultural management scenarios for the Vermont section of MBB.

			Cropped Land Use				Cropped Land Use	MBB
			Corn	Soybean	Hay	Other [2]	Total	Total [3]
Baseline scenario	**Area**	**(ha)**	8,240	86	26,696	153	35,175	184,072
	Sediment loading	**(T TSS)**	84,326	218	42,768	665	127,978	
	Total P loading	**(kg Total P)**	38,579	149	44,020	1,293	84,041	109,951
Scenario BMP-1	**Sediment loading**	**(T TSS)**	84,326	218	42,768	665	127,978	
(Nutrient MGT)	**Abatement**	**(%)**	0%	0%	0%	0%	**0%**	
	Total P loading [1]	**(kg Total P)**	38,579	149	3 4291 [1]	1,293	74,312	100,222
	Abatement	**(%)**	0%	0%	-22%	0%	**-11.6%**	-8.8%
Scenario BMP-2	**Sediment loading**	**(T TSS)**	25,385	131	42,768	665	68,950	
(Crop system MGT)	**Abatement**	**(%)**	-69.9%	-40.0%	0.0%	0.0%	**-46.1%**	
	Total P loading	**(kg Total P)**	17,038	106	44,020	1,293	62,458	88,367
	Abatement	***(%)***	-55.8%	-28.7%	0.0%	0.0%	**-25.7%**	-19.6%
Scenario BMP-3	**Sediment loading**	**(T TSS)**	68,533	177	34,759	541	104,010	
(Riparian zone MGT)	***Abatement***	***(%)***	-18.7%	-18.7%	-18.7%	-18.7%	**-18.7%**	
	Total P loading	**(kg Total P)**	31,754	124	38,833	1,058	71,770	97,569
	Abatement	***(%)***	-17.7%	-16.9%	-11.8%	-18.2%	**-14.6%**	-11.3%
Scenario BMP-1 + 2	**Sediment loading**	**(T TSS)**	25,385	131	42,768	665	68,950	
		(%)	-69.9%	-40.0%	0.0%	0.0%	**-46.1%**	
	Total P loading	**(kg Total P)**	17,038	106	34,291	1,293	52,729	78,638
	Abatement	***(%)***	-55.8%	-28.7%	-22.1%	0.0%	**-37.3%**	-28.5%
Scenario BMP-1+2+3	**Sediment loading**	**(T TSS)**	20,631	106	42,768	541	64,047	
	Abatement	***(%)***	-75.5%	-51.2%	0.0%	-18.7%	**-50.0%**	
	Total P loading	**(kg Total P)**	14,248	89	34,291	1,058	49,686	75,596
	Abatement	***(%)***	-63.1%	-40.2%	-22.1%	-18.2%	**-40.9%**	-31.2%
Scenario BMP-4	**Sediment loading**	**(T TSS)**	2,319	12	20,773	53	23,157	
(Land conversion)	***Abatement***	***(%)***	-97.2%	-94.5%	-51.4%	-92.1%	**-81.9%**	
	Total P loading	**(kg Total P)**	3,894	25	22,709	79	26,706	*52,516*
	Abatement	***(%)***	-89.9%	-83.0%	-48.4%	-93.9%	**-68.2%**	-52.2%

[1] Considering only the hay acreages where manure P is applied (2 4476 ha), the P loading abatement from BMP-1 correspond to 23,6% of the baseline scenario.

[2] The land use class "Other agricultural" (no available data on crop type) has been treated as unfertilized hay.

[3] Includes points sources from residential and urban land uses (waste water treatment plants).

Table 27. Projected average sediment and P loadings for baseline and alternate agricultural management scenarios for the Quebec section of MBB.

			Cropped Land Use							MBB
			Grain corn	Hay	Silage corn	Small grain	Soybean	Other [2]	Total	Total [3]
Baseline scenario	**Area**	**(ha)**	8,869	10,960	957	1,578	5,640	396	28,401	135,978
	Sediment loading	**(T TSS)**	4,984	3,894	1,321	857	7,793	312	19,161	
	Total P loading	**(kg Total P)**	13,594	8,394	2,210	1,888	12,434	426	38,945	75,652
Scenario PGO-1	**Sediment loading**	**(T TSS)**	4,984	3,894	1,321	857	7,793	312	19,161	
(Nutrient MGT) [1]	**Abatement**	**(%)**	0.0%	0.0%	0.0%	0.0%	0.0%	0.0%	**0.0%**	
	Total P loading	**(kg Total P)**	12,254	7 599 [1]	2,017	1,644	12,053	423	35,991	72,692
	Abatement	**(%)**	-9.9%	-9.5%	-8.7%	-12.9%	-3.1%	-0.6%	**-7.6%**	-3.9%
Scenario PGO-2	**Sediment loading**	**(T TSS)**	2,278	3,894	355	777	2,544	272	10,120	
(Crop system MGT)	**Abatement**	**(%)**	-54.3%	0.0%	-73.1%	-9.4%	-67.4%	-12.7%	**-47.2%**	
	Total P loading	**(kg Total P)**	9,790	8,394	1,087	1,791	6,629	370	28,062	64,789
	Abatement	**(%)**	-28.0%	0.0%	-50.8%	-5.1%	-46.7%	-13.1%	**-27.9%**	-14.4%
Scenario PGO-3	**Sediment loading**	**(T TSS)**	4,049	3,161	1,074	697	6,334	253	15,567	
(Riparian zone MGT)	**Abatement**	**(%)**	-18.8%	-18.8%	-18.7%	-18.7%	-18.7%	-18.7%	**-18.8%**	
	Total P loading	**(kg Total P)**	11,981	7,407	1,872	1,652	10,578	364	33,855	70,557
	Abatement	**(%)**	-11.9%	-11.8%	-15.3%	-12.5%	-14.9%	-14.5%	**-13.1%**	-6.7%
Scenario PGO-1 + 2	**Sediment loading**	**(T TSS)**	2,278	3,894	355	777	2,544	272	10,120	
	Abatement	**(%)**	-54.3%	0.0%	-73.1%	-9.4%	-67.4%	-12.7%	**-47.2%**	
	Total P loading	**(kg Total P)**	8,812	7,599	965	1,578	6,344	368	25,666	62,388
	Abatement	**(%)**	-35.2%	-9.5%	-56.3%	-16.4%	-49.0%	-13.7%	**-34.1%**	-17.5%
Scenario PGO-1+2+3	**Sediment loading**	**(T TSS)**	1,851	3,894	289	631	2,068	221	8,953	
	Abatement	**(%)**	-62.9%	0.0%	-78.2%	-26.4%	-73.5%	-29.0%	**-53.3%**	
	Total P loading	**(kg Total P)**	7,956	7,599	843	1,371	5,588	316	23,673	60,387
	Abatement	**(%)**	-41.5%	-9.5%	-61.8%	-27.4%	-55.1%	-25.7%	**-39.2%**	-20.2%
Scenario PGO-4	**Sediment loading**	**(T TSS)**	260	1,754	46	78	291	33	2,463	
(Land conversion)	**Abatement**	**(%)**	-94.8%	-54.9%	-96.5%	-90.9%	-96.3%	-89.5%	**-87.1%**	
	Total P loading	**(kg Total P)**	5,558	6,046	497	782	3,128	142	16,154	50,906
	Abatement	**(%)**	-59.1%	-28.0%	-77.5%	-58.6%	-74.8%	-66.5%	**-58.5%**	-32.7%

[1] Considering only the hay acreages where manure P is applied (3,590 ha), the P loading abatement from PGO-1 correspond to 21.5% of the baseline scenario.

[2] The land use class "Other agricultural" (no available data on crop type) has been treated as unfertilized hay.

[3] Includes points sources from residential and urban land uses (waste water treatment plants).

Nutrient Management Group Effects (BMP-1)

The BMP-1 group reflects the effect of an alternate management of manure inputs, namely a transition to an incorporation mode and the exclusion of late fall inputs. The MM algorithm was developed from local rainfall simulation research. Based on runoff P data, the MM routine empirically projects the surface runoff enrichment in soluble P resulting from the spreading of unincorporated manure. The effect of the BMP on the projected P emission depends on the surface runoff rate, soil P saturation level, and the rate of P inputs. Only fields parameterized with unincorporated manure are affected by BMP-1. The MM do not project any runoff enrichment from P mineral fertilizer, considering that the material is typically incorporated at seeding.

The nutrient management scenario results in 11.6% and 7.6% P abatements for Vermont and Quebec crop lands, respectfully. The difference reflects their distinct cropping systems. In Vermont, only the P loadings from hay fields are affected by the BMP, where the manure was considered non incorporated in the baseline scenario. Conversely, all Vermont corn land have manure incorporated in the baseline scenario. When considering only the manured hay fields, the P abatement resulting from the incorporation of manure averages 22.6%.

In Quebec, the surface area in hay production is relatively less important, while variable acreages of field crops (corn, soybean and small grains) were considered in no-till system in the baseline scenario. Part of the P abatement from the BMP scenario is thus related to manure incorporation on no-till fields. Most of P abatement though is for manured hay field, which averages 21.5% in Québec, which is close to what is projected for Vermont.

Figure 17 illustrates the HRU-level deviation in projected specific P loadings in Vermont and Quebec resulting from the nutrient management scenario compared to the baseline scenario. Notwithstanding the high variability in baseline P emissions, the deviation in abatement ratios between the two territories illustrates the preponderance of hay production in Vermont's cropping systems, where manure incorporation proportionally results in higher abatement in P emissions.

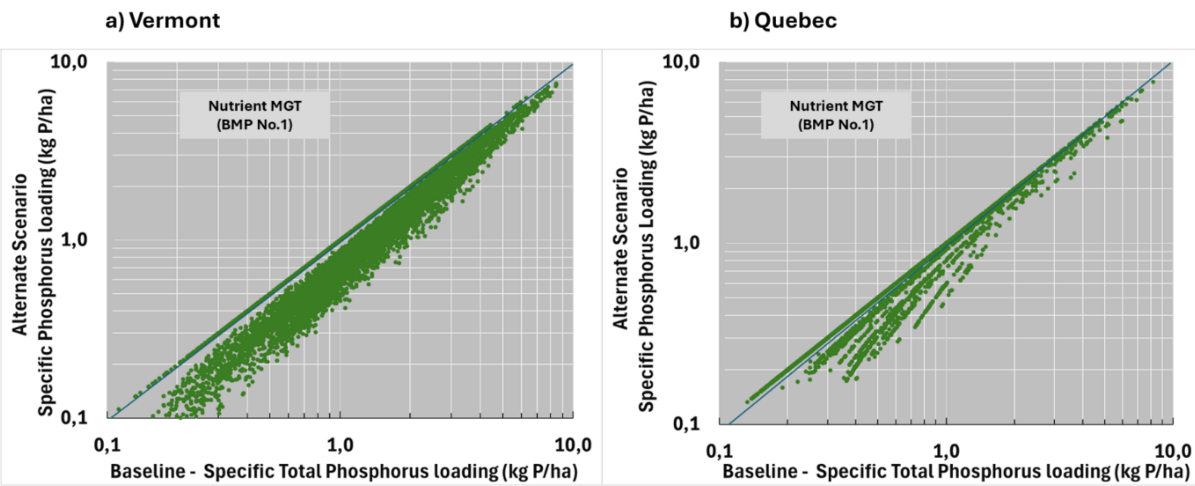

Figure 17. Distribution of specific phosphorus loading rates (kg P/ha) for hay fields in Vermont (a) and Quebec (b), projected by the nutrient management scenario (BMP-1) vs the baseline scenario (MM outputs at hydrological response units (HRUs) scale).

Cropping System Group Effects (BMP-2)

The cropping system scenario group (BMP-2 group) projects the effects of complete anti-erosive protection of annually cropped fields. The cover cropping of vulnerable silage corn and soybean stubbles, together with abundant crop residue cover on grain corn and small grains provide an effective reduction in sediment loadings. Projected average abatement rates in sediment loadings are maximal on silage corn in Vermont and Quebec, with 70% and 73% reductions, respectfully (Tables 26-27). On particularly vulnerable soybean ground, the 67%

(QC) and 40% (VT) average abatement rates in sediment loadings also reflect elevated baseline sediment loads. The conversion of grain corn acreages to no-till in Quebec also results in a 54% average reduction in projected sediment loadings. A relatively lower abatement rate than with silage corn or soybean reflect the protective effect of residue cover from fall minimum tillage systems documented in the baseline scenario.

Figure 18 illustrates the HRU-level deviation of projected abatements in sediment and phosphorus loadings resulting from the implementation of erosion control on Vermont and Quebec fields. Most important reductions in sediment mass loadings in Vermont for silage corn reflect the initially elevated loads from baseline conditions. Sediment load reductions from erosion controls in Quebec are lower than in Vermont, reflecting geophysical and cropping system baseline conditions. Indeed, flatter topography, subsurface drainage, lower soil erodibility and prevalence of crop residue covers all contribute to relatively lower baseline sediment yields, and concurrently lower sediment loads reduction than in Vermont. Sediment abatement rates projected in Vermont and Quebec essentially translate the MUSLE equation "C" crop cover factors of the MM's erosion module, which lead to linearized abatement ratios pictured in Figure 18.

The effective erosion protection given by the BMP-2 scenario leads to the most effective P abatements amongst the three BMP groups. The overall average reductions in P loadings from cropped land resulting from BMP-2 reaches 26% to 28% in Vermont and Quebec, respectfully (Tables 26-27). Abatement rates in P loadings significantly lower than the ones for sediment reflect the MM algorithms and are consistent with the literature on P mobility. The MM simulates a P enrichment of sediment from fields covered by crop residues and/or cover crop, through the incorporation of a P sediment enrichment ratio. Lower erosion rates imply finer grain sizes of sediment and resulting higher particulate P levels. Erosion protection affects solely particulate P loadings within the MM, without effects on soluble P emission. A practical implication of these phenomena is that cropping system BMP-2 is less effective in reducing P loadings from rich soils, which yield higher soluble P loadings. Relatively richer soils in Quebec, together with relatively lower baseline sediment loadings are reflected in the distinct patterns of specific P loadings reductions in Vermont and Quebec (Figure 18).

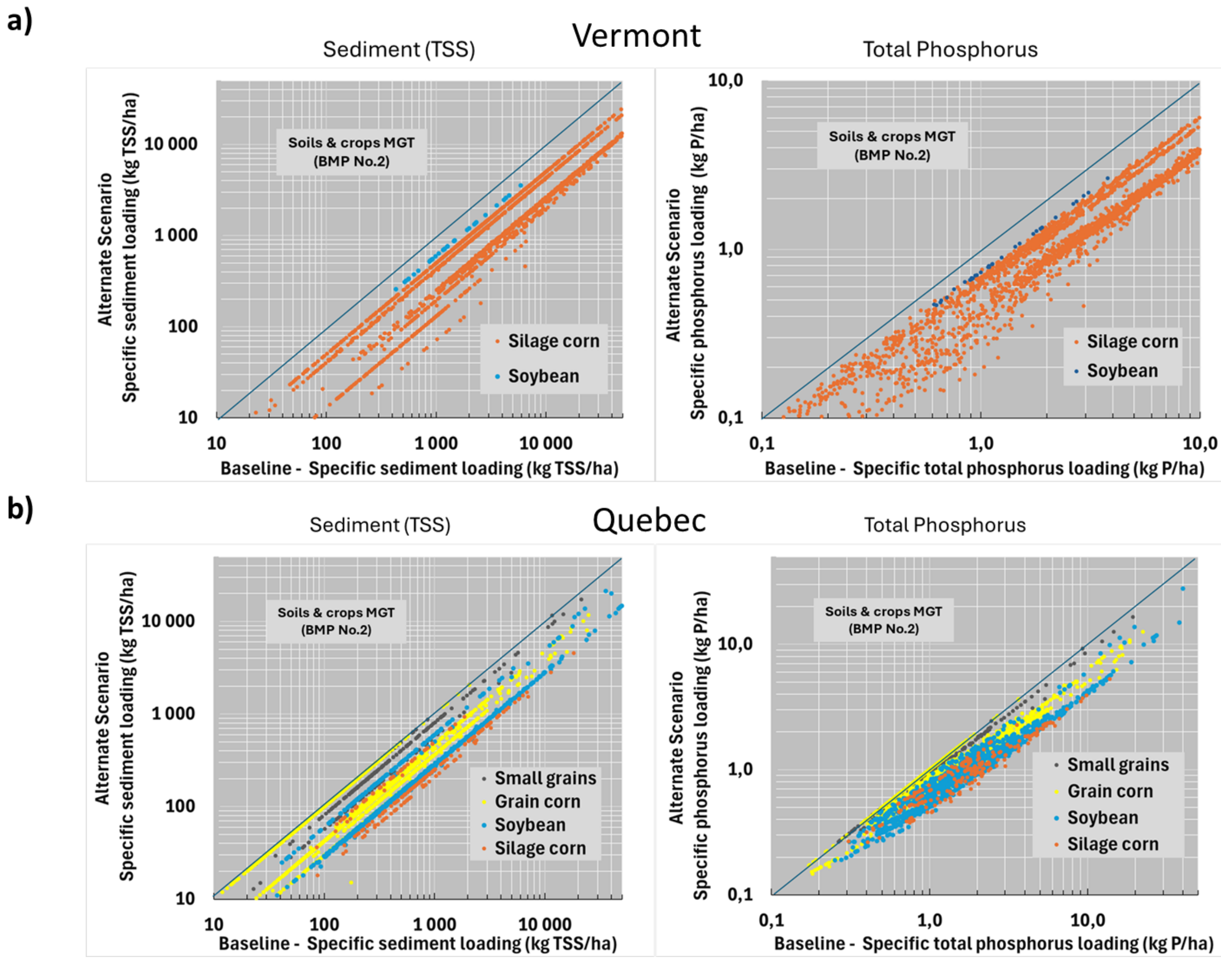

Figure 18. Distribution of specific sediment and phosphorus loading rates (kg P/ha) for fields in Vermont (a) and Quebec (b), projected by the cropping system management scenario (BMP-2) vs the baseline scenario (MM outputs at hydrological response units (HRUs) scale).

Riparian Zone Management (Buffers and Sedimentation Structures, BMP-3)

The riparian zone management scenario (BMP-3) generated a uniform abatement rate of 18.7% for sediment P loading over all crop classes in Vermont and Quebec (Figure 19 and Tables 26-27). These results reflect the generalized empirical abatement factor applied to the sediment loading in surface runoff of individual HRUs in the metamodel. Conceptually, the MM empirical abatement rate is projecting the effect of extended riparian strips and in-ditch catch basins on water quality, as documented at catchment scale for a tributary of downstream Pike River (Michaud et al., 2005),

A similar abatement rate of sediment loading in Vermont and Quebec generated, however, different P loading abatement rates, namely 14.6% and 13.1% for Vermont and Quebec, respectively (Tables 26-27). This difference in P loadings abatement is explained by relatively higher levels of soil phosphorus in Quebec, which resulted in higher soluble P yields in the baseline scenario. Because the riparian zone management scenario (BMP-3) solely affects the particulate P fraction of surface runoff, the effect on total P loading is relatively lower in Quebec.

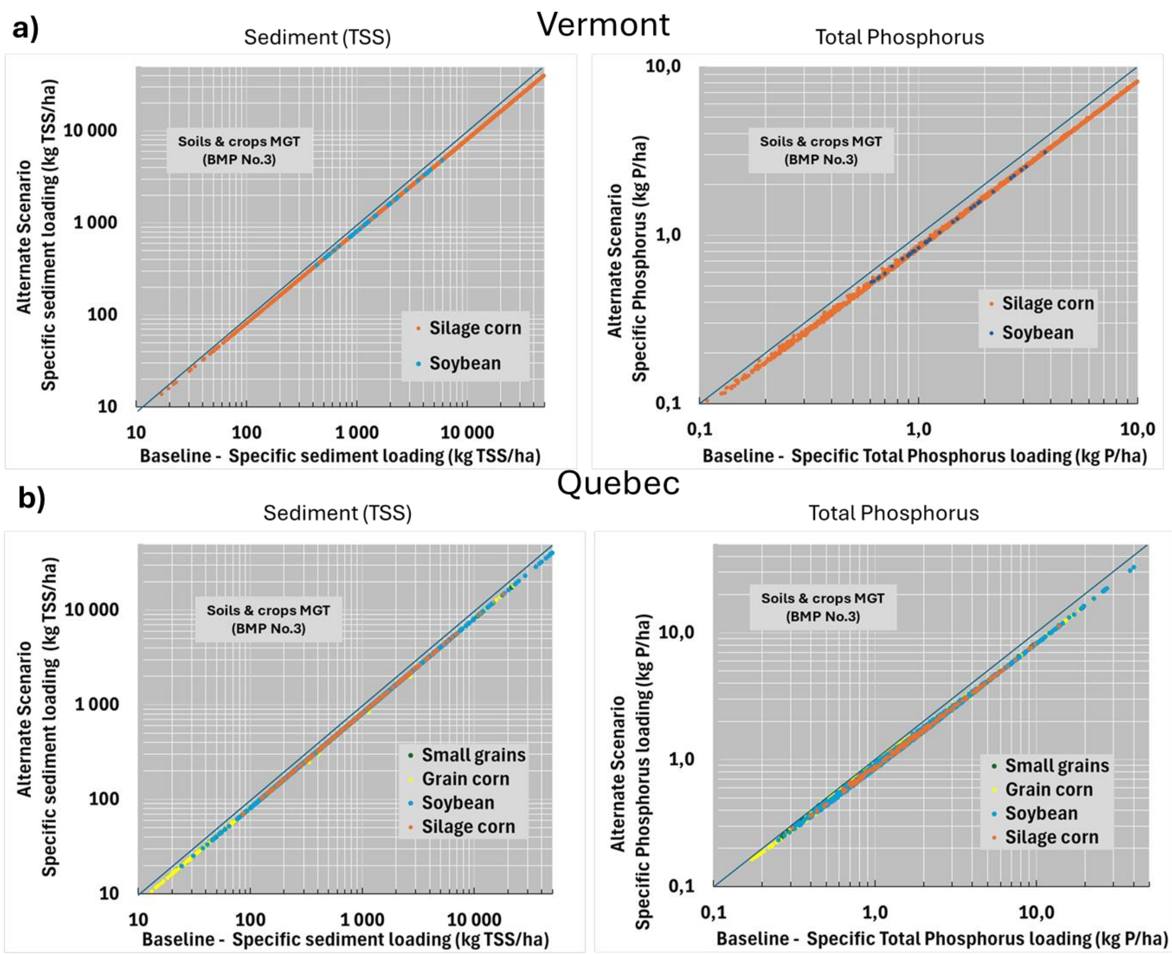

Figure 19. Distribution of specific sediment and phosphorus loading rates (kg P/ha) for fields in Vermont (a) and Quebec (b), projected by the riparian zone management scenario (BMP-3) vs the baseline scenario (MM outputs at hydrological response units (HRUs) scale).

Multi-Group Agricultural BMPs Effects

The simultaneous input of nutrient MGT group (BMP-1) and cropping system MGT group (BMP-2) generates a cumulative effect on P loadings, with total abatement rates of 37.3% and 34.1% for Vermont and Quebec crop lands, respectfully. The additive effect of BMP-1 and BMP-2 on P loadings is due to these individual scenarios influencing different sources of phosphorus. Although nutrient MGT has an effect on soluble P loadings, mostly for hay fields, cropping system MGT lowers particulate P loadings, mostly for annual crops.

The addition of Riparian Zone management (BMP-3), however, does not generate such a cumulative effect. Because cropping scenario (BMP-2) reduces the projected emissions of sediment and particulate P from the field, the effect of riparian protection (BMP-3), expressed by a fixed abatement rate, no longer reduces the P loading with the same efficiency as with the baseline loading. Although the “simple” effect of BMP-3 scenario on baseline sediment loads averages 19% for both regions, the marginal effect of BMP-3 (BMP(1+2+3) – BMP(1+2)) is reduced to 3.9% and 6.1 %, respectively for Vermont and Quebec. The same logic applies to P loadings, with marginal effects of 3.6% and 5.1% for Vermont and Quebec (Tables 26-27).

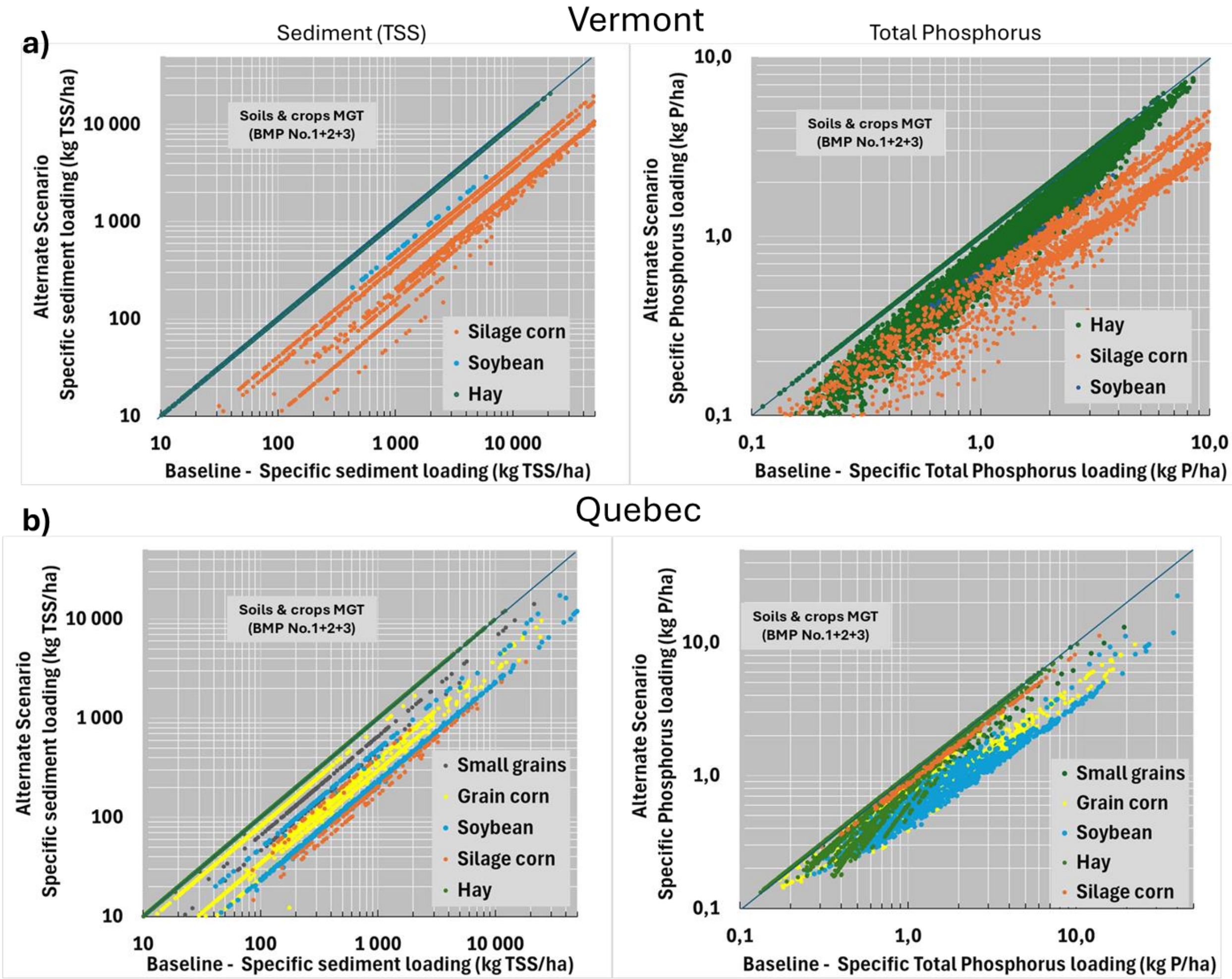

Figure 20. Distribution of specific sediment and phosphorus loading rates (kg P/ha) for fields in Vermont (a) and Quebec (b), projected by the multi-group BMP 1+2+3 vs the baseline scenario (MM outputs at hydrological response units (HRUs) scale).

Land Conversion (BMP-4)

The land conversion scenario implies a change in the land use of the targeted land units. Conceptually, the new parameterization of the land units is representative of a dense meadow, without fertilizer inputs. The substitution of the baseline “C” cover factor (MUSLE erosion equation) by a low value (C=0.017) results in drastic reductions in sediment emissions, from 82 to 87% abatement rates for annual crops, and from 50 to 55% for hay fields (Tables 26-27). These reductions in sediment yields translate into very high particulate P loading abatement rates, averaging 68% in Vermont, and 59% in Quebec. This difference in average abatement rates for P among territories reflects relatively higher soil P levels in Quebec. If the land conversion scenario severely reduces the sediment loadings, it does not change the baseline P level of the soils. Soluble P loading is still predicted by the metamodel, essentially driven by the baseline soil P level.

Residential and Urban Land Uses Point Sources (BMP-5 and BMP-6)

Table 28 summarizes the baseline and alternate scenarios P loadings projected for the septic systems within residential areas (BMP-5) and the wastewater treatment plants (BMP-6). Considering the baseline P loadings projected for the septic systems of 3.96 T P (QC) and 4.11 T P (VT), the 34% abatement in septic P loadings resulting from the BMP-5 alternate scenario results in a global reduction of 2.74 T P load for the MMB. The projected reduction in P loadings from septic systems are nearly equivalent in Quebec and Vermont, with 1.35 and 1.40 T P for Vermont and Quebec, respectively. The projected reduction in P loadings for Quebec owes more to the high-density residential areas than in Vermont, where the low-density residential areas largely dominate (Table 28). Because high density residential areas were attributed baseline septic specific P loadings two times higher than for low density residential areas, both regions show similar P loads reductions from the BMP-5 scenario, despite their contrasting distribution in residential densities.

For the wastewater treatment plant scenario (BMP-6) the 34% abatement rate results in a similar projection in P load reduction in Vermont (0.32 T-P) and Quebec (0.36 T P). This projection essentially reflects the baseline respective P loadings of Vermont and Quebec wastewater plants documented in the watershed P inventory.

Table 28. Projection of developed residential and urban P loadings for septic systems and wastewater treatment plant alternate management scenarios (BMP-5 and BMP-6).

Developed Residential and Urban Area and Quantity	Quebec	Vermont
Developed, residential Low density area (ha)	429	868
Developed, residential High Density area (ha)	398	39
Total Residential area (ha)	827	906
Septic load, Residential, Low Density (kg P)	1,387	3,774
Septic load, Residential High Density (kg P) [2]	2,573	339
Total septic load (kg P) [1]	3,960	4,113
Septic specific Load, Residential, Low Density (kg P/ha)	3.23	4.35
Septic specific Load, Residential High Density (kg P/ha) [2]	6.47	8.70
Specific Non-Point P load, Residential, Low Density (kg P/ha)	0.68	0.68
Specific Non-Point P load, Residential, High Density (kg P/ha)	1.1	1.1
Total specific P load, Residential, Low Density (kg P/ha)	3.91	5.03
Total specific P load, Residential, High Density (kg P/ha)	7.57	9.80
Total P load, Residential, Low Density (kg P)	1,679	4,364
Total P load, Residential, High Density (kg P)	3,011	382
BMP-5 Septic P load, Residential, Low Density (kg P) [3]	915	2,491
BMP-5 Septic P load, Residential, High Density (kg P) [3]	1,698	224
BMP-5 P load, Residential, Low Density (kg P) [3]	1,207	3,081
BMP-5 P load, Residential, high Density (kg P) [3]	2,136	267
Total wastewater treatment plants load (kg P)	1,070	950
BMP-6 P load, wastewater treatment plants [3]	706	627

[1] Derived from population census.
[2] High density residential areas were attributed to septic-specific P loadings two times higher than for low density residential areas.
[3] The P loading abatement rate is 34%.

Composite Scenarios (Multiple Groups Combined)

The rationale behind the projection of composite scenarios is to optimize the reduction in P loadings through the cumulative effects of best management practices (BMPs), while targeted implementations favor their cost-efficiency. The spatial heterogeneity in soil properties, landscape pattern, land use, and management over the Missisquoi Bay watershed leads to an important spatial discrimination in non-point P loading rates projected across the watershed landscape. Figure 21 illustrates the phenomenon through cumulative distribution functions of baseline P loading rates for Quebec and Vermont agricultural cropped lands. Both regions show similar distributions, where 20% of cropped land of Vermont (7,036 ha) or Québec (5,682 ha), generate from 54% (QC) to 56% (VT) of the baseline projected total P loading. When considering 50% of their respective cropland (17,591 ha for VT; 14,196 ha for QC), the P baseline loading rates are reaching respectively 85% and 81% of total P loadings from Vermont and Québec.

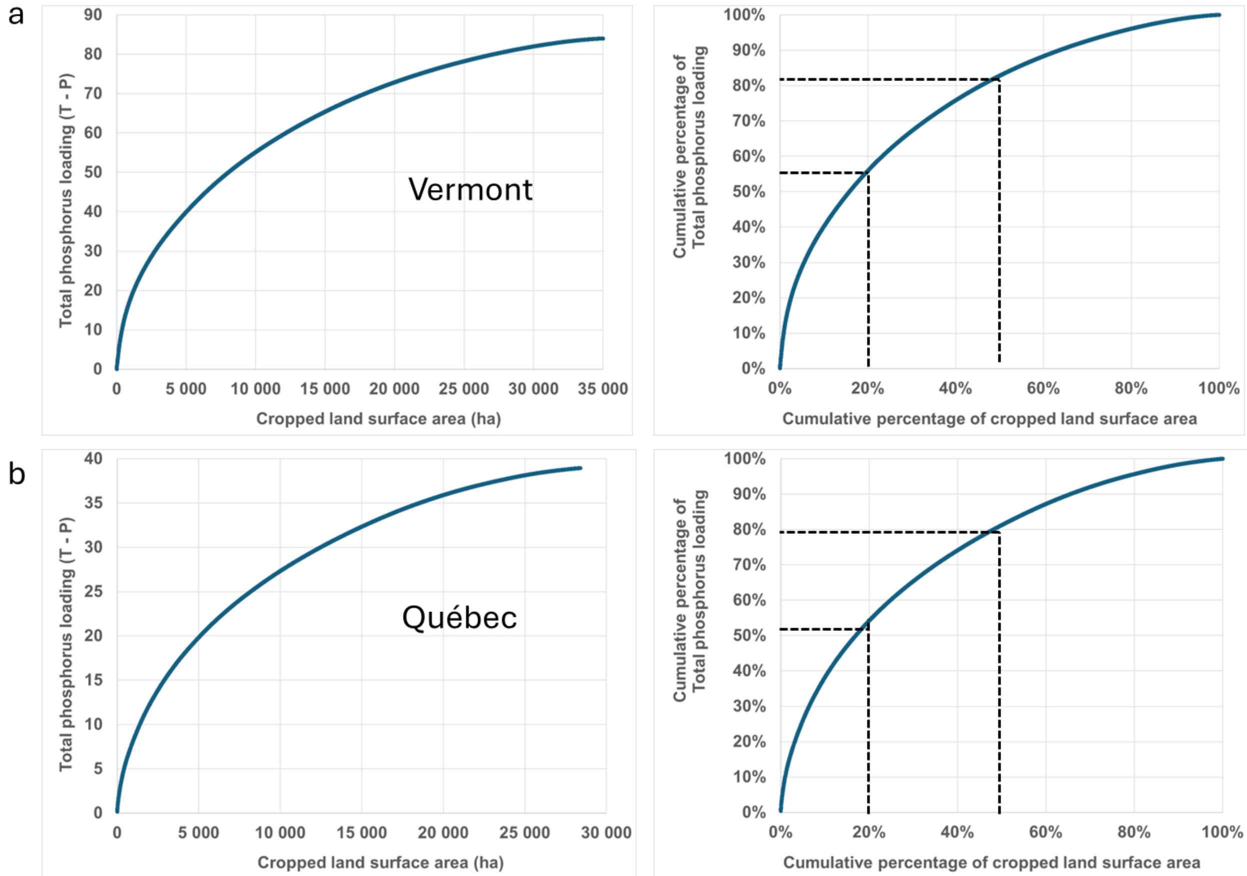

Figure 21. Surface area distribution of baseline total phosphorus loadings from cropped land in Vermont (a) and Quebec (b), following a decreasing order of individual HRU-specific P loading rates.

The important spatial discrimination in baseline P loading has a definite impact on the effects of agricultural BMPs implementation. Figure 22 compares the total P projected abatement rates at full MBB watershed scale resulting from a random or targeted strategy of BMPs implementation on cropped land. Projected results on BMP effects are highly contrasted and demonstrate the full benefit of adopting a targeted strategy when it comes to P non-point sources control. For example, a 7.4% P abatement rate is projected at watershed scale for a random implementation of composite scenario BMP 1+2+3 (nutrient, crop system and riparian management) over 20% of the cropland. A targeted implementation over the same total surface area (20% of the cropland) would generate more than a three-fold increase in P loading abatement rate (23%). A similar pattern is projected with a rate of 50% BMP implementation over cropland. Although the random implementation is projecting a 15.6% reduction of watershed P loading, the abatement rate nearly doubles (26.8%) with a targeted strategy.

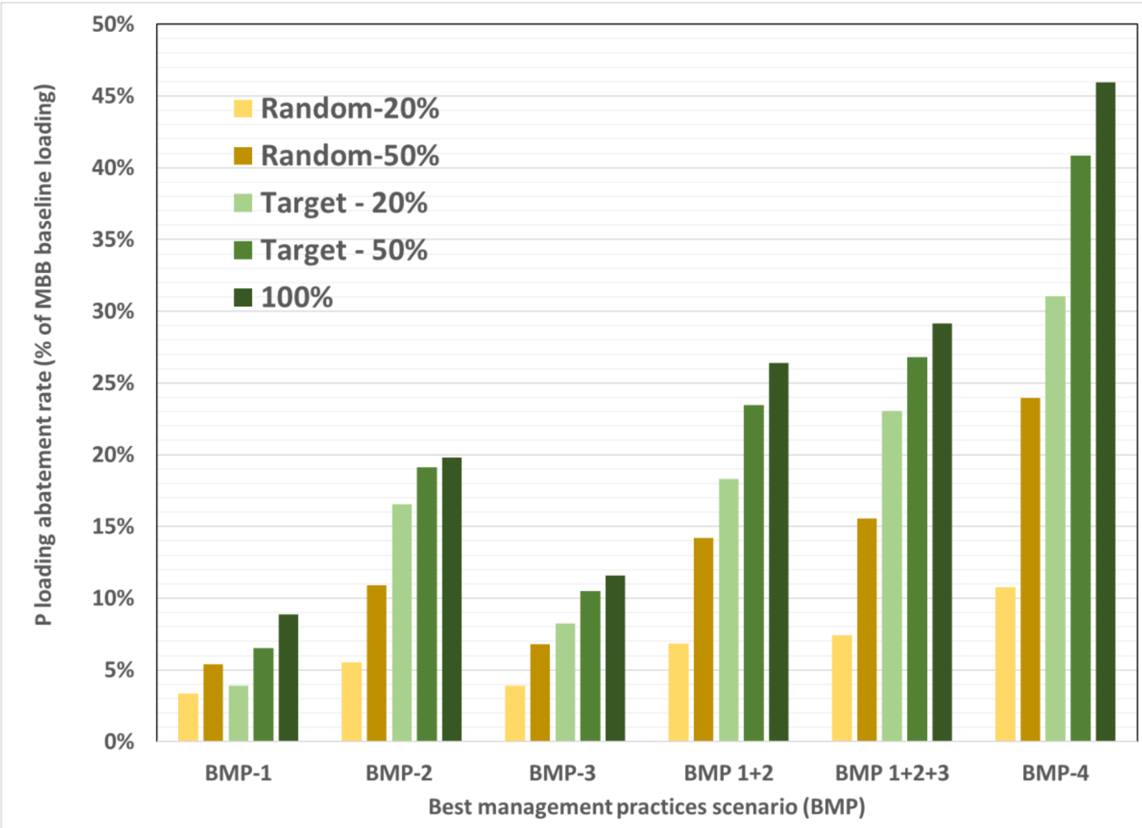

Figure 22. Projected phosphorus loading abatement rates with respect to Missisquoi Bay watershed baseline loading from random, targeted, and global implementation of best management practices (BMP) scenarios on cropped land (including a 34% abatement rate systematically applied to residential and urban point sources).

The effect of spatial heterogeneity in baseline P loadings has a strong effect on the effeciency of land conversion scenarios (BMP-4). In fact, the land conversion scenario has the most effective abatement rate of P loading, compared to the other agricultural BMPs. When applied to most vulnerable farm land (target CSAs), the projected reduction in P loading is thus highly significant. Figure 23 illustrates the effect of including land conversion scenarios to a targeted strategy (50% of cropped land) for composite BMPs (BMP 1+2+3). Without land conversion, the watershed scale P loading abatement rate resulting from BMP 1+2+3 is projected to be 26.8%. The substitution of 5% most critical surface areas to permanent forage cover leads to a projected abatement rate of 32.2%. The same logic applies to 10% and 20% substitution of composite BMPs (BMP 1+2+3) by land conversion, for resulting P abalement rates of 34.4% and 37.3% at watershed scale. The marginal effect of land conversion diminishes with the importance of targeted area. Considering the important spatial discrimination in baseline P loadings, the 5% land conversion scenario has a significanly higher efficiency on its target area than the 10% or 20% scenarios. Given that land conversion scenarios would presumably involve the largest cost-share costs, as compared to other agricultural BMPs, a practical implication of these projections would be to restrain land conversion scenarios to the most critical CSAs.

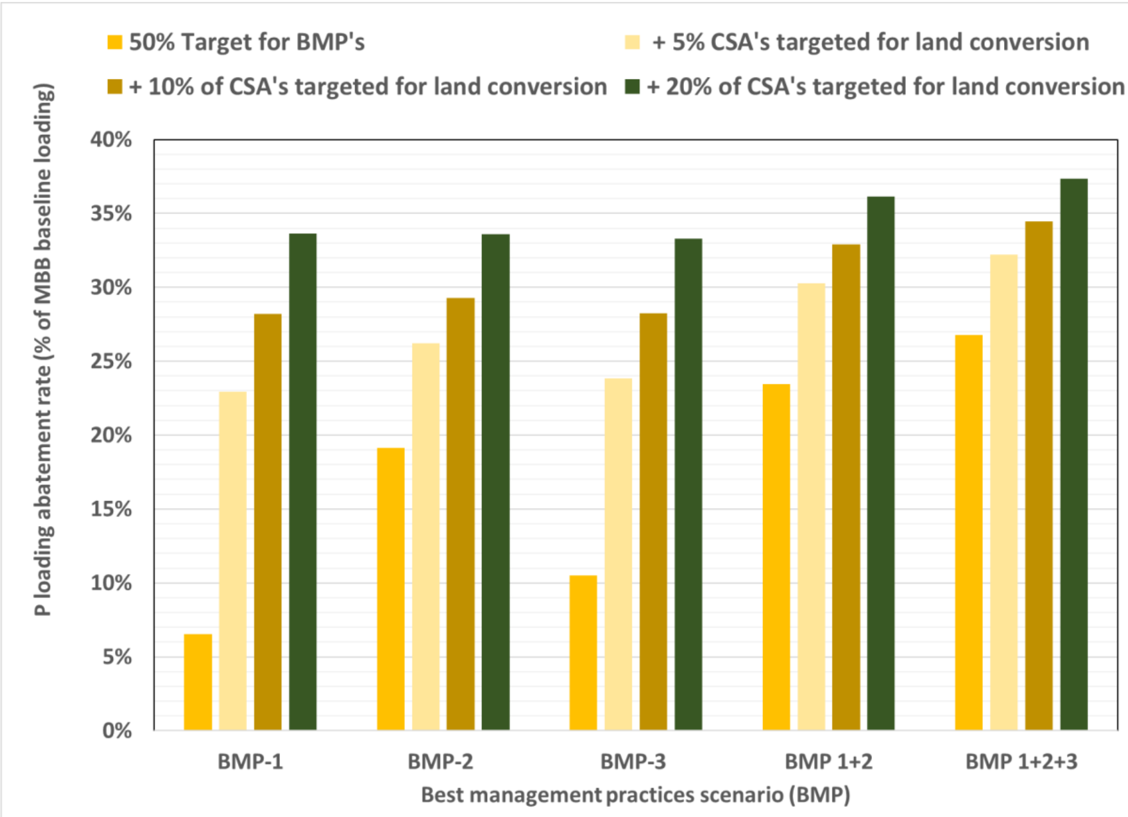

Figure 23. Projected phosphorus loading abatement rates with respect to Missisquoi Bay watershed baseline loading from a targeted (50% of CSAs area) composite BMPs scenario (BMP 1+2+3), together with an increasing level of land conversion scenarios (0, 5%, 10%, 20%). (A 34% abatement rate was systematically applied to residential and urban point sources).

From a tributary scale perspective, alternate management scenarios also generate contrasting effects on sediment and phosphorus loadings. Table 29 documents the contrast in P abalement rates amongst the Misssiquoi, Pike and Rock river subwatersheds resulting from the composite scenario, where BMPs are applied to 50% of agricultural critical source areas (CSAs), including a conversion of 10% of most critical CSAs, together with point source control of residential and urban sources. Overall, a global 33.7% reduction in P loadings is projected at the MBB watershed scale, when considering the combined agricultural BMPs (BMP 1+2+3). However, the abalement rates vary considerably amongst the MBB tributaries. For example, a much higher abalement rate in P loadings (56.6%) is projected for Rock River transboudary subwatershed. The contrast in land use between the subwatersheds largely explains the differences in projected P abatement rates. First, the agricultural land use is much more important in the Rock River watershed, as compared to Missisquoi and Pike watersheds. Consequently, the implementation of agricultral BMPs will have a greater relative impact on the global P loading. Conversely, the important forest and wetland cover in the Missisquoi and Pike watersheds, together with the small cathments that directly flow to the bay, has a mitigation effect on the abatement rates resulting from the projection of agricultural BMPs.

Table 29. Annual phosphous loadings and abatements resulting from the implementation of agricultural BMPs on 50% of agricultural critical source areas (CSAs), including the land conversion of 10% of most critical CSAs, together with point source control of residential and urban sources.

Tributaries	Area (ha)	Annual Baseline Loading [1] (kg Total-P)	Annual Phosphorous Loading (kg Total-P)[2]				
			Nutrient MGT BMP-1	Crop and Soil MGT BMP-2	Riparian Zone MGT BMP-3	Combined BMP 1+2	Combined BMP1+2+3
Total direct discharge (QC + VT)	18,617	6,733	6,465	6,174	6,398	6,114	5,864
Total Missisquoi (QC + VT)	221,537	109,226	80,178	81,672	80,848	76,767	76,253
Total Pike (QC + VT)	65,542	51,737	38,972	36,641	38,630	35,269	33,253
Total Rock (QC + VT)	14,354	17,907	9,313	8,173	8,845	8,008	7,768
Total MBB	320,050	185,603	134,929	132,659	134,721	126,159	123,138
			% Abatement from Baseline Scenario				
Total direct discharge (QC + VT)			-4.0%	-8.3%	-5.0%	-9.2%	-12.9%
Total Missisquoi (QC + VT)			-26.6%	-25.2%	-26.0%	-29.7%	-30.2%
Total Pike (QC + VT)			-24.7%	-29.2%	-25.3%	-31.8%	-35.7%
Total Rock (QC + VT)			-48.0%	-54.4%	-50.6%	-55.3%	-56.6%
Total MBB			-27.3%	-28.5%	-27.4%	-32.0%	-33.7%

[1] Includes point sources loadings from residential and urban land uses.
[2] Scenario includes 50% target BMPs on cropland, land conversion of 10% agricultural CSAs and point sources control (34% abatement)

TASK 7: SIMULATE AND QUANTIFY P FATE AND TRANSPORT WITHIN AND FROM MISSISQUOI BAY

Bay-Wide P Mass Balance

Throughout the model output time series, baseline model results demonstrate that there is a substantial P imbalance in the bay with more P coming into the bay from its tributaries relative to what the bay exports (positive P imbalance) at an annual scale (Figure 24). While the numbers are relatively similar in scale to those in the previously developed model by Limnotech (Limnotech, 2012), the projected P imbalance in this study is more variable and generally higher, particularly in high flow and riverine phosphorus input years (Figure 24, 25, Limnotech, 2012). As landscape P reduction scenarios are implemented, the magnitude of P imbalance decreases, with dryer years with less riverine loading approaching equilibrium under maximum P reduction (P imbalance near zero and inputs are similar to outputs). However, higher external loading years with extreme high flow events, even under maximum P reduction, remain well above P balance with substantial accumulation of P in the bay's sediment (Figure 24, 25). Compared to the Limnotech model, our simulation years capture some very high riverine P loading years due to extreme hydrological events (Figure 25), the scale of which were not captured in Limnotech's riverine forcing data. In those years, external loads are extremely high and notably high P imbalance persists irrespective of P load reduction simulations (Figure 25). This result highlights the relative importance of large events in impacting the overall system's P budget, as has been demonstrated elsewhere (Vidon et al., 2018), which has substantial relevance to climate change impacts on P imbalance given the increasing occurrence of such events in recent years (VT Climate Assessment, 2021). For example, had 2024 and 2025 also been included as repeated simulation years, the range of variability and magnitude of P imbalance/accumulation in the bay would be much higher due to the notable extreme events of those years.

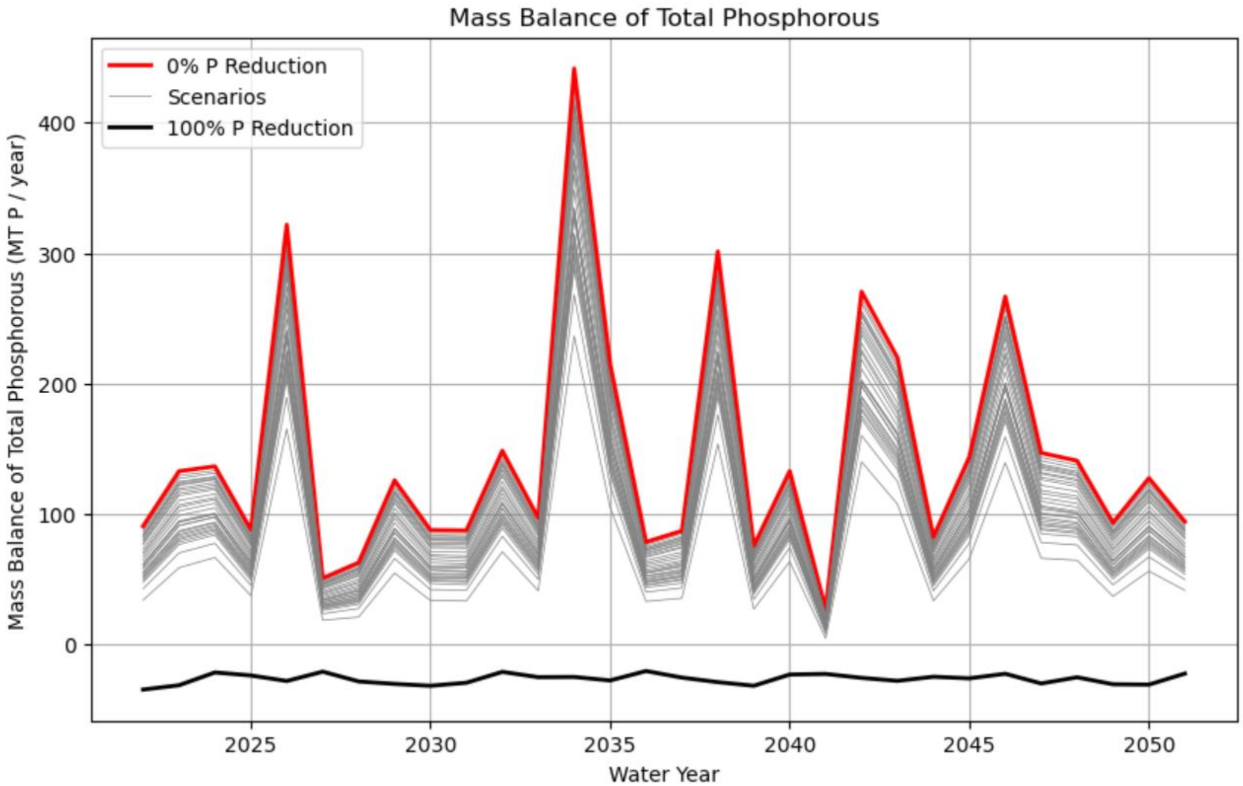

Figure 24. Bay-wide P mass balance for simulation years (inputs from tributaries-output from the causeway) in metric tons (MT). Positive values indicate that P is accumulating in the bay, whereas negative values indicate scenarios where the bay is becoming depleted in P and zero would be P equilibrium where P inventories would theoretically remain constant. The red line is the baseline scenario, the grey lines are the range of watershed P reduction scenarios implemented. The black line shows results when tributary loading of P is zero and represents annual export of legacy P from the bay's sediment.

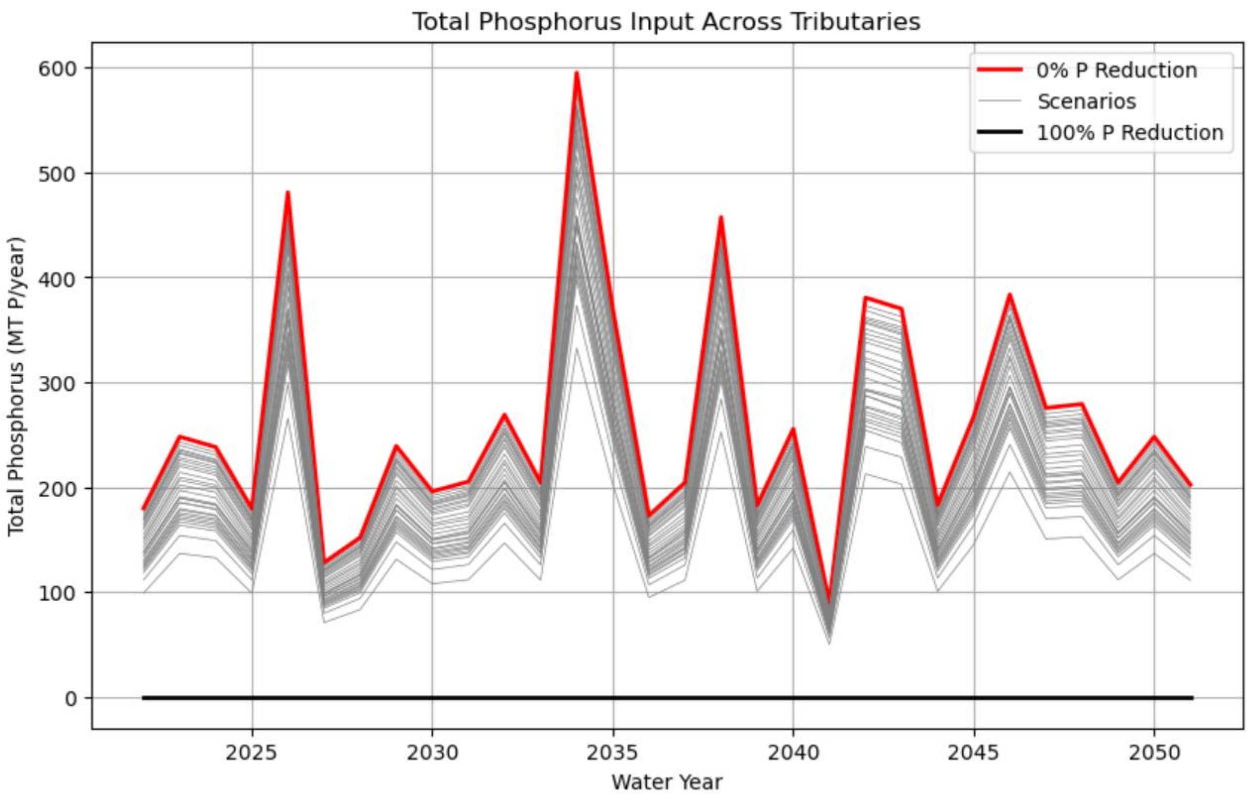

Figure 25. WRTDS tributary inputs of total phosphorus for model simulation years. The red line is the baseline scenario and the grey lines span the range of P reduction scenarios implemented.

Export from the bay via the causeway (Figure 26) generally tracks inputs from the tributaries, which is hydrodynamically intuitive given that periods when riverine inputs are high (high flow events) (Figure 24), the residence time of water will be very short in the bay, and thus a substantial portion of the riverine P load will exit the bay into the Inland Sea and dominate the annual load coming from the bay (Mendelsohn et al., 1997). Furthermore, the magnitude of internal loading does not respond to changing inputs and inventories of sediment P over simulation time (black and red lines are almost the same in Figure 27). It is also useful to examine the magnitude of P export from the causeway under the scenario where external loading of P from the watershed is zero given that this time series is representative of the export of legacy sediment P from the bay. Based on these results, we can conservatively estimate that the bay is exporting between 20 and 40 metric tons of P associated with internal loading from the sediment annually. Interannual variability in internal loading is primarily driven by variability in the occurrence and persistence of sediment-water interface anoxia, which is ultimately driven by the cumulative duration of a stable water column (Kirol et al., 2024), particularly in summer. Windy conditions in the summer suppress internal loading, whereas prolonged periods of calm winds will promote internal loading in Missisquoi Bay by promoting sediment-water interface anoxia. Additional positive feedbacks exist between internal loading water temperature (warmer water promotes internal loading by increasing sediment oxygen demand and the kinetics of subsequent reaction rates) and cyanobacteria bloom (adding labile carbon that enhance oxygen consumption) that are represented in the model and likely also impact interannual variability in internal loading. Annual sediment fluxes of P in this modeling effort (Figure 27) are of comparable range, albeit slightly lower than sediment phosphorus inputs derived from the Limnotech Model (35-56 MT/yr), whereas our tributary loads are slightly higher than the

Limnotech model due to the previously mentioned recurrence of years with extreme external loading events. Additionally, there is far less variability from year to year in internal loading of P relative to the fluctuations observed in the tributary loading dataset, which also agrees with our understanding of the bay and its tributaries (e.g., Isles et al., 2015, Vaughan, 2019). In general, model results suggest that on an annual scale, internal loading represents roughly 10 to 20% of the annual P flux into the bay (Figure 28). Overall, our modeling efforts further confirm that the dominant source of P during any given year is the bay's tributaries, but there is a large degree of variability in the scale of P imbalance because there is large variability in tributary P loading within the years simulated for this study.

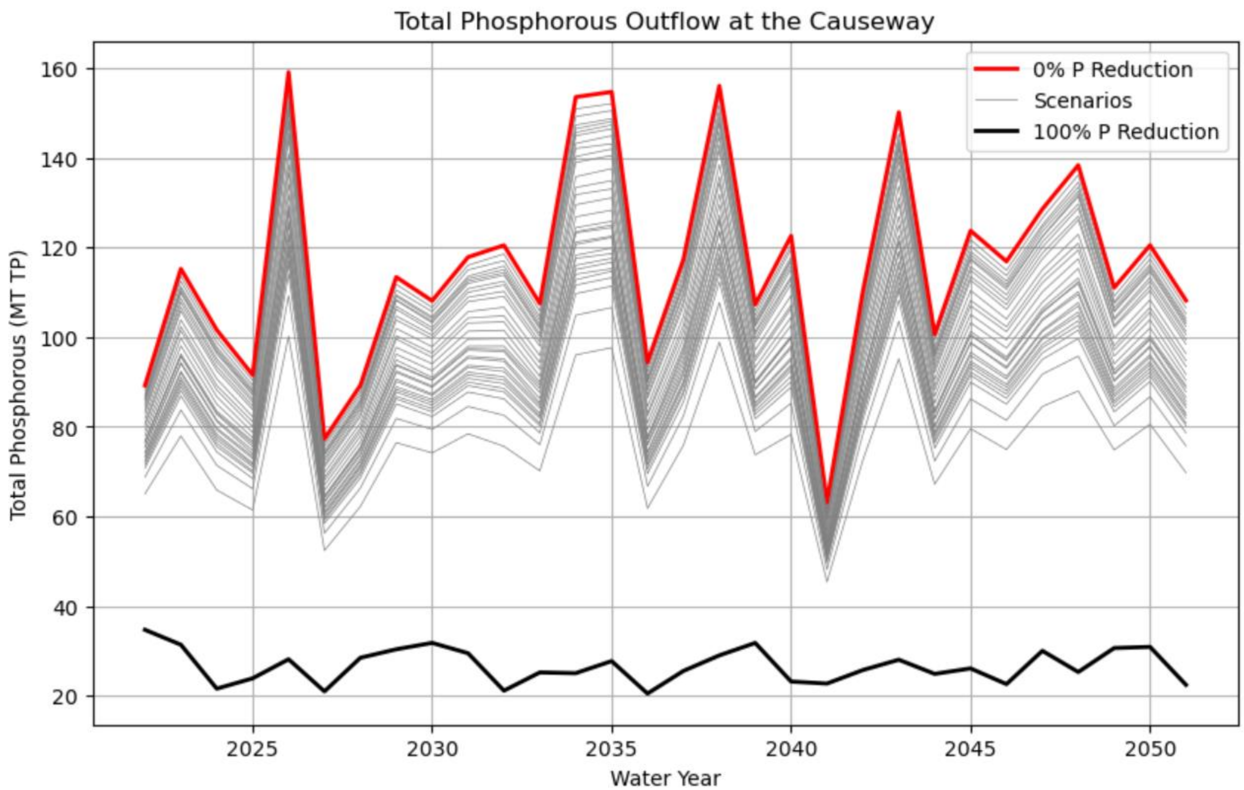

Figure 26. Total phosphorus exported from the bay into the Inland Sea across model simulation years. The red line is the baseline scenario, the grey lines are watershed P reduction scenarios implemented. The black line is the simulation when tributary loading of P is eliminated and represents annual export of legacy P from the bay's sediment.

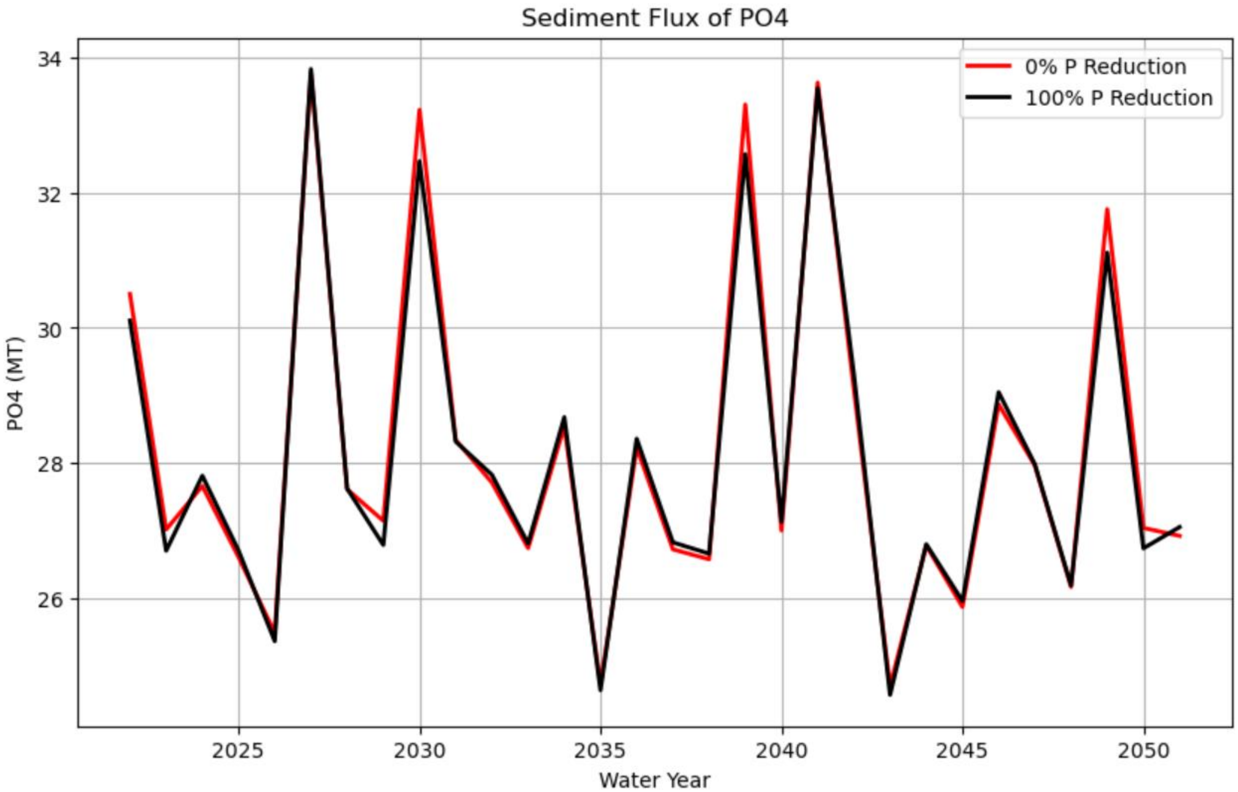

Figure 27. Annual flux of phosphate from bay sediment inventories. Only the baseline (red) and 100% reduction scenarios are shown because P reductions do not have substantial impacts on internal loading in this model (red and black lines are almost identical).

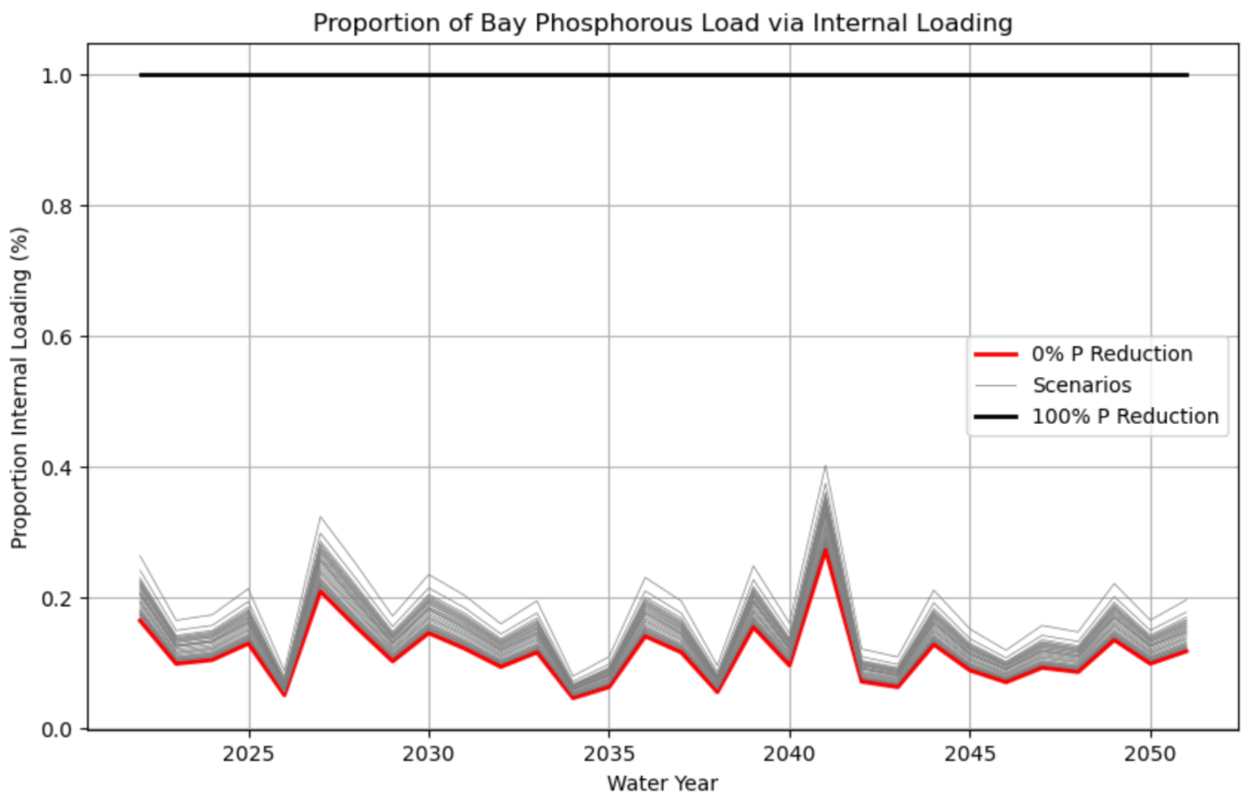

Figure 28. The annual proportion of phosphorus loading to the bay from internal loading. The remaining portion can be attributed to inputs from the bay's tributaries (summing to 1). The red line is the baseline scenario and the grey lines are the range of watershed P scenarios implemented.

Seasonal P Imbalance and the Relative Roles of Internal and External Loading

Through examination of the phosphorus model output at the monthly scale, the anticipated seasonal trend of P imbalance was observed. During the shoulder seasons (spring and late fall), external loading drove high P imbalance and P accumulation in the bay. Conversely, in summer seasons, the bay under some simulations was actually a net exporter of phosphorus in the months of July and August when internal loading can be the dominant P flux (Table 31, Figure 29). This phenomenon is driven by the export of dissolved P released by the bay's sediment during periods of transient anoxia at the sediment-water interface (Giles et al., 2016; Schroth et al., 2015). Summer is also a period where internal loading often provides the majority of P to the water column of the bay (Figure 29). The phosphorus that is leaving the bay during the summer consists of a relatively high fraction of dissolved P from internal loading which is concentrated in July through September. Interestingly, we found that there is a substantial flux of P from the bay associated with cyanobacteria cells that peaks in the fall (Figure 30). This is likely due to the fall blooms being transported out of the bay by north winds and/or fall storms. This process has been observed visually by our team, as well as via remote sensing from satellite data and illustrates that the bay can be a nontrivial (metric tons) source of phosphorus and cyanobacteria to the adjacent northern waters of the Inland Sea segment of Lake Champlain. This export of dissolved and cyanobacteria P could enhance bloom activity in that region of the lake and also continue to degrade the water quality of that lake segment in future years.

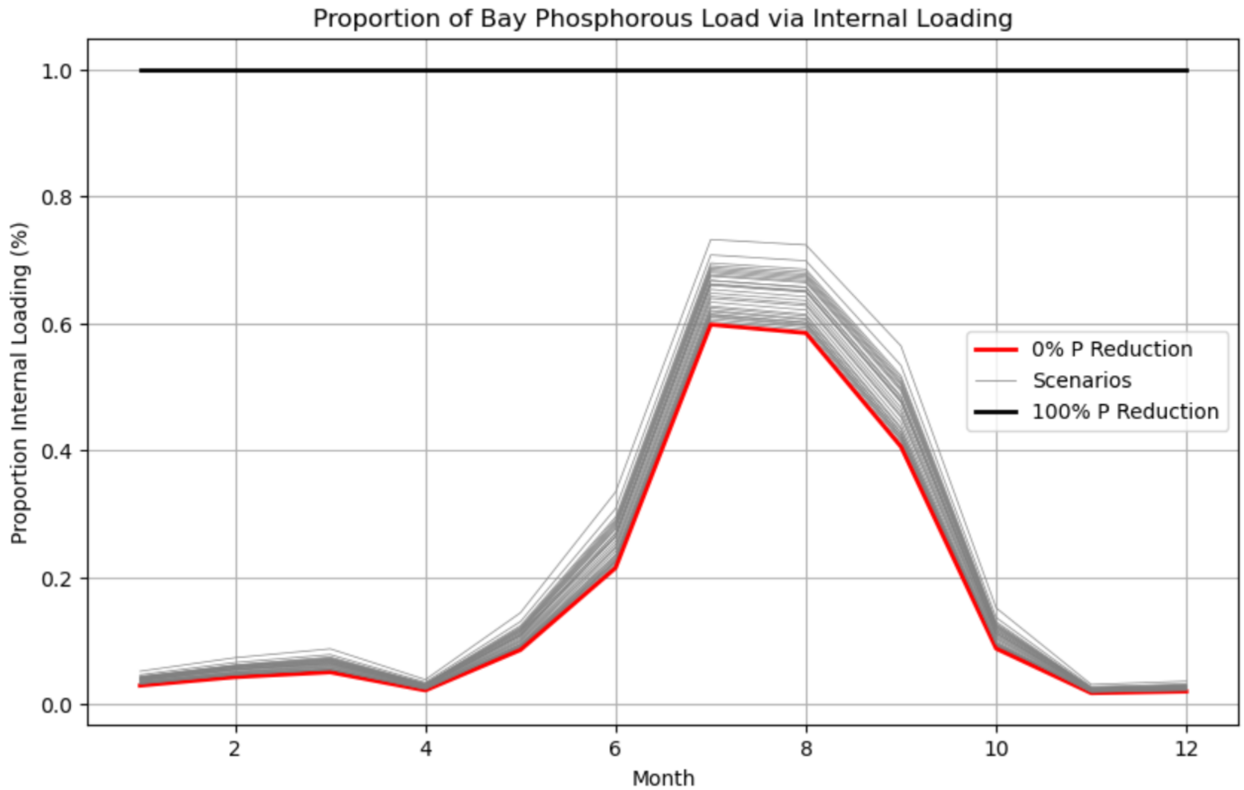

Figure 29. Monthly proportions of P fluxes to the bay. A value of one indicates that for the simulation only internal loading from lake sediments provided phosphorus to the bay whereas a value of zero would indicate that all P was sourced in the bay's tributaries.

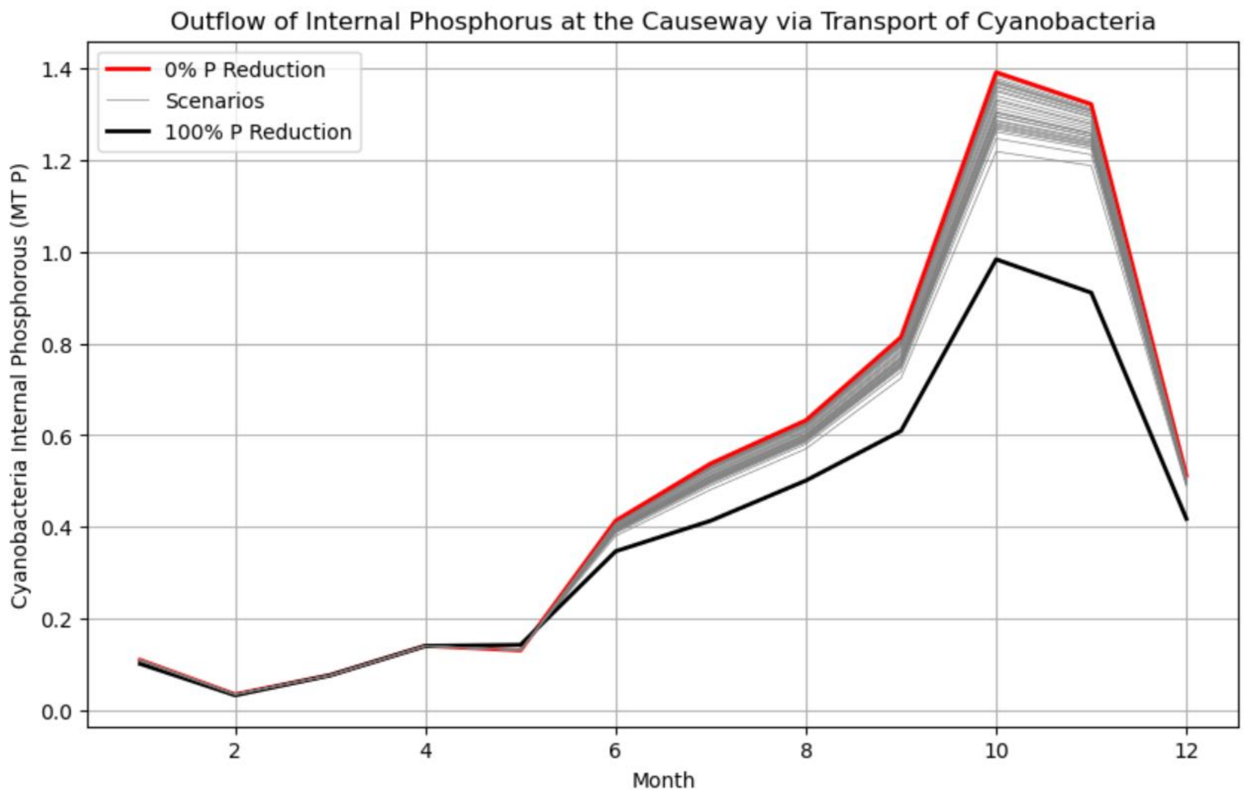

Figure 30. The average monthly mass of phosphorus exported via cyanobacteria from Missisquoi Bay to the Inland Sea. Red line is baseline scenario, grey lines are P reduction scenarios and the black line is a simulation with no watershed P input.

Impacts of P Reductions on Cyanobacteria Blooms and Achieving the TMDL Target Concentration

Unfortunately, all P reduction scenarios had minimal impact on the number of days that the bay is simulated to have bloom conditions at a threshold of 20 μg/L or higher bay-wide average chlorophyll concentration. Under the largest P reduction scenario, the bloom decreased by only a few days in the summer or up to a week when considering the entire year (Figure 31, Tables 31 and 30, respectively). In general, this result agrees with previous model simulations of the bay's biogeochemistry and ecology with this model (Braun et al., 2024) and the Limnotech model (Zia et al., 2022; Limnotech, 2012), as well as our process-based understanding of the bay (e.g., Isles et al., 2015, 2017a). These process-based modeling studies have all indicated that large reductions, almost double the maximum P reduction scenario used here, are required to have an appreciable decrease in cyanobacteria blooms (e.g., Zia et al., 2022). This result is due to the persistence of large stores of legacy phosphorus in the bay's sediment that provide P to cyanobacteria under conditions where they naturally thrive (hot and dry portions summer). Once initiated, those blooms are often resilient and can persist well into fall. Conversely, watershed P input reductions impact water column P inventories in Missisquoi Bay most during shoulder seasons when conditions are often unfavorable for cyanobacteria dominance (turbid, cool water).

Not surprisingly given the annual dominance of tributary P input to annual P balance (Figure 25), phosphorus concentrations are much more responsive to the landscape P reduction scenarios when compared to the scenarios' minimal impacts on bloom dynamics. The average yearly TP concentrations in the bay were between 47 and 61 μg/L in the baseline scenario. Average TP concentrations decreased to a range of 30 to 39 μg/L under maximum reduction scenarios (see ranges in Table 30). Average total P concentrations are higher in the summers than the annual average under maximum P reduction because that is the time of the year when internal loading of P is most prevalent (Figure 29, Table 31). Thus, we can conclude that while the bay would not meet the TMDL target concentration of 25 μg/L under any of these scenarios, they would get the bay substantially closer to its target concentration relative to current conditions.

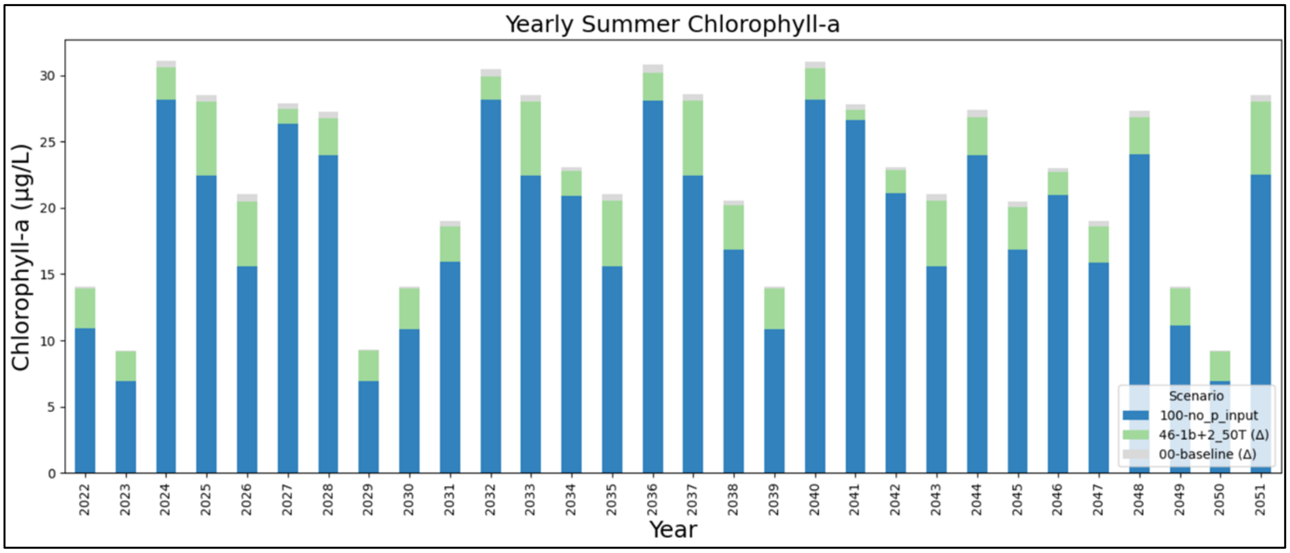

Figure 31. Average annual summer (June through September) chlorophyll-a concentrations in Missisquoi Bay in response to baseline (0% reduction) in blue, maximum achieved reduction in metamodel simulations in green, and no riverine P input in blue.

Table 30. Model P mass balance (total P inputs – total P outputs) and water quality output by simulation year for baseline scenarios with the range of data output for the minimum and maximum P reduction scenario in parentheses.

Yr	Trib Input (MT/yr)	Outflow (MT/yr)	Bloom Days	TP in Water (mg/L)	Internal Load (MT/yr)	TP Mass Balance (MT/yr)
2022	179.8 (179.8 - 98.9)	89.2 (89.2 - 65.0)	26 (26 - 23)	47.3 (47.3 - 32.3)	30.5 (30.5 - 30.6)	90.6 (90.6 - 33.9)
2023	248.0 (248.0 - 136.7)	115.3 (115.3 - 78.0)	8 (8 - 0)	50.0 (50.0 - 32.6)	27.0 (27.0 - 26.9)	132.8 (132.8 - 58.7)
2024	238.1 (238.1 - 132.5)	101.6 (101.6 - 65.9)	102 (102 - 101)	51.0 (51.0 - 33.2)	27.7 (27.7 - 27.7)	136.5 (136.5 - 66.6)
2025	179.5 (179.5 - 98.8)	91.6 (91.6 - 61.4)	110 (110 - 108)	48.3 (48.3 - 31.9)	26.6 (26.6 - 26.7)	88.0 (88.0 - 37.4)
2026	481.0 (481.0 - 265.5)	159.2 (159.2 - 100.3)	66 (66 - 62)	56.9 (56.9 - 35.3)	25.5 (25.5 - 25.5)	321.8 (321.8 - 165.2)
2027	128.0 (128.0 - 70.8)	77.3 (77.3 - 52.4)	120 (120 - 118)	56.2 (56.2 - 38.0)	33.8 (33.8 - 33.8)	50.7 (50.7 - 18.5)
2028	151.9 (151.9 - 83.2)	89.3 (89.3 - 62.2)	114 (114 - 111)	47.5 (47.5 - 32.7)	27.6 (27.6 - 27.7)	62.7 (62.7 - 21.0)
2029	239.2 (239.2 - 131.1)	113.4 (113.4 - 76.4)	0 (0 - 0)	47.8 (47.8 - 31.0)	27.2 (27.2 - 27.1)	125.8 (125.8 - 54.7)
2030	195.8 (195.8 - 107.9)	108.1 (108.1 - 74.2)	26 (26 - 23)	52.7 (52.7 - 34.5)	33.2 (33.2 - 33.1)	87.6 (87.6 - 33.7)
2031	205.2 (205.2 - 111.7)	117.9 (117.9 - 78.4)	56 (56 - 46)	51.5 (51.5 - 32.9)	28.4 (28.4 - 28.4)	87.3 (87.3 - 33.2)
2032	269.0 (269.0 - 146.7)	120.5 (120.5 - 75.6)	99 (99 - 99)	54.5 (54.5 - 34.4)	27.7 (27.7 - 27.8)	148.5 (148.5 - 71.0)
2033	204.4 (204.4 - 111.2)	107.5 (107.5 - 70.2)	113 (113 - 112)	52.9 (52.9 - 33.9)	26.8 (26.8 - 26.8)	96.9 (96.9 - 41.1)
2034	595.2 (595.2 - 332.6)	153.6 (153.6 - 96.1)	77 (77 - 76)	61.1 (61.1 - 38.7)	28.6 (28.6 - 28.6)	441.5 (441.5 - 236.5)
2035	370.0 (370.0 - 202.7)	154.8 (154.8 - 97.7)	77 (77 - 70)	61.5 (61.5 - 38.5)	24.7 (24.7 - 24.8)	215.2 (215.2 - 105.0)
2036	172.9 (172.9 - 94.7)	94.4 (94.4 - 61.8)	118 (118 - 117)	56.3 (56.3 - 36.7)	28.2 (28.2 - 28.3)	78.5 (78.5 - 32.9)
2037	204.4 (204.4 - 111.2)	117.4 (117.4 - 75.9)	113 (113 - 112)	57.3 (57.3 - 36.4)	26.7 (26.7 - 26.8)	87.0 (87.0 - 35.4)
2038	457.4 (457.4 - 252.6)	156.1 (156.1 - 98.9)	67 (67 - 66)	55.1 (55.1 - 33.7)	26.6 (26.6 - 26.6)	301.3 (301.3 - 153.7)
2039	182.8 (182.8 - 100.7)	107.3 (107.3 - 73.8)	52 (52 - 48)	54.2 (54.2 - 35.5)	33.3 (33.3 - 33.2)	75.5 (75.5 - 26.9)

Yr	Trib Input (MT/yr)	Outflow (MT/yr)	Bloom Days	TP in Water (mg/L)	Internal Load (MT/yr)	TP Mass Balance (MT/yr)
2040	255.5 (255.5 - 141.9)	122.6 (122.6 - 78.4)	110 (110 - 102)	56.5 (56.5 - 36.5)	27.0 (27.0 - 27.1)	132.8 (132.8 - 63.5)
2041	90.0 (90.0 - 50.0)	63.2 (63.2 - 45.4)	122 (122 - 119)	47.5 (47.5 - 33.8)	33.6 (33.6 - 33.6)	26.8 (26.8 - 4.6)
2042	380.6 (380.6 - 212.6)	110.2 (110.2 - 72.6)	100 (100 - 98)	54.0 (54.0 - 36.8)	29.1 (29.1 - 29.2)	270.4 (270.4 - 140.0)
2043	370.0 (370.0 - 202.7)	150.2 (150.2 - 95.2)	76 (76 - 70)	58.3 (58.3 - 36.8)	24.7 (24.7 - 24.7)	219.7 (219.7 - 107.5)
2044	183.1 (183.1 - 100.5)	100.7 (100.7 - 67.2)	107 (107 - 103)	51.9 (51.9 - 34.0)	26.8 (26.8 - 26.8)	82.4 (82.4 - 33.4)
2045	267.4 (267.4 - 145.3)	123.8 (123.8 - 79.6)	64 (64 - 61)	48.8 (48.8 - 30.4)	25.9 (25.9 - 25.9)	143.6 (143.6 - 65.7)
2046	383.6 (383.6 - 214.3)	116.9 (116.9 - 74.9)	100 (100 - 98)	54.3 (54.3 - 35.5)	28.9 (28.9 - 28.9)	266.7 (266.7 - 139.4)
2047	275.4 (275.4 - 150.6)	128.6 (128.6 - 84.5)	61 (61 - 57)	55.6 (55.6 - 35.3)	28.0 (28.0 - 28.0)	146.8 (146.8 - 66.1)
2048	279.2 (279.2 - 152.5)	138.4 (138.4 - 88.0)	88 (88 - 86)	56.5 (56.5 - 35.3)	26.2 (26.2 - 26.2)	140.8 (140.8 - 64.5)
2049	204.3 (204.3 - 111.6)	111.1 (111.1 - 74.8)	26 (26 - 23)	53.1 (53.1 - 34.2)	31.8 (31.8 - 31.6)	93.3 (93.3 - 36.8)
2050	248.0 (248.0 - 136.7)	120.5 (120.5 - 80.6)	8 (8 - 0)	51.4 (51.4 - 33.3)	27.1 (27.1 - 27.0)	127.5 (127.5 - 56.1)
2051	202.3 (202.3 - 111.2)	108.2 (108.2 - 69.8)	90 (90 - 89)	51.7 (51.7 - 32.8)	26.9 (26.9 - 27.1)	94.1 (94.1 - 41.4)

Table 31. Summer model P balance (total P inputs – total P outputs) and water quality output by simulation year for baseline scenario with the range of data output for the minimum and maximum P reduction scenario in parentheses. To be consistent with previous modeling studies, June through September was considered 'summer'.

Yr	Trib Input (MT/yr)	Outflow (MT/yr)	Bloom Days	TP in Water (ug/L)	Internal Load (MT/yr)	TP Mass Balance (MT/yr)
2022	84.9 (84.9 - 46.9)	32.5 (32.5 - 22.8)	26 (26 - 23)	54.8 (54.8 - 37.9)	20.1 (20.1 - 20.1)	50.1 (50.1 - 22.0)
2023	29.2 (29.2 - 15.6)	25.9 (25.9 - 19.0)	0 (0 - 0)	48.6 (48.6 - 34.5)	18.0 (18.0 - 18.0)	1.1 (1.1 - -5.4)
2024	3.3 (3.3 - 1.8)	9.8 (9.8 - 7.4)	102 (102 - 101)	47.4 (47.4 - 35.7)	19.2 (19.2 - 19.3)	-8.6 (-8.6 - -7.5)
2025	5.9 (5.9 - 3.2)	16.5 (16.5 - 11.2)	90 (90 - 89)	51.9 (51.9 - 35.7)	18.5 (18.5 - 18.6)	-13.1 (-13.1 - -10.1)
2026	23.2 (23.2 - 12.1)	20.3 (20.3 - 14.0)	63 (63 - 59)	52.0 (52.0 - 35.1)	15.7 (15.7 - 15.7)	0.4 (0.4 - -4.1)
2027	1.2 (1.2 - 0.7)	5.9 (5.9 - 4.4)	101 (101 - 100)	56.3 (56.3 - 42.5)	22.0 (22.0 - 22.1)	-5.6 (-5.6 - -4.7)
2028	29.9 (29.9 - 16.0)	13.9 (13.9 - 10.5)	88 (88 - 86)	42.3 (42.3 - 31.3)	17.3 (17.3 - 17.4)	13.1 (13.1 - 2.9)
2029	29.2 (29.2 - 15.6)	26.5 (26.5 - 19.4)	0 (0 - 0)	48.9 (48.9 - 34.7)	18.1 (18.1 - 18.1)	0.4 (0.4 - -5.8)
2030	84.9 (84.9 - 46.9)	33.9 (33.9 - 23.5)	26 (26 - 23)	56.4 (56.4 - 38.7)	20.1 (20.1 - 20.1)	48.7 (48.7 - 21.3)
2031	49.1 (49.1 - 26.5)	22.2 (22.2 - 15.8)	48 (48 - 46)	45.4 (45.4 - 31.6)	18.7 (18.7 - 18.7)	21.6 (21.6 - 6.1)
2032	4.1 (4.1 - 2.2)	8.0 (8.0 - 6.2)	99 (99 - 99)	48.1 (48.1 - 36.0)	19.3 (19.3 - 19.4)	-5.7 (-5.7 - -5.6)
2033	5.9 (5.9 - 3.2)	16.4 (16.4 - 11.1)	90 (90 - 89)	51.6 (51.6 - 35.7)	18.5 (18.5 - 18.6)	-12.9 (-12.9 - -10.1)
2034	4.0 (4.0 - 2.2)	13.2 (13.2 - 9.7)	74 (74 - 73)	61.4 (61.4 - 44.7)	20.0 (20.0 - 20.0)	-10.7 (-10.7 - -8.8)
2035	23.2 (23.2 - 12.1)	21.7 (21.7 - 14.8)	63 (63 - 59)	55.8 (55.8 - 37.3)	15.7 (15.7 - 15.7)	-1.0 (-1.0 - -4.9)
2036	4.1 (4.1 - 2.2)	9.3 (9.3 - 6.9)	99 (99 - 99)	54.9 (54.9 - 39.9)	19.3 (19.3 - 19.4)	-7.0 (-7.0 - -6.3)
2037	5.9 (5.9 - 3.2)	17.5 (17.5 - 11.7)	90 (90 - 89)	54.7 (54.7 - 37.3)	18.5 (18.5 - 18.6)	-14.0 (-14.0 - -10.7)
2038	28.1 (28.1 - 14.6)	22.3 (22.3 - 15.3)	64 (64 - 63)	48.3 (48.3 - 32.2)	17.4 (17.4 - 17.5)	2.0 (2.0 - -3.9)
2039	84.9 (84.9 - 46.9)	35.7 (35.7 - 24.5)	26 (26 - 23)	58.2 (58.2 - 39.7)	20.1 (20.1 - 20.1)	46.9 (46.9 - 20.3)
2040	3.3 (3.3 - 1.8)	10.3 (10.3 - 7.7)	102 (102 - 101)	48.7 (48.7 - 36.4)	19.3 (19.3 - 19.3)	-9.1 (-9.1 - -7.8)
2041	1.2 (1.2 - 0.7)	5.4 (5.4 - 4.2)	102 (102 - 100)	51.1 (51.1 - 39.6)	22.0 (22.0 - 22.0)	-5.2 (-5.2 - -4.4)
2042	4.0 (4.0 - 2.2)	12.8 (12.8 - 9.5)	74 (74 - 73)	57.3 (57.3 - 42.4)	20.0 (20.0 - 20.0)	-10.3 (-10.3 - -8.6)
2043	23.2 (23.2 - 12.1)	21.0 (21.0 - 14.4)	63 (63 - 59)	53.1 (53.1 - 35.8)	15.7 (15.7 - 15.7)	-0.2 (-0.2 - -4.5)
2044	29.9 (29.9 - 16.0)	14.6 (14.6 - 10.9)	88 (88 - 86)	44.9 (44.9 - 32.8)	17.3 (17.3 - 17.4)	12.3 (12.3 - 2.5)
2045	28.1 (28.1 - 14.6)	20.8 (20.8 - 14.4)	64 (64 - 61)	44.3 (44.3 - 29.9)	17.4 (17.4 - 17.5)	3.6 (3.6 - -3.0)

Yr	Trib Input (MT/yr)	Outflow (MT/yr)	Bloom Days	TP in Water (ug/L)	Internal Load (MT/yr)	TP Mass Balance (MT/yr)
2046	4.0 (4.0 - 2.2)	12.7 (12.7 - 9.4)	74 (74 - 73)	57.1 (57.1 - 42.2)	20.0 (20.0 - 20.0)	-10.2 (-10.2 - - 8.5)
2047	49.1 (49.1 - 26.5)	24.3 (24.3 - 17.1)	48 (48 - 46)	50.5 (50.5 - 34.4)	18.7 (18.7 - 18.7)	19.4 (19.4 - 4.8)
2048	29.9 (29.9 - 16.0)	14.0 (14.0 - 10.5)	88 (88 - 86)	43.8 (43.8 - 32.1)	17.3 (17.3 - 17.4)	12.9 (12.9 - 2.9)
2049	84.9 (84.9 - 46.9)	33.8 (33.8 - 23.4)	26 (26 - 23)	56.3 (56.3 - 38.6)	20.1 (20.1 - 20.1)	48.8 (48.8 - 21.4)
2050	29.2 (29.2 - 15.6)	26.6 (26.6 - 19.4)	0 (0 - 0)	49.4 (49.4 - 34.9)	18.0 (18.0 - 18.0)	0.3 (0.3 - -5.8)
2051	5.9 (5.9 - 3.2)	16.7 (16.7 - 11.3)	90 (90 - 89)	52.7 (52.7 - 36.1)	18.5 (18.5 - 18.6)	-13.2 (-13.2 - - 10.2)

Task 8: Develop the Missisquoi Basin P Mass Balance Assessment Toolkit

The results of the development of the Missisquoi Bason P Mass Balance Toolkit included two components. The first component was the linear regression models used to determine Bay P mass balance outcomes based in reductions in watershed P loadings to the Bay. The second component was the web-based application itself.

Linear Regression Models for Bay P Mass Balance from Watershed Load Reductions

Linear regression models were developed to enable the determination of Bay P mass balance components (P mass balance, P concentration, and cyanobacteria bloom days) based on any user-defined alternative management scenario. This was necessary for two reasons. First, only a subset (30) of all 90 alternative management scenarios simulated with the metamodel were used as inputs to the AEM3D Bay simulations from which Bay P results were quantified. Second, users of the Toolkit can construct their own watershed P loading scenario by combining HUC12-scale loadings from multiple different alternative scenarios simulations, resulting in a unique watershed scale load estimate not directly associated with any of the 90 alternatives originally generated. The linear regression models provide the mechanism to associate Bay P quantities with any possible watershed P reduction between the baseline conditions and the most impactful combination of P reduction practices evaluated.

The first linear regression model quantifies the Bay total P mass balance (Bay P inputs – Bay P outputs) as a function of the watershed P load reduction and is shown in Figure 32. As shown, there is a strong linear relationship, with an R^2 value of 0.9994.

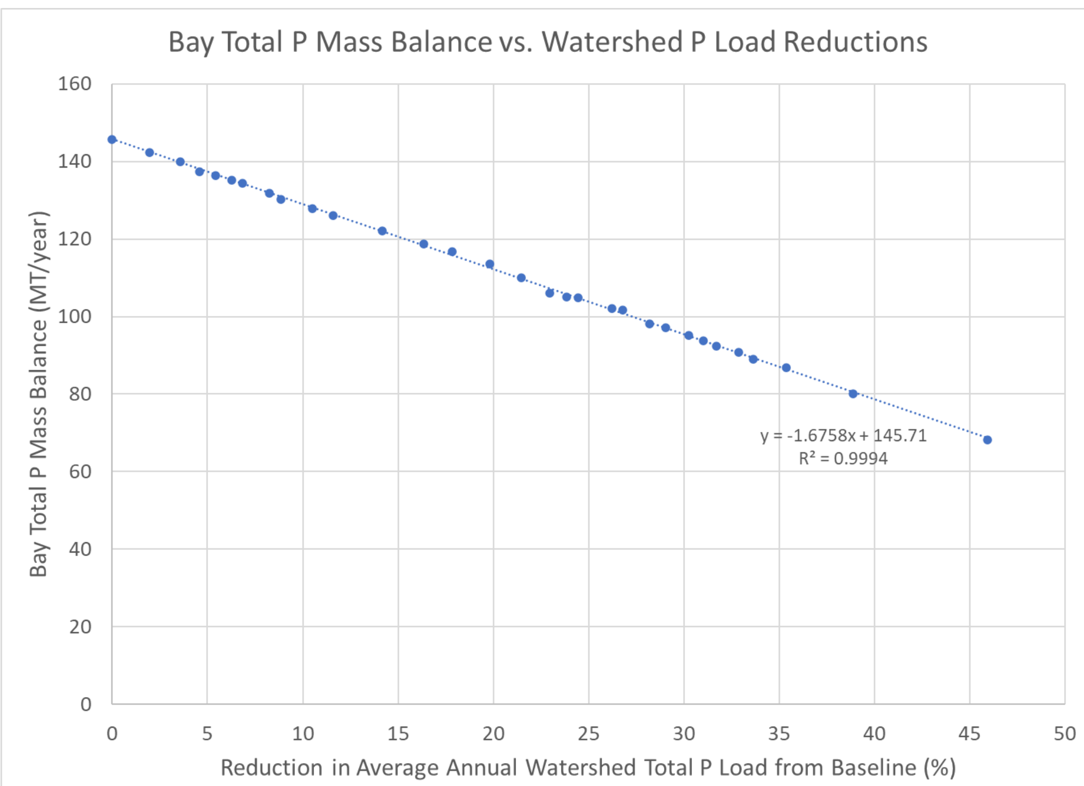

Figure 32. Linear regression model for Bay P mass balance (total P inputs – total P outputs) as a function of watershed average annual P loading reduction.

The second regression model quantifies the Bay average annual aquatic total P concentration as a function of the watershed P load reduction. The linear regression is shown in Figure 33. As shown, there is a strong linear relationship, with an R^2 value of 0.9999. The lower slope of this regression line (-0.4106) compared to the slope of the P mass balance regression in Figure 32 (-1.6758) indicates that the aquatic P concentration is less responsive to the loading reductions, likely due to legacy P in the benthic sediment partitioning into the water column. This supposition is supported by the maximum watershed P load reduction (46%) resulting in a 53% reduction in the Bay P mass balance (Figure 32) but only a 35% reduction in the Bay's aquatic P concentration (Figure 33).

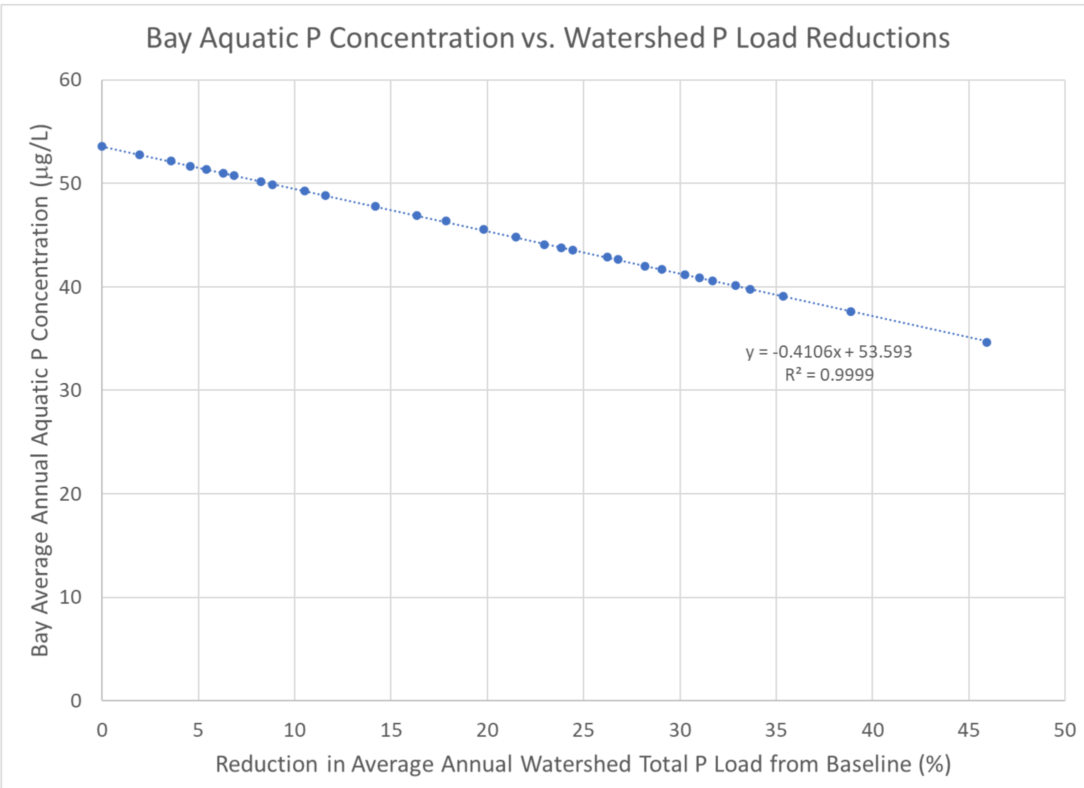

Figure 33. Linear regression model for Bay average annual aquatic P concentration as a function of watershed average annual P loading reduction.

The third regression model quantifies the Bay average annual days with cyanobacteria blooms as a function of the watershed P load reduction. The days with cyanobacteria blooms are assumed to occur when the daily aquatic P concentration exceeds 20 µg/L. The result of this linear regression is shown in Figure 34. The linear relationship between watershed P load reduction and the days of cyanobacteria blooms is also quite strong (R^2 value of 0.9717), although we see slightly higher residuals, and a much lower slope (-0.0842), indicating that even with large reductions in watershed P loads, the cyanobacteria bloom days decrease only slightly. The previous section of this report provides more expansive discussion of these same observations.

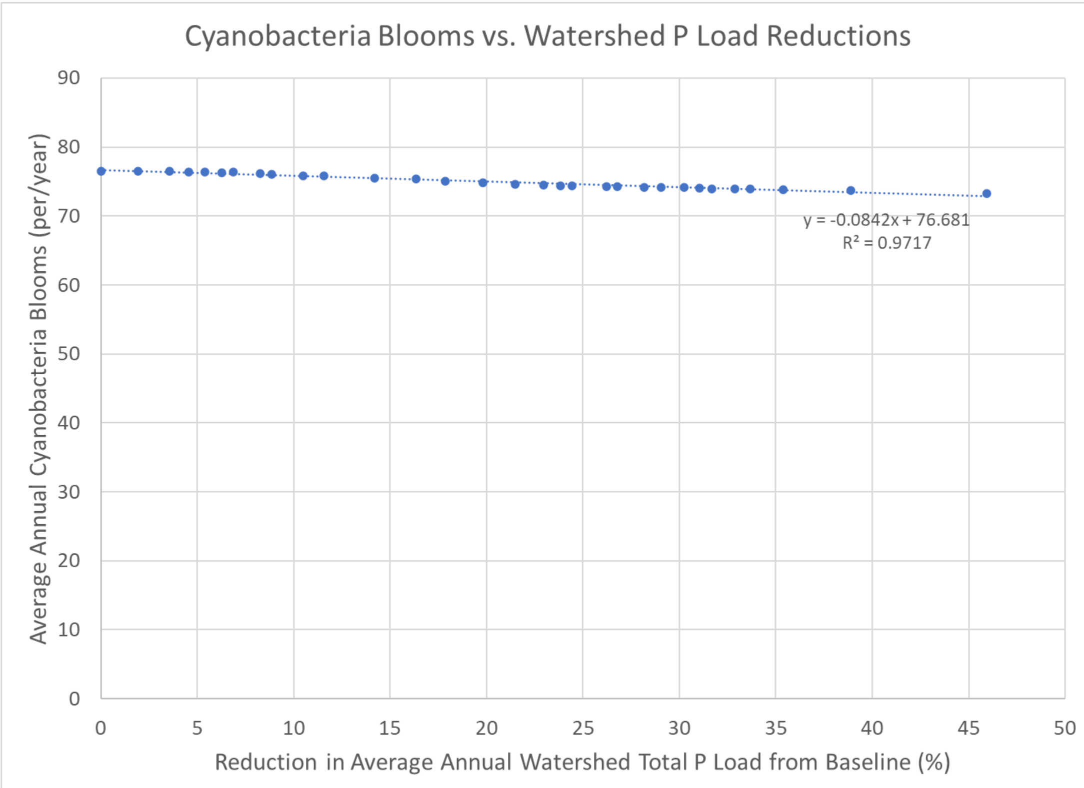

Figure 34. Linear regression model for Bay average annual cyanobacteria bloom days as a function of watershed average annual P loading reduction.

The three linear regression models described above were incorporated into the P Mass Balance Toolkit to provide the linkage between user-defined alternative management scenarios and the P quantity outcomes in the Bay.

Web-Based Toolkit

The Toolkit is a web-based mapping application enabling users to evaluate how changes P management practices across the watershed impact the P mass balance in Missisquoi Bay. The functionality of the application will be demonstrated in a stepwise fashion through an example analysis session with accompanying screenshots. The Toolkit can be accessed at: https://www.stone-env.net/mass_balance/

1. Upon arriving at the Toolkit web site, a map of the average annual total P yield at the HUC12 scale is shown (see Figure 35). The legend provides the scale for P yield in kg/ha-yr. These results are directly from the metamodel.
2. Clicking a HUC12 in the map will bring up information on the HUC12 watershed, including name, scenario being mapped, and the P quantity being mapped and shown on the legend (see Figure 36).
3. Clicking on the *Show Table* tab expands a table that shows results of the *Baseline Condition*, including watershed P loading and yield, and resulting Missisquoi P mass balance, P water concentration, and cyanobacteria bloom days (Figure 37). At this point, an *Alternative Scenario* has not yet been defined, thus that entries in the results table

are shown as *NA*. The table can be removed from the display by clicking the *Hide Table Results* tab.

4. To begin an *Alternative Scenario* analysis, the user clicks on the *Analyze Alternative P Management Scenario* button, which opens the first data entry interface (see Figure 38) to select the P mass balance quantity to map (Total P Load, Total P Yield, or Total P Load Change).

5. Once a P mass balance quantity is selected, the interface to describe the characteristics of an *Alternative Scenario* opens within the sidebar (see Figure 39). The options to define an *Alternative Scenario* include Septic Improvement, BMP Implementation, BMP, and Land Conversion. The options to define the scenario must be entered sequentially from top to bottom in the sidebar interface. As each option is defined, only valid alternatives for the next option are allowed for selection.

6. The *Septic Improvement* option has values of *Yes* or *No* (Figure 40). When *Yes* is selected, both septic system and centralized wastewater treatment average annual P loads are reduced by 34% (details provided in Task 6 discussion in Sections 3 and 5). When *No* is selected, the Baseline septic system and wastewater P loads are assumed.

7. The *BMP Implementation* option has values of *100%*, *20% Random*, *20% Targeted*, *50% Random*, and *50% Targeted* (Figure 41). Each of these implementation options are relevant to the agricultural land BMPs only and are applied to all eligible agricultural land cover classes.

8. The *BMP option* is enabled after a *BMP Implementation* value is selected (Figure 42). There will always be six choices for the BMP option, including *Nutrient Management (Manure* Incorporated, No Late Fall Application), *Erosion Control (Combined Cover Crop and No Till/Conservation Till)*, *Landscape/Structural Controls (Riparian Buffers and Water/Sediment Control Basins)*, *Nutrient Management & Erosion Controls*, and *Nutrient Management & Erosion Controls & Landscape/Structural Controls*, and *Land Conversion (Annual Crops to Permanent Grassland)*. Details concerning the modeling of these BMPs are provided in descriptions of Task 6 in Sections 3 and 5.

9. The *Land Conversion* option is enabled after a *BMP* value is selected (Figure 43). The number of choices for the *Land Conversion* option will vary from one to four options, depending upon the previous option selection. For the *BMP* options selected with 50% targeted implementation, *Land Conversion* rate values of None, 5%, 10%, or 20% are available. For the other combinations of *BMP* and *BMP Implementation* selected, only one Land Conversion option will be available (none, 20%, 50%, or 100%).

10. Once all the *Alternative Scenario* input options have been selected, the single final *Alternative Scenario* should result (see Figure 44).

11. The user can then apply the alternative scenario created to 1 or more HUC12 watersheds, with 40 sub-watersheds covering the entire Missisquoi Bay watershed. Clicking the *Select All Regions* button chooses the entire Bay watershed. Users may choose to individually remove HUC12 watersheds from the analysis by clicking on the “x” next to the HUC12 name. Clicking on the *Submit* button initiates the back-end analysis which constructs the watershed-level alternative scenario analysis, applies

linear regression models to determine Bay P mass balance outputs, and updates the map and results table to report the impacts of the alternative scenario on the watershed and Bay P mass balance (see Figure 45).

12. The watershed map of HUC12s is updated with the quantity selected for the Alternative Scenario (Figure 46), with the characteristics describing the *Alternative Scenario* displayed in the sidebar.

13. Showing the results table now includes model outputs from the *Alternative Scenario* in addition to the *Baseline* (Figure 47). The percent reductions in each P mass balance quantity are also displayed.

14. *Alternative Scenarios* applied to a sub-set of HUC12 sub-watersheds assume that *Baseline* conditions apply to the remainder of the HUC12s within the Bay watershed (Figure 48). The results displayed in the *Results Table* still reflect changes in P mass balance quantities for the entire watershed, with alternative P management practices applied to the selected HUC12s only (Figure 49).

15. *Clicking Clear All Scenarios* clear the map and *Results Table (Figure 50)*.

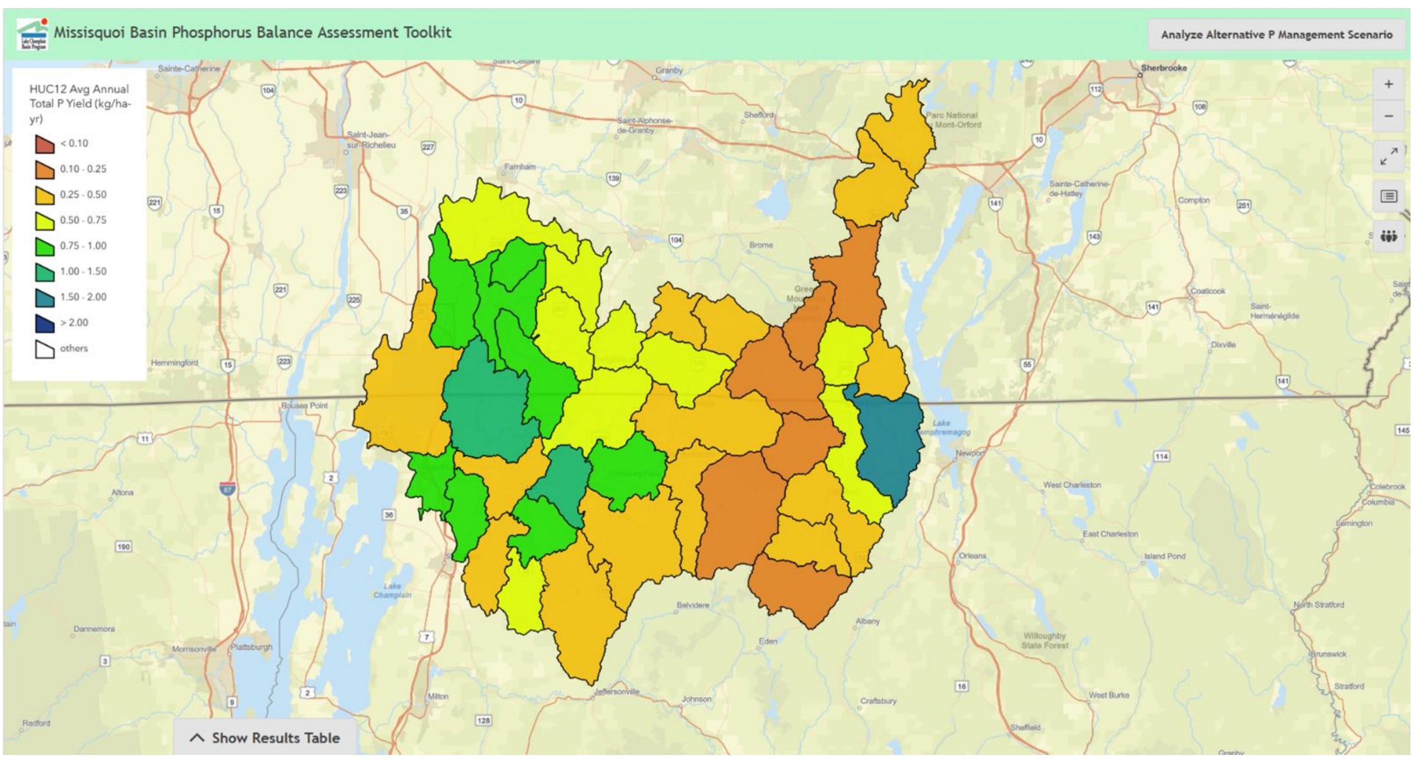

Figure 35. P Mass Balance Toolkit opening map.

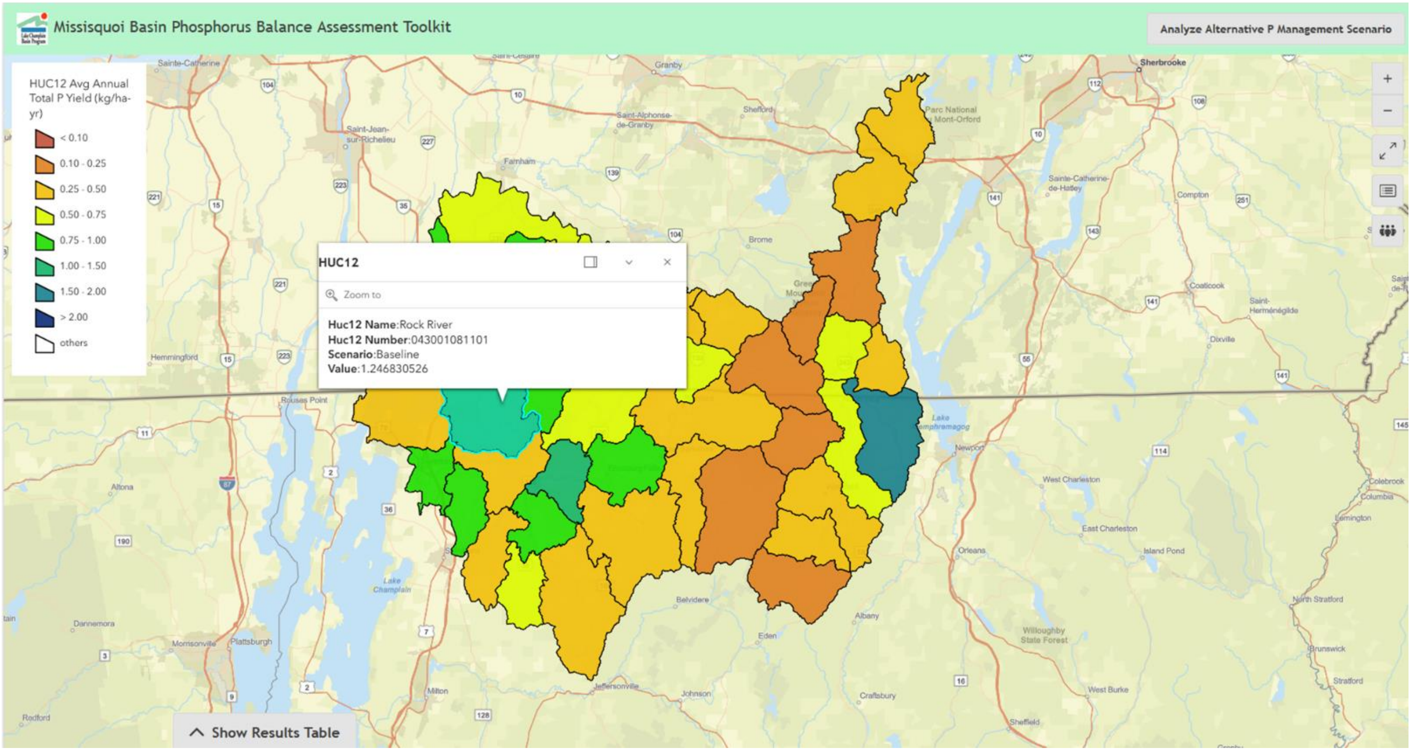

Figure 36. Information about a HUC12 shown upon clicking the map.

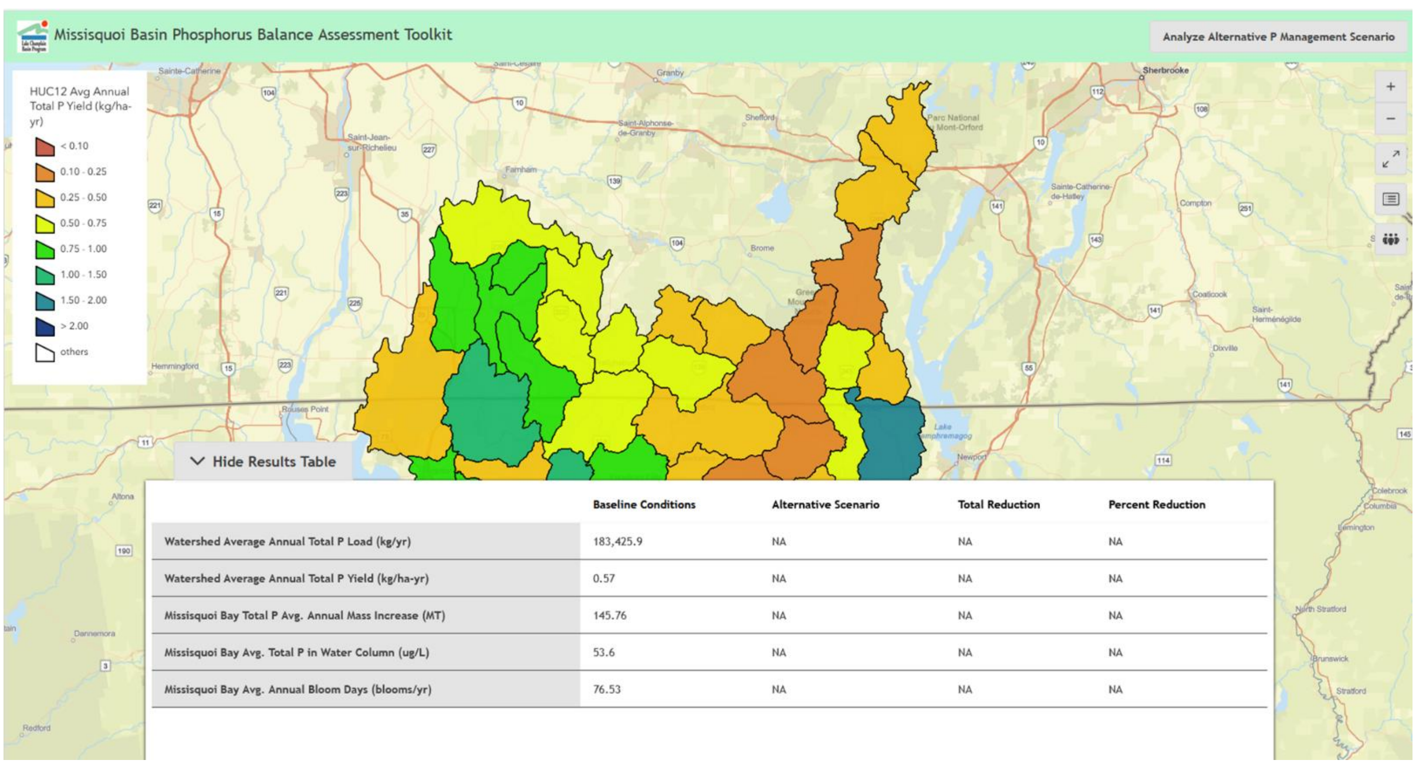

	Baseline Conditions	Alternative Scenario	Total Reduction	Percent Reduction
Watershed Average Annual Total P Load (kg/yr)	183,425.9	NA	NA	NA
Watershed Average Annual Total P Yield (kg/ha-yr)	0.57	NA	NA	NA
Missisquoi Bay Total P Avg. Annual Mass Increase (MT)	145.76	NA	NA	NA
Missisquoi Bay Avg. Total P in Water Column (ug/L)	53.6	NA	NA	NA
Missisquoi Bay Avg. Annual Bloom Days (blooms/yr)	76.53	NA	NA	NA

Figure 37. Tabular results of the Baseline Condition, including watershed P loading and yield, and resulting Missisquoi P mass balance, P water concentration, and cyanobacteria bloom days.

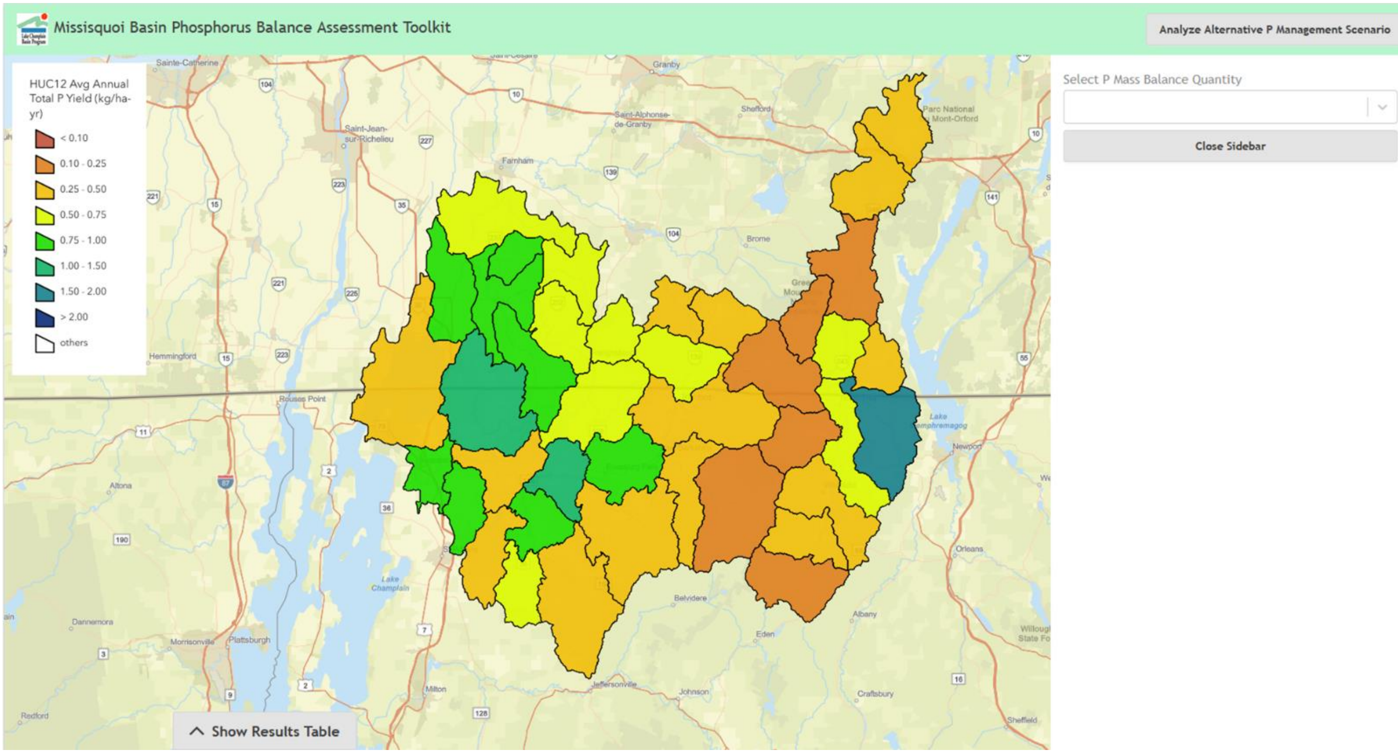

Figure 38. Clicking on the Analyze Alternative P Management Scenario button opens the first data entry interface to select the P Mass Balance quantity to map.

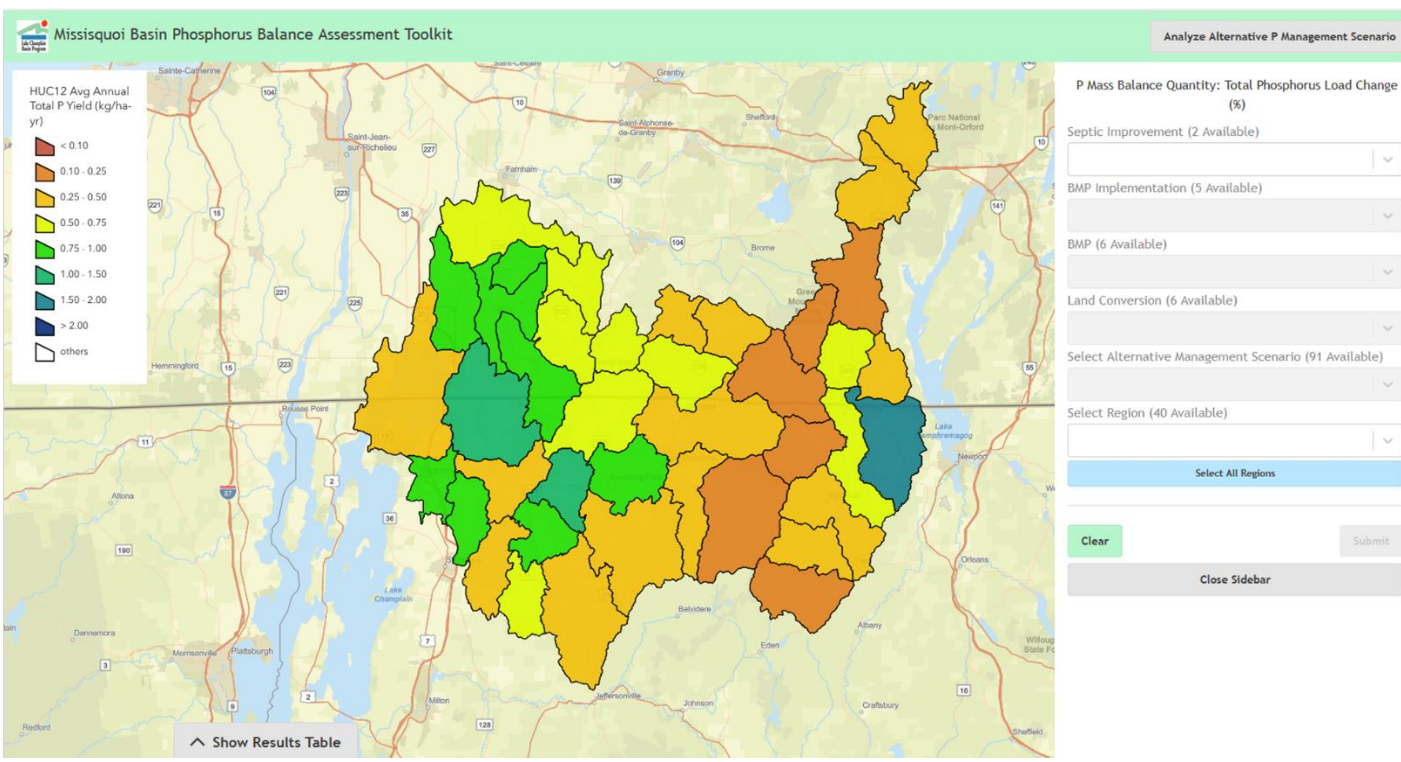

Figure 39. Sidebar for defining an Alternative Scenario after having chosen a P mass balance quantity to evaluate and map.

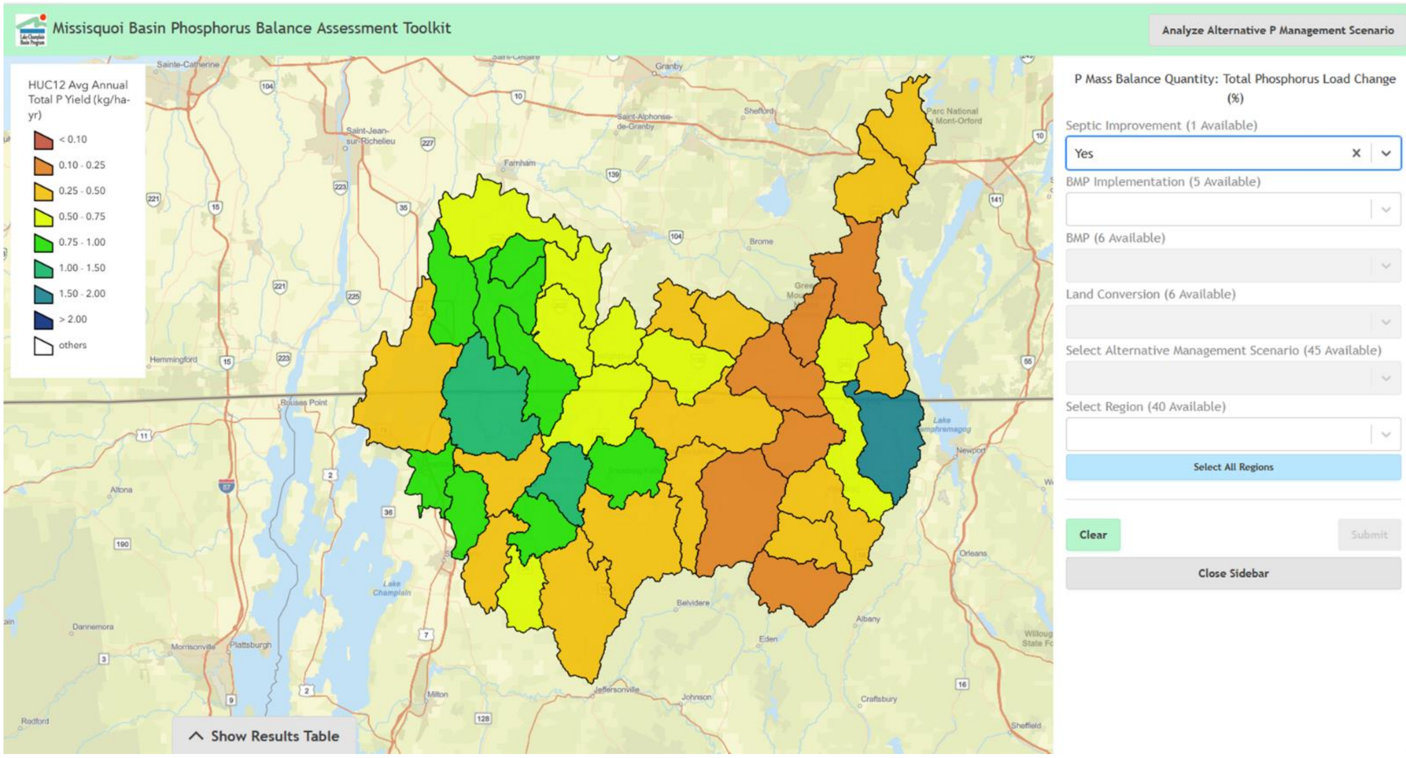

Figure 40. Selection of the Septic Improvement option for Alternative Scenario definition.

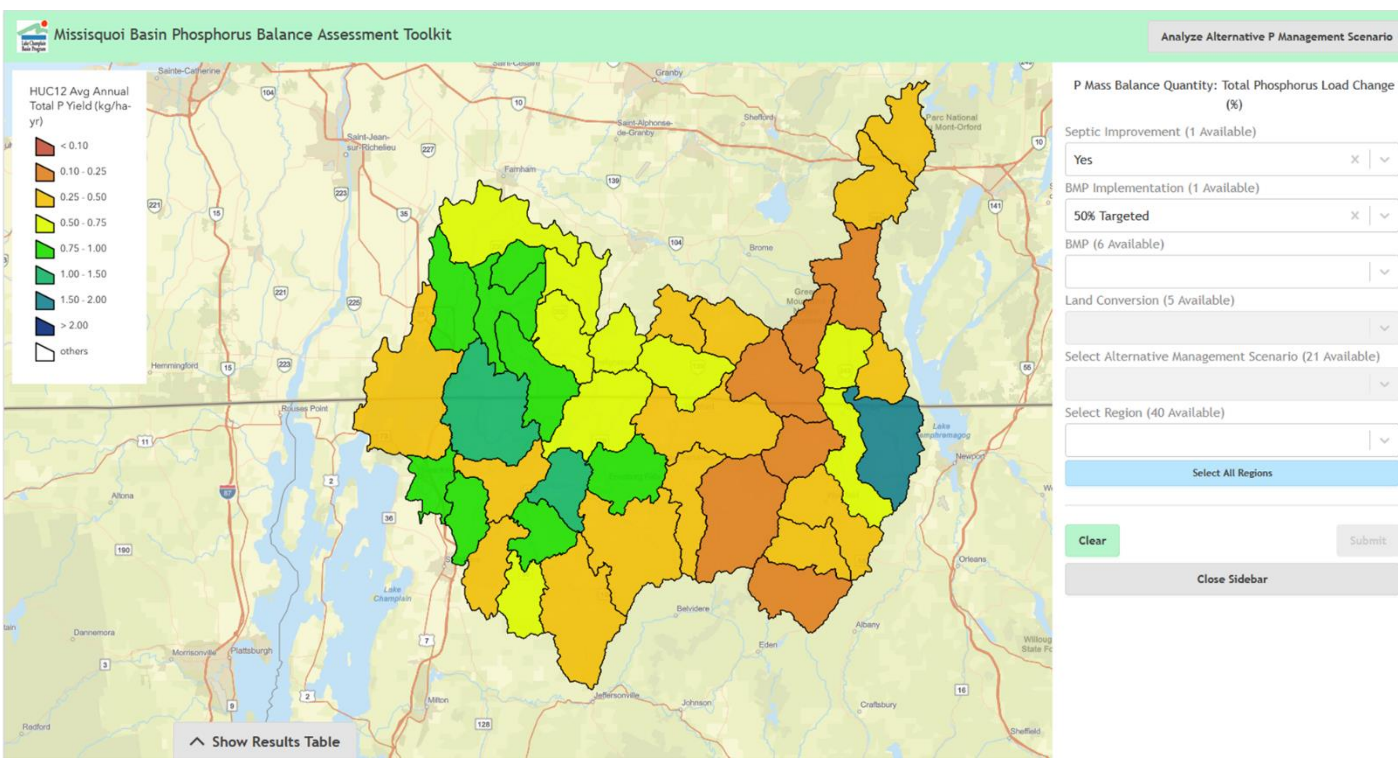

Figure 41. Selection of BMP Implementation option for Alternative Scenario definition.

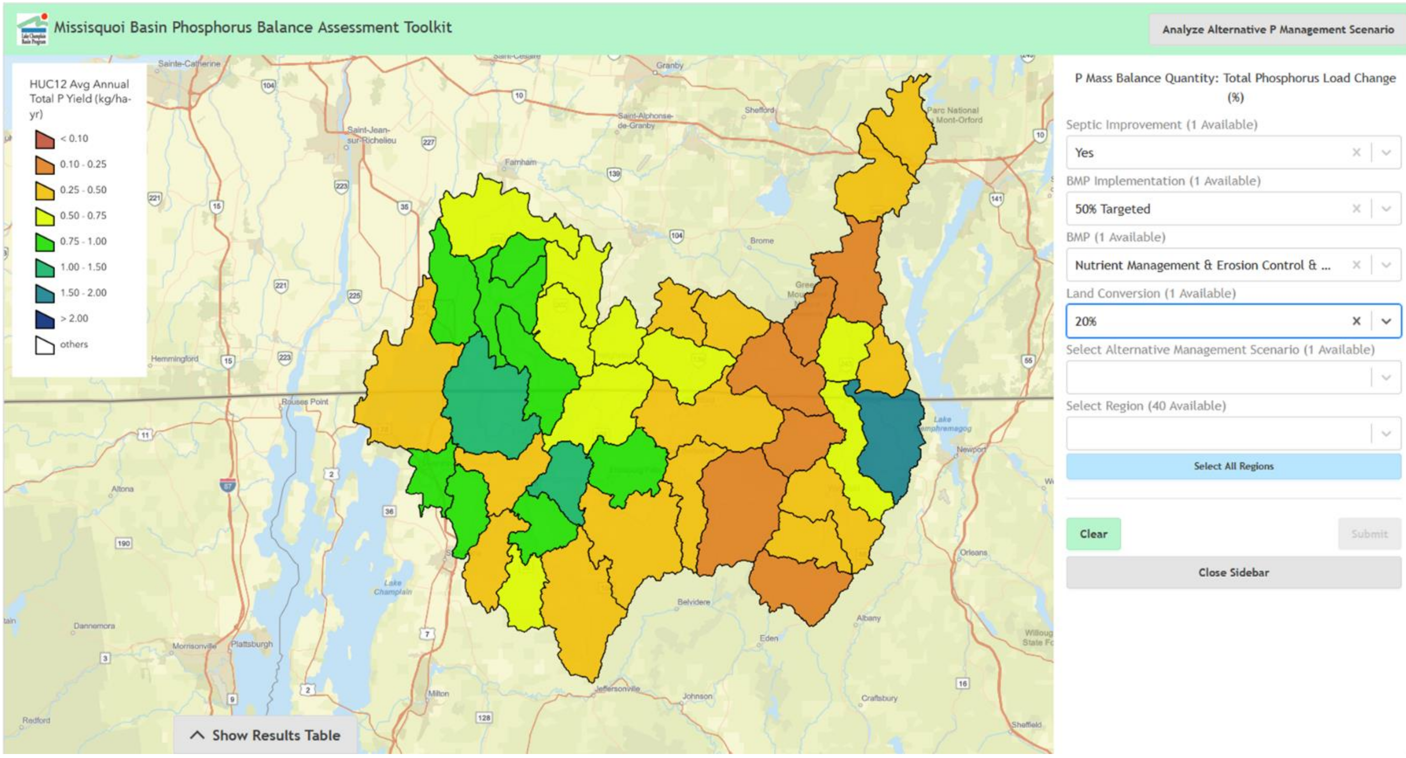

Figure 42. Selection of BMP option for Alternative Scenario definition.

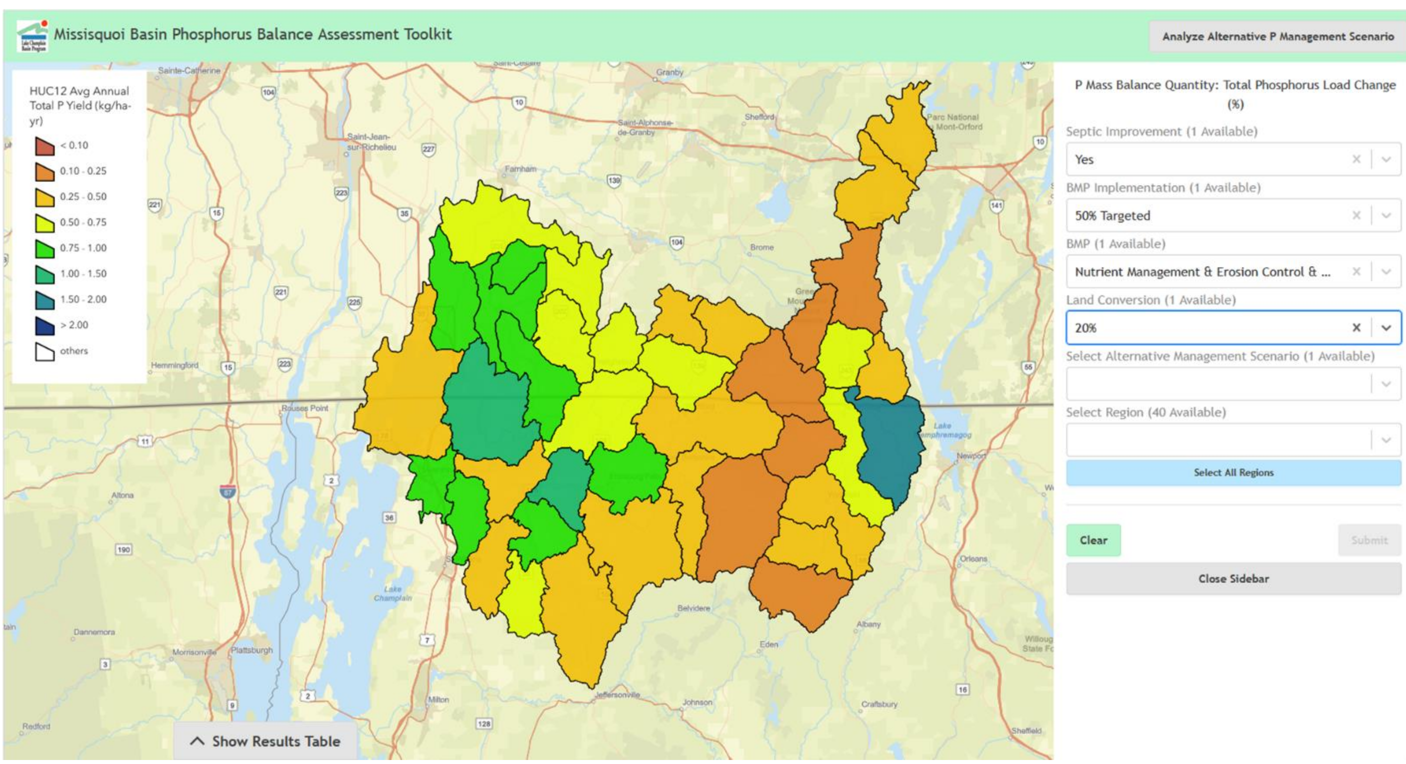

Figure 43. Land Conversion option for Alternative Scenario definition.

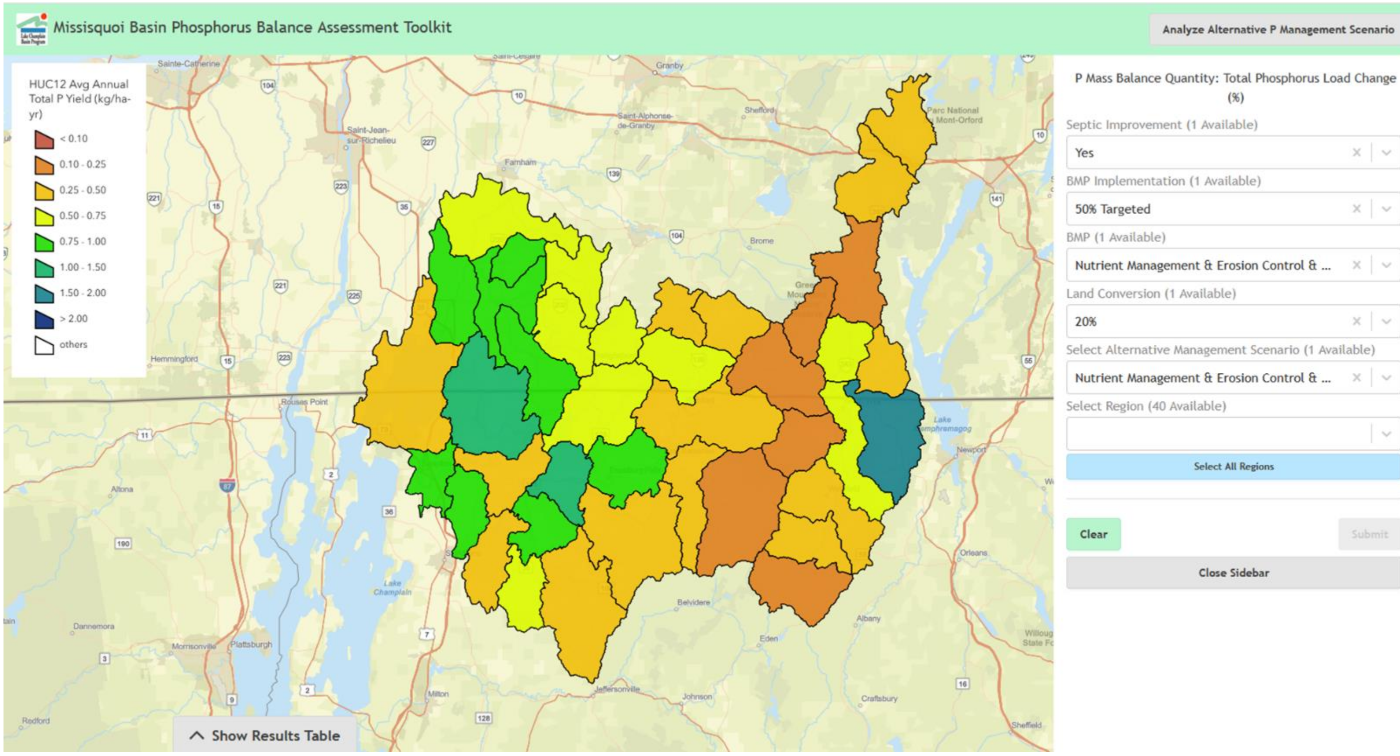

Figure 444. Final Alternative Management Scenario selection based on previous option selections.

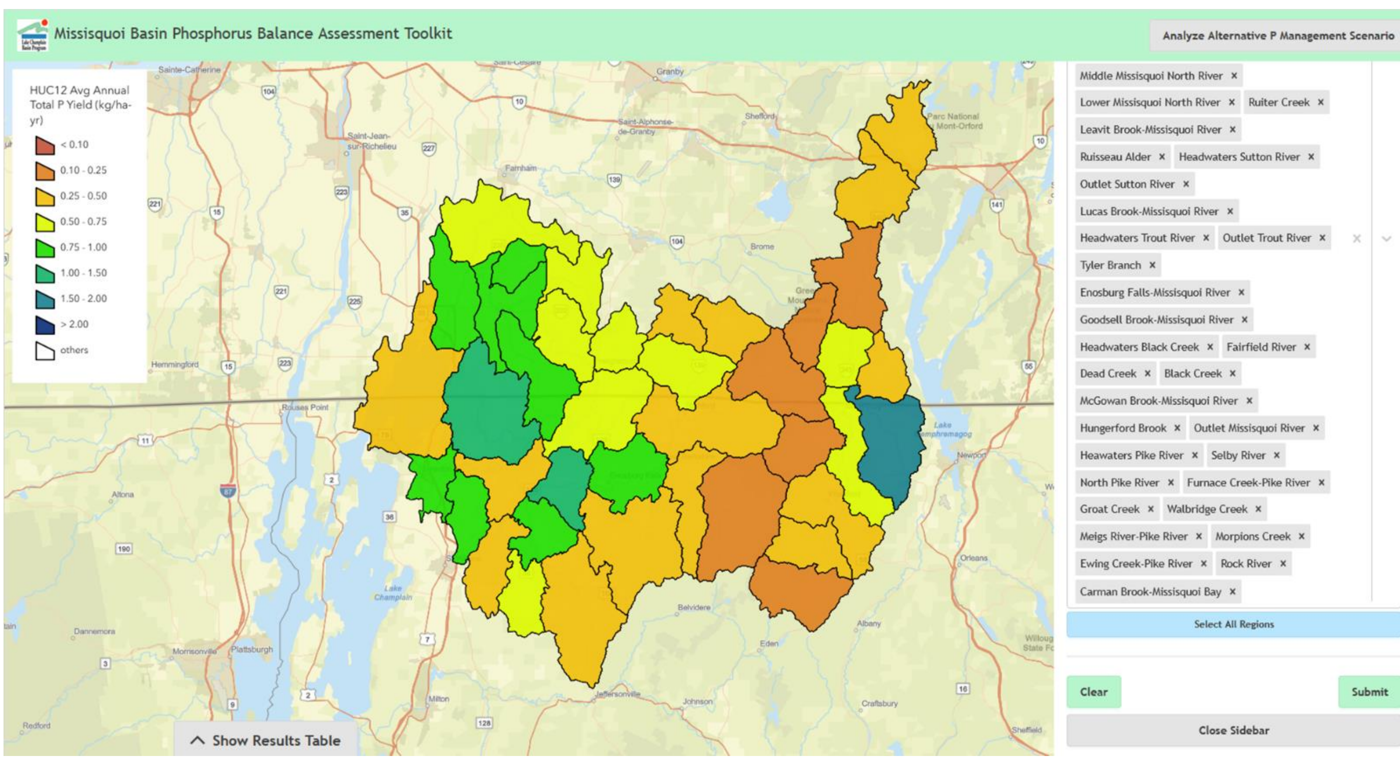

Figure 45. Selection of HUC12 regions to apply P management Alternative Scenario to.

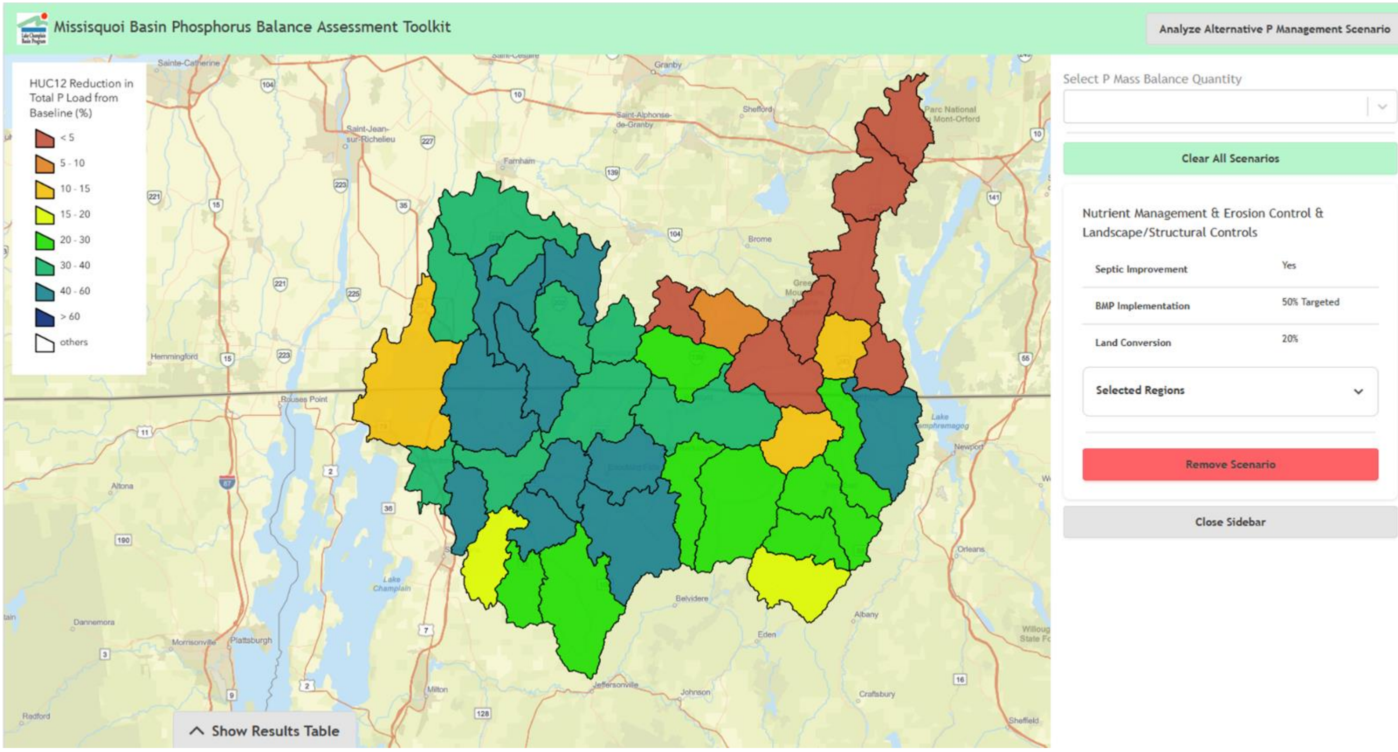

Figure 46. Map update after submitting alternative analysis request. Characteristics of the Alternative Scenario are documented in the sidebar.

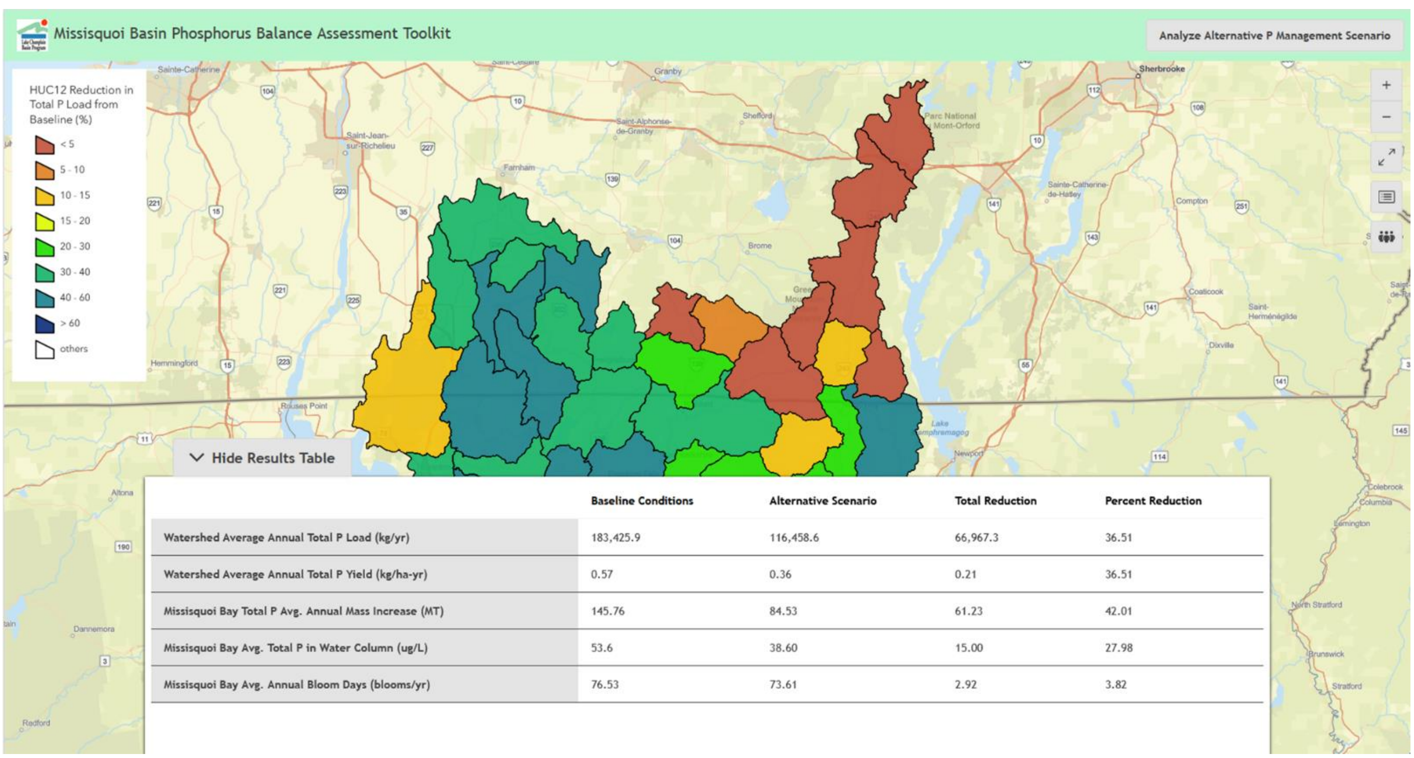

	Baseline Conditions	Alternative Scenario	Total Reduction	Percent Reduction
Watershed Average Annual Total P Load (kg/yr)	183,425.9	116,458.6	66,967.3	36.51
Watershed Average Annual Total P Yield (kg/ha-yr)	0.57	0.36	0.21	36.51
Missisquoi Bay Total P Avg. Annual Mass Increase (MT)	145.76	84.53	61.23	42.01
Missisquoi Bay Avg. Total P in Water Column (ug/L)	53.6	38.60	15.00	27.98
Missisquoi Bay Avg. Annual Bloom Days (blooms/yr)	76.53	73.61	2.92	3.82

Figure 47. Updated table results showing changes in watershed and Bay P mass balance quantities resulting from Alternative Scenario implementation.

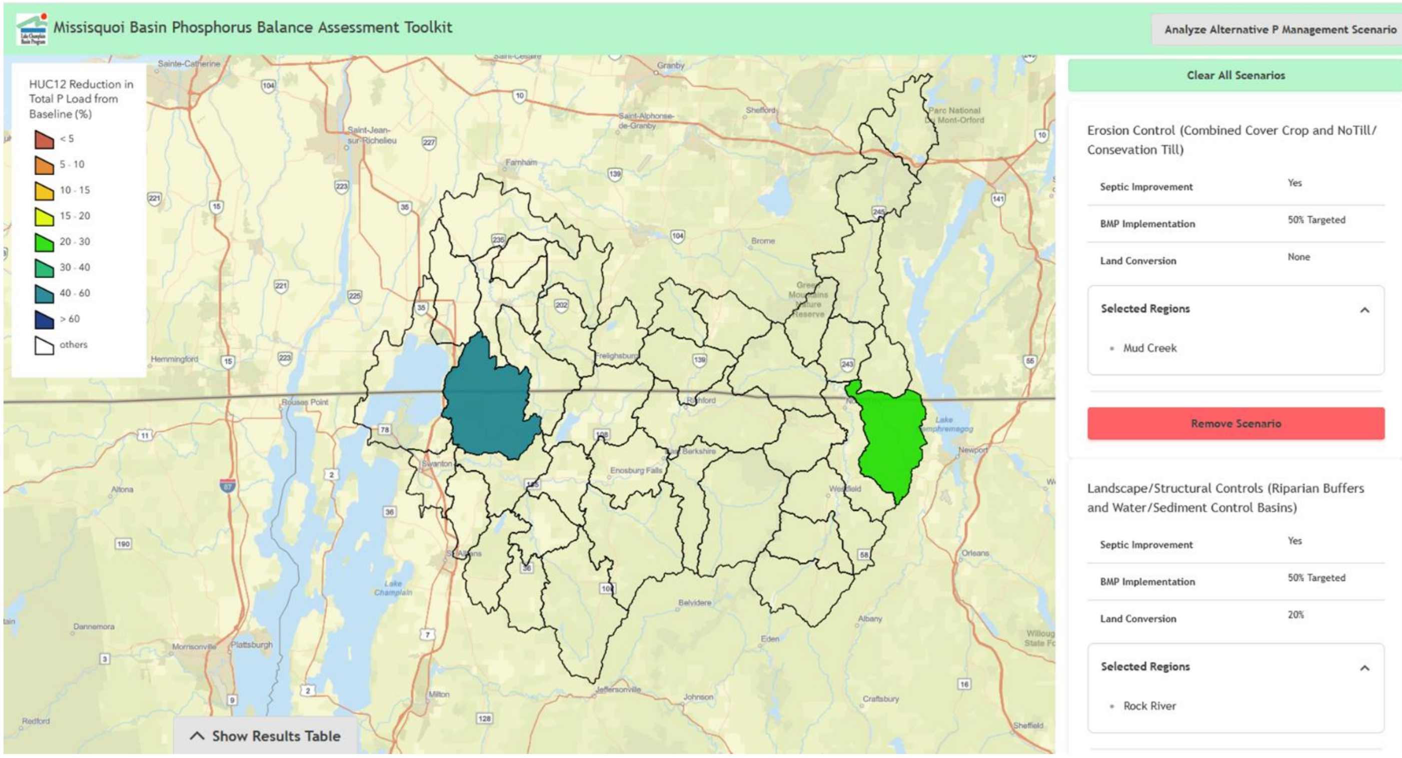

Figure 48. Map update after submitting an Alternative Scenario analysis request for two HUC12 sub-watersheds (Rock River and Mud Creek).

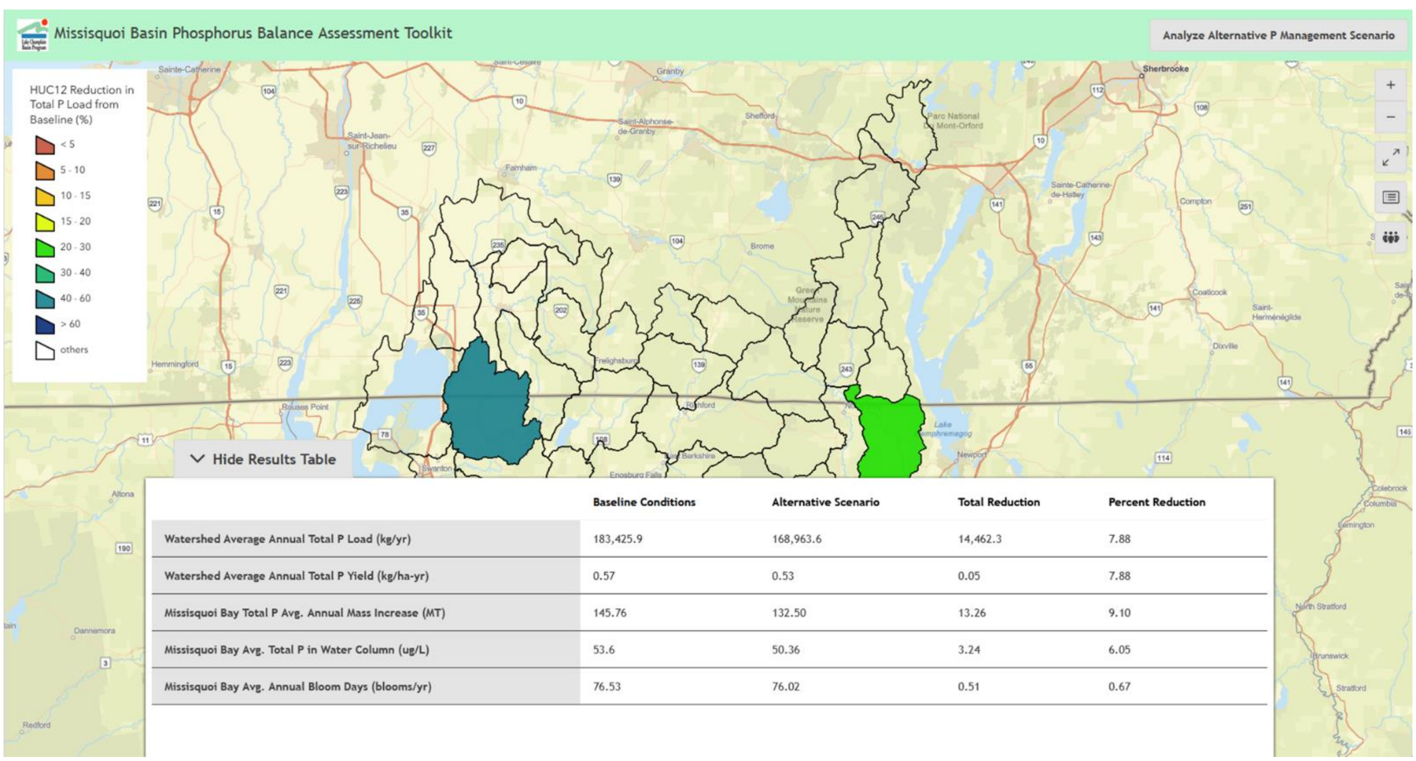

	Baseline Conditions	Alternative Scenario	Total Reduction	Percent Reduction
Watershed Average Annual Total P Load (kg/yr)	183,425.9	168,963.6	14,462.3	7.88
Watershed Average Annual Total P Yield (kg/ha-yr)	0.57	0.53	0.05	7.88
Missisquoi Bay Total P Avg. Annual Mass Increase (MT)	145.76	132.50	13.26	9.10
Missisquoi Bay Avg. Total P in Water Column (ug/L)	53.6	50.36	3.24	6.05
Missisquoi Bay Avg. Annual Bloom Days (blooms/yr)	76.53	76.02	0.51	0.67

Figure 49. Results Table update submitting an Alternative Scenario analysis request for two HUC12 sub-watersheds (Rock River and Mud Creek).

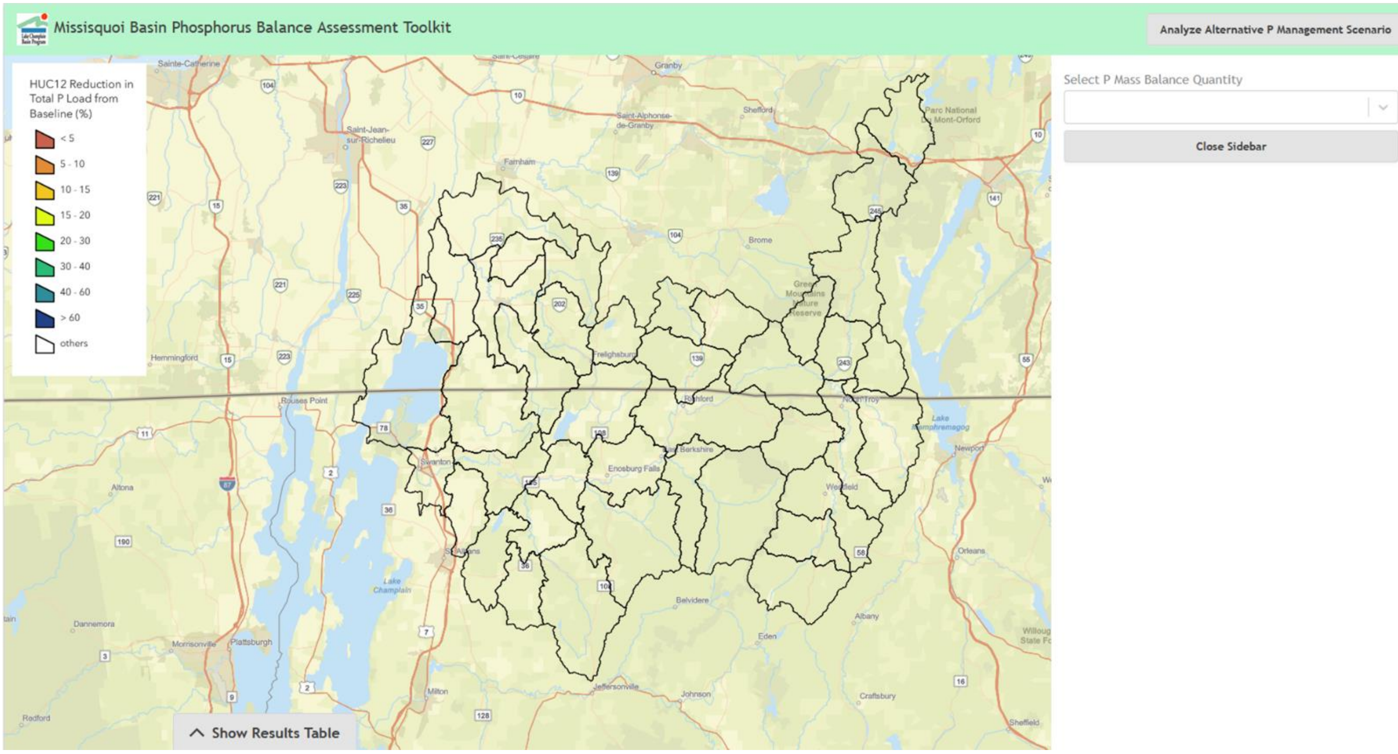

Figure 50. Map and application update after clicking Clear All Scenarios.

6. CONCLUSIONS

This project to develop a comprehensive binational P mass balance analysis toolkit for the Missisquoi Bay watershed has produced several important outputs and provided valuable insights into how modifications to P management practices, implemented following a range of approaches throughout the watershed, are projected to translate to quantifiable changes in water quality within the Bay. The comprehensive terrestrial P inventory brought together the best available data and current science in quantifying current P inputs and stores throughout the entire watershed. This compilation will provide value to future efforts within the MBB which require knowledge of the spatial distribution and magnitude of P, which could include studies to evaluate targeted P input reduction strategies, evaluation of data gaps, and identification of opportunities for refined P inventory quantification, or the development of spatio-temporal datasets to track changes in P inputs and stores over time. The creation of the binational SWAT-based metamodel, inclusive of over 175,000 landscape units (HRUs), represents the only comprehensive basin-wide P loading model for the MBB that combines the benefits of a well-vetted SWAT modeling approach with extensive validation with both field scale monitoring studies and in-stream monitoring studies throughout the entire watershed. This project demonstrated the utility of this modeling approach in generating Missisquoi Bay loading projections for 90 different alternative management scenarios covering a range of agricultural BMPs and improvements to residential (septic) wastewater systems and urban wastewater treatment plant upgrades. Integration of the terrestrial metamodel with the AEM3D Bay model has provided a comprehensive view of how the Bay, given its current inventory or P in water and sediment, will respond to a wide range of projected P loadings directly derived from the alternative P management scenarios simulated using the metamodel. The coupled terrestrial metamodel/AEM3D modeling approach developed in this study could be utilized in future analyses that may wish to explore new alternative management practices, different approaches to terrestrial reductions in P inputs, or modifications to assumptions concerning P storage dynamics within the terrestrial landscape and the Bay. Finally, the analysis approach built into the P Mass Balance Toolkit took advantage of the 90 independent alternative scenarios simulated with the metamodel and 30 alternative scenarios simulated with the AEM3D Bay model to enable evaluation of a nearly limitless range of possible conditions that fall between the current (baseline) P loading and the alternative P loading representing the most aggressive P abatement strategy (converting all cultivated agricultural land to unmanaged grassland). This extensive flexibility was achieved by enabling Toolkit users to construct Bay loading scenarios at the HUC12-scale and through the development of empirical regression models to relate tributary P load reductions to the Bay's water quality metrics (P mass balance, P concentration, and cyanobacteria bloom days). The Toolkit's framework has been designed such that future updates to the metamodel's alternative loading scenarios could be readily added to the application, as well as the results of additional AEM3D Bay P dynamics simulations.

The modeling approach taken in this study demonstrated several alternative management scenarios whereby the average annual reduction in total P loads to the Bay would be reduced by 35% - 45%. For example, the scenario that includes improvements to septic systems and wastewater treatment plants, combined with adopting erosion control, and riparian zone management to a targeted 50% of critical source areas, combined with converting 20% of the most critical cropland to grassland yielded an average watershed total P load reduction of 36.1%. The Bay model predicts that this reduction will translate to a 41.6% reduction in average annual P mass imbalance, with a somewhat lower reduction in the average annual total P concentration in water (27.7% reduction), representing an average annual P concentration of near 38 μg/L. As has been discussed in this report, the legacy P within the Bay's sediment provides an internal loading source that is resilient to watershed reductions on this timescale and leads to a more modest decrease in average P concentration than the reduction in watershed loading would otherwise suggest. Likewise, the average number of cyanobacteria bloom days per year is projected to only decrease by two to three days per year under a 36.1% external P loading reduction scenario (based on a 20 μg/L concentration threshold for bloom conditions). This last finding of apparently limited end-user water quality benefit may prompt some to ask whether substantial efforts in reducing P loads to Missisquoi Bay are worth the cost. To this question, we offer several points to consider:

- Given the findings of Braun et al. (2024), attainable watershed P reductions of the scale simulated by our metamodel, when coupled with approaches to limit internal loading, would be the most timely and efficient way to substantially suppress cyanobacteria blooms and meet the TMDL target. Furthermore, given that global climate change projections suggest that conditions that promote internal loading of P will become more prevalent in the future, aggressive watershed reductions across sectors are critical to keep water quality conditions from further deterioration.
- The projections in this project's P mass balance modeling make several simplifying assumptions, namely constant soil P saturation levels and constant levels of legacy P stores in Missisquoi Bay over a 30-year time period, which might result in conservative estimates of the reduction in P concentration in the Bay over longer timescales than simulated here.

- Although the reduction in cyanobacteria bloom frequency associated with a 35%-45% reduction in watershed loads was small, substantial improvements to the P mass imbalance and P concentrations were predicted to occur. This bodes well for longer-term water quality improvements, as these trends will directly lead to a gradual lowering of legacy P in the Bay's sediment, which will eventually result in the visible and tangible water quality improvements we are looking to achieve.
- The lowering of P concentration in the Bay, though not predicted to be enough to substantially reduce cyanobacteria bloom frequency, is expected to have a beneficial impact by reducing the severity of these blooms.

As previous studies have demonstrated (Braun et al., 2024; Zia et al., 2022), legacy P in shallow water bodies like Missisquoi Bay poses a difficult challenge for long term water quality improvement efforts. In addition to the very beneficial land management practices aimed at reducing watershed terrestrial source P loads, additional research into cost-effective approaches to reducing legacy P stores (both aquatic and terrestrial components) would provide the potential to expedite the water quality improvement outcomes we are looking to achieve. In the meantime, the modeling analysis and P Mass Balance Toolkit developed in this study can inform which alternative practices implemented in what locations will provide the greatest benefit in closing the P imbalance gap in the Bay. As new technologies for reducing P stores and transport are developed, these may be similarly assessed at the full watershed scale and incorporated into the modeling and Toolkit framework developed in this project.

7. References

Albrecht, G., Q. M. Ketterings, J. and Beckman. 2005. Soil pH for Field Crops. *In* Agronomy Fact Sheet Series. Vol. 5.

Beaudet, P., M. Grenier, M. Giroux et V. Girard. 2009. Base de données sur les statistiques des propriétés chimiques des sols minéraux du Québec.

Bernard, C. et D. Côté. 1997. Rapport final de projet. Centre de Recherche et D'expérimentation en Sols, MAPAQ.

Biron, P., T. Buffin-Bélanger, M. Larocque,S. Demers, T. Olsen, M.-A. Ouellet, G. Choné, C.-A. Cloutier et M. Needelman. 2013. Espace de liberté: Un cadre de gestion intégrée pour la conservation des cours d'eau dans un contexte de changements climatiques. Rapport Ouranos, projet #510014-101, 122 p. https://belsp.uqtr.ca/id/eprint/1253/1/Biron%20et%20al_2013_Gestion_int%C3%A9gr%C3%A9e_eau_A.pdf

Bondeson, F.A., 2023. Technological and spatial analysis techniques to improve outcomes of agricultural nutrient management. Graduate College Dissertations and Theses. University of Vermont, Burlington, Vermont. 1682. https://scholarworks.uvm.edu/graddis/1682

Bondeson, F.A., J. Faulkner, T. Chin, A. Schroth, A. Michaud, M. Winchell, M. Niang and E. Roy. 2024. Watershed-scale spatial prediction of agricultural land phosphorus mass balance and soil phosphorus metrics: A bottom-up approach. Journal of Environmental Quality

53(6):1152-1163. DOI: 10.1002/jeq2.20633
https://acsess.onlinelibrary.wiley.com/doi/10.1002/jeq2.20633

Braun, D., A. Schroth, A. Kirol, C. Marti and K. Wagner. 2024. Evaluating alternatives to control internal phosphorus loading in Missisquoi Bay using a three-dimensional coupled hydrodynamic-aquatic ecosystem model. Prepared for the Lake Champlain Basin Program under contract to NEIWPCC. Stone Environmental, Montpelier, Vermont.

Cliche, G. and A. Saladzius. 2020. Évaluation de performance des ouvrages municipaux d'assainissement des eaux - Bassin versant de la bais Missisquoi, années 2016 à 2018. Fondation Rivières.

Centre de référence en agriculture et agroalimentaire du Québec (CRAAQ). 2010. Guide de référence en fertilisation, 2e édition.

Côté, D., A.R. Michaud, T.S. Tran and C. Bernard. 1999. Slurry sidedressing and topdressing can improve soil and water quality in the Lake Champlain Basin. Lake Champlain in Transition: From Research Toward Restoration. *In* T.O. Manley and P.L. Manley (eds.). Water Science and Application 1. American Geophysical Union. ISBN 0-87590-350-9. pp 225-238.

Daryanto, D., S. Daryanto, L. Wang, P.A. Jacinthe. 2017. Meta-Analysis of Phosphorus Loss from No-Till Soils. J. Environ. Qual., 46 (2017), pp. 1028-1037, 10.2134/jeq2017.03.0121

Deslandes, J., I. Beaudin, A.R. Michaud, F. Bonn and C.A. Madramootoo. 2006. Influence of landscape and cropping system on phosphorus mobility within the Pike River watershed of Southwestern Quebec. Canadian Water Resources Journal 32(1):21-42.
https://irda.qc.ca/media/1i5b5yhy/irda-influencelandscapecroppingphosphorusmobilitypikeriver-articlesscientifiques-2007.pdf

Dodd, R.J. et A.N. Sharpley. 2016. Conservation practice effectiveness and adoption: Unintended consequences and implications for sustainable phosphorus management. Nutrient Cycling in Agroecosystems 104:373-392. https://doi.org/10.1007/s10705-015-9748-8

Drouin, A., I. Beaudin, A. et Michaud.A 2014. GEODEP: L'outil de diagnostic des exportations de phosphore spatialisé. Fiche technique. IRDA. https://irda.qc.ca/media/zp1dq4ny/irda-diagnosticexportationsphosphorespatialise-fichessyntheses-2014.pdf

Enright, P. and C.A. Madramootoo. 2004. Phosphorus losses in surface runoff and subsurface drainage waters on two agricultural fields in Quebec. pp 160-170. *In* R.A. Cooke (ed.). Drainage VIII – Proceedings of the Eight International Drainage Symposium. Published by ASAS, St. Joseph, Michigan.

ESRI. 2011. Arc Hydro Geoprocessing Tools - Tutorial. Version 2.0 – October 2011.

Fenton, M., C. Albers and Q. and Ketterings. 2008. Soil Organic Matter. *In* Agronomy Fact Sheet Series, Vol. 41. http://franklin.cce.cornell.edu/resources/soil-organic-matter-fact-sheet

Financière Agricole du Québec (FAQ). 2021. Banque de données des cultures assurées (BDPPAD) for the reference year 2021. https://www.fadq.qc.ca/documents/donnees/base-de-donnees-des-parcelles-et-productions-agricoles-declarees/

Gagné G., I. Beaudin, M. Leblanc, A. Drouin, G. Veilleux, J.D. Sylvain et A.R. Michaud. 2013. Classement des séries de sols minéraux du Québec selon les groupes hydrologiques. Rapport final. IRDA, Québec, Canada. 81 p. https://irda.qc.ca/media/imupistp/irda-solsminerauxquebecgroupeshydrologiques-rapport-decembre2013.pdf

Galford, G.L., Faulkner, J., Dupigny-Giroux, L.-A., Posner, S. and Edling, L. (eds.) (2021). The Vermont Climate Assessment 2021. Gund Institute of Environment, University of Vermont, Burlington, VT. DOI: 10.18125/kowgvg

Gangbazo, G., A.R. Pesant and G.M. Barnett. 1996. Effets de l'épandage des engrais minéraux et de grandes quantités de lisier de porc sur l'eau, le sol et les cultures. Ministère de l'Environnement et de la Faune, Dir. Écosystèmes Aquatiques.

Giles, C.D., P.D.F. Isles, T. Manley, Y. Xu, G.K. Druschel and A. Schroth. 2016. The mobility of phosphorus, iron, and manganese through the sediment–water continuum of a shallow eutrophic freshwater lake under stratified and mixed water-column conditions. Biogeochemistry 127:15–34. DOI:10.1007/s10533-015-0144-x.

Giroux, M. and R. Royer. 2006a. Influence des modes de fertilisation sur les pertes d'éléments nutritifs dans les drains agricoles sous prairies et orge grainée. Cahier No. 5 de l'Observatoire de la qualité des sols du Québec. Institut de Recherche et de Développement en Agroenvironnement Inc (IRDA), Québec, Québec, Canada. 57 p. https://irda.qc.ca/media/usnbsilb/irda-influencefertilisationpertesnutritifsdrains-rapport-mai2006.pdf

Giroux, M., and R. Royer. 2006b. Influence des modes de fertilisation sur les pertes d'éléments nutritifs dans les drains agricoles sous le maïs-grain, l'orge et le canola. Cahier No. 6 de l'Observatoire de la qualité des sols du Québec. Institut de Recherche et de Développement en Agroenvironnement Inc (IRDA) Québec, Québec, Canada. 84 p. https://irda.qc.ca/media/ezilg25b/irda-pertesnutritifsdrainsmais-rapport-juin2006.pdf

Giroux, M., M. Duchemin, A.R. Michaud, I. Beaudin, C. Landry and M.R. Laverdière. 2008. Relation entre les concentrations en phosphore particulaire et dissous dans les eaux de ruissellement et les teneurs en P total et assimilable des sols pour différentes cultures. Agrosolutions 19(1):4-14. https://irda.blob.core.windows.net/media/2183/giroux-et-al-2008_article_relation_p_m3_sols_eaux_ruissellement.pdf

Gollamudi, A., C.A. Madramootoo and P. Enright. 2007. Water quality modeling of two agricultural fields in southern Quebec using SWAT. Transactions of the ASABE 50(6):1973-1980.

Hartigan, J. A. and M.A. Wong. 1979. A K-Means clustering algorithm. Journal of the Royal Statistical Society: Series C of Applied Statistics28(1):100–108. https://www.jstor.org/stable/2346830

Institut de la Statistique du Québec (ISQ). 2017. Le bilan démographique du Québec. https://bdso.gouv.qc.ca/docs-ken/multimedia/PB01614FR_Bilandemo2017F00.pdf

Institut de Recherche et Développement en Agroenvironnement (IRDA). 2017. Banque de données hydro-pédologiques. Unpublished report.

Institut de Recherche et Développement en Agroenvironnement (IRDA). 2022. Laboratoire d'analyse agroenvironnementale. https://www.irda.qc.ca/fr/a-propos/installations/laboratoire-d-analyse-agroenvironnementale/

International Joint Commission (IJC). 2020. Nutrient Loading and Impacts in Lake Champlain – Missisquoi Bay and Lake Memphremagog. 219 pp. https://www.ijc.org/sites/default/files/2020-07/Government_Package_English_Revised.pdf

Isaaks, E.H. and M.R. Srivastava. 1989. Applied Geostatistics. Oxford University Press, New York, New York. 582 p.

Isles, P.D.F., C.D. Giles, T.A. Gearhart, Y. Xu, G.K. Druschel and A.W. Schroth. 2015. Dynamic internal drivers of a historically severe cyanobacteria bloom in Lake Champlain revealed through comprehensive monitoring. Journal of Great Lakes Research 41:818-829.

Isles, P.D.F., D.M. Rizzo, Y.Y. Xu and A.W. Schroth. 2017a. Modeling the drivers of interannual variability in cyanobacterial bloom severity using self-organizing maps and high-frequency data. Inland Waters7(3):333-347. DOI:10.1080/20442041.2017.1318640

Isles, P.D.F., Y.Y. Xu, J. D. Stockwell and A.W. Schroth. 2017b. Climate-driven changes in energy and mass inputs systematically alter nutrient concentration and stoichiometry in deep and shallow regions of Lake Champlain. Biogeochemistry133(2):201-217. DOI:10.1007/s10533-017-0327-8

John, K., S.M. Afu, I.A. Isong, , E.E. Aki, N.M. Kebonye, E.O. Ayito, P.A. Chapman, M.O.Eyong, and V. Penížek. 2021. Mapping soil properties with soil-environmental covariates using geostatistics and multivariate statistics: International Journal of Environmental Science and Technology18:3327-3342.

Joung, D., M. Leduc, B. Ramcharitar, Y. Xu, P.D.F. Isles, J.D. Stockwell, G.K. Druschel, T. Manley A.W. Schroth. 2017. Winter weather and lake-watershed physical configuration drive phosphorus, iron, and manganese dynamics in water and sediment of ice-covered lakes. Limnology and Oceanography. 62 (4)1620-1635. DOI: 10.1002/lno.10521

Khiari, L., L.E. Parent, A. Pellerin, A.R.A. Alimi, C. Tremblay, R.R. Simard, and J. Fortin. 2000. An agri-environmental phosphorus saturation index for acid coarse-textured soils. Journal of Environmental Quality 29(6):2052-2052. https://doi.org/10.2134/jeq2000.00472425002900060053x

Kirol, A.P., A.M. Morales-Williams, D.C. Braun, C.L. Marti, K.J. Wagner, A.W. Schroth. 2024. Linking sediment and water column phosphorus dynamics to oxygen, temperature, and aeration in shallow eutrophic lakes. Water Resources Research 60(1):1-20.

Kodinariya, T.M. and P.R. Makwana,. 2013. Review on determining of cluster in K-means. International Journal of Advance Research in Computer Science and Management Studies1(6):90-95. https://www.researchgate.net/publication/313554124

Krivoruchko, K. and A. Gribov. 2019 Evaluation of empirical Bayesian kriging: Spatial Statistics 32:100-368. DOI:10.1016/j.spasta.2019.100368

La Financière Agricole du Québec (FAQ). 2021. Banque de données des cultures assurées (BDPPAD) for the reference year 2021. https://www.fadq.qc.ca/documents/donnees/base-de-donnees-des-parcelles-et-productions-agricoles-declarees/

Landry, C. 2006. Impact à long terme de l'application de lisier de porc sur les flux de nutriments du sol. IRDA. https://irda.blob.core.windows.net/media/2255/landry-2006_fiche_impact_lt_lisier_porcin.pdf

LimnoTech. 2012. Development of a phosphorus mass balance model for Missisquoi Bay. Prepared for the Lake Champlain Basin Program under contract to NEIWPCC. LimnoTech, Ann Arbor, Michigan.

Liu, J., P.J.A. Kleinman, H. Aronsson, D. Flaten, R.W. McDowell, M. Bechmann, D.B. Beegle, T.P. Robinson, R.B. Bryant, H. Liu, A.N. Sharpley, and T.L. Veith. 2018. A review of regulations and guidelines related to winter manure application. Ambio 47(6) :657-670. https://doi.org/10.1007/s13280-018-1012-4

Madramootoo, C.A., A.R. Michaud, J. Whalen et S.-C. Poirier. 2012. Mesures précises et approches innovantes en modélisation de la dynamique des nutriments en bassin et en plan d'eau contribuant aux fleurs des cyanobactéries. Rapport final n° 2009-CY-130646. Programme de recherche en partenariat sur les cyanobactéries. Fonds Québécois de la Recherche sur la Nature et les Technologies et Fonds de la Recherche en Santé du Québec, Québec, Québec. 30 p. https://irda.qc.ca/media/wswgnf3r/irda-modelisationnutrimentseaufleurscyanobacteries-rapport-decembre2012.pdf

Magdoff, F.R., C. Hryshko, W.E. Jokela, R.P. Durieux and Y. Bu. 1999. Comparison of phosphorus soil test extractants for plant availability and environmental assessment. Soil Science Society of America Journal 63(4):999-1006. https://doi.org/10.2136/sssaj1999.634999x

Mallarino, A.P., B.M. Stewart, J.L. Baker, J.A. Downing and J.E. Sayer. 2005. Background and basic concepts of the Iowa phosphorus index. A support document of the USDA-NRCS field Office Technical Note 25. United States Department of Agriculture, Washington, D.C. 11 p.

Medalie, L. 2013. Concentration, flux, and the analysis of trends of total and dissolved phosphorus, total nitrogen, and chloride in 18 tributaries to Lake Champlain, Vermont and New York, 1990–2011: U.S. Geological Survey Scientific Investigations Report, 2013–5021. U.S. Geological Survey, Washington, D.C. 29 p. http://pubs.usgs.gov/sir/2013/5021/

Mendelsohn, D., C. Swanson and T. Isaji. 1997. Hydrodynamic modeling of Missisquoi Bay in Lake Champlain. Prepared for Vermont Department of Conservation, Waterbury, Vermont.

Michaud, A.R., R. Lauzier et M.R. Laverdière. 2002. Description du système de transfert du phosphore dans le bassin versant du ruisseau au Castor. Agrosol 13(2):124-139. https://www.researchgate.net/publication/238755546_Description_du_systeme_de_transfert_du_phosphore_dans_le_bassin-versant_du_ruisseau_au_Castor

Michaud, A.R., M.R. Laverdière. 2004. Effects of cropping, soil type and manure application on phosphorus export and bioavaibility. Canadian Journal of Soil Science, 84(3): 295-305. Erratum 84 (4) p. 525.

Michaud, A.R., R. Lauzier et M.R. Laverdière. 2004. Temporal and spatial variability in non-point source phosphorus in relation to agricultural production and terrestrial indicators. *In* T.O. Manley, P.L. Manley and T.B. Mihuc (eds.), Lake Champlain: Partnerships and Research in the New Millennium. Kluwer Academic/Plenum Pub., New York, NY. pp 97-121.

Michaud, A.R., R. Lauzier et M.R. Laverdière. 2005. Mobilité du phosphore et intervention agroenvironnementale en bassin versant agricole: Etude de cas du bassin versant du ruisseau au Castor, tributaire de la rivière aux Brochets, Québec. Agrosol 16(1) :57-59. https://irda.qc.ca/media/ctbnukx0/irda-mobilitephosphoreruisseaucastor-articlesscientifiques-2005.pdf

Michaud, A.R., I. Beaudin, J. Deslandes, F. Bonn et C.A. Madramootoo. 2007. SWAT-predicted influence of different landscape and cropping systems alterations on phosphorus mobility within the Pike River watershed of Southwestern Quebec. 2007. Canadian Journal of Soil Science 87(3) :329-344. https://irda.qc.ca/media/bk4cu5rr/irda-swatpredictedphosphorusmobilitypikeriver-articlesscientifiques-2007.pdf

Michaud, A.R, J. Desjardins, M. Grenier et R. Lauzier. 2009a. Suivi de la qualité de l'eau des bassins versants expérimentaux Ewing et Aux Castor – Dans le cadre du projet Lisière verte. Rapport final de projet. Institut de Recherche et de Développement en Agroenvironnement (IRDA), Coopérative de Solidarité du Bassin Versant de la Rivière aux Brochets, AAC (PASCAA) et MAPAQ, Québec, Québec. 27 p. http://www.irda.qc.ca/resultats/publications/197.html

Michaud, A.R., J. Deslandes, J. Desjardins et M. Grenier. 2009b. Réseau d'actions concertées en bassins versants agricoles. Rapport final de projet. Institut de Recherche et de Développement en Agroenvironnement (IRDA), MAPAQ, Club du Bassin LaGuerre, Dura-Club, Club de Fertilisation de la Beauce, Fonds D'action Québécois pour le Développement Durable, Conseil pour le Développement de L'agriculture du Québec et Programme d'aide Technique de Couverture Végétale du Canada, Québec, Québec. 155 p. https://irda.qc.ca/media/kgkj0v2g/irda-actionsconcertees-rapport-aout2009.pdf

Michaud, A.R., M. Giroux, I. Beaudin, J. Desjardins, G. Gagné, M. Duchemin, J. Deslandes, C. Landry, P. Beaudet et J. Lagacé. 2009c. ODEP; un Outil de diagnostic des exportations de phosphore. Manuel de l'utilisateur. Projet Gestion du risque associé aux facteurs source et transport du phosphore des sols cultivés au Québec, réalisé dans le cadre de l'Initiative d'appui aux conseillers agricoles (PIACA-204). Institut de Recherche et de Développement en Agroenvironnement Inc. (IRDA) et Centre de Référence en Agriculture et Agroalimentaire du Québec (CRAAQ), Québec, Canada.

Michaud, A.R., J. Desjardins, N. Coté, I. Beaudin, A. Drouin, S. Seydoux et I. Saint-Laurent. 2012. Rapport de l'observatoire de la qualité de l'eau de surface en bassins versants agricoles. Rapport sommaire pour la période de référence 2009-2011. Rapport réalisé dans le cadre du projet Observatoire de la qualité de l'eau de surface en bassins versants agricoles. Institut de Recherche et de Développement en Agroenvironnement Inc. (IRDA), Québec, Canada. 82 p. et annexes. https://irda.blob.core.windows.net/media/7905/irda_rapportscientifique_observatoire_10-bassins_periode_reference_2012.pdf

Michaud, A.R., M.A. Niang, A. Blais-Gagnon, F. Landry, W. Huertas, J. Desjardins et M. Grenier. 2018. Outil de diagnostic et de prédiction des exportations diffuses de sédiments et de nutriments GéODEP+N. Rapport scientifique de projet No. IA113111, Programme Innov'action Agroalimentaire, Ministère de l'Agriculture, des Pêcheries et de l'Alimentation du Québec (MAPAQ), Québec, Canada. 83 p. https://www.researchgate.net/publication/380365620_Outil_de_diagnostic_et_de_prediction_des_exportations_diffuses_de_sediments_et_de_nutriments_-_GEODEPN_GeODEPN_A_Tool_kit_for_the_diagnosis_and_prediction_of_diffuse_sediment_and_nutrients_exports

Michaud, A., M. Niang, L. Belzile, F. Chouinard and J. Bérubé. 2019a. Cost-benefit analysis of proposed actions needed to reduce phosphorus loads from the Rock River subwatershed to Missisquoi Bay by 40%. OBVBM, IRDA. LCBP. https://irda.qc.ca/media/5k3ds0sc/irda-reduction40phosphorerivierelaroche-rapport-avril2019.pdf

Michaud, A.R., S-C Poirier et J.K Whalen. 2019b. Tile drainage as a hydrologic pathway for phosphorus export from an agricultural subwatershed. Journal of Environmental Quality 48(1):64-72 https://acsess.onlinelibrary.wiley.com/doi/abs/10.2134/jeq2018.03.0104

Michaud, A.R., C. Gombault, M. Niang, A. Blais-Gagnon, W. Huertas, G. Labrie et M. Landry. 2021. Suivi hydrométrique et modélisation hydrologique des sédiments et des nutriments des bassins versants de la MRC de la Haute-Yamaska. 92 p. https://irda.qc.ca/media/xwzerdbd/irda-sedimentsnutrimentsmrchauteyamaska-rapport-mars2021.pdf

Ministère de l'Énergie et des Ressources Naturelles (MERN). 2021a. Base de données topographiques du Québec (BDTQ). https://www.donneesquebec.ca/recherche/dataset/grhq

Ministère de l'Énergie et des Ressources Naturelles (MERN). 2021b. Carte écoforestière. https://www.donneesquebec.ca/recherche/dataset/carte-ecoforestiere-avec-perturbations

Ministère de l'Environnement, Lutte Contre les Changements Climatiques, Faune et Parcs (MELCCFP). 2020. Guide de référence du Règlement sur les exploitations agricoles. https://www.environnement.gouv.qc.ca/milieu_agri/agricole/guide-reference-rea.htm

Ministère de l'Environnement, Lutte Contre les Changements Climatiques, Faune et Parcs (MELCCFP). 2021a. Phosphorus loadings reports for Missisquoi Bay region. Data obtained under data privacy protection protocol.

Ministère de l'Environnement, Lutte Contre les Changements Climatiques, Faune et Parcs (MELCCFP). 2021b. Suivi des ouvrages municipaux d'assainissement des eaux usées (SOMAEU). https://www.environnement.gouv.qc.ca/eau/eaux-usees/somaeu/index.htm

Ministère de l'Environnement, de la Lutte Contre les Changements Climatiques, Faune et des Parcs (MELCCFP). 2022. Atlas hydroclimatique méridional 2022, Québec, Direction de l'expertise hydrique (DEH). https://services-mddelcc.maps.arcgis.com/apps/webappviewer/index.html?id=371faa9786634167a7bdefdead35e43e

Municipalité Régionale de Comté de Brome-Missisquoi (MRCBM). 2016. Plan de Gestion des matières résiduelles (PGMR) modifié et révisé de la MRC Brome-Missisquoi 2016-

2020.https://mrcbm.qc.ca/common/documentsContenu/PGMR%20modifi%C3%A9%20et%20r%C3%A9vis%C3%A9%20adopt%C3%A9%2021%20juin%202016_partie_1.pdf

Municipalité Régionale de Comté de Memphrémagog (MRC de Memphrémagog). 2009. Schéma d'aménagement et de développement. https://www.mrcmemphremagog.com/download/Schema/PSAD_premier_projet_v2009.pdf

NRCS-IOWA. 2004. Iowa Technical Note no. 25. Iowa phosphorus index. Natural Resources Conservation Service, Des Moines, Iowa. 32 p.

NRCS. 2022. Soil Survey Geographic (SSURGO) Database. Soil survey staff, Natural Resources Conservation Service, United States Department of Agriculture, Washington, D.C. https://sdmdataaccess.sc.egov.usda.gov

Organisme de Bassin Versant de la Baie Missisquoi (OBVBM). 2015. Plan directeur de l'eau du Bassin Versant de la Baie Missisquoi: Portrait 2015. https://obvbm.org/wp-content/uploads/2021/05/portrait_2015.pdf

Organisme de Bassin Versant Baie Missisquoi (OBVBM). 2017. Questionnaire de suivi des installations septiques du bassin versant de la baie Missisquoi. Unpublished report.

Organisme de Bassin Versant de la Baie Missisquoi (OBVBM). 2021. Plan directeur de l'eau du Bassin Versant de la Baie Missisquoi: Portrait 2021. Draft Report.

Oldfield, L., S. Rakhimbekova, J.W. Roy and C.E. Robinson. 2020. Estimation of phosphorus loads from septic systems in tributaries in the Canadian Lake Erie Basin. Journal of Great Lakes Research 46(6):1559-1569. https://doi.org/10.1016/j.jglr.2020.08.021

Olea, R.A. 2006. A six-step practical approach to semivariogram modeling. Stochastic Environmental Research and Risk Assessment 20:307-318. DOI:10.1007/s00477-005-0026-1

Perica, S., S. Pavlovic, M. St. Laurent, C. Trypaluk, D. Unruh, D. Martin and O. Wilhite. 2019. NOAA Atlas 14, Precipitation-Frequency Atlas of the United States. Volume 10 Version 3.0: Northeastern States. US Department of Commerce, Washington, D.C.. 265 p.

Puttonen, I., J. Mattila, P. Jonsson, O.M. Karlsson, T. Kohonen, A. Kotilainen, K. Lukkari, J.M. Malmaeus and E. Rydin. 2014. Distribution and estimated release of sediment phosphorus in the northern Baltic Sea archipelagos: Estuarine, Coastal and Shelf Science 145: 9-21. DOI:10.1016/j.ecss.2014.04.010

R Core Team. 2022. R: A language and environment for statistical computing (4.2.2). R Foundation for Statistical Computing, Vienna, Austria. https://www.r-project.org/

Ricard, S., A. Blais-Gagnon, W. Huertas, A. Michaud et M. Wu. 2022. Caractérisation Hydrométrique des Branches 5 du Ruisseau Au Castor et 46 du Ruisseau Morpions. Rapport Final. IRDA et partenaires. 17 p. https://irda.blob.core.windows.net/media/7223/irda_rapport_castorsmorpions_2022.pdf

Samsonova, V.P., Yu.N. Blagoveshchenskii and Yu.L. Meshalkina. 2017. Use of empirical Bayesian kriging for revealing heterogeneities in the distribution of organic carbon on agricultural lands: Eurasian Soil Science 50:305-311. DOI:10.1134/S1064229317030103

Schroth, A.W., C.D. Giles, P.D.F. Isles, Y. Xu, Z. Perzan and G.K. Druschel. 2015. Dynamic coupling of iron, manganese, and phosphorus behavior in water and sediment of shallow ice-covered eutrophic lakes. Environmental Science and Technology 49: 9758–9767. DOI:10.1021/acs.est.5b02057

Simoneau, M. 2019. Qualité de l'eau des tributaires de la baie Missisquoi: Evolution temporelle 1999-2017 et portrait récent 2015-2017. Ministère de l'Environnement et de la Lutte Contre les Changements Climatiques, Direction Générale du Suivi de L'état de L'environnement, Québec, Québec. 92 p. + 12 annexes. https://www.environnement.gouv.qc.ca/eau/bassinversant/bassins/missisquoi/evolution1999-2017-portrait2015-2017/rapport.pdf

Smeltzer, E. and M. Simoneau. 2008. Phosphorus loading to Missisquoi Bay from sub-basins in Vermont and Québec, 2002-2005. VT DEC, Vermont, and MELCCFP, Quebec.

US Census Bureau. 2020. 2020 Census Results. https://www.census.gov/programs-surveys/decennial-census/decade/2020/2020-census-results.html

US EPA. 2002. Onsite Wastewater Treatment Systems Manual Revised 2002. National Service Center for Environmental Publications (NSCEP), Washington, D.C.

US EPA. 2016. Phosphorus TMDLs for Vermont segments of Lake Champlain. US EPA Region 1, New England, Boston, Massachusetts. https://attains.epa.gov/attains-public/api/documents/actions/1VTDECWQ/66080/104776

USDA NASS. 2016. USDA national agricultural statistics service cropland data layer. https://nassgeodata.gmu.edu/CropScape/

USDA NASS. 2017. 2017 Census of Agriculture. www.nass.usda.gov/AgCensus

USGS. 2021. Watershed boundary dataset, National Geodatabase. Accessed July 2021 at: https://prd-tnm.s3.amazonaws.com/index.html?prefix=StagedProducts/Hydrography/WBD/National/GDB/

Vaughan, M.C.H. 2019. Concentration, load, and trend estimates for nutrients, chloride, and total suspended solids in Lake Champlain tributaries, 1990-2017. Technical Report No. 86. Lake Champlain Basin Program, Grand Isle, Vermont.

VCGI. 2016. Vermont open geodata portal. https://geodata.vermont.gov/

Vidon, P., D.L. Karwan, A.S. Andres, S. Inamdar, S. Kaushal, J. Morrison, J. Mulaney, D. Ross, A.W. Schroth, J.B. Shanley and B. Yoon. 2018. In the path of the hurricane: Impact of Hurricane Irene and Tropical Storm Lee on watershed hydrology and biogeochemistry from North Carolina to Maine, USA. Biogeochemistry 141:351-364. https://doi.org/10.1007/s10533-018-0423-4

VTANR. 2023. National pollutant discharge elimination system (NPDES) permits. https://anrweb.vt.gov/DEC/IWIS/ReportViewer2.aspx?Report=WWActiveNPDESPermitsandViewParms=False

Wall, G.J., D.R. Coote, E.A. Pringle and I.J. Shelton (eds). 2002. RUSLE-CAN - Équation universelle révisée des pertes de sol pour application au Canada: Manuel pour l'évaluation des pertes de sols causées par l'érosion hydrique au Canada. Direction Générale de la Recherche, Agriculture et Agroalimentaire Canada, Gatineau, Québec. No de contribution Vol. 02 (91). 117 p.

Williams, R. 1995. The EPIC model. *In* Computer Models of Watershed Hydrology. pp 909-1000.

Winchell, M., D. Meals, S. Folle, J. Moore, D. Braun, C. DeLeo, R. Schiff and K. Budreski. 2011. Identification of Critical Source Areas of Phosphorus Within the Vermont Sector of the Missisquoi Bay Basin (Technical Report No. 63B). Grand Isle, VT: Lake Champlain Basin Program. Stone Environmental, Inc., Montpelier, Vermont and Milone and MacBroom, Inc. https://www.lcbp.org/publications/identification-critical-source-areas-phosphorus-within-vermont-sector-missisquoi-bay-basin-technical-report-63b/

Zhang, Q. and R.M. Hirsch. 2019. River water-quality concentration and flux estimation can be improved by accounting for serial correlation through an autoregressive model. Water Resources Research 55(11):9705-9723. https://doi.org/10.1029/2019WR025338

Zia, A., A.W. Schroth, J.S. Hecht, P. Isles, P.J. Clemins, S. Turnbull, P. Bitterman, Y. Tsai, I.N. Mohammed, G. Bucini, E.M.B. Doran, C. Koliba, A. Bomblies, B. Beckage, J. Winter, E.C. Adair, D.M. Rizzo, W. Gibson and G. Pinder. 2022. Climate change-legacy phosphorus synergy hinders lake response to aggressive water policy targets. Earth's Future, Vol. 10. DOI:10.1029/2021EF002234. Appendices

Appendix 1: Results tables of Terrestrial P Inventories Throughout the Missisquoi Basin, Quebec

This appendix, provided as an Excel spreadsheet, contains higher resolution (subwatershed-level) quantifications of the agricultural P sources, non-agricultural P sources, and current P storage in soils, and supporting data for Quebec. The name of this spreadsheet is *Appendix1_TerrestrialPInventory_QC_Tables.xlsx*. The list of tables contained in the appendix is provided here.

Table A1-1: Land Use Distribution within Individual Subwatersheds of Missisquoi bay Basin.

Table A1-2: Distribution of Phosphorus Inputs, Crop Uptakes and Balances per Land Use Classes for Individual Subwatersheds (HUC12) of Missisquoi Bay Basin

Table A1-3: Area Weighted Mehlich-3 Soil Test Phosphorus, Aluminium and P Saturation per Land Use Classes for Individual Subwatersheds (HUC12) of Missisquoi Bay Basin

Table A1-4: Soil Phosphorus Saturation Distribution

Table A1-5: Wastewater Treatment Plant Characteristics

Table A1-6: Population and Estimated Loadings from Septic Systems for Missisquoi Bay Watershed

Appendix 2: Results tables of Terrestrial P Inventories Throughout the Missisquoi Basin, Vermont

This appendix, provided as an Excel spreadsheet, contains higher resolution (subwatershed-level) quantifications of the agricultural P sources, non-agricultural P sources, and current P storage in soils, and supporting data for Vermont. The name of this spreadsheet is *Appendix2_TerrestrialPInventory_VT_Tables.xlsx*. The list of tables contained in the appendix is provided here.

Table A2-1: Agricultural P Inputs by HUC12 and Land Use

Table A2-2: Agricultural P Inputs Variability by HUC12 and Land Use

Table A2-3: Soil Characteristics by HUC12 and Land Use

Table A2-4: Soil Characteristics Variability by HUC12 and Land Use

Table A2-5: Wastewater P Effluent Concentrations

Table A2-6: Wastewater P Solids

Table A2-7: Septic System P Load Estimations

Appendix 3: Results tables of Missisquoi Bay P Inventories

This appendix, provided as an Excel spreadsheet, contains additional sample-level details of the water column and sediment P concentrations within the bay. The name of this spreadsheet is *Appendix3_MissisquoiBay_PInventory_Tables.xlsx*. The list of tables contained in the appendix is provided here.

Table A3-1: Sediment Samples, Ascorbate Extraction

Table A3-2: Sediment Samples, Total Digestion

Table A3-3: Water Samples, DEC

Table A3-4: Water Samples, UVM Platform

Table A3-5: Water Samples, UVM Spatial

Appendix 4: Metadata of Key Inputs to the Terrestrial Metamodel

This appendix, provided as table in Word format, list the metamodel input parameters and their classes or units description.

Appendix 5: Quality Assurance Project Plan

This appendix provides the project's Quality Assurance Project Plan (QAPP) as document in PDF format.